

EXPLORING THE NORTH AMERICAN ARCTIC BENTHOS: COMMUNITY STRUCTURE
AND OIL DEGRADATION POTENTIAL OF SEDIMENT BACTERIA AND ARCHAEA

By

Alexis M. Walker, B.S.

A Dissertation Submitted in Partial Fulfillment of the Requirements

for the Degree of

Doctor of Philosophy

in

Marine Biology

University of Alaska Fairbanks

December 2022

APPROVED:

Dr. Sarah L. Mincks, Committee Chair
Dr. Mary Beth Leigh, Committee Co-Chair
Dr. Ana Aguilar Islas, Committee Member
Dr. Andres Lopez, Committee Member
Dr. Eric R. Collins, Committee Member
Dr. Lara Horstmann, Chair
Department of Marine Biology
Dr. Bradley Moran, Dean
College of Fisheries and Ocean Sciences
Dr. Richard Collins
Director of the Graduate School

ABSTRACT

The Chukchi and Beaufort seas benthic habitats are home to a multitude of ecologically and commercially important organisms that are subject to ongoing environmental changes, including the impacts of climate change and increased exposure to contaminants. Benthic bacteria and archaea can be considered biogeochemical engineers. They play a major role in organic matter (OM) degradation and nutrient cycling and their community structure can reflect changes in environmental conditions such as OM composition and quantity, nutrient availability, redox conditions, and natural/anthropogenic contaminants (e.g. petroleum hydrocarbons). Yet, sediment microbial communities have rarely been examined in these marginal seas of North American Arctic. In this dissertation, I characterized marine sediment microbial communities along environmental gradients in the Beaufort (Chapter 2) and Chukchi seas (Chapter 3) and assess Arctic benthic microbial community response to oil exposure (Chapter 4). I assessed diversity, community structure, and environmental correlates of prokaryotic communities via 16S rRNA amplicon sequencing in surface sediments (upper 1 cm) from the Northern Bering Sea to the Amundsen Gulf in the southern Beaufort Sea. On a broad spatial scale encompassing the whole study area, I observed three distinct microbial assemblages. One assemblage was characteristic of the Northern Bering-Chukchi seas shelf, and two distinguished nearshore and offshore sediments in the Beaufort Sea. Within the Beaufort Sea, four assemblages were identified, reflecting habitat heterogeneity with respect to OM loading, water depth, and nearshore/riverine input, including a major influence of the Mackenzie River. Two assemblages were distinguished within the Bering-Chukchi region, including one representative of suboxic sediments and one suggesting influence of phytodetrital OM input as evidenced by the abundance of diatom/particle-associated microbes. These two assemblages may also reflect

differences between local versus advective OM inputs. Incubation experiments exposing Arctic marine sediments to fresh and weathered crude oil under anaerobic and aerobic conditions were performed to assess oil biodegradation potential and identify putative oil-degrading microbes in the benthos. Molecular analyses revealed that significant community shifts occurred in the oiled treatments, with distinct communities emerging following exposure to fresh versus weathered oil, and in oxic versus anoxic conditions. The work presented here constitutes the first large-scale survey of benthic microbes in this region of the North American Arctic, including their response to petroleum contamination, generating valuable baseline data for the changes to come.

TABLE OF CONTENTS

ABSTRACT	iii
LIST OF FIGURES	ix
LIST OF APPENDICES	xiii
ACKNOWLEDGEMENTS	xv
CHAPTER 1: GENERAL INTRODUCTION	1
1.1 REFERENCES	5
CHAPTER 2: PATTERNS IN BENTHIC MICROBIAL COMMUNITY STRUCTURE ACROSS ENVIRONMENTAL GRADIENTS IN THE BEAUFORT SEA SHELF AND SLOPE	15
2.1 ABSTRACT	15
2.2 INTRODUCTION	16
2.3 METHODS	20
2.3.1 <i>Sample Collection</i>	20
2.3.2 <i>Sediment Characteristics</i>	21
2.3.3 <i>Microbial Community Analysis</i>	22
2.3.4 <i>Data Analyses</i>	23
2.4 RESULTS	25
2.4.1 <i>Prokaryotic Community Structure and Diversity</i>	25
2.4.2 <i>Taxonomic Composition and Indicator Taxa</i>	26
2.4.3 <i>Environmental Correlates of Community Structure</i>	28
2.4.4 <i>Broader Geographical Context</i>	30
2.5 DISCUSSION	31
2.5.1 <i>Upper Slope Assemblage (A)</i>	31
2.5.2 <i>Generalist Assemblage (B)</i>	34
2.5.3 <i>Shallow Shelf Assemblage (C)</i>	35
2.5.4 <i>Anoxic Assemblage (D)</i>	37
2.5.5 <i>Broader Geographical Context</i>	40
2.5.6 <i>Synthesis</i>	42
2.6 ACKNOWLEDGMENTS	45
2.7 REFERENCES	46
2.8 FIGURES	76
2.9 APPENDICES	82

CHAPTER 3: BENTHIC BACTERIA AND ARCHAEA IN THE NORTH AMERICAN ARCTIC REFLECT FOOD SUPPLY REGIMES AND IMPACTS OF COASTAL AND RIVERINE INPUTS	88
3.1 ABSTRACT	88
3.2 INTRODUCTION	89
3.3 METHODS	92
3.3.1 <i>Collection</i>	92
3.3.2 <i>Environmental Data</i>	93
3.3.3 <i>16S rRNA Amplicon Sequencing</i>	95
3.3.4 <i>Data Analysis</i>	96
3.4 RESULTS	98
3.4.1 <i>Vertical Distribution of Prokaryotic Communities Within Sediments (N Bering, SE Chukchi)</i>	98
3.4.2 <i>Spatial Distribution of Sediment Prokaryotic Communities on a Broader Spatial Scale</i>	99
3.4.3 <i>Chukchi vs. Beaufort Sediments</i>	101
3.5 DISCUSSION	102
3.5.1 <i>Vertical Distribution of Prokaryotic Communities Within Sediments (N Bering, SE Chukchi)</i>	103
3.5.2 <i>Spatial Patterns in Bering-Chukchi Surface Sediments</i>	107
3.5.3 <i>Prokaryotic Community Structure in North American Arctic Sediments</i>	113
3.6 CONCLUSIONS	115
3.7 ACKNOWLEDGEMENTS	117
3.8 REFERENCES	118
3.9 FIGURES	145
APPENDICES	153
CHAPTER 4: MICROBIAL COMMUNITY RESPONSE TO CRUDE OIL EXPOSURE IN ARCTIC MARINE SEDIMENTS	161
4.1 ABSTRACT	161
4.2 INTRODUCTION	162
4.3 METHODS	165
4.3.1 <i>Experimental Design</i>	165
4.3.2 <i>Sequencing, Bioinformatics, and Data Analysis</i>	167
4.4 RESULTS	168
4.4.1 <i>Community Structure</i>	168
4.4.2 <i>Core Community</i>	169
4.4.3 <i>Putative Oil Degradars</i>	170

4.4.4 Diversity	171
4.5 DISCUSSION	172
4.5.1 Conclusions	179
4.6 REFERENCES	180
4.7 FIGURES	202
CHAPTER 5: GENERAL CONCLUSION	207
5.1.1 Context in a changing Arctic	211
5.1.2 Future work	213
5.2 REFERENCES	215

LIST OF FIGURES

Figure 2.1. Prokaryotic cluster assemblages and spatial distribution in Beaufort Sea sediments. This figure shows the dendrogram of the four assemblages revealed via hierarchical clustering above the study area map which exhibits sample locations colored by assemblage. The map was created using ArcGIS online with the following layers: Northwest Territories, Esri, Garmin, FAO, NOAA, USGS, EPA, NRCan, and Parks Canada.....	76
Figure 2.2. Substructure of prokaryotic assemblages. This dendrogram highlights the substructure within each assemblage and the differing east to west gradients reflected by the substructure. Assemblage A was divided by location and depth, with one sub-cluster dominated by Amundsen Gulf (AG) samples combined with broader Beaufort (AKCA) slope samples deeper than 350 m. The other assemblage A sub-cluster was dominated by broader Beaufort slope samples with AG samples shallower than 350 m. Assemblage B divided cleanly between broader Beaufort and Amundsen Gulf samples. Assemblage C divided between the west of the Mackenzie River, AK samples, and east of the Mackenzie River, CA Beaufort and AG samples. Assemblage D divided into combinations of AG samples with either AK or CA samples with no obvious demarcations.....	77
Figure 2.3. Top 25 abundant families in Beaufort Sea surface sediments. The stacked barplot illustrates the proportion of the top 25 families for each assemblage on the left-hand y-axis. The plot is arranged such that the most abundant taxa starts from the top and decreases toward the bottom. Note that Gammaproteobacteria Inc. sed., NB1-j, Actinomarinales, Sva1033, OM190, BD7-8, AT-s2-59, and UBA10353 are not classified to family, but order level.	78
Figure 2.4. Proportion of assemblage-specific indicator taxa across prokaryotic assemblages. Indicator taxa are identified to the lowest taxonomic level possible. The plot is colored by functional groups which provide insight into characteristics associated with specific assemblages. *Indicates those taxa that were not yielded as indicators, but represent OTUs belonging to the same family as unidentified indicator taxa.	79
Figure 2.5. Distribution of environmental parameters for each assemblage. Each violin plot shows the distribution, within each assemblage, of the environmental parameters indicated as significant correlates in the ideal model for CAP analysis. Note that salinity is also included in this figure, though it was not run in CAP analysis due to the covariance inflation factor with depth. The symbols † and * indicate significant differences between un-matching symbols with other assemblages. $\delta^{13}\text{C}$ values for ice, marine, and terrestrial OM sources was derived from Dunton et al. (2006).	80
Figure 2.6. Environmental parameters influencing prokaryotic assemblage structure. The ordination plots above depict the results of Constrained Analysis of Principal Coordinates. All included environmental parameters are significant correlates ($P < 0.001$) to the first four CAP axes (A–C) and, in total, explained 18% of the variation in prokaryotic community structure ($R^2 = 0.18$). The corresponding correlations are reported in the table for all axes.	81
Figure 2.7. Top 10 abundant prokaryotes at class level exhibited in marine sediments. The colored grid above is arranged with surface sediment microbiomes on the y-axis, Beaufort,	

global benthic, Norwegian Arctic, and deep-sea (Zinger et al., 2011; Bienhold et al., 2016). The *x*-axis represents the rank from the most abundant taxa on the left to the least abundant taxa on the right exhibited by these microbiomes. The colors represent the class-level taxonomy of these prokaryotes. 82

Figure 3.1. Map of ASGARD sample stations and associated vertical sediment depth distributions of prokaryotic assemblages. Map (a). The stations on this map show where sediment cores were collected for prokaryotic community and environmental parameter analyses in 2018 as a part of the ASGARD program. The different symbols marking each station indicate the assemblage profile group across different sediment depth horizons (b). A depiction of the assemblage profile groups (Group 1, Group 2, Group 3, Group 4), which exhibited similar assemblage patterns with sediment depth. 145

Figure 3.2. Map and dendrograms of prokaryotic community structure exhibited in Bering-Chukchi surface sediments from ASGARD and DBO samples. The dendrogram above the map shows the assemblages for ASGARD surface sediments and the dendrogram to the left shows the assemblages exhibited in DBO surface sediments. The stations on the map are colored by assemblage and shaped based on year. The stations on the map are also put into context with respect to the DBO 1-5 transects located on the Bering-Chukchi Shelf. St. Lawrence Island is denoted by the abbreviation SLI. 146

Figure 3.3. Depth trends in relative abundance of 10 dominant taxa (family-level) for groups sharing the same downcore microbial assemblage patterns. Overlaid on each plot are letters denoting the assemblage exhibited by each group and dotted lines where a transition between assemblages occurred. The figure legend is organized such that the aerobic and/or facultative taxa are depicted in lighter colors and anaerobic taxa are depicted in darker colors. Depth is measure as cm below seafloor (cmbsf). 147

Figure 3.4. Sediment characteristics profiles for prokaryotic assemblage structure with sediment depth. Depth profiles of environmental parameters (porosity, TOC, and TN) that were significantly correlated with microbial community structure for each group. Groups are denoted by different line patterns, and colors of the points reflect the assemblage that was exhibited at the corresponding sediment depth on the y-axis. Sediment depth is measure as cm below seafloor (cmbsf). 148

Figure 3.5. Heatmap of indicator taxa and most abundant genus-level taxa for assemblages A and B across Bering-Chukchi sediments. Indicator taxa included in the heatmap are *R76-B128*, *MSBL3*, *Blastopirellula*, *Dokdonia*, *Rubritalea*, *Geopsychrobacter*, and *Oleiphilus*. The symbols above the heatmap represent functional groups reported in the literature for each taxon. 149

Figure 3.6. Distribution of oil degraders and iron reducers in relation to isoprenoid III and Fe concentrations in Northern Bering and Chukchi sediments on the Bering Chukchi Shelf. Maps of the distribution and relative abundance (%) of oil degraders (*Oleispira* and *Oleiphilus*) and iron reducers (*Geopsychrobacter*) in sediments collected from a) ASGARD (2018) and d) DBO (2014). Concentrations of highly branched isoprenoid III in b) 2014 and c) 2017 (Koch et al., 2020). Iron (Fe) content (%) measured in Chukchi sediments in 2012 (e) (Astakhov et al., 2013). 150

Figure 3.7. Environmental parameters correlating with prokaryotic assemblage structure in Bering-Chukchi surface sediments. Ordination plots exhibiting the significant environmental correlates with the community structure of Bering-Chukchi sediment prokaryotes and are depicted in 2 different axes combinations: a) CAP1 and CAP4 axes and b) CAP2 and CAP3 axes. The table provides the correlation strength (R^2) between the statistically significant ($P < 0.001$) environmental variables and associated axes. Note that DBO5 was not included as all three samples were lacking Chl-*a* measurements. 151

Figure 3.8. Dendrogram and map of prokaryotic community structure in surface sediments of the North American Arctic. The dotted line in the dendrogram denotes the division between the Bering-Chukchi and Beaufort seas and depicts the differences between the 3 major assemblages in the North American Arctic: The Bering-Chukchi assemblage and the nearshore and offshore assemblages within the Beaufort Sea. The substructure within the Bering-Chukchi assemblage was such that the transects overlaying corresponding benthic hotspots DBO1 (SLIP) and DBO4 (NECS) hotspots were clustered together (SL+NE*), and the DBO5 (BC), DBO3 (SECS), and DBO2 (Chirikov) hotspots were clustered together (BC* +SECS + Chirikov). The asterisks denote that there is one station within the NECS (DBO4) transect which clusters with the BC +SECS + Chirikov (DBO5+DBO3+DBO2) samples, and one station in the BC (DBO5) transect that were clustered with the SLIP+NECS (DBO1 + DBO4) samples. In the Beaufort Sea, substructure within the offshore shelf assemblage was such that there were offshore sub-assemblages west and east of the Mackenzie River. The stations on the map are colored by substructure. 152

Figure 4.1. Experimental design for sediment oil biodegradation incubation tests. Oil degradation rates and community composition shifts were observed at 6 time points at 12-day intervals over the course of 60 days. For all incubation treatments, i.e., unoiled, fresh oil, weathered oil, oxic, and anoxic, there were 3 replicates. Oxic treatments were analyzed at time 0, 12, 24, 36, 48 and 60 days. Anoxic incubations were only analyzed at 790 days. 202

Figure 4.2. Cluster dendrogram of oxic and anoxic sediment samples. In this dendrogram, unoiled, oxic oiled, and Anoxic oiled assemblages are enclosed in boxes, and the substructure and time points in days are highlighted in color. The unoiled assemblage is in quotations as it does include samples with oil in them from day 0 of the experiment. Shapes are used to denote the treatment for each node on the dendrogram where “*in situ*” represents samples upon collection from the Chukchi Sea benthos, which were collected 10 days prior to the start of the experiment (-10). 203

Figure 4.3. Change in core community genera with respect to oil treatment over time. The line plots above depict the proportion (y-axis), which are differing in scale for each taxon, of a given genus within unoiled, fresh oil, and weathered oil samples. The x-axis is such that 0 days is the start of experiment for anoxic and oxic samples, 60 days marks the end of the oxic experiment, and 72 days marks day 790, which is when the anoxic samples were harvested. Taxa with an * are clustered at genus level but could only be classified to order level. 204

Figure 4.4. Change in most abundant taxa over time across treatments (unoiled fresh oil, and weathered oil under oxic and anoxic conditions) in Chukchi Sea sediments. The area plots above depict the proportional change in core community overtime with select top 50 genera of unoled,

fresh oil, and weathered oil treatments. The x-axis is such that -10 days is the time of sample collection (10 days before experiment start), then day 0 (start of experiment for anoxic and oxic samples), then 12-day intervals when oxic samples were harvested, and finally one anoxic time point at day 790. Asterisks denote taxa which were clustered at genus-level but identified only down to order-level. 205

Figure 4.5. Change in prokaryotic diversity overtime across treatments as barplots of unoiled, fresh oil, and weathered oil replicate samples under oxic and anoxic conditions from day 0 to 790 (x-axis) are shown above. The y-axis is the change in inverse Simpson indices from the mean diversity found *in situ* (samples upon collection). All samples from 0-60 days are oxic, and all samples at day 790 are anoxic. 206

LIST OF APPENDICES

Appendix 2.1. Distribution of <i>Methyloceanibacter</i> at different levels of sequence removal. The pie chart above illustrates an example, using the genus <i>Methyloceanibacter</i> , of how relative abundances change with removal of singletons and doubletons compared to no removal (none). The difference in abundance is attributed to the removal of OTUs that would likely not have been removed if clustered at 97% similarity as they belong to the same genus. This is an important consideration when using amplicon sequence variants (ASVs), and software which automatically remove singletons and doubletons such as DADA2.	83
Appendix 2.2. Indicator OTUs for individual and combinations of prokaryotic assemblages. This Venn diagram illustrates the number of indicator OTUs in parentheses identified for individual assemblages and those shared in different combinations of assemblages.	83
Appendix 2.3. Indicator taxa for each prokaryotic assemblage. Taxa are arranged from most abundant starting at the top to least abundant toward the bottom. Those without a semi-colon indicate OTUs which could not be IDed past the taxonomic level provided.	84
Appendix 2.4. Proportion of top 10 most abundant taxa in Beaufort sediments at class level. This bubble plot illustrates the proportion of the 10 most abundant taxa at class level for Beaufort Sea surface sediments.	87
Appendix Table 3.1. Sediment characteristic data for ASGARD samples.....	153
Appendix Table 3.2. Environmental data for ASGARD and DBO surface samples (0-1cm)....	155
Appendix 3.3. Dendrogram depicting the three prokaryotic assemblage clusters resulting from hierarchical clustering analysis.	157
Appendix 3.4. Most abundant prokaryotic families across 3 assemblages exhibited in Chukchi sediments in 2018. The stacked barplot illustrates the relative abundance of the top 25 families for each cluster found in the upper 5-10cm in Chukchi Sea sediments collected in 2018. The plot is arranged such that the most abundant taxa starts from the top and decreases towards the bottom. Note that Gammaproteobacteria (Gamma.) Incertae Sedis, B2M28, Sva1033, NB1-j, Actinomarinales, and Sva0485 are not classified to family, but order level.	158
Appendix 3.5. Dendrogram from hierarchical clustering analysis with combined OTU table for ASGARD and DBO sediment samples.....	159
Appendix 3.6. Top-25 most abundant prokaryotic families across 2 assemblages exhibited in Chukchi sediments in 2014 and 2018. The stacked barplot illustrates the relative abundance of the top 25 families for each assemblage found in the upper 1cm layer in Northern Bering and Chukchi sediments collected in 2014 and 2018. The plot is arranged such that the most abundant taxa start from the top and decreases towards the bottom. Note that Gammaproteobacteria (Gamma.) Incertae Sedis, Sva1033, B2M28, NB1-j, and BD2-2 1 are not classified to family, but to order level.	160

ACKNOWLEDGEMENTS

My sincerest thank you to my advisors, Dr. Sarah Mincks and Dr. Mary Beth Leigh, who gave me the guidance, support, patience, and space for creativity, passion, and life circumstances. You were both an integral part of this journey and I cannot thank you enough. Much gratitude to my committee, Dr. Ana Aguilar-Islas, Dr. Andres Lopez, and Dr. Eric Collins, for providing pivotal feedback and pointing me in the right direction, whether it was steering me away from a tangent or towards the most useful literature, analysis, and questions. A huge thank you to Shannon MacPhee for coordinating and collaborating with us, without you we would not have had such an expansive dataset from the Canadian Beaufort Sea. Chapter 1 sample sequencing, student stipend, and tuition were funded by the US Department of the Interior, Bureau of Ocean Energy Management (BOEM) through the Coastal Marine Institute graduate student fellowship program (Grant# M16AC00004). Stipend and tuition support during chapter 1 preparation was provided in part by the North Pacific Research Board (Project #1303). This work was also supported via in-kind match from the high-performance computing and data storage resources operated by the Research Computing Systems Group at the University of Alaska Fairbanks Geophysical Institute. Sample sequencing, student stipend, and tuition for chapter 2 were funded by the North Pacific Research Board (Project #1907). Stipend and tuition support was provided in part by the Oil Spill Recovery Institute (Project #19-10-06). Thanks to Brittany Charrier for providing insight into corresponding macrofaunal community patterns in the Chukchi Sea Benthos. Thank you to the crew of the *Norseman II* and the *R/V Sikuliaq*. Sincerest gratitude to the many ASGARD scientists who collected samples for the Chukchi 2018 project (Andrew Thurber, Sarah Seabrook, Jessica Pretty, Opik Ahkinga, Sylvana Gonzales) and who shared supporting environmental data. Jackie Grebmeier was instrumental in collecting surface sediment samples

for microbial community analysis across the broader Bering-Chukchi seas in 2014. So much appreciation goes out to Taylor Gofstein for assisting with oil and sediment extraction methods and protocol creation for Chapter 3. Support for the use of the UAF Institute of Arctic Biology Genomics Core lab, which was utilized throughout every chapter in this thesis was provided by the Institutional Development Award (IDeA) from the National Institute of General Medical Sciences of the National Institutes of Health (NIH) under grant number 2P20GM103395. The content of this dissertation is solely the responsibility of the authors and does not necessarily reflect the official views of the NIH

CHAPTER 1: GENERAL INTRODUCTION

Benthic bacteria and archaea perform diverse metabolic functions that mediate biogeochemical processes, including OM degradation and early diagenesis of organic matter in marine sediments (Deming and Baross, 1993). Although taxonomic identity is generally not a reliable predictor of ecological function for most prokaryotes, a growing body of research indicates that the presence of certain prokaryotic families or genera can provide insight into the quantity and quality of available OM, trace metals, bioturbation, presence of naturally- or anthropogenically-derived hydrocarbons, and even redox conditions in downcore sediments (Baltar et al., 2018; Chen et al., 2017; Deng et al., 2020; Ferguson et al., 2017; Hoffmann et al., 2017; Kostka et al., 2011; Steenbergh et al., 2014). Additionally, certain taxonomic groups have been strongly correlated with environmental parameters, such as chlorophyll-*a* (an indicator of phytodetritus deposition) and bathymetry, measured along natural environmental gradients (Bienhold et al., 2012; Jacob et al., 2013). Benthic prokaryotes are also key players in both the production and mitigation of greenhouse gases such as methane and nitrous oxide and represent a first line of defense in remediating contamination by oil and other petroleum-based products (Boetius et al., 2000; Casciotti and Buchwald, 2012; Head et al., 2006). Thus, benthic microbial community characterization could be an invaluable tool for assessing changes in the environment and provide clues to processes that are difficult to observe or measure directly in offshore regions such as the North American Arctic.

The North American Arctic encompasses the Chukchi and Beaufort seas, marginal seas characterized by a broad inflow and narrow interior shelf respectively (Carmack and Wassmann, 2006). The broad Bering-Chukchi shelf is considered a highly productive and ecologically

important habitat that supports foraging by an array of organisms including whales, pinnipeds, and sea birds, which in turn support subsistence hunting by coastal Indigenous communities (Grebmeier et al., 2015; Grebmeier and Maslowski, 2014; Huntington et al., 2021, 2016). The high productivity of this region is fueled by the northward flow of three major water masses: nutrient-rich Anadyr-influenced water in the west, centrally located summer and winter variants of Bering Sea water, and warmer lower-nutrient Alaska Coastal Water to the east along the Alaskan coast (Gong and Pickart, 2015; Thomas Weingartner et al., 2005; Woodgate, 2018). By comparison, the narrower Beaufort Sea shelf experiences less primary production, but exhibits sharper biological and physical gradients largely due to varying bathymetry and terrestrial input via erosion and riverine influence (Carmack and Wassmann, 2006). In the Beaufort Sea, summer depth-stratified water-mass structure includes a fresher surface Polar Mixed Layer (PML; ~0–50 m), the Pacific-influenced Arctic Halocline Layer (AHL; ~50 – 200 m), and warmer, more saline Atlantic Water (AW) at depths greater than 200 m (Lansard et al., 2012; Miquel et al., 2015; Smoot and Hopcroft, 2017). Eastern Beaufort Sea shelf (< 100 m water depth) and slope habitats are particularly influenced by riverine input, including the vast Mackenzie River which is the fourth largest in the Arctic in terms of freshwater discharge (330 km³/year), and the largest in terms of sediment transport (124 × 10⁶ t/year) (Holmes et al., 2012; Macdonald et al., 1998; Rachold et al., 2004). The Mackenzie River primarily influences the water and sediment characteristics near the US-Canada border and areas further east, whereas the western Beaufort is influenced by warmer, more nutrient-rich waters entering from the Chukchi Sea and forming the Beaufort Shelf Jet, which flows due east from Barrow Canyon (Dunton et al., 2006; Pickart, 2004; Weingartner et al., 2005) This benthic habitat may also be heavily influenced by methane

derived from organic matter burial, mud volcanoes, subsurface permafrost, and/or gas hydrates (Brothers et al., 2016; Coffin et al., 2017; Paull et al., 2015; Retelletti Brogi et al., 2019).

The naturally dynamic environment of the Arctic shelves is also highly susceptible to climate change effects, which have already manifested in reduced sea-ice extent, species range shifts, and changes in pelagic primary productivity, OM deposition, and hydrography, all of which may have major and varying impacts on macro- to microorganisms (Arrigo and van Dijken, 2015, 2011; Grebmeier, 2012; Moore and Stabeno, 2015; Nelson et al., 2014). Furthermore, due to climbing atmospheric temperatures, current projections predict that the Beaufort and Chukchi seas will be ice-free in summer for 4-5 months, respectively, by 2040 (Årthun et al., 2021; Wang and Overland, 2015). Thus, previously ice-covered waters will become more accessible to human activities, increasing the likelihood of anthropogenic disturbance and contaminant exposure through oil and gas development and the expansion of maritime transportation.

Understanding microbially-mediated oil biodegradation potential is important to accurately predicting the fate and effects of oil exposure in marine sediments, because microbial metabolism is the primary mechanism of oil-spill remediation in the marine environment (Braddock et al., 1995; Hazen et al., 2015; McFarlin et al., 2014; Prince et al., 2013, 2002). This information is also valuable to developing appropriate spill response strategies, including those that rely on biodegradation. Despite conservative estimates that 20-30% of total oil from a spill event is transported to the benthos, oil spill effects on benthic microbial communities have not yet been studied in the North American Arctic (Muschenheim and Lee, 2002). Oil in the benthos can adversely impact the health of the marine ecosystems, including benthic and pelagic food webs, immediately following an oil spill and for decades into the future (Peterson et al., 2003;

Shigenaka, 2014). Oil can be toxic or fatal to a multitude of demersal fishes and invertebrates and is persistent in the environment and the tissues of exposed organisms years after a spill event (Jewett et al., 2002; Short et al., 2003; Sun et al., 2018). Ten years following the Exxon-Valdez oil spill (EVOS), oil compounds persisted in marine sediments and at toxic levels within the tissues of organisms such as Pacific halibut (*Hippoglossus stenolepis*), mussels, and clams (Jewett et al., 2002). In Arctic ecosystems, benthic fishes and invertebrates compose all or some of the diets of marine birds and mammals including walrus (*Odobenus rosmarus divergens*), seals, and whales, which are also important for subsistence hunting by Indigenous communities (Huntington et al., 2021). Thus, understanding the fate of oil in Arctic marine sediments is important to assessing the potential environmental and human health impacts of an oil spill in this ecosystem.

Microbial community structure varies across multiple spatiotemporal scales, along biogeochemical gradients, and in response to contaminant exposure (Ladau and Elie-Fadrosh, 2019; Shade et al., 2018). I characterized benthic microbial communities of the Beaufort (Chapter 1) and Chukchi (Chapter 2) seas using 16S rRNA amplicon (V4) metabarcoding surveys from sediment samples, and investigated how these communities might be impacted in the event of an oil spill (Chapter 3).

1.1 REFERENCES

- Arrigo, K.R., van Dijken, G.L., 2015. Continued increases in Arctic Ocean primary production. *Prog. Oceanogr.* 136, 60–70. <https://doi.org/10.1016/j.pocean.2015.05.002>
- Arrigo, K.R., van Dijken, G.L., 2011. Secular trends in Arctic Ocean net primary production. *J. Geophys. Res.* 116, C09011. <https://doi.org/10.1029/2011JC007151>
- Årthun, M., Onarheim, I.H., Dörr, J., Eldevik, T., 2021. The Seasonal and Regional Transition to an Ice-Free Arctic. *Geophys. Res. Lett.* 48, e2020GL090825. <https://doi.org/10.1029/2020GL090825>
- Baltar, F., Gutiérrez-Rodríguez, A., Meyer, M., Skudelny, I., Sander, S., Thomson, B., Nodder, S., Middag, R., Morales, S.E., 2018. Specific Effect of Trace Metals on Marine Heterotrophic Microbial Activity and Diversity: Key Role of Iron and Zinc and Hydrocarbon-Degrading Bacteria. *Front. Microbiol.* 9, 3190. <https://doi.org/10.3389/fmicb.2018.03190>
- Bienhold, C., Boetius, A., Ramette, A., 2012. The energy–diversity relationship of complex bacterial communities in Arctic deep-sea sediments. *ISME J.* 6, 724–732. <https://doi.org/10.1038/ismej.2011.140>
- Boetius, A., Ravenschlag, K., Schubert, C.J., Rickert, D., Widdel, F., Gleseke, A., Amann, R., Jørgensen, B.B., Witte, U., Pfannkuche, O., 2000. A marine microbial consortium apparently mediating anaerobic oxidation methane. *Nature* 407, 623–626. <https://doi.org/10.1038/35036572>

- Braddock, J.F., Lindstrom, J.E., Brown, E.J., 1995. Distribution of hydrocarbon-degrading microorganisms in sediments from Prince William Sound, Alaska, following the Exxon Valdez oil spill. *Mar. Pollut. Bull.* 30, 125–132. [https://doi.org/10.1016/0025-326X\(94\)00110-U](https://doi.org/10.1016/0025-326X(94)00110-U)
- Brothers, L.L., Herman, B.M., Hart, P.E., Ruppel, C.D., 2016. Subsea ice-bearing permafrost on the U.S. Beaufort Margin: 1. Minimum seaward extent defined from multichannel seismic reflection data. *Geochemistry, Geophys. Geosystems* 17, 4354–4365. <https://doi.org/10.1002/2016GC006584>
- Carmack, E., Wassmann, P., 2006. Food webs and physical–biological coupling on pan-Arctic shelves: Unifying concepts and comprehensive perspectives. *Prog. Oceanogr.* 71, 446–477. <https://doi.org/10.1016/j.pocean.2006.10.004>
- Casciotti, K.L., Buchwald, C., 2012. Insights on the marine microbial nitrogen cycle from isotopic approaches to nitrification. *Front. Microbiol.* 3, 356. <https://doi.org/10.3389/fmicb.2012.00356>
- Chen, X., Andersen, T.J., Morono, Y., Inagaki, F., Jørgensen, B.B., Lever, M.A., 2017. Bioturbation as a key driver behind the dominance of Bacteria over Archaea in near-surface sediment. *Sci. Rep.* 7, 2400. <https://doi.org/10.1038/s41598-017-02295-x>
- Coffin, R., Smith, J., Yoza, B., Boyd, T., Montgomery, M., 2017. Spatial Variation in Sediment Organic Carbon Distribution across the Alaskan Beaufort Sea Shelf. *Energies* 10, 1265. <https://doi.org/10.3390/en10091265>

- Deming, J.W., Baross, J.A., 1993. The Early Diagenesis of Organic Matter: Bacterial Activity, in: *Organic Geochemistry*. Springer, pp. 119–144. https://doi.org/10.1007/978-1-4615-2890-6_5
- Deng, L., Bölsterli, D., Kristensen, E., Meile, C., Su, C.-C., Bernasconi, S.M., Seidenkrantz, M.-S., Glombitza, C., Lagostina, L., Han, X., Jørgensen, B.B., Røy, H., Lever, M.A., 2020. Macrofaunal control of microbial community structure in continental margin sediments. *Proc. Natl. Acad. Sci. U. S. A.* 117, 15911–15922. <https://doi.org/10.1073/pnas.1917494117>
- Dunton, K.H., Weingartner, T., Carmack, E.C., 2006. The nearshore western Beaufort Sea ecosystem: Circulation and importance of terrestrial carbon in arctic coastal food webs. *Prog. Oceanogr.* 71, 362–378. <https://doi.org/10.1016/j.pocean.2006.09.011>
- Ferguson, R.M.W., Gontikaki, E., Anderson, J.A., Witte, U., 2017. The variable influence of dispersant on degradation of oil hydrocarbons in subarctic deep-sea sediments at low temperatures (0-5 °C). *Sci. Rep.* 7, 1–13. <https://doi.org/10.1038/s41598-017-02475-9>
- Gong, D., Pickart, R.S., 2015. Summertime circulation in the eastern Chukchi Sea. *Deep Sea Res. Part II Top. Stud. Oceanogr.* 118, 18–31. <https://doi.org/10.1016/J.DSR2.2015.02.006>
- Grebmeier, J.M., 2012. Shifting Patterns of Life in the Pacific Arctic and Sub-Arctic Seas. *Ann. Rev. Mar. Sci.* 4, 63–78. <https://doi.org/10.1146/annurev-marine-120710-100926>
- Grebmeier, J.M. and, Maslowski, W., 2014. *The Pacific Arctic Region*. Springer Netherlands, Dordrecht. <https://doi.org/10.1007/978-94-017-8863-2>

- Grebmeier, J.M., Bluhm, B.A., Cooper, L.W., Danielson, S.L., Arrigo, K.R., Blanchard, A.L., Clarke, J.T., Day, R.H., Frey, K.E., Gradinger, R.R., Kędra, M., Konar, B., Kuletz, K.J., Lee, S.H., Lovvorn, J.R., Norcross, B.L., Okkonen, S.R., 2015. Ecosystem characteristics and processes facilitating persistent macrobenthic biomass hotspots and associated benthivory in the Pacific Arctic. *Prog. Oceanogr.* 136, 92–114.
<https://doi.org/10.1016/j.pocean.2015.05.006>
- Hazen, T.C., Prince, R.C., Mahmoudi, N., 2015. Marine Oil Biodegradation. *Environ. Sci. Technol.* 50, 2121–2129. <https://doi.org/10.1021/acs.est.5b03333>
- Head, I.M., Jones, D.M., Röling, W.F.M., 2006. Marine microorganisms make a meal of oil. *Nat. Rev. Microbiol.* 4, 173–182. <https://doi.org/10.1038/nrmicro1348>
- Hoffmann, K., Hassenrück, C., Salman-Carvalho, V., Holtappels, M., Bienhold, C., 2017. Response of Bacterial Communities to Different Detritus Compositions in Arctic Deep-Sea Sediments. *Front. Microbiol.* 8, 1–18. <https://doi.org/10.3389/fmicb.2017.00266>
- Holmes, R.M., Coe, M.T., Fiske, G.J., Gurtovaya, T., McClelland, J.W., Shiklomanov, A.I., Spencer, R.G.M., Tank, S.E., Zhulidov, A. V., 2012. Climate Change Impacts on the Hydrology and Biogeochemistry of Arctic Rivers, in: *Climatic Change and Global Warming of Inland Waters*. John Wiley & Sons, Ltd, Chichester, UK, pp. 1–26.
<https://doi.org/10.1002/9781118470596.ch1>
- Huntington, H.P., Quakenbush, L.T., Nelson, M., 2016. Effects of changing sea ice on marine mammals and subsistence hunters in northern Alaska from traditional knowledge

interviews. *Biol. Lett.* 12, 20160198. <https://doi.org/10.1098/rsbl.2016.0198>

Huntington, H.P., Raymond-Yakoubian, J., Noongwook, G., Naylor, N., Harris, C., Harcharek, Q., Adams, B., 2021. “We Never Get Stuck:” A Collaborative Analysis of Change and Coastal Community Subsistence Practices in the Northern Bering and Chukchi Seas, Alaska. *ARCTIC* 74, 113–126. <https://doi.org/10.14430/ARCTIC72446>

Jacob, M., Soltwedel, T., Boetius, A., Ramette, A., 2013. Biogeography of Deep-Sea Benthic Bacteria at Regional Scale (LTER HAUSGARTEN, Fram Strait, Arctic). *PLoS One* 8, e72779. <https://doi.org/10.1371/journal.pone.0072779>

Jewett, S.C., Dean, T.A., Woodin, B.R., Hoberg, M.K., Stegeman, J.J., 2002. Exposure to hydrocarbons 10 years after the Exxon Valdez oil spill: Evidence from cytochrome P4501A expression and biliary FACs in nearshore demersal fishes. *Mar. Environ. Res.* 54, 21–48. [https://doi.org/10.1016/S0141-1136\(02\)00093-4](https://doi.org/10.1016/S0141-1136(02)00093-4)

Kostka, J.E., Prakash, O., Overholt, W.A., Green, S.J., Freyer, G., Canion, A., Delgardio, J., Norton, N., Hazen, T.C., Huettel, M., 2011. Hydrocarbon-degrading bacteria and the bacterial community response in Gulf of Mexico beach sands impacted by the deepwater horizon oil spill. *Appl. Environ. Microbiol.* 77, 7962–7974. <https://doi.org/10.1128/AEM.05402-11>

Ladau, J., Eloie-Fadrosch, E.A., 2019. Spatial, Temporal, and Phylogenetic Scales of Microbial Ecology. *Trends Microbiol.* 27, 662–669. <https://doi.org/10.1016/J.TIM.2019.03.003>

Lansard, B., Mucci, A., Miller, L.A., Macdonald, R.W., Gratton, Y., 2012. Seasonal variability

of water mass distribution in the southeastern Beaufort Sea determined by total alkalinity and $\delta^{18}\text{O}$. *J. Geophys. Res. Ocean.* 117, n/a-n/a. <https://doi.org/10.1029/2011JC007299>

Macdonald, R.W., Solomon, S.M., Cranston, R.E., Welch, H.E., Yunker, M.B., Gobeil, C., 1998. A sediment and organic carbon budget for the Canadian beaufort shelf. *Mar. Geol.* 144, 255–273. [https://doi.org/10.1016/S0025-3227\(97\)00106-0](https://doi.org/10.1016/S0025-3227(97)00106-0)

McFarlin, K.M., Prince, R.C., Perkins, R., Leigh, M.B., 2014. Biodegradation of dispersed oil in Arctic seawater at -1°C . *PLoS One* 9, 1–8. <https://doi.org/10.1371/journal.pone.0084297>

Miquel, J.C., Gasser, B., Martín, J., Marec, C., Babin, M., Fortier, L., Forest, A., 2015. Downward particle flux and carbon export in the Beaufort Sea, Arctic Ocean; the role of zooplankton. *Biogeosciences* 12, 5103–5117. <https://doi.org/10.5194/bg-12-5103-2015>

Moore, S.E., Stabeno, P.J., 2015. Synthesis of Arctic Research (SOAR) in marine ecosystems of the Pacific Arctic. *Prog. Oceanogr.* 136, 1–11. <https://doi.org/10.1016/j.pocean.2015.05.017>

Muschenheim, D.K., Lee, K., 2002. Removal of oil from the sea surface through particulate interactions: Review and prospectus. *Spill Sci. Technol. Bull.* 8, 9–18. [https://doi.org/10.1016/S1353-2561\(02\)00129-9](https://doi.org/10.1016/S1353-2561(02)00129-9)

Nelson, R.J., Ashjian, C.J., Bluhm, B.A., Conlan, K.E., Gradinger, R.R., Grebmeier, J.M., Hill, V.J., Hopcroft, R.R., Hunt, B.P.V., Joo, H.M., Kirchman, D.L., Kosobokova, K.N., Lee, S.H., Li, W.K.W., Lovejoy, C., Poulin, M., Sherr, E., Young, K. V., 2014. Biodiversity and biogeography of the lower trophic taxa of the pacific arctic region: Sensitivities to climate change, in: *The Pacific Arctic Region: Ecosystem Status and Trends in a Rapidly Changing*

Environment. Springer Netherlands, pp. 269–336. https://doi.org/10.1007/978-94-017-8863-2_10

Paull, C.K., Dallimore, S.R., Caress, D.W., Gwiazda, R., Melling, H., Riedel, M., Jin, Y.K., Hong, J.K., Kim, Y.G., Graves, D., Sherman, A., Lundsten, E., Anderson, K., Lundsten, L., Villinger, H., Kopf, A., Johnson, S.B., Hughes Clarke, J., Blasco, S., Conway, K., Neelands, P., Thomas, H., Côté, M., 2015. Active mud volcanoes on the continental slope of the Canadian Beaufort Sea. *Geochemistry, Geophys. Geosystems* 16, 3160–3181. <https://doi.org/10.1002/2015GC005928>

Peterson, C.H., Rice, S.D., Short, J.W., Esler, D., Bodkin, J.L., Ballachey, B.E., Irons, D.B., 2003. Long-Term Ecosystem Response to the Exxon Valdez Oil Spill. *Science* (80-.). 302, 2082–2086. https://doi.org/10.1126/SCIENCE.1084282/SUPPL_FILE/PETERSON.SOM.PDF

Pickart, R.S., 2004. Shelfbreak circulation in the Alaskan Beaufort Sea: Mean structure and variability. *J. Geophys. Res. C Ocean.* 109, 1–14. <https://doi.org/10.1029/2003JC001912>

Prince, R.C., McFarlin, K.M., Butler, J.D., Febbo, E.J., Wang, F.C.Y., Nedwed, T.J., 2013. The primary biodegradation of dispersed crude oil in the sea. *Chemosphere* 90, 521–526. <https://doi.org/10.1016/j.chemosphere.2012.08.020>

Prince, R.C., Owens, E.H., Sergy, G.A., 2002. Weathering of an Arctic oil spill over 20 years: the BIOS experiment revisited. *Mar Pollut Bull* 44, 1236–1242. [https://doi.org/10.1016/s0025-326x\(02\)00214-x](https://doi.org/10.1016/s0025-326x(02)00214-x)

Rachold, V., Eicken, H., Gordeev, V. V., Grigoriev, M.N., Hubberten, H., 2004. The Organic Carbon Cycle in the Arctic Ocean. *Org. Carbon Cycle Arct. Ocean*.

<https://doi.org/10.1007/978-3-642-18912-8>

Retelletti Brogi, S., Kim, J.-H., Ryu, J.-S., Jin, Y.K., Lee, Y.K., Hur, J., 2019. Exploring sediment porewater dissolved organic matter (DOM) in a mud volcano: Clues of a thermogenic DOM source from fluorescence spectroscopy. *Mar. Chem.*

<https://doi.org/10.1016/J.MARCHEM.2019.03.009>

Shade, A., Dunn, R.R., Blowes, S.A., Keil, P., Bohannan, B.J.M., Herrmann, M., Küsel, K., Lennon, J.T., Sanders, N.J., Storch, D., Chase, J., 2018. Macroecology to Unite All Life, Large and Small. *Trends Ecol. Evol.* 33, 731–744.

<https://doi.org/10.1016/J.TREE.2018.08.005>

Shigenaka, G., 2014. Twenty-Five Years After the Exxon Valdez Oil Spill ; National Oceanic and Atmospheric Administration Scientific Support, Monitoring and Research.

Short, J.W., Rice, S.D., Heintz, R.A., Carls, M.G., Moles, A., 2003. Long-term effects of crude oil on developing fish: Lessons from the Exxon Valdez oil spill. *Energy Sources* 25, 509–517. <https://doi.org/10.1080/00908310390195589>

Smoot, C.A., Hopcroft, R.R., 2017. Depth-stratified community structure of Beaufort Sea slope zooplankton and its relations to water masses. *J. Plankton Res.* 39, 79–91.

<https://doi.org/10.1093/plankt/fbw087>

Steenbergh, A.K., Bodelier, P.L.E., Slomp, C.P., Laanbroek, H.J., 2014. Effect of Redox

Conditions on Bacterial Community Structure in Baltic Sea Sediments with Contrasting Phosphorus Fluxes. *PLoS One* 9, e92401. <https://doi.org/10.1371/journal.pone.0092401>

Sun, R., Sun, Y., Li, Q.X., Zheng, X., Luo, X., Mai, B., 2018. Polycyclic aromatic hydrocarbons in sediments and marine organisms: Implications of anthropogenic effects on the coastal environment. *Sci. Total Environ.* 640–641, 264–272.
<https://doi.org/10.1016/J.SCITOTENV.2018.05.320>

Wang, M., Overland, J.E., 2015. Projected future duration of the sea-ice-free season in the Alaskan Arctic. (J.E. Overland). *Prog. Oceanogr.* 136, 50–59.
<https://doi.org/10.1016/j.pocean.2015.01.001>

Weingartner, Thomas, Aagaard, K., Woodgate, R., Danielson, S., Sasaki, Y., Cavalieri, D., 2005. Circulation on the north central Chukchi Sea shelf. *Deep Sea Res. Part II Top. Stud. Oceanogr.* 52, 3150–3174. <https://doi.org/10.1016/J.DSR2.2005.10.015>

Weingartner, T, Okkonen, S., Danielson, S., 2005. Circulation and water property variations in the nearshore Alaskan Beaufort Sea. *US Miner. Manag. Serv. Outer Cont. Shelf Study* 2005–028, 1–103.

Woodgate, R.A., 2018. Increases in the Pacific inflow to the Arctic from 1990 to 2015, and insights into seasonal trends and driving mechanisms from year-round Bering Strait mooring data. *Prog. Oceanogr.* 160, 124–154.
<https://doi.org/10.1016/J.POCEAN.2017.12.007>

CHAPTER 2: PATTERNS IN BENTHIC MICROBIAL COMMUNITY STRUCTURE ACROSS ENVIRONMENTAL GRADIENTS IN THE BEAUFORT SEA SHELF AND SLOPE¹

2.1 ABSTRACT

The paradigm of tight pelagic-benthic coupling in the Arctic suggests that current and future fluctuations in sea ice, primary production, and riverine input resulting from global climate change will have major impacts on benthic ecosystems. To understand how these changes will affect benthic ecosystem function, we must characterize diversity, spatial distribution, and community composition for all faunal components. Bacteria and archaea link the biotic and abiotic realms, playing important roles in organic matter (OM) decomposition, biogeochemical cycling, and contaminant degradation, yet sediment microbial communities have rarely been examined in the North American Arctic. Shifts in microbial community structure and composition occur with shifts in OM inputs and contaminant exposure, with implications for shifts in ecological function. Furthermore, the characterization of benthic microbial communities provides a foundation from which to build focused experimental research. We assessed diversity and community structure of benthic prokaryotes in the upper 1 cm of sediments in the southern Beaufort Sea (United States and Canada), and investigated environmental correlates of prokaryotic community structure over a broad spatial scale (spanning 1,229 km) at depths ranging from 17 to 1,200 m. Based on hierarchical clustering, we identified four prokaryotic

¹ Walker AM, Leigh MB and Mincks SL (2021) Patterns in Benthic Microbial Community Structure Across Environmental Gradients in the Beaufort Sea Shelf and Slope. *Front. Microbiol.* 12:581124. doi: 10.3389/fmicb.2021.581124

assemblages from the 85 samples analyzed. Two were largely delineated by the markedly different environmental conditions in shallow shelf vs. upper continental slope sediments. A third assemblage was mainly comprised of operational taxonomic units (OTUs) shared between the shallow shelf and upper slope assemblages. The fourth assemblage corresponded to sediments receiving heavier OM loading, likely resulting in a shallower anoxic layer. These sites may also harbor microbial mats and/or methane seeps. Substructure within these assemblages generally reflected turnover along a longitudinal gradient, which may be related to the quantity and composition of OM deposited to the seafloor; bathymetry and the Mackenzie River were the two major factors influencing prokaryote distribution on this scale. In a broader geographical context, differences in prokaryotic community structure between the Beaufort Sea and Norwegian Arctic suggest that benthic microbes may reflect regional differences in the hydrography, biogeochemistry, and bathymetry of Arctic shelf systems.

2.2 INTRODUCTION

The Arctic marine ecosystem is undergoing pronounced changes due to climbing atmospheric temperatures, occurring two to three times faster than the global average (ACIA, 2005; Walsh et al., 2011). Resulting shifts in sea-ice cover, primary production, and riverine input will likely affect the quality and quantity of organic material (OM) deposited to the seafloor and the tight pelagic-benthic coupling characteristic of Arctic ecosystems may emphasize the effects of these changes (Grebmeier, 2012; Kortsch et al., 2015). Impacts of climate change on Arctic benthic eukaryotes have varied among size classes, but benthic prokaryotic communities have not been described well enough to monitor change (Kędra et al., 2015; Nelson et al., 2014; Renaud et al., 2019).

Benthic bacteria and archaea perform diverse metabolic functions that mediate biogeochemical processes, including degradation and early diagenesis of organic matter in marine surface sediments (Deming and Baross, 1993). Prokaryotes provide a link between the abiotic and biotic realms, such that prokaryotic community structure reflects environmental gradients in, for example, OM deposition. Studies conducted in the Norwegian Arctic suggest that prokaryotic community structure shifts with varying quality and quantity of OM inputs, with possible consequences for ecosystem function (Braeckman et al., 2018; Hoffmann et al., 2017). Certain taxonomic groups have been strongly correlated with environmental parameters, such as Chl-*a* and bathymetry, measured along natural environmental gradients (Bienhold et al., 2012; Jacob et al., 2013). Benthic prokaryotes are also key players in both the production and degradation of greenhouse gases such as methane and nitrous oxide and represent a first line of defense in remediating contamination by oil and other petroleum-based products (Boetius et al., 2000; Casciotti and Buchwald, 2012; Head et al., 2006). In some cases, these important functions are attributable to specific taxonomic groups (Kostka et al., 2011; Otte et al., 2019; Ruff et al., 2015). Thus, characterization of benthic prokaryotic community structure may yield valuable insights into ecosystem function in Arctic marine sediments, particularly those permeated with methane and subjected to active mineral resource exploration such as the Beaufort Sea sites examined here (BOEM, 2019; Coffin et al., 2013).

The Beaufort Sea is an Arctic marginal sea that crosses a border between the United States and Canada, stretching from Point Barrow (Alaska, United States) to Banks Island (Northwest Territories, Canada). Prior studies of benthic prokaryotes in the southern Beaufort Sea have focused on subsurface sediments (20–70 cm) to assess the influence of either methane or mud volcanoes on bacterial community structure (Hamdan et al., 2013; Kirchman et al., 2014;

Lee et al., 2018; Treude et al., 2014). Communities in these deeper sediments typically differ substantially from the active surface layer (Bienhold et al., 2016; Durbin and Teske, 2011; Fry et al., 2006; Inagaki, 2003; Jorgensen et al., 2012; Roussel et al., 2009). Thus, there is no established baseline for benthic prokaryotes in southern Beaufort Sea surface sediments to date, and only limited data from deeper sediment horizons. Most information on Arctic benthic prokaryotes comes from the Norwegian Arctic, largely from deep-sea or fjord habitats, which differ from the Beaufort Sea in terms of primary production, terrestrial/riverine input, and bathymetry (Arnosti, 2008; Bienhold et al., 2016; Buttigieg and Ramette, 2015; Carmack and Wassmann, 2006; Holmes et al., 2002; Li et al., 2009; Ravensschlag et al., 2001; Zeng et al., 2017).

Across the southern Beaufort Sea, summer depth-stratified water-mass structure includes a fresher surface Polar Mixed Layer (PML; ~0–50 m), the Pacific-influenced Arctic Halocline Layer (AHL; ~50 – 200 m), and warmer, more saline Atlantic Water (AW) at depths greater than 200 m (Lansard et al., 2012; Miquel et al., 2015; Smoot and Hopcroft, 2017). Eastern Beaufort Sea shelf (< 100 m water depth) and slope habitats are particularly influenced by riverine input, including the vast Mackenzie River which is the fourth largest in the Arctic in terms of freshwater discharge (330 km³/year), and the largest in terms of sediment transport (124 × 10⁶ t/year) (Holmes et al., 2002; Macdonald et al., 1998; Rachold et al., 2004). The Mackenzie River primarily influences the water and sediment characteristics of the Canadian sector of the shelf and slope, and to a lesser extent the Amundsen Gulf and easternmost section of the Alaskan sector (Figure 1). The Mackenzie shelf functions as a vast estuary influenced by freshwater runoff, receiving inputs of both terrestrial and marine sources of organic matter (Carmack and Macdonald, 2002; Magen et al., 2010). The Amundsen Gulf, which connects the

Canadian Arctic Archipelago with the southeast Beaufort Sea, is characterized by several peripheral bays, straights, and inlets and ringed by a narrow shelf surrounding a central basin (Forest et al., 2010; Gamboa et al., 2017; Stokes et al., 2006). Water mass properties in the Alaskan Beaufort Sea are influenced by warmer, more nutrient-rich waters entering from the Chukchi Sea and forming the Beaufort Shelf Jet, which flows due east from Barrow Canyon (Dunton et al., 2006; Pickart, 2004; Weingartner et al., 2005). These longitudinal environmental gradients from Point Barrow to Banks Island have been reflected in the benthic distributions of OM and certain epi-/infaunal groups (Bell et al., 2016; Goñi et al., 2013; Magen et al., 2010; Naidu et al., 2000). This benthic habitat may also be heavily influenced by methane derived from organic matter burial, mud volcanoes, subsurface permafrost, and/or gas hydrates (Brothers et al., 2016; Coffin et al., 2017; Lee et al., 2018; Paull et al., 2015; Retelletti Brogi et al., 2019).

We sought to describe prokaryote communities across this broad, heterogeneous benthic habitat, specifically by (1) assessing the diversity, structure, and composition of archaeal and bacterial communities in the upper 1 cm of sediments, and (2) investigating environmental correlates of prokaryote community structure over a broad area of the southern Beaufort Sea shelf and slope. Expanding knowledge of functional taxonomic groups of marine prokaryotes provides insight into this unstudied microbial habitat, and a framework for developing more targeted experimental studies in this dynamic polar environment (Bier et al., 2015; Fuhrman, 2009; Fuhrman et al., 2015).

2.3 METHODS

2.3.1 *Sample Collection*

Our study area covers a broad section of the continental shelf and upper slope of the Alaskan and Canadian Beaufort Sea, from areas offshore of the Colville River in the west to Banks Island in the east, and into the Amundsen Gulf (Figure 2.1). A total of 85 sediment samples were collected opportunistically at water depths between 17 and 1,200 m from 2012 to 2014 as part of two international collaborative field programs: the US-Transboundary Fish and Lower Trophic Communities Project (USTB) and the Canadian Beaufort Regional Environmental Assessment Project (BREA). Fifteen sediment samples, 8 in 2012 and 7 in 2013, were collected using a 5 cm diameter sub-core from the upper 1 cm layer of a 0.25 m² box core. In 2014, 70 sediment samples were collected using a 60-cc, 2.5 cm diameter, sterilized syringe from the upper 1 cm surface layer of a double van Veen grab (0.1 m², USTB) or a 0.25 m² box core (BREA). As preliminary analyses indicated that neither year or sampling gear were significant factors affecting prokaryotic community structure here, all samples were used in this study. The samples were immediately frozen at -20°C following collection aboard respective vessels, transported to the University of Alaska Fairbanks (UAF) Institute of Arctic Biology Genomics Core Laboratory, and then stored at -80°C . Environmental variables such as depth, bottom water temperature, and salinity were recorded from CTD profiles conducted at corresponding sampling locations (Eert et al., 2012; Smoot and Hopcroft, 2017).

2.3.2 Sediment Characteristics

We quantified several common indicators of quality, quantity, and origin of sediment OM including chlorophyll-*a* concentration (Chl-*a*), phaeopigment concentration (Phaeo), total organic carbon (TOC), total nitrogen (TN), ratio of carbon to nitrogen (C:N), and bulk sediment $\delta^{13}\text{C}$ and $\delta^{15}\text{N}$. All parameters were measured using sediment samples taken from the upper 1 cm of the same box core or grab as the genomic samples from each sampling station. Chl-*a* and phaeopigment concentrations were measured fluorometrically (Arar and Collins, 1997). Briefly, samples were suspended in 5 ml 100% acetone, sonicated in an ice-water bath for 10 min, and allowed to extract overnight at -20°C . Samples were then centrifuged to remove sediment, and transferred to a clean test tube. Chl-*a* concentration was determined using a TD-700 fluorometer (Turner Designs). After recording fluorescence values, samples were acidified with HCl, and fluorescence readings were taken of the acidified samples to produce phaeopigment values. A standard curve produced using commercially available Chl-*a* standard was used to convert fluorescence readings into concentrations.

Stable isotope and elemental analysis were performed on freeze-dried sediment samples at the Alaska Stable Isotope Facility (ASIF). Data for USTB samples were generated and previously reported by Bell et al. (2016); additional samples were analyzed here using the same protocol. Stable isotope data, $\delta^{13}\text{C}$ and $\delta^{15}\text{N}$, were generated using a ThermoFinnigan DeltaVPlus isotope ratio mass spectrometer with Pee Dee Belemite (PDB) and atmospheric nitrogen as standards for carbon and nitrogen, respectively. Percent carbon and nitrogen content was obtained using a Costech ESC 4010 elemental analyzer, and used to calculate TOC, TN, and C:N ratios.

Sediment porosity (Φ), i.e., volume of water within sediments (V_w), was calculated as an indicator of sediment permeability/O₂ penetration using Eq. 1 (Bennett and Lambert, 1971; Ullman and Aller, 1982). Sediment wet (W_{sw}) and dry (W_{sd}) weights were recorded before and after freeze-drying, and used to calculate the mass of water (W_w). Sediment density (ρ_s) was held constant at 2.50 g/cm³, based on Coffin et al. (2017). Seawater density (ρ_w) was calculated based on bottom-water temperatures and salinities recorded at sampled sites.

$$\text{Porosity } (\Phi) = V_w = \frac{(W_{sw} - W_{sd})}{\rho_w} \div \left(\frac{W_{sd}}{\rho_s} + \frac{W_w}{\rho_w} \right)$$

2.3.3 Microbial Community Analysis

16S ribosomal (rRNA) gene amplicon sequencing was conducted on freeze-dried sediments in order to assess the diversity and taxonomic composition of prokaryotes. Total genomic DNA was extracted from sediment samples using the Qiagen PowerSoil kit, and revised forward (515FB) and reverse (806RB) primers from the Earth Microbiome Project (EMP) were used to amplify the V4 region of the 16S rRNA gene (Apprill et al., 2015; Caporaso et al., 2012, 2011; Parada et al., 2016). Library preparation was conducted using iTru adapters for sequencing and a one-step PCR protocol with indexed primers, which is the current standard protocol used by the EMP (Apprill et al., 2015; Caporaso et al., 2012, 2011; Parada et al., 2016; Walters et al., 2016). Samples were sequenced on an Illumina MiSeq at the UAF Genomics Core Lab.

Raw sequences were de-multiplexed using the Mr. Demuxy package (Cock et al., 2009). Demultiplexed sequences were run with mothur v1.40.0 on a high performance-computing cluster through UAF Research Computing Systems using a modified MiSeq standard operating procedure (Schloss et al., 2009). Operational taxonomic units (OTUs) were clustered at 100%

similarity using the OptiClust option in mothur, taxonomy was assigned to OTUs using the SILVA 132 mothur formatted reference database with a bootstrap cutoff of 100%, and the samples in the resulting OTU table were normalized to 30,000 sequences and converted to relative abundances (Edgar, 2018; Glöckner et al., 2017; Wang et al., 2007; Westcott and Schloss, 2017). This OTU table (relative abundance of sequence reads per OTU for each sample) was used to conduct analyses of diversity and community structure of prokaryotes and to assess correlations with environmental variables.

2.3.4 Data Analyses

All statistical analyses were conducted using R, primarily using the vegan package (Oksanen, 2015; R Core Team, 2017). Diversity was quantified using the inverse Simpson index ($1/\lambda$) which reflects evenness and richness (Morris et al., 2014). Community structure was investigated via hierarchical clustering analysis with the Ward method (ward.D2) based on a Bray-Curtis dissimilarity derived from the OTU table. Cluster tests were used to assess the validity (heterogeneity, significance) and characteristics (silhouette, stability) of the hierarchical clusters. The heterogeneity of and significance between hierarchical clusters were investigated using Bray Curtis distances with the betadisper and adonis functions, respectively (Oksanen et al., 2017). OTUs that distinguished each cluster were identified via indicator taxa analysis using the indicpecies package (De Cáceres et al., 2010; De Cáceres and Legendre, 2009). The multipatt function was used to identify taxa specific to a single cluster, or indicative of combinations of clusters, with a significance of ≤ 0.001 and a strength of ≥ 0.900 (i.e., >90% probability of occurrence within a given cluster or combination of clusters (De Cáceres and Legendre, 2009). Given the complexity of the prokaryotic species concept and the lack of taxonomic resolution for many taxa, we used this indicator analysis to identify OTUs potentially

indicative of certain habitat features and/or assemblages. We assessed the distribution of these indicator taxa at varying taxonomic levels, from phylum to genus, to characterize representative assemblages for each cluster.

Differences in the median values of environmental parameters among clusters were evaluated using Kruskal-Wallis tests followed by pairwise Wilcoxon Rank Sum tests with a Benjamini and Yekutieli (BY) correction (Yekutieli and Benjamini, 2002). Relationships between prokaryotic community structure and environmental variables were modeled using Constrained Analysis of Principle Coordinates, i.e., the capscale function in the R vegan package (Oksanen, 2015; R Core Team, 2017). The best model for capscale analyses was identified based on variance inflation factors for each environmental parameter and a forward and backward stepwise model selection via permutation tests on adjusted R^2 and P -values using the ordistep function. The significance of the environmental correlates yielded via Constrained Analysis of Principle Coordinates was investigated in R using the adonis function; correlation strengths were calculated using the cor function (Oksanen et al., 2017). All bioinformatic and statistical scripts can be found here on GitHub².

In order to put Beaufort Sea surface sediment microbes into a broader geographical context, we qualitatively compared the 10 most abundant taxa at class level with those reported for global benthic surface sediments, global deep-sea sediments, and Norwegian-Arctic sediments (Bienhold et al., 2016; Zinger et al., 2011). We refer to the Arctic microbiome published by Bienhold et al. (2016) as the Norwegian Arctic microbiome because all but one dataset included in that study was generated from the Norwegian Arctic (Bienhold et al., 2016).

² <https://github.com/amwalker/Beaufort-benthos>

2.4 RESULTS

2.4.1 Prokaryotic Community Structure and Diversity

The total number of OTUs yielded was 295,115. No OTUs were removed (e.g., singletons or doubletons) because removals resulted in substantial changes in certain taxonomic groups (Appendix A2.1). Hierarchical clustering analysis identified four clusters, i.e., assemblages of prokaryotes which have significantly different (adonis: $F = 12.6$, $P < 0.001$) taxonomic composition (Figure 2.1). However, the silhouette test yielded an average cluster width of 0.11, indicating a high degree of similarity between clusters which suggests that the four assemblages may exist more so as a gradient rather than as discrete communities in particular locations. The number of samples within each cluster, herein referred to as assemblages A, B, C, and D, was as follows: A = 23, B = 35, C = 11, and D = 16. Assemblage A is most distinct, whereas C and D are most similar (Figure 2.1). The distribution of values for Inverse Simpson diversity differed for each assemblage, with the highest prokaryotic diversity exhibited in assemblage A, then B, D, and C.

Each assemblage is represented by sampling locations distributed across the study area (Figure 2.1), such that assemblages were not restricted to particular geographic areas that might reflect distinct environmental characteristics. However, when delving into the substructure of individual assemblages, patterns emerged at smaller spatial scales (Figure 2.2). Assemblage A contained two clusters, with one containing mostly Alaskan and Canadian Beaufort (AKCA) samples and some shallower (<350 m) Amundsen Gulf and Banks Island (AGBI) samples, and the other containing mostly AGBI samples with a few deeper (>350 m) AKCA samples. Assemblage B was clearly divided into AKCA and AGBI samples. Sub-structure for assemblage

C was delineated by the Mackenzie River into the AK Beaufort shelf (west of the river) and the CA Beaufort with AG samples (east of the river). Assemblage D divides into two groups with no obvious geographical demarcations.

2.4.2 Taxonomic Composition and Indicator Taxa

There were 350 prokaryotic families represented in this dataset; we focused on the 25 most abundant families (or in some cases, orders) to assess broad-scale patterns in community structure and compare relative abundance of these dominant taxa among individual assemblages. Abundant taxa consisting of multiple unclassified OTUs within a class or phylum, specifically Alpha- and Gammaproteobacteria, were ignored. The 25 most abundant taxa accounted for 58% of the total sequence reads, and are listed in order of decreasing abundance in Figure 2.3. Family-level composition differed among assemblages, with inverse relationships in abundance of particular taxa in assemblages A and C. Families that were relatively abundant in assemblage A also tended to be abundant in assemblage B, whereas assemblages C and D also showed similar trends. The families Nitrosopumilaceae, Woeseiaceae, NB1-j, Actinomarinales, Kiloniellaceae, Subgroup 22, OM190, and AT-s2-59 were particularly abundant in assemblage A. Haliaceae, BD7-8, and Methyloiligellaceae were most prominent in assemblage B. In assemblage C, Flavobacteraceae, Rhodobacteraceae, Rubritalaceae, and Psychromonadaceae were more abundant. Gammaproteobacteria *Incertae sedis*, Desulfobulbaceae, Sva1033, Anaerolineaceae, and Desulfobacteraceae were abundant in assemblage D.

Indicator taxa analyses revealed that assemblage A had the highest number of indicator OTUs (294), followed by C (61) and D (27), and no OTUs were identified as indicators for assemblage B (Appendices A2.2, A2.3). Taxa indicative of a combination of assemblages will be referred to as indicative taxa, to differentiate from assemblage-specific indicator taxa. Mirroring

trends shown in Figure 2.3, assemblages A + B and C + D shared relatively high numbers of indicative OTUs. No indicative taxa were shared between assemblages A + C alone, but some were shared between A + B + C, suggesting B represents a transitional community with representatives from both of the distinct A and C assemblages. Assemblages B + D also shared very few indicative taxa, but more were found when combined with either assemblage A or C (A+B+D or B+C+D).

In light of the numerous uncultured and indicative OTUs, we limit our discussion to selected assemblage-specific indicator taxa, identified to the highest taxonomic resolution possible, for which published information could be used with confidence to infer function or distribution of a specific assemblage, and/or metabolic type or relationship to environmental variables (Figure 4). Indicator OTUs for assemblage A belonged to the class Acidobacteria (Subgroups 6, 9, 10, 21, 22, and 26), clades SAR202 and 324, and the families Thermoanaerobaculaceae, Magnetospiraceae (*Magnetospira*), Nitrosopumilaceae (*Candidatus Nitrosopumilus*), Nitrospiraceae (*Nitrospira*), and Scalinduaceae (*Scalindua*). Representative taxa under Thermoanaerobaculaceae belong to Acidobacteria subgroup 10 which was recently assigned to this family (Dedysh and Yilmaz, 2018). Indicator taxa for assemblage C included representatives from the families Flavobacteriaceae (*Polaribacter* and *Ulvibacter*), Rhodobactereaceae (*Loktanella* and *Octadecabacter*), Thiovulaceae (*Cocleimonas*), Thiotrichaceae (*Sulfurimonas*), and Desulfobulbaceae (*Desulfobulbus*) (Figure 2.4). Assemblage D indicator taxa were within the families Anaerolineaceae, Desulfobacteraceae, Desulfobulbaceae, orders PHOS-HE36 and SBR1031, and phyla Bathyarchaeota, and Schekmanbacteria. The only indicator OTU identified down to genus level here was *Desulfococcus* (Desulfobacteraceae), therefore other abundant genus-level OTUs that belonged

to the families Desulfobacteraceae and Desulfobulbaceae, were also queried and further explored with the indicator taxa (Figure 2.4).

2.4.3 *Environmental Correlates of Community Structure*

Overall, the suite of environmental variables measured here explained relatively little (18%; Adj. $R^2 = 0.18$) of the variation in prokaryote community structure among sites (Figure 2.6). Nonetheless, results of the CAP analysis did suggest significant correlations (adonis: $P < 0.001$) with different habitat characteristics for each assemblage. Assemblage A was found solely on the continental slope in 23 samples ranging from 171 to 1,200 m water depth (median depth 350 m), thus generally consisting of “deep-sea” locations further offshore and below the photic zone. Sediments at these locations exhibited significantly higher $\delta^{15}\text{N}$ and porosity, and lower values of Chl-*a* concentration and C:N; bottom waters were warmer and more saline (Figure 2.5). Assemblage A largely differentiated from the other assemblages on the CAP1 axis (Figures 2.6a,c). CAP1 was most strongly and positively correlated with depth, $\delta^{15}\text{N}$, and porosity and exhibited a moderate to weak negative correlation with Chl-*a* and TOC. Variation within assemblage A was most apparent on the CAP4 axis suggesting Amundsen Gulf and Banks Island samples (+CAP4) are more influenced by degraded and marine derived OM (higher $\delta^{15}\text{N}$ and $\delta^{13}\text{C}$) whereas Beaufort slope samples (-CAP4) had higher porosity sediments with comparatively more phaeopigment and terrestrial OM (Figure 2.6C).

Assemblage B consisted of 35 samples ranging between 36 and 350 m water depth (median depth 75 m), with a little more than half (19) located on the shelf and the remainder (16) on the slope. Median values of all environmental parameters for assemblage B were not significantly different than those for any of the other assemblages (Figure 2.5). CAP analysis showed a separation of assemblage B largely along the CAP2, axis suggesting that stations in

this assemblage are characterized by more degraded OM (positive correlation with phaeopigment and $\delta^{15}\text{N}$) and less influence from terrestrial organic matter (higher $\delta^{13}\text{C}$ suggesting marine or ice-algal source; Dunton et al., 2006; Figures 5, 6A). Differences among samples within assemblage B were most apparent on both the CAP3 and CAP4 axes, indicating that Amundsen Gulf and Banks Island samples (-CAP3) were generally characterized by higher TOC and lower porosity, whereas samples from the open shelf and slope (+CAP3) were characterized by higher porosity sediments with comparatively less TOC and more degraded phytodetritus (higher phaeopigment). Easternmost samples from the Amundsen Gulf (+CAP4) were separated from all other samples (-CAP4), with potentially sea-ice derived OM (higher $\delta^{13}\text{C}$), compared to more degraded marine and terrestrial OM (lower $\delta^{13}\text{C}$ and higher phaeopigment) in the western Beaufort. Depth was also moderately or highly correlated with the CAP 3 and 4 axes, although this may reflect effects of other environmental variables that co-vary with depth.

The 11 samples represented by assemblage C were located solely in shallow shelf sediments ranging from 17 to 42 m water depth (median depth 21 m) with significantly lower values of $\delta^{15}\text{N}$, $\delta^{13}\text{C}$, and salinity. Assemblages C, B, and D were largely separated along the CAP2 axis, with assemblage C samples more correlated with fresh phytodetritus (higher Chl-a, lower $\delta^{15}\text{N}$) and terrestrial OM (lower $\delta^{13}\text{C}$). Samples within assemblage C varied along CAP3 axis which is most strongly correlated with TOC and porosity (Figure 6B). Nearshore samples from the Alaskan Beaufort shelf (+CAP3) were characterized by lower TOC and higher porosity, whereas those from the Canadian Beaufort and Amundsen Gulf (-CAP3) had higher TOC and lower porosity.

Assemblage D consisted of 16 samples which were collected almost exclusively at shelf locations (=100 m; median depth 72 m), except for 3 deep sites (=200 m) offshore of the Colville

River plume where high concentrations of Chl-*a* were found. Environmental characterization for and correlations with assemblage D were not well captured with parameters measured here (Figures 2.5, 2.6). Variation within assemblage D was most apparent on the CAP3 axis, which suggests that several samples had comparatively higher organic matter input and lower porosity.

2.4.4 Broader Geographical Context

Comparisons of the top 10 class-level taxa between Beaufort Sea, global benthic, deep-sea, and Norwegian-Arctic surface sediments indicate that all four sediment microbiomes share five major taxa: Gammaproteobacteria, Alphaproteobacteria, Deltaproteobacteria, Bacteroidia, and Actinobacteria (Figure 2.7). The Beaufort Sea sediment microbiome included taxa that were also highly abundant in either the combination of global benthic and deep-sea microbiomes (Plantomycetia) or the Norwegian-Arctic microbiome (Phycisphaera). Interestingly, four classes prevalent in the other three microbiomes were not among the 10 most abundant in Beaufort Sea sediments: Clostridia, Betaproteobacteria, Bacilli, and Acidobacteria. Nonetheless, Acidobacteria was quite abundant in the Beaufort Sea, falling within the top 13 most abundant classes. Class Betaproteobacteria was not detected in Beaufort Sea surface sediments, whereas Clostridia and Bacilli were present but in relatively low abundances. Nitrososphaeria, Verrucomicrobia, and Anaerolineae were among the top 10 taxa of the Beaufort Sea sediment microbiome, but were not abundant in the other datasets.

2.5 DISCUSSION

We identified four distinct assemblages, A, B, C, and D, across a broad area in southern Beaufort Sea surface sediments. Assemblage A occurred only at sites on the upper continental slope with lower concentrations of more degraded OM and higher porosity sediments. A distinct community (assemblage C) was found in shallow shelf sediments, with higher OM content and terrestrial OM influence. The wide distribution of assemblage B across shelf and slope depths and overlap in taxonomic composition with assemblages A and C, may reflect a transition zone between the shelf and slope sites containing generalists found in both bathymetric zones.

Assemblage D was found primarily at shelf depths, but included a few deeper slope sites in the westernmost part of the study area with high OM content. Indicator taxa with known metabolic functions and/or ecological context suggest that assemblage D was not merely comprised of generalists. In order to provide ecological context and better understand what distinguishes these assemblages, we examined taxa that were assemblage-specific and/or exhibited higher abundances associated to an individual assemblage together with environmental correlates.

2.5.1 *Upper Slope Assemblage (A)*

The indicator taxa of assemblage A, specifically Acidobacteria subgroups and SAR clades, reflect the deeper sampling depths (171–1,200 m) typified by reduced inputs of more degraded organic matter (Figure 1.5). Representatives of the phylum Acidobacteria found in Arctic deep-sea sediments have been proposed as potential indicators of oligotrophic conditions, and found to be more abundant in highly permeable sub-Arctic and Arctic sediments indicating an affinity for low-molecular-weight OM; subgroups 6, 10, and 26 in particular were more active under oligotrophic conditions (Bienhold et al., 2012; Hoffmann et al., 2017; Probandt et al.,

2017). Here, Acidobacteria subgroups 6, 9, 10, 21, 22, and 26 along with SAR clades 324 and 202, were prevalent in slope assemblage A. The clades SAR324 and SAR202, like the Acidobacteria subgroups, are also indicative of deep, oligotrophic environments (Galand et al., 2010; Landry et al., 2017; Li et al., 2015; Morris et al., 2004; Nunoura et al., 2018; Orcutt et al., 2011; Zinke et al., 2018).

Slope assemblage A may also reflect some of the unique biogeochemical characteristics on the Beaufort Sea slope. In the Arctic Halocline waters over the Canada Basin, SAR 202 have been implicated in terrestrial OM degradation, consistent with the relatively strong terrestrial signal exhibited throughout the Southern Beaufort, even in the upper slope sediments (Figure 2.5; Colatriano et al., 2018). SAR202 has also been linked with deep-sea mud volcanoes and SAR324 with methane-rich hydrothermal plumes (Coelho et al., 2016; Sheik et al., 2014). Acidobacteria subgroup 10 was recently placed in the family Thermoanaerobaculaceae which encompasses thermophilic obligate anaerobes isolated from marine hydrothermal vents and freshwater hot springs (Dedysh and Yilmaz, 2018; Losey et al., 2013). Several mud volcanoes on the Beaufort Sea slope release subsurface methane and produce temperatures $\geq 23^{\circ}\text{C}$ within a few centimeters of the sediment-water interface, creating suitable habitat for thermophilic anaerobes such as those within subgroup 10 (Gamboa et al., 2017; Lee et al., 2018; Paull et al., 2015; Paull, pers. comm). Subgroup 10 is widespread across the study area, yet to date, mud volcanoes have only been reported on the Canadian Beaufort Slope. These microbes may be spore-forming, similar to other thermophilic anaerobes reported from Arctic marine sediments that produce spores that lie dormant until favorable conditions arise (Hubert et al., 2010; Müller et al., 2014). However, previous reports of thermo-anaerobic bacterial spores belonged to the phylum Firmicutes, and not Acidobacteria, and none of the current taxa within Acidobacteria subgroup

10 are known to be spore-forming (Hubert et al., 2010; Losey et al., 2013; Müller et al., 2014). Given their occurrence in Arctic sediments from other regions, it is more likely that bacteria in subgroup 10 inhabit a wider temperature range than previously recognized (Hoffmann et al., 2017).

Beaufort sediment mineralogical properties may be influenced by the abundant indicator OTUs within Magnetospiraceae, a family composed of magnetotactic bacteria. Magnetotactic bacteria are unique in that they biosynthesize a mineral nanocrystal which they can use as a “compass” to navigate toward favorable redox conditions found at the oxic-anoxic interface in marine sediments (Lefevre and Bazylinski, 2013). Though indicator OTUs were all uncultured, *Magnetospira* is the most abundant taxon identified to genus-level within this family. Members of the genus *Magnetospira* produce magnetite crystals, which are the predominant magnetic grain found in Canadian Beaufort sediments and are more prevalent on the slope (Gamboa et al., 2017; Lefevre and Bazylinski, 2013; Williams et al., 2012).

Genera tightly linked to nitrification and anaerobic ammonia oxidation were relatively more abundant in slope assemblage A. *Nitrospira* are exclusively chemoautotrophic nitrite-oxidizing bacteria, oxidizing nitrite to nitrate, but have recently been found to perform complete nitrification, oxidizing ammonia to nitrate (Daims, 2014; Daims et al., 2015). *Candidatus Nitrosopumilus* encompasses ammonia-oxidizing archaea (AOA), which are aerobic nitrifiers that exhibit an extremely high affinity for ammonia, and can oxidize ammonia to nitrate, nitrite, or nitrous oxide (Könneke et al., 2014; Martens-Habbena et al., 2015; Qin et al., 2016; Stahl and de la Torre, 2012). AOA can perform mixotrophy and heterotrophy, but are largely chemoautotrophs (Könneke et al., 2014; Offre et al., 2013; Qin et al., 2014; Stahl and de la Torre, 2012). They also exhibit photoinhibition and increased autotrophic activity, which is

consistent with the distribution of this assemblage at deeper sampling stations (Alonso-Sáez et al., 2012; Qin et al., 2014). In the pelagic zone of the Beaufort Sea, AOA are relatively more abundant in bottom waters on the slope and may be capable of urea degradation to fuel nitrification, as has been observed for *Candidatus Nitrosopumilus sediminis* in Arctic sediments near Svalbard (Alonso-Sáez et al., 2012; Damashek et al., 2017; Park et al., 2012). In the portion of our study area characterized by assemblage A, a peak in urea concentration occurs at 250–300 m water depth due to zooplankton and fish excretion, which may fuel the activity of AOA in this region (Simpson et al., 2008).

The genus *Candidatus Scalindua* encompasses anaerobic ammonia oxidizing (anammox) bacteria which convert ammonia to N₂ via autotrophic metabolism and can utilize nitrite, nitrate, metal oxides, and even oligopeptides and small organic molecules as electron acceptors (Penton et al., 2006; Van de Vossenberg et al., 2013). Anaerobic ammonia oxidation may be a major sink for nitrate in the marine system, and has been reported in Arctic shelf slope sediments in the Chukchi Sea, near Greenland, and in deep-sea sediments from the Arctic mid-ocean ridge (Jorgensen et al., 2012; Penton et al., 2006; Rysgaard et al., 2004). The predominance of anammox bacteria at the deeper slope sites occupied by assemblage A supports previous claims that anammox is more likely to occur in areas with less organic matter loading (Burgin and Hamilton, 2007; McTigue et al., 2016; Rysgaard et al., 2004; Thamdrup and Dalsgaard, 2002).

2.5.2 Generalist Assemblage (B)

While no indicator taxa were identified for assemblage B, one abundant taxon included members of the bacterial family Methyloiligellaceae, dominated in this study by the genus *Methyloceanibacter* which contains known methylotrophs (Takeuchi et al., 2014; Vekeman et al., 2016a). Some species of *Methyloceanibacter* oxidize methanol, while others exhibit methane

oxidation and include the methane monooxygenase gene in their genome (Takeuchi et al., 2014; Vekeman et al., 2016a, 2016b). We have detected a relatively high abundance of the methane monooxygenase gene in these sediments through metagenomics analyses, although further analyses are needed to attribute these genes to a specific taxonomic group (Walker et al. unpublished data). Nonetheless, the presence of *Methyloceanibacter* coupled with the abundant distribution of the methane monooxygenase gene in methane-permeated Beaufort Sea sediments suggests that aerobic methane oxidation may be an active process in this region, although further research confirming this activity would be required. As there are multiple sources of methane in these sediments, methane oxidation in the Beaufort Sea is likely an important process constraining methane concentrations reaching the sea surface (Lorenson et al., 2016). However, no evidence for methanotrophy has yet been reported in the water column or subsurface sediments, despite chemical evidence that oxidation of methane derived from ancient sources may be occurring near the sediment-water interface (Hamdan et al., 2013; Sparrow et al., 2018).

2.5.3 Shallow Shelf Assemblage (C)

Indicator taxa for assemblage C were characteristic of a shallow- shelf environment influenced by fresh phytodetritus, riverine input, and sea ice, in keeping with elevated Chl-a and significantly lower values of $\delta^{13}\text{C}$ and salinity observed at assemblage C locations. Many of these taxa may be deposited to the seafloor in association with sinking particles.

Flavobacteriaceae occur in conjunction with phytoplankton blooms and subsequent deposition of phytodetritus (Bienhold et al., 2012; Hoffmann et al., 2017; Junge et al., 2002; Teeling et al., 2012). Genera within this family are typically aerobic, though there are some facultative anaerobic heterotrophs capable of degrading complex polysaccharides (McBride, 2014; Teeling et al., 2012; Xing et al., 2015). Two of the genus-level indicator taxa found here, *Ulvibacter* and

Polaribacter, are often particle attached and tightly connected with phytoplankton blooms and sea ice (Bowman and McCuaig, 2003; Brinkmeyer et al., 2003; Junge et al., 2002; Teeling et al., 2012; Xing et al., 2015). *Ulvibacter* is one of the first and most abundant genera to respond to a phytoplankton bloom following algal lysis, whereas *Polaribacter* is most abundant in later stages of an algal bloom and can use sulfatases to access highly sulfated algal material (Helbert, 2017; Teeling et al., 2016, 2012; Xing et al., 2015). *Polaribacter* species generally include psychrophilic bacteria that are most commonly found in polar and temperate regions. Until recently, they had only been identified in sea ice and seawater, but are now described from Arctic sediments offshore of Svalbard (Bowman et al., 2012; Gosink et al., 1998; Li et al., 2014; Rapp et al., 2018).

A few of the indicator taxa for assemblage C suggest that light availability may be a major factor influencing community composition. Genomic analyses of *Polaribacter* species, along with *Loktanella* and *Octadecabacter*, indicator taxa from the Rhodobacteraceae family, contain various rhodopsins (light- driven proton pumps) and other light responsive genes, indicating an affinity for well-lit shallower waters (Boeuf et al., 2013; Dogs et al., 2017; González et al., 2008; Vollmers et al., 2013; Wu et al., 2014; Xing et al., 2015). *Loktanella*, described as anoxygenic photoheterotrophs (AAP), have been found in Beaufort Sea surface waters including the Mackenzie River outflow where they were positively correlated with Chl- *a* (Boeuf et al., 2013). AAP photosynthesize but also require oxygen for breaking down organic matter with light-harvested energy, and are most abundant in coastal waters and eutrophic estuaries (Boeuf et al., 2013; Waidner and Kirchman, 2007). Photoheterotrophy could be an advantage in such environments that are heavily influenced by terrestrial material, providing an energy source to fuel more costly metabolic processes such as the degradation of humic

substances (Boeuf et al., 2013). *Octadecabacter* species are psychrophilic, aerobic heterotrophs with gas vesicles and are abundant in sea ice, though a few taxa have been isolated from seawater and marine sediments (Billerbeck et al., 2015; Brinkmeyer et al., 2003; Gosink et al., 1997; Lee et al., 2014; Vollmers et al., 2013). *Octadecabacter* spp. have also been linked to phytoplankton blooms and detrital aggregates in the Arctic and elsewhere (Grossart et al., 2005; Koedooder et al., 2019; Rapp et al., 2018).

The remaining indicator taxa for assemblage C belong to the bacterial families Thiotrichaceae, Thiovolaceae, and Desulfobulbaceae, all of which are involved in the marine sulfur cycle. Members of the Desulfobulbaceae family, which are anaerobic sulfate reducers, were also found in assemblage D and discussed further below (Kuever, 2014a). Thiotrichaceae and Thiovolaceae, represented here by *Cocleimonas* and *Sulfurimonas*, respectively, are sulfur oxidizers (Garrity et al., 2015; Han and Perner, 2015; Tanaka et al., 2011). Sulfur oxidizing bacteria are generally limited by the availability of necessary electron donors (typically reduced sulfur compounds) and acceptors (oxygen, nitrate) favored in anoxic and oxic conditions, respectively (Jørgensen et al., 2019; Wasmund et al., 2017). Adaptations exhibited by *Sulfurimonas* and *Cocleimonas* provide a competitive advantage in the oxidation of elemental sulfur and other sulfur intermediates (Han and Perner, 2015; Pjevac et al., 2014; Tanaka et al., 2011; Wasmund et al., 2017).

2.5.4 Anoxic Assemblage (D)

The indicator taxa for assemblage D suggest a greater extent of anoxic sediment within the upper 1 cm layer. All indicator OTUs for Assemblage D are strict anaerobes within the families Desulfobulbaceae, Desulfobacteraceae, Anaerolineaceae, PHOS- HE36, the order SBR1033, and the phyla Bathyarchaeota and Schekmanbacteria (Anantharaman et al., 2018;

Evans et al., 2015; Kuever, 2014a, 2014b; Yamada and Sekiguchi, 2018). Members of the archaeal phylum Bathyarchaeota and candidate bacterial phylum Schekmanbacteria consisted of uncultured OTUs with less than 85% matches to published sequences in BLAST. Though inferences based on this level of taxonomy are highly speculative, representatives from both phyla have been most commonly sequenced from subsurface marine sediments (Anantharaman et al., 2018; Biddle et al., 2006; Evans et al., 2015; Inagaki et al., 2003; Lopez-Fernandez et al., 2018; Sørensen and Teske, 2006; Winkel et al., 2018).

Anaerolineaceae are comprised of anaerobic heterotrophs with a fermentative metabolism and have been sequenced in anoxic, organic-rich habitats such as sludge digesters, hydrothermal vents, and glacial fjord sediments off the coast of Svalbard (McIlroy et al., 2017; Yamada and Sekiguchi, 2018; Zeng et al., 2017). They are typically abundant in biofilms and implicated as hydrogenotrophs and alkane degraders, though few studies have examined marine representatives (Al-Thani et al., 2014; Liang et al., 2015; Siegert et al., 2011; Sinkko et al., 2013; van der Waals et al., 2017). Similarly, bacteria in the order SBR1031 have been primarily investigated in waste-water treatment plants where they produce biofilms (X. Wang et al., 2018; Xia et al., 2016). Marine representatives have been found in oil-contaminated estuarine sediments, and increase in abundance in seasonal microbial mats in the North Sea (Cardoso et al., 2019; Obi et al., 2017). Bacteria from the family PHOS-HE36 have also been predominately studied in the context of sludge digesters and biofilms, often sequenced with bacteria in the Anaerolineaceae family, but have also been found in marine sediments near methane seeps, hydrothermal vents, and within microbial mats (Dabert et al., 2001; Fujii et al., 2002; Trembath-Reichert et al., 2016; L. Wang et al., 2018; Zinke et al., 2018).

Indicator taxa from assemblage D are also connected to the sulfur cycle, specifically sulfate reduction, which is the dominant process responsible for anaerobic degradation of organic matter in marine sediments (Jørgensen et al., 2019; Wasmund et al., 2017). The abundance of several taxa within the families Desulfobacteraceae and Desulfobulbaceae suggest that sulfate reduction is prevalent in both shallow shelf assemblage C and anoxic assemblage D. At family level, Desulfobacteraceae taxa were more abundant in assemblage D, whereas Desulfobulbaceae taxa were more evenly distributed between assemblages C and D, albeit with specific genera that were more abundant in shallow assemblage C. These families have shown responses to different substrates in Arctic sulfidic sediments, suggesting the taxonomic differences between assemblages C and D reflect differences in substrate availability among sites (Dyksma et al., 2018; Müller et al., 2018).

Desulfocapsa and *Desulfobulbus* (Desulfobulbaceae) were more abundant in shallow shelf assemblage C, and have often been sequenced in Arctic fjord sediments alongside sulfur-oxidizing bacteria (SOB) such as *Sulfurimonas* and *Cocleimonas*; which were also identified as indicator taxa for assemblage C (Buongiorno et al., 2019; Trivedi et al., 2018; Zeng et al., 2017). This repeated co-occurrence in Arctic marine sediments suggests an affinity for similar environmental/redox conditions, and further exemplifies subtle differences between sulfur cycling in assemblages C and D.

The more abundant SRB taxa in assemblage D, particularly SEEP-SRB1 and SEEP-SRB4 clades, are most commonly sequenced from cold seeps (Kleindienst et al., 2012; Ruff et al., 2015; Schreiber et al., 2010). SEEP-SRB have been implicated in coupling sulfate reduction to the anaerobic oxidation of non-methane and methane hydrocarbons, however they remain largely uncultured (Petro et al., 2019). *Desulfococcus* spp., though commonly found in sulfidic

sediments, are also associated with marine seeps, and may be major players in anaerobic hydrocarbon degradation in association with seeps (Boetius et al., 2000; Kleindienst et al., 2014, 2012; Orphan et al., 2001).

The majority of samples in this assemblage were located in shallow shelf sediments, some of which were characterized by heavy OM loading and low porosity, conducive to oxygen depletion. Samples collected on the slope in assemblage D exhibited some of the highest concentrations of Chl-*a* measured here, and may have received a recent pulse of fresh phytodetritus leading to shallow anoxic conditions in sediments. Moreover, multiple indicator taxa for assemblage D are also associated with biofilms, microbial mats, seep environments, or subsurface sediments, suggesting the presence of these features at some sites. Microbial mats have been reported on Beaufort Sea sediments, mostly surrounding slow gas seeps (Paull et al., 2011). The inherently patchy distribution of benthic seeps and microbial mats coupled with the varying conditions that foster anoxic sediments may explain the lack of definable substructure exhibited by assemblage D and weak correlations with environmental parameters in this study.

2.5.5 Broader Geographical Context

Benthic prokaryotic community substructure on the Beaufort Sea shelf and upper slope broadly reflected longitudinal gradients in OM quality and quantity, as well as the influence of bathymetry. While bathymetric effects were particularly apparent in distinguishing slope assemblage A, shallow shelf assemblage C, and generalist assemblage B, redox conditions likely played a role in differentiating assemblages C and D. These findings highlight the importance of assessing prokaryotic communities on a broad spatial scale, given that community structure reflected environmental variation occurring over scales of meters to kilometers. This raises the

question of how prokaryotic community structure in the Beaufort Sea compares to other regions within the Arctic and beyond.

At class-level, 60% of the top 10 taxa from Beaufort Sea sediments were shared with those from the global, deep-sea, and Norwegian Arctic sediment microbiomes (Figure 2.7). The classes Anaerolineae, Nitrososphaeria, and Verrucomicrobiae were abundant and unique to the Beaufort Sea surface sediment microbiome. The bacterial class Anaerolineae and archaeal class Nitrososphaeria are typified by the families Anaerolinaceae and Nitrosopumilaceae which, as mentioned above, primarily contain anaerobic bacteria associated with heavy OM loading as was prevalent in anoxic assemblage D, and ammonia-oxidizing archaea prevalent in slope assemblage A, respectively. Not surprisingly, Nitrososphaeria was not among the most abundant taxa in the global, deep-sea, or Norwegian Arctic sediment microbiomes. Though common in marine surface sediments and typically more abundant than ammonia oxidizing bacteria, archaea have been overlooked in previous studies solely focused on bacteria (Bienhold et al., 2016; Park et al., 2010; Zinger et al., 2011). Their relatively high abundance here highlights the under-appreciated role of archaea in marine surface sediments. If archaea are excluded, the bacterial taxon Thermoanaerobaculia joins the top 10 most abundant taxa in our study. This group encompasses the anaerobic, thermophilic organisms largely represented by subgroup 10 an indicator taxon for slope assemblage A. This class was not among the most abundant taxa in sediments globally, in the deep sea, or in the Norwegian Arctic. Thermoanaerobaculia together with Anaerolineae suggest comparatively shallower anoxic conditions in Beaufort Sea surface sediments, spanning both slope and shallow shelf locations.

Betaproteobacteria, Gemmatimonadetes, Bacilli, and Clostridia were among the 10 most abundant taxa from global benthic, deep-sea, and Norwegian-Arctic microbiomes, yet were not

prominent in Beaufort sediments. Betaproteobacteria, which were not present even at low abundances in Beaufort Sea sediments, were discovered to be potential laboratory contaminants in other studies (Grahm et al., 2003; Kulakov et al., 2002; Laurence et al., 2014; Salter et al., 2014). On a global scale Zinger et al. (2011) observed Bacilli and Clostridia in higher abundances in coastal sediments vs. open water or deep-sea sediments. Bacilli and Clostridia can be indicators of urban fecal contamination in coastal watersheds, lagoons, and nearshore seawater (Dai et al., 2018; Dubinsky et al., 2012; Wu et al., 2010). As the Beaufort Sea is extremely remote from urban life, it is not surprising that these taxa were less prevalent. Clostridia was included in the Norwegian-Arctic microbiome and Bacilli in the deep-sea microbiome, which are also presumably more pristine than typical coastal areas, suggesting that there are bacteria in these classes which are not necessarily correlated with urban waste (Bienhold et al., 2016).

The prokaryotic community structure in the Beaufort Sea differed somewhat from the Norwegian-Arctic, even at the relatively coarse taxonomic level of class, suggesting benthic microbes may reflect regional differences in hydrography, biogeochemistry, and bathymetry of Arctic shelf systems (Carmack and Wassmann, 2006). However, samples from the Norwegian-Arctic were largely collected at depths > 1,000 m, so these regional differences need to be further explored particularly across wider depth ranges.

2.5.6 Synthesis

The occurrence of strictly anaerobic taxa in all assemblages identified here indicates that Beaufort Sea surface sediments exhibit widespread anoxia within the 0–1 cm depth horizon, consistent with oxygen penetration studies conducted in other Arctic sediments (Jørgensen et al., 2005; Kostka et al., 1999). A larger proportion of anaerobic taxa occurred in shallow shelf (C)

and anoxic (D) assemblages, indicating that, in general, oxygen depletion in nearshore sediments is comparatively more widespread than offshore, particularly in areas where organic matter loading and Chl-*a* were higher and porosity lower. Although this is a common trend when comparing shelf to slope sediments, it may be of particular importance in the Beaufort Sea when viewed through the lens of climate change (Orcutt et al., 2011). An overall net increase of river runoff and terrestrial organic matter has already been established for the Mackenzie River, and is predicted to continue over the coming years (Doxaran et al., 2015; Holmes et al., 2012). Thus, we might expect an increase in abundance of anaerobic taxa in shallow shelf assemblage C, with potentially more stations resembling or overlapping with anoxic assemblage D. There may also be increased taxonomic overlap between microbial communities associated with the Mackenzie River outflow and shallow shelf assemblage C. In addition to riverine input, shifts in primary production and sea-ice extent will likely be most apparent in the shallow shelf sediments, as the majority of indicator taxa in assemblage C have been strongly correlated to both phytoplankton blooms and sea-ice microbial communities.

An increase in OM input, whether terrestrial or marine derived, will likely translate to an increase in OM burial and subsequent methanogenesis in the already methane-permeated Beaufort Sea sediments (Coffin et al., 2013). Characterizing the microbes involved in both methane production/degradation and associated processes in these sediments is thus of particular interest. The high relative abundance of potential methanotrophs exhibited in this study could, in addition to highlighting the presence of methane throughout sediments in the region, indicate an important constraint on methane efflux that requires further investigation.

This study also highlights the vast array of uncultured and unclassified microbes in Arctic marine sediments, particularly exemplified by slope assemblage A, which was the most

divergent and diverse and contained the highest number of uncultured taxa across all assemblages. Anoxic assemblage D also exhibited a comparatively high abundance of uncultured microbes with representatives which are more rarely studied in the context of the marine system. The lack of knowledge regarding these taxa points to a need for more experimental and culture-based studies to elucidate their role in biogeochemical processes, that would provide insights into the links between microbial community structure and benthic ecosystem function. Although taxonomic classification does not directly equate to function, known microbes from slope assemblage A highlight how taxonomic composition may provide a framework for future studies. For instance, research investigating the role of nitrification and anammox in the Beaufort Sea would be most beneficial in slope sediments where microbes involved in aerobic/anaerobic ammonia oxidation and nitrite oxidation were abundant, and could reveal useful information about regional nitrogen cycling and upwelling dynamics. Additionally, microbial taxonomy can provide insights into environmental conditions that are not typically measured with surveys of larger benthic epi- and infaunal organisms, such as sediment oxygen penetration and the presence of biofilms, microbial mats, and/or seeps seemingly reflected by the taxonomic composition of anoxic assemblage D. Overall, these insights provided by prokaryotic community structure emphasize the value of incorporating microbial surveys more broadly into field sampling programs in the North American Arctic and elsewhere. This study establishes a baseline for Beaufort Sea benthic microbes, however without long-term datasets we cannot assess how these communities will respond to and reflect shifts related to climate change or other disturbances such as energy resource exploration.

2.6 ACKNOWLEDGMENTS

Samples for this project were collected opportunistically through field work funded by BOEM and Department of Fisheries and Oceans Canada. Sincerest gratitude goes out to Dr. Holly Bik for providing the bioinformatics and genomics foundation needed for this project to happen.

Appreciation also goes to Dr. Eric Collins for ongoing bioinformatic and statistical assistance. A huge thank you to Shannon MacPhee for coordinating and collaborating with us, without you we would not have had such an expansive dataset from the Canadian Beaufort Sea. The majority of environmental variables incorporated in this study were provided through the hard work of Julia Dissen.

2.7 REFERENCES

- ACIA, 2005. Arctic Climate Impact Assessment. ACIA overview report, Cambridge University Press.
- Al-Thani, R., Al-Najjar, M.A.A., Al-Raei, A.M., Ferdelman, T., Thang, N.M., Shaikh, I. Al, Al-Ansi, M., de Beer, D., 2014. Community Structure and Activity of a Highly Dynamic and Nutrient-Limited Hypersaline Microbial Mat in Um Alhool Sabkha, Qatar. *PLoS One* 9, e92405. <https://doi.org/10.1371/journal.pone.0092405>
- Alonso-Sáez, L., Waller, A.S., Mende, D.R., Bakker, K., Farnelid, H., Yager, P.L., Lovejoy, C., Tremblay, J.É., Potvin, M., Heinrich, F., Estrada, M., Riemann, L., Bork, P., Pedrós-Alió, C., Bertilsson, S., 2012. Role for urea in nitrification by polar marine Archaea. *Proc. Natl. Acad. Sci. U. S. A.* 109, 17989–17994. <https://doi.org/10.1073/pnas.1201914109>
- Anantharaman, K., Hausmann, B., Jungbluth, S.P., Kantor, R.S., Lavy, A., Warren, L.A., Rappé, M.S., Pester, M., Loy, A., Thomas, B.C., Banfield, J.F., 2018. Expanded diversity of microbial groups that shape the dissimilatory sulfur cycle. *ISME J.* 12, 1715–1728. <https://doi.org/10.1038/s41396-018-0078-0>
- Apprill, A., McNally, S., Parsons, R., Weber, L., 2015. Minor revision to V4 region SSU rRNA 806R gene primer greatly increases detection of SAR11 bacterioplankton. *Aquat. Microb. Ecol.* 75, 129–137. <https://doi.org/10.3354/ame01753>
- Arar, E.J., Collins, G.B., 1997. Method 445.0: In vitro determination of chlorophyll a and pheophytin a in marine and freshwater algae by fluorescence. Ohio: United States Environmental Protection Agency, Office of Research and Development, National Exposure Research Laboratory.
- Arnosti, C., 2008. Functional differences between Arctic seawater and sedimentary microbial

- communities: contrasts in microbial hydrolysis of complex substrates. *FEMS Microbiol. Ecol.* 66, 343–351. <https://doi.org/10.1111/j.1574-6941.2008.00587.x>
- Bell, L.E., Bluhm, B.A., Iken, K., 2016. Influence of terrestrial organic matter in marine food webs of the Beaufort Sea shelf and slope. *Mar. Ecol. Prog. Ser.* 550, 1–24. <https://doi.org/10.3354/meps11725>
- Bennett, R.H., Lambert, D.N., 1971. Rapid and reliable technique for determining unit weight and porosity of deep-sea sediments. *Mar. Geol.* 11, 201–207. [https://doi.org/10.1016/0025-3227\(71\)90007-7](https://doi.org/10.1016/0025-3227(71)90007-7)
- Biddle, J.F., Lipp, J.S., Lever, M.A., Lloyd, K.G., Sørensen, K.B., Anderson, R., Fredricks, H.F., Elvert, M., Kelly, T.J., Schrag, D.P., Sogin, M.L., Brenchley, J.E., Teske, A., House, C.H., Hinrichs, K.U., 2006. Heterotrophic Archaea dominate sedimentary subsurface ecosystems off Peru. *Proc. Natl. Acad. Sci. U. S. A.* 103, 3846–3851. <https://doi.org/10.1073/pnas.0600035103>
- Bienhold, C., Boetius, A., Ramette, A., 2012. The energy–diversity relationship of complex bacterial communities in Arctic deep-sea sediments. *ISME J.* 6, 724–732. <https://doi.org/10.1038/ismej.2011.140>
- Bienhold, C., Zinger, L., Boetius, A., Ramette, A., 2016. Diversity and Biogeography of Bathyal and Abyssal Seafloor Bacteria. *PLoS One* 11, e0148016. <https://doi.org/10.1371/journal.pone.0148016>
- Bier, R.L., Bernhardt, E.S., Boot, C.M., Graham, E.B., Hall, E.K., Lennon, J.T., Nemergut, D., Osborne, B.B., Ruiz-González, C., Schimel, J.P., Waldrop, M.P., Wallenstein, M.D., 2015. Linking microbial community structure and microbial processes: an empirical and conceptual overview. *FEMS Microbiol. Ecol.* fiv113. <https://doi.org/10.1093/femsec/fiv113>

- Billerebeck, S., Orchard, J., Tindall, B.J., Giebel, H.-A., Brinkhoff, T., Simon, M., 2015. Description of *Octadecabacter Temperatus* Sp. Nov., Isolated From the Southern North Sea, Emended Descriptions of the Genus *Octadecabacter* and Its Species and Reclassification of *Octadecabacter jejudonensis* Park and Yoon 2014 as *Pseudooctadecabacter Jejudon*. *Int. J. Syst. Evol. Microbiol.* 65, 1967–1974. <https://doi.org/10.1099/ijjs.0.000205>
- BOEM, n.d. Leasing and Plans | BOEM [WWW Document]. URL <https://www.boem.gov/Alaska-Leasing-and-Plans/> (accessed 1.14.19).
- Boetius, A., Ravenschlag, K., Schubert, C.J., Rickert, D., Widdel, F., Gleseke, A., Amann, R., Jørgensen, B.B., Witte, U., Pfannkuche, O., 2000. A marine microbial consortium apparently mediating anaerobic oxidation methane. *Nature* 407, 623–626. <https://doi.org/10.1038/35036572>
- Boeuf, D., Cottrell, M.T., Kirchman, D.L., Lebaron, P., Jeanthon, C., 2013. Summer community structure of aerobic anoxygenic phototrophic bacteria in the western Arctic Ocean. *FEMS Microbiol. Ecol.* 85, 417–432. <https://doi.org/10.1111/1574-6941.12130>
- Bowman, J.P., McCuaig, R.D., 2003. Biodiversity, Community Structural Shifts, and Biogeography of Prokaryotes within Antarctic Continental Shelf Sediment. *Appl. Environ. Microbiol.* 69, 2463–2483. <https://doi.org/10.1128/AEM.69.5.2463-2483.2003>
- Bowman, J.S., Rasmussen, S., Blom, N., Deming, J.W., Rysgaard, S., Sicheritz-Ponten, T., 2012. Microbial community structure of Arctic multiyear sea ice and surface seawater by 454 sequencing of the 16S RNA gene. *ISME J.* 6, 11–20. <https://doi.org/10.1038/ismej.2011.76>
- Braeckman, U., Janssen, F., Lavik, G., Elvert, M., Marchant, H., Buckner, C., Bienhold, C., Wenzhöfer, F., 2018. Carbon and nitrogen turnover in the Arctic deep sea: in situ benthic community response to diatom and coccolithophorid phytodetritus. *Biogeosciences* 15,

6537–6557. <https://doi.org/10.5194/bg-15-6537-2018>

Brinkmeyer, R., Knittel, K., Jürgens, J., Weyland, H., Amann, R., Helmke, E., 2003. Diversity and Structure of Bacterial Communities in Arctic versus Antarctic Pack Ice. *Appl. Environ. Microbiol.* 69, 6610–6619. <https://doi.org/10.1128/AEM.69.11.6610-6619.2003>

Brothers, L.L., Herman, B.M., Hart, P.E., Ruppel, C.D., 2016. Subsea ice-bearing permafrost on the U.S. Beaufort Margin: 1. Minimum seaward extent defined from multichannel seismic reflection data. *Geochemistry, Geophys. Geosystems* 17, 4354–4365. <https://doi.org/10.1002/2016GC006584>

Buongiorno, J., Herbert, L.C., Wehrmann, L.M., Michaud, A.B., Laufer, K., Røy, H., Jørgensen, B.B., Szykiewicz, A., Faiia, A., Yeager, K.M., Schindler, K., Lloyd, K.G., 2019. Complex Microbial Communities Drive Iron and Sulfur Cycling in Arctic Fjord Sediments. *Appl. Environ. Microbiol.* 85, e00949-19. <https://doi.org/10.1128/AEM.00949-19>

Burgin, A.J., Hamilton, S.K., 2007. Have we overemphasized the role of denitrification in aquatic ecosystems? A review of nitrate removal pathways. *Front. Ecol. Environ.* [https://doi.org/10.1890/1540-9295\(2007\)5\[89:HWOTRO\]2.0.CO;2](https://doi.org/10.1890/1540-9295(2007)5[89:HWOTRO]2.0.CO;2)

Buttigieg, P.L., Ramette, A., 2015. Biogeographic patterns of bacterial microdiversity in Arctic deep-sea sediments (HAUSGARTEN, Fram Strait). *Front. Microbiol.* 5, 1–12. <https://doi.org/10.3389/fmicb.2014.00660>

Caporaso, J.G., Lauber, C.L., Walters, W. a, Berg-Lyons, D., Huntley, J., Fierer, N., Owens, S.M., Betley, J., Fraser, L., Bauer, M., Gormley, N., Gilbert, J. a, Smith, G., Knight, R., 2012. Ultra-high-throughput microbial community analysis on the Illumina HiSeq and MiSeq platforms. *ISME J.* 6, 1621–1624. <https://doi.org/10.1038/ismej.2012.8>

Caporaso, J.G., Lauber, C.L., Walters, W.A., Berg-Lyons, D., Lozupone, C.A., Turnbaugh, P.J.,

- Fierer, N., Knight, R., 2011. Global patterns of 16S rRNA diversity at a depth of millions of sequences per sample. *Proc. Natl. Acad. Sci.* 108, 4516–4522.
<https://doi.org/10.1073/pnas.1000080107>
- Cardoso, D.C., Cretoiu, M.S., Stal, L.J., Bolhuis, H., 2019. Seasonal development of a coastal microbial mat. *Sci. Rep.* 9. <https://doi.org/10.1038/s41598-019-45490-8>
- Carmack, E., Wassmann, P., 2006. Food webs and physical–biological coupling on pan-Arctic shelves: Unifying concepts and comprehensive perspectives. *Prog. Oceanogr.* 71, 446–477.
<https://doi.org/10.1016/j.pocean.2006.10.004>
- Carmack, E.C., Macdonald, R.W., 2002. Oceanography of the Canadian Shelf of the Beaufort Sea: A Setting for Marine Life. *ARCTIC* 55, 29–45. <https://doi.org/10.14430/arctic733>
- Casciotti, K.L., Buchwald, C., 2012. Insights on the marine microbial nitrogen cycle from isotopic approaches to nitrification. *Front. Microbiol.* 3, 356.
<https://doi.org/10.3389/fmicb.2012.00356>
- Cock, P.J.A., Antao, T., Chang, J.T., Chapman, B.A., Cox, C.J., Dalke, A., Friedberg, I., Hamelryck, T., Kauff, F., Wilczynski, B., de Hoon, M.J.L., 2009. Biopython: freely available Python tools for computational molecular biology and bioinformatics. *Bioinformatics* 25, 1422–1423. <https://doi.org/10.1093/bioinformatics/btp163>
- Coelho, F.J.R.C., Louvado, A., Domingues, P.M., Cleary, D.F.R., Ferreira, M., Almeida, A., Cunha, M.R., Cunha, Â., Gomes, N.C.M., 2016. Integrated analysis of bacterial and microeukaryotic communities from differentially active mud volcanoes in the Gulf of Cadiz. *Sci. Rep.* 6, 35272. <https://doi.org/10.1038/srep35272>
- Coffin, R., Smith, J., Yoza, B., Boyd, T., Montgomery, M., 2017. Spatial Variation in Sediment Organic Carbon Distribution across the Alaskan Beaufort Sea Shelf. *Energies* 10, 1265.

<https://doi.org/10.3390/en10091265>

- Coffin, R.B., Smith, J.P., Plummer, R.E., Yoza, B., Larsen, R.K., Millholland, L.C., Montgomery, M.T., 2013. Spatial variation in shallow sediment methane sources and cycling on the Alaskan Beaufort Sea Shelf/Slope. *Mar. Pet. Geol.* 45, 186–197.
<https://doi.org/10.1016/j.marpetgeo.2013.05.002>
- Colatriano, D., Tran, P.Q., Guéguen, C., Williams, W.J., Lovejoy, C., Walsh, D.A., 2018. Genomic evidence for the degradation of terrestrial organic matter by pelagic Arctic Ocean Chloroflexi bacteria. *Commun. Biol.* 1. <https://doi.org/10.1038/s42003-018-0086-7>
- Dabert, P., Sialve, B., Delgenès, J.-P., Moletta, R., Godon, J.-J., 2001. Characterisation of the microbial 16S rDNA diversity of an aerobic phosphorus-removal ecosystem and monitoring of its transition to nitrate respiration. *Appl. Microbiol. Biotechnol.* 55, 500–509.
<https://doi.org/10.1007/s002530000529>
- Dai, T., Zhang, Y., Ning, D., Su, Z., Tang, Y., Huang, B., Mu, Q., Wen, D., 2018. Dynamics of Sediment Microbial Functional Capacity and Community Interaction Networks in an Urbanized Coastal Estuary. *Front. Microbiol.* 9. <https://doi.org/10.3389/fmicb.2018.02731>
- Daims, H., 2014. The Family Nitrospiraceae, in: *The Prokaryotes*. Springer Berlin Heidelberg, Berlin, Heidelberg, pp. 733–749. https://doi.org/10.1007/978-3-642-38954-2_126
- Daims, H., Lebedeva, E. V., Pjevac, P., Han, P., Herbold, C., Albertsen, M., Jehmlich, N., Palatinszky, M., Vierheilig, J., Bulaev, A., Kirkegaard, R.H., von Bergen, M., Rattei, T., Bendinger, B., Nielsen, P.H., Wagner, M., 2015. Complete nitrification by Nitrospira bacteria. *Nature* 528, 504–509. <https://doi.org/10.1038/nature16461>
- Damashek, J., Pettie, K.P.K., Brown, Z.W.Z., Mills, M.M.M., Arrigo, K.R.K., Francis, C.A.C., 2017. Regional patterns in ammonia-oxidizing communities throughout Chukchi Sea waters

- from the Bering Strait to the Beaufort Sea. *Aquat. Microb. Ecol.* 79, 273–286.
<https://doi.org/10.3354/ame01834>
- De Cáceres, M., Legendre, P., 2009. Associations between species and groups of sites: indices and statistical inference. *Ecology* 90, 3566–3574. <https://doi.org/10.1890/08-1823.1>
- De Cáceres, M., Legendre, P., Moretti, M., 2010. Improving indicator species analysis by combining groups of sites. *Oikos* 119, 1674–1684. <https://doi.org/10.1111/j.1600-0706.2010.18334.x>
- Dedysh, S.N., Yilmaz, P., 2018. Refining the taxonomic structure of the phylum Acidobacteria. *Int. J. Syst. Evol. Microbiol.* 68, 3796–3806. <https://doi.org/10.1099/ijsem.0.003062>
- Deming, J.W., Baross, J.A., 1993. The Early Diagenesis of Organic Matter: Bacterial Activity, in: *Organic Geochemistry*. Springer, pp. 119–144. https://doi.org/10.1007/978-1-4615-2890-6_5
- Dogs, M., Wemheuer, B., Wolter, L., Bergen, N., Daniel, R., Simon, M., Brinkhoff, T., 2017. Rhodobacteraceae on the marine brown alga *Fucus spiralis* are abundant and show physiological adaptation to an epiphytic lifestyle. *Syst. Appl. Microbiol.* 40, 370–382.
<https://doi.org/10.1016/j.syapm.2017.05.006>
- Doxaran, D., Devred, E., Babin, M., 2015. A 50% increase in the amount of terrestrial particles delivered by the Mackenzie River into the Beaufort Sea (Canadian Arctic Ocean) over the last 10 years. *Biogeosciences Discuss.* 12, 305–344. <https://doi.org/10.5194/bgd-12-305-2015>
- Dubinsky, E.A., Esmaili, L., Hulls, J.R., Cao, Y., Griffith, J.F., Andersen, G.L., 2012. Application of Phylogenetic Microarray Analysis to Discriminate Sources of Fecal Pollution. *Environ. Sci. Technol.* 46, 4340–4347. <https://doi.org/10.1021/es2040366>

- Dunton, K.H., Weingartner, T., Carmack, E.C., 2006. The nearshore western Beaufort Sea ecosystem: Circulation and importance of terrestrial carbon in arctic coastal food webs. *Prog. Oceanogr.* 71, 362–378. <https://doi.org/10.1016/j.pocean.2006.09.011>
- Durbin, A.M., Teske, A., 2011. Microbial diversity and stratification of South Pacific abyssal marine sediments. *Environ. Microbiol.* 13, 3219–3234. <https://doi.org/10.1111/j.1462-2920.2011.02544.x>
- Dyksma, S., Lenk, S., Sawicka, J.E., Mußmann, M., 2018. Uncultured Gammaproteobacteria and Desulfobacteraceae Account for Major Acetate Assimilation in a Coastal Marine Sediment. *Front. Microbiol.* 9, 3124. <https://doi.org/10.3389/fmicb.2018.03124>
- Edgar, R.C., 2018. Updating the 97% identity threshold for 16S ribosomal RNA OTUs. *Bioinformatics* 34, 2371–2375. <https://doi.org/10.1093/bioinformatics/bty113>
- Eert, J., Meisterhans, G., Michel, C., Niemi, A., Reist, J., Williams, W.J., Dempsey, M., 2012. Physical, chemical and biological oceanographic data from the Beaufort Regional Environmental Assessment: Marine Fishes Project , August- September 2012, Can Data Rep Hydrogr Ocean Sci.
- Evans, P.N., Parks, D.H., Chadwick, G.L., Robbins, S.J., Orphan, V.J., Golding, S.D., Tyson, G.W., 2015. Methane metabolism in the archaeal phylum Bathyarchaeota revealed by genome-centric metagenomics. *Science* (80-.). 350, 434–438. <https://doi.org/10.1126/science.aac7745>
- Forest, A., Bélanger, S., Sampei, M., Sasaki, H., Lalande, C., Fortier, L., 2010. Three-year assessment of particulate organic carbon fluxes in Amundsen Gulf (Beaufort Sea): Satellite observations and sediment trap measurements. *Deep. Res. Part I Oceanogr. Res. Pap.* 57, 125–142. <https://doi.org/10.1016/j.dsr.2009.10.002>

- Fry, J.C., Webster, G., Cragg, B.A., Weightman, A.J., Parkes, R.J., 2006. Analysis of DGGE profiles to explore the relationship between prokaryotic community composition and biogeochemical processes in deep seafloor sediments from the Peru Margin. *FEMS Microbiol. Ecol.* 58, 86–98. <https://doi.org/10.1111/j.1574-6941.2006.00144.x>
- Fuhrman, J.A., 2009. Microbial community structure and its functional implications. *Nature* 459, 193–9. <https://doi.org/10.1038/nature08058>
- Fuhrman, J.A., Cram, J.A., Needham, D.M., 2015. Marine microbial community dynamics and their ecological interpretation. *Nat. Rev. Microbiol.* 13, 133–146. <https://doi.org/10.1038/nrmicro3417>
- Fujii, T., Sugino, H., Rouse, J.D., Furukawa, K., 2002. Characterization of the microbial community in an anaerobic ammonium-oxidizing biofilm cultured on a nonwoven biomass carrier. *J. Biosci. Bioeng.* 94, 412–418. [https://doi.org/10.1016/S1389-1723\(02\)80218-3](https://doi.org/10.1016/S1389-1723(02)80218-3)
- Galand, P.E., Potvin, M., Casamayor, E.O., Lovejoy, C., 2010. Hydrography shapes bacterial biogeography of the deep Arctic Ocean. *ISME J.* 4, 564–576. <https://doi.org/10.1038/ismej.2009.134>
- Gamboa, A., Montero-Serrano, J.-C., St-Onge, G., Rochon, A., Desjage, P.-A., 2017. Mineralogical, geochemical, and magnetic signatures of surface sediments from the Canadian Beaufort Shelf and Amundsen Gulf (Canadian Arctic). *Geochemistry, Geophys. Geosystems* 18, 488–512. <https://doi.org/10.1002/2016GC006477>
- Garrity, G.M., Bell, J.A., Lilburn, T., 2015. Thiotrichaceae fam. nov., in: *Bergey's Manual of Systematics of Archaea and Bacteria*. John Wiley & Sons, Ltd, Chichester, UK, pp. 1–1. <https://doi.org/10.1002/9781118960608.fbm00236>
- Glöckner, F.O., Yilmaz, P., Quast, C., Gerken, J., Beccati, A., Ciuprina, A., Bruns, G., Yarza, P.,

- Peplies, J., Westram, R., Ludwig, W., 2017. 25 years of serving the community with ribosomal RNA gene reference databases and tools. *J. Biotechnol.* 261, 169–176.
<https://doi.org/10.1016/j.jbiotec.2017.06.1198>
- Goñi, M. a., O'Connor, A.E., Kuzyk, Z.Z., Yunker, M.B., Gobeil, C., Macdonald, R.W., 2013. Distribution and sources of organic matter in surface marine sediments across the North American Arctic margin. *J. Geophys. Res. Ocean.* 118, 4017–4035.
<https://doi.org/10.1002/jgrc.20286>
- González, J.M., Fernández-Gómez, B., Fernández-Guerra, A., Gómez-Consarnau, L., Sánchez, O., Coll-Lladó, M., del Campo, J., Escudero, L., Rodríguez-Martínez, R., Alonso-Sáez, L., Latasa, M., Paulsen, I., Nedashkovskaya, O., Lekunberri, I., Pinhassi, J., Pedrós-Alió, C., 2008. Genome analysis of the proteorhodopsin-containing marine bacterium *Polaribacter* sp. MED152 (Flavobacteria). *Proc. Natl. Acad. Sci.* 105, 8724–8729.
<https://doi.org/10.1073/pnas.0712027105>
- Gosink, J.J., Herwig, R.P., Staley, J.T., 1997. *Octadecabacter arcticus* gen. nov., sp. nov., and *O. antarcticus*, sp. nov., Nonpigmented, Psychrophilic Gas Vacuolate Bacteria from Polar Sea Ice and Water. *Syst. Appl. Microbiol.* 20, 356–365. [https://doi.org/10.1016/S0723-2020\(97\)80003-3](https://doi.org/10.1016/S0723-2020(97)80003-3)
- Gosink, J.J., Woese, C.R., Staley, J.T., 1998. *Polaribacter* gen. nov., with three new species, *P. irgensii* sp. nov., *P. franzmannii* sp. nov. and *P. filamentus* sp. nov., gas vacuolate polar marine bacteria of the Cytophaga-Flavobacterium-Bacteroides group and reclassification of *Flectobacillus glomera*. *Int. J. Syst. Bacteriol.* 48, 223–235.
<https://doi.org/10.1099/00207713-48-1-223>
- Grahn, N., Olofsson, M., Ellnebo-Svedlund, K., Monstein, H.-J., Jonasson, J., 2003.

- Identification of mixed bacterial DNA contamination in broad-range PCR amplification of 16S rDNA V1 and V3 variable regions by pyrosequencing of cloned amplicons. *FEMS Microbiol. Lett.* 219, 87–91. [https://doi.org/10.1016/S0378-1097\(02\)01190-4](https://doi.org/10.1016/S0378-1097(02)01190-4)
- Grebmeier, J.M., 2012. Shifting Patterns of Life in the Pacific Arctic and Sub-Arctic Seas. *Ann. Rev. Mar. Sci.* 4, 63–78. <https://doi.org/10.1146/annurev-marine-120710-100926>
- Grossart, H.-P., Levold, F., Allgaier, M., Simon, M., Brinkhoff, T., 2005. Marine diatom species harbour distinct bacterial communities. *Environ. Microbiol.* 7, 860–873. <https://doi.org/10.1111/j.1462-2920.2005.00759.x>
- Hamdan, L.J., Coffin, R.B., Sikaroodi, M., Greinert, J., Treude, T., Gillevet, P.M., 2013. Ocean currents shape the microbiome of Arctic marine sediments. *ISME J.* 7, 685–96. <https://doi.org/10.1038/ismej.2012.143>
- Han, Y., Perner, M., 2015. The globally widespread genus *Sulfurimonas*: versatile energy metabolisms and adaptations to redox clines. *Front. Microbiol.* 6, 989. <https://doi.org/10.3389/fmicb.2015.00989>
- Head, I.M., Jones, D.M., Røling, W.F.M., 2006. Marine microorganisms make a meal of oil. *Nat. Rev. Microbiol.* 4, 173–182. <https://doi.org/10.1038/nrmicro1348>
- Helbert, W., 2017. Marine Polysaccharide Sulfatases. *Front. Mar. Sci.* 4, 6. <https://doi.org/10.3389/fmars.2017.00006>
- Hoffmann, K., Hassenrück, C., Salman-Carvalho, V., Holtappels, M., Bienhold, C., 2017. Response of Bacterial Communities to Different Detritus Compositions in Arctic Deep-Sea Sediments. *Front. Microbiol.* 8, 1–18. <https://doi.org/10.3389/fmicb.2017.00266>
- Holmes, R.M., Coe, M.T., Fiske, G.J., Gurtovaya, T., McClelland, J.W., Shiklomanov, A.I., Spencer, R.G.M., Tank, S.E., Zhulidov, A. V., 2012. Climate Change Impacts on the

Hydrology and Biogeochemistry of Arctic Rivers, in: Climatic Change and Global Warming of Inland Waters. John Wiley & Sons, Ltd, Chichester, UK, pp. 1–26.

<https://doi.org/10.1002/9781118470596.ch1>

Holmes, R.M., McClelland, J.W., Peterson, B.J., Shiklomanov, I.A., Shiklomanov, A.I.,

Zhulidov, A. V., Gordeev, V. V., Bobrovitskaya, N.N., 2002. A circumpolar perspective on fluvial sediment flux to the Arctic ocean. *Global Biogeochem. Cycles* 16, 45-1-45–14.

<https://doi.org/10.1029/2001GB001849>

Hubert, C., Arnosti, C., Brüchert, V., Loy, A., Vandieken, V., Jørgensen, B.B., 2010.

Thermophilic anaerobes in Arctic marine sediments induced to mineralize complex organic matter at high temperature. *Environ. Microbiol.* 12, 1089–1104.

<https://doi.org/10.1111/j.1462-2920.2010.02161.x>

Inagaki, F., 2003. *Sulfurimonas autotrophica* gen. nov., sp. nov., a novel sulfur-oxidizing -

proteobacterium isolated from hydrothermal sediments in the Mid-Okinawa Trough. *Int. J.*

Syst. Evol. Microbiol. 53, 1801–1805. <https://doi.org/10.1099/ijs.0.02682-0>

Inagaki, F., Suzuki, M., Takai, K., Oida, H., Sakamoto, T., Aoki, K., Nealson, K.H., Horikoshi,

K., 2003. Microbial Communities Associated with Geological Horizons in Coastal

Subseafloor Sediments from the Sea of Okhotsk. *Appl. Environ. Microbiol.* 69, 7224–7235.

<https://doi.org/10.1128/AEM.69.12.7224-7235.2003>

Jacob, M., Soltwedel, T., Boetius, A., Ramette, A., 2013. Biogeography of Deep-Sea Benthic

Bacteria at Regional Scale (LTER HAUSGARTEN, Fram Strait, Arctic). *PLoS One* 8,

e72779. <https://doi.org/10.1371/journal.pone.0072779>

Jørgensen, B., Glud, R., Holby, O., 2005. Oxygen distribution and bioirrigation in Arctic fjord

sediments (Svalbard, Barents Sea). *Mar. Ecol. Prog. Ser.* 292, 85–95.

<https://doi.org/10.3354/meps292085>

Jørgensen, B.B., Findlay, A.J., Pellerin, A., 2019. The Biogeochemical Sulfur Cycle of Marine Sediments. *Front. Microbiol.* 10, 849. <https://doi.org/10.3389/fmicb.2019.00849>

Jørgensen, S.L., Hannisdal, B., Lanzén, A., Baumberger, T., Flesland, K., Fonseca, R., Øvreås, L., Steen, I.H., Thorseth, I.H., Pedersen, R.B., Schleper, C., 2012. Correlating microbial community profiles with geochemical data in highly stratified sediments from the Arctic Mid-Ocean Ridge. *Proc. Natl. Acad. Sci.* 109, 16764–16765.

<https://doi.org/10.1073/pnas.1207574109>

Junge, K., Imhoff, F., Staley, T., Deming, W., 2002. Phylogenetic Diversity of Numerically Important Arctic Sea-Ice Bacteria Cultured at Subzero Temperature. *Microb. Ecol.* 43, 315–328. <https://doi.org/10.1007/s00248-001-1026-4>

Kędra, M., Moritz, C., Choy, E.S., David, C., Degen, R., Duerksen, S., Ellingsen, I., Górska, B., Grebmeier, J.M., Kirievskaya, D., van Oevelen, D., Piwosz, K., Samuelsen, A., Węśławski, J.M., 2015. Status and trends in the structure of Arctic benthic food webs. *Polar Res.* 34, 23775. <https://doi.org/10.3402/polar.v34.23775>

Kirchman, D.L., Hanson, T.E., Cottrell, M.T., Hamdan, L.J., 2014. Metagenomic analysis of organic matter degradation in methane-rich Arctic Ocean sediments. *Limnol. Oceanogr.* 59, 548–559. <https://doi.org/10.4319/lo.2014.59.2.0548>

Kleindienst, S., Herbst, F.A., Stagars, M., Von Netzer, F., Von Bergen, M., Seifert, J., Peplies, J., Amann, R., Musat, F., Lueders, T., Knittel, K., 2014. Diverse sulfate-reducing bacteria of the *Desulfosarcina/Desulfococcus* clade are the key alkane degraders at marine seeps. *ISME J.* 8, 2029–2044. <https://doi.org/10.1038/ismej.2014.51>

Kleindienst, S., Ramette, A., Amann, R., Knittel, K., 2012. Distribution and in situ abundance of

- sulfate-reducing bacteria in diverse marine hydrocarbon seep sediments. *Environ. Microbiol.* 14, 2689–2710. <https://doi.org/10.1111/j.1462-2920.2012.02832.x>
- Koedooder, C., Stock, W., Willems, A., Mangelinckx, S., De Troch, M., Vyverman, W., Sabbe, K., 2019. Diatom-bacteria interactions modulate the composition and productivity of benthic diatom biofilms. *Front. Microbiol.* 10, 1255. <https://doi.org/10.3389/fmicb.2019.01255>
- Könneke, M., Schubert, D.M., Brown, P.C., Hügler, M., Standfest, S., Schwander, T., Schada von Borzyskowski, L., Erb, T.J., Stahl, D.A., Berg, I.A., 2014. Ammonia-oxidizing archaea use the most energy-efficient aerobic pathway for CO₂ fixation. *Proc. Natl. Acad. Sci. U. S. A.* 111, 8239–44. <https://doi.org/10.1073/pnas.1402028111>
- Kortsch, S., Primicerio, R., Fossheim, M., Dolgov, A. V., Aschan, M., 2015. Climate change alters the structure of arctic marine food webs due to poleward shifts of boreal generalists. *Proc. R. Soc. B Biol. Sci.* 282. <https://doi.org/10.1098/rspb.2015.1546>
- Kostka, J., Thamdrup, B., Glud, R., Canfield, D., 1999. Rates and pathways of carbon oxidation in permanently cold Arctic sediments. *Mar. Ecol. Prog. Ser.* 180, 7–21. <https://doi.org/10.3354/meps180007>
- Kostka, J.E., Prakash, O., Overholt, W.A., Green, S.J., Freyer, G., Canion, A., Delgado, J., Norton, N., Hazen, T.C., Huettel, M., 2011. Hydrocarbon-degrading bacteria and the bacterial community response in Gulf of Mexico beach sands impacted by the deepwater horizon oil spill. *Appl. Environ. Microbiol.* 77, 7962–7974. <https://doi.org/10.1128/AEM.05402-11>
- Kuever, J., 2014a. The Family Desulfobacteraceae, in: *The Prokaryotes*. Springer Berlin Heidelberg, Berlin, Heidelberg, pp. 45–73. https://doi.org/10.1007/978-3-642-39044-9_266

- Kuever, J., 2014b. The Family Desulfobulbaceae, in: The Prokaryotes. Springer Berlin Heidelberg, Berlin, Heidelberg, pp. 75–86. https://doi.org/10.1007/978-3-642-39044-9_267
- Kulakov, L.A., McAlister, M.B., Ogden, K.L., Larkin, M.J., O’Hanlon, J.F., 2002. Analysis of bacteria contaminating ultrapure water in industrial systems. *Appl. Environ. Microbiol.* 68, 1548–55. <https://doi.org/10.1128/aem.68.4.1548-1555.2002>
- Landry, Z., Swa, B.K., Herndl, G.J., Stepanauskas, R., Giovannoni, S.J., 2017. SAR202 genomes from the dark ocean predict pathways for the oxidation of recalcitrant dissolved organic matter. *MBio* 8. <https://doi.org/10.1128/mBio.00413-17>
- Lansard, B., Mucci, A., Miller, L.A., Macdonald, R.W., Gratton, Y., 2012. Seasonal variability of water mass distribution in the southeastern Beaufort Sea determined by total alkalinity and $\delta^{18}\text{O}$. *J. Geophys. Res. Ocean.* 117, n/a-n/a. <https://doi.org/10.1029/2011JC007299>
- Laurence, M., Hatzis, C., Brash, D.E., 2014. Common contaminants in next-generation sequencing that hinder discovery of low-abundance microbes. *PLoS One* 9, e97876. <https://doi.org/10.1371/journal.pone.0097876>
- Lee, D.H., Kim, J.H., Lee, Y.M., Stadnitskaia, A., Jin, Y.K., Niemann, H., Kim, Y.G., Shin, K.H., 2018. Biogeochemical evidence of anaerobic methane oxidation on active submarine mud volcanoes on the continental slope of the Canadian Beaufort Sea. *Biogeosciences* 15, 7419–7433. <https://doi.org/10.5194/bg-15-7419-2018>
- Lee, Y.M., Jung, Y.-J., Hong, S.G., Kim, J.H., Lee, H.K., 2014. Diversity and Physiological Characteristics of Culturable Bacteria from Marine Sediments of Ross Sea, Antarctica. *Korean J. Microbiol.* 50, 119–127. <https://doi.org/10.7845/kjm.2014.4014>
- Lefevre, C.T., Bazylinski, D.A., 2013. Ecology, Diversity, and Evolution of Magnetotactic Bacteria. *Microbiol. Mol. Biol. Rev.* 77, 497–526. <https://doi.org/10.1128/mubr.00021-13>

- Li, H., Yu, Y., Luo, W., Zeng, Y., Chen, B., 2009. Bacterial diversity in surface sediments from the Pacific Arctic Ocean. *Extremophiles* 13, 233–246. <https://doi.org/10.1007/s00792-009-0225-7>
- Li, H., Zhang, X.-Y., Liu, C., Lin, C.-Y., Xu, Z., Chen, X.-L., Zhou, B.-C., Shi, M., Zhang, Y.-Z., 2014. *Polaribacter huanghezhanensis* sp. nov., isolated from Arctic fjord sediment, and emended description of the genus *Polaribacter*. *Int. J. Syst. Evol. Microbiol.* 64, 973–978. <https://doi.org/10.1099/ijs.0.056788-0>
- Li, Y., Liu, Q., Li, C., Dong, Y., Zhang, W.W., Zhang, W.W., Xiao, T., 2015. Bacterial and archaeal community structures in the Arctic deep-sea sediment. *Acta Oceanol. Sin.* 34, 93–113. <https://doi.org/10.1007/s13131-015-0624-9>
- Liang, B., Wang, L.-Y.Y., Mbadinga, S.M., Liu, J.-F.F., Yang, S.-Z.Z., Gu, J.-D.D., Mu, B.-Z.Z., 2015. Anaerolineaceae and Methanosaeta turned to be the dominant microorganisms in alkanes-dependent methanogenic culture after long-term of incubation. *AMB Express* 5, 37. <https://doi.org/10.1186/s13568-015-0117-4>
- Lopez-Fernandez, M., Simone, D., Wu, X., Soler, L., Nilsson, E., Holmfeldt, K., Lantz, H., Bertilsson, S., Dopson, M., 2018. Metatranscriptomes Reveal That All Three Domains of Life Are Active but Are Dominated by Bacteria in the Fennoscandian Crystalline Granitic Continental Deep Biosphere. *MBio* 9. <https://doi.org/10.1128/mBio.01792-18>
- Lorenson, T.D., Griener, J., Coffin, R.B., 2016. Dissolved methane in the Beaufort Sea and the Arctic Ocean, 1992–2009; sources and atmospheric flux. *Limnol. Oceanogr.* 61, S300–S323. <https://doi.org/10.1002/lno.10457>
- Losey, N.A., Stevenson, B.S., Busse, H.-J., Damste, J.S.S., Rijpstra, W.I.C., Rudd, S., Lawson, P.A., 2013. *Thermoanaerobaculum aquaticum* gen. nov., sp. nov., the first cultivated

- member of Acidobacteria subdivision 23, isolated from a hot spring. *Int. J. Syst. Evol. Microbiol.* 63, 4149–4157. <https://doi.org/10.1099/ijs.0.051425-0>
- Macdonald, R.W., Solomon, S.M., Cranston, R.E., Welch, H.E., Yunker, M.B., Gobeil, C., 1998. A sediment and organic carbon budget for the Canadian beaufort shelf. *Mar. Geol.* 144, 255–273. [https://doi.org/10.1016/S0025-3227\(97\)00106-0](https://doi.org/10.1016/S0025-3227(97)00106-0)
- Magen, C., Chaillou, G., Crowe, S.A., Mucci, A., Sundby, B., Gao, A., Makabe, R., Sasaki, H., 2010. Origin and fate of particulate organic matter in the southern Beaufort Sea - Amundsen Gulf region, Canadian Arctic. *Estuar. Coast. Shelf Sci.* 86, 31–41. <https://doi.org/10.1016/j.ecss.2009.09.009>
- Martens-Habbena, W., Qin, W., Horak, R.E.A., Urakawa, H., Schauer, A.J., Moffett, J.W., Armbrust, E.V., Ingalls, A.E., Devol, A.H., Stahl, D.A., 2015. The production of nitric oxide by marine ammonia-oxidizing archaea and inhibition of archaeal ammonia oxidation by a nitric oxide scavenger. *Environ. Microbiol.* 17, 2261–2274. <https://doi.org/10.1111/1462-2920.12677>
- McBride, M.J., 2014. The Family Flavobacteriaceae, in: *The Prokaryotes*. Springer Berlin Heidelberg, Berlin, Heidelberg, pp. 643–676. https://doi.org/10.1007/978-3-642-38954-2_130
- McIlroy, S.J., Kirkegaard, R.H., Dueholm, M.S., Fernando, E., Karst, S.M., Albertsen, M., Nielsen, P.H., 2017. Culture-Independent Analyses Reveal Novel Anaerolineaceae as Abundant Primary Fermenters in Anaerobic Digesters Treating Waste Activated Sludge. *Front. Microbiol.* 8, 1134. <https://doi.org/10.3389/fmicb.2017.01134>
- McTigue, N.D., Gardner, W.S., Dunton, K.H., Hardison, A.K., 2016. Biotic and abiotic controls on co-occurring nitrogen cycling processes in shallow Arctic shelf sediments. *Nat.*

Commun. 7, 13145. <https://doi.org/10.1038/ncomms13145>

Miquel, J.C., Gasser, B., Martín, J., Marec, C., Babin, M., Fortier, L., Forest, A., 2015.

Downward particle flux and carbon export in the Beaufort Sea, Arctic Ocean; the role of zooplankton. *Biogeosciences* 12, 5103–5117. <https://doi.org/10.5194/bg-12-5103-2015>

Morris, E.K., Caruso, T., Buscot, F., Fischer, M., Hancock, C., Maier, T.S., Meiners, T., Müller, C., Obermaier, E., Prati, D., Socher, S.A., Sonnemann, I., Wäschke, N., Wubet, T., Wurst, S., Rillig, M.C., 2014. Choosing and using diversity indices: insights for ecological applications from the German Biodiversity Exploratories. *Ecol. Evol.* 4, 3514–24.

<https://doi.org/10.1002/ece3.1155>

Morris, R.M., Rappé, M.S., Urbach, E., Connon, S.A., Giovannoni, S.J., 2004. Prevalence of the Chloroflexi-related SAR202 bacterioplankton cluster throughout the mesopelagic zone and deep ocean. *Appl. Environ. Microbiol.* 70, 2836–2842.

<https://doi.org/10.1128/AEM.70.5.2836-2842.2004>

Müller, A.L., de Rezende, J.R., Hubert, C.R.J., Kjeldsen, K.U., Lagkouravdos, I., Berry, D., Jørgensen, B.B., Loy, A., 2014. Endospores of thermophilic bacteria as tracers of microbial dispersal by ocean currents. *ISME J.* 8, 1153–1165. <https://doi.org/10.1038/ismej.2013.225>

Müller, A.L., Pelikan, C., de Rezende, J.R., Wasmund, K., Putz, M., Glombitza, C., Kjeldsen, K.U., Jørgensen, B.B., Loy, A., 2018. Bacterial interactions during sequential degradation of cyanobacterial necromass in a sulfidic arctic marine sediment. *Environ. Microbiol.* 20, 2927–2940. <https://doi.org/10.1111/1462-2920.14297>

Naidu, A.S., Cooper, L.W., Finney, B.P., Macdonald, R.W., Alexander, C., Semiletov, I.P., 2000. Organic carbon isotope ratio ($\delta^{13}\text{C}$) of Arctic Amerasian Continental shelf sediments. *Int. J. Earth Sci.* 89, 522–532. <https://doi.org/10.1007/s005310000121>

- Nelson, R.J., Ashjian, C.J., Bluhm, B.A., Conlan, K.E., Gradinger, R.R., Grebmeier, J.M., Hill, V.J., Hopcroft, R.R., Hunt, B.P.V., Joo, H.M., Kirchman, D.L., Kosobokova, K.N., Lee, S.H., Li, W.K.W., Lovejoy, C., Poulin, M., Sherr, E., Young, K. V., 2014. Biodiversity and biogeography of the lower trophic taxa of the pacific arctic region: Sensitivities to climate change, in: *The Pacific Arctic Region: Ecosystem Status and Trends in a Rapidly Changing Environment*. Springer Netherlands, pp. 269–336. https://doi.org/10.1007/978-94-017-8863-2_10
- Nunoura, T., Nishizawa, M., Hirai, M., Shimamura, S., Harnvoravongchai, P., Koide, O., Morono, Y., Fukui, T., Inagaki, F., Miyazaki, J., Takaki, Y., Takai, K., 2018. Microbial diversity in sediments from the bottom of the challenger deep, the mariana trench. *Microbes Environ.* 33, 186–194. <https://doi.org/10.1264/jsme2.ME17194>
- Obi, C.C., Adebusoye, S.A., Amund, O.O., Ugoji, E.O., Ilori, M.O., Hedman, C.J., Hickey, W.J., 2017. Structural dynamics of microbial communities in polycyclic aromatic hydrocarbon-contaminated tropical estuarine sediments undergoing simulated aerobic biotreatment. *Appl. Microbiol. Biotechnol.* 101, 4299–4314. <https://doi.org/10.1007/s00253-017-8151-6>
- Offre, P., Spang, A., Schleper, C., 2013. Archaea in Biogeochemical Cycles. *Annu. Rev. Microbiol.* 67, 437–457. <https://doi.org/10.1146/annurev-micro-092412-155614>
- Oksanen, J., 2015. *Multivariate Analysis of Ecological Communities in R: vegan tutorial*.
- Oksanen, J., Blanchet, F.G., Friendly, M., Kindt, R., Legendre, P., Mcglinn, D., Minchin, P.R., O'hara, R.B., Simpson, G.L., Solymos, P., Henry, M., Stevens, H., Szoecs, E., Wagner, H., Oksanen, M.J., 2017. *Community Ecology Package*.
- Orcutt, B.N., Sylvan, J.B., Knab, N.J., Edwards, K.J., 2011. Microbial Ecology of the Dark Ocean above, at, and below the Seafloor. *Microbiol. Mol. Biol. Rev.* 75, 361–422.

<https://doi.org/10.1128/MMBR.00039-10>

- Orphan, V.J., Hinrichs, K.U., Ussler, W., Paull, C.K., Taylor, L.T., Sylva, S.P., Hayes, J.M., Delong, E.F., 2001. Comparative Analysis of Methane-Oxidizing Archaea and Sulfate-Reducing Bacteria in Anoxic Marine Sediments. *Appl. Environ. Microbiol.* 67, 1922–1934. <https://doi.org/10.1128/AEM.67.4.1922-1934.2001>
- Otte, J.M., Blackwell, N., Ruser, R., Kappler, A., Kleindienst, S., Schmidt, C., 2019. N₂O formation by nitrite-induced (chemo)denitrification in coastal marine sediment. *Sci. Rep.* 9, 10691. <https://doi.org/10.1038/s41598-019-47172-x>
- Parada, A.E., Needham, D.M., Fuhrman, J.A., 2016. Every base matters: assessing small subunit rRNA primers for marine microbiomes with mock communities, time series and global field samples. *Environ. Microbiol.* 18, 1403–1414. <https://doi.org/10.1111/1462-2920.13023>
- Park, B.J., Park, S.J., Yoon, D.N., Schouten, S., Damsté, J.S.S., Rhee, S.K., 2010. Cultivation of autotrophic ammonia-oxidizing archaea from marine sediments in coculture with sulfur-oxidizing bacteria. *Appl. Environ. Microbiol.* 76, 7575–7587. <https://doi.org/10.1128/AEM.01478-10>
- Park, S.J., Kim, J.G., Jung, M.Y., Kim, S.J., Cha, I.T., Ghai, R., Martín-Cuadrado, A.B., Rodríguez-Valera, F., Rhee, S.K., 2012. Draft genome sequence of an ammonia-oxidizing archaeon, “*Candidatus Nitrosopumilus sediminis*” AR2, from svalbard in the arctic circle. *J. Bacteriol.* 194, 6946–6947. <https://doi.org/10.1128/JB.01869-12>
- Paull, C., Dallimore, S., Hughes-Clarke, J., Blasco, S., Lundsten, E., Iii, W.U., Graves, D., Sherman, A., Conway, K., Melling, H., Vagle, S., Collett, T., 2011. Tracking the decomposition of submarine permafrost and gas hydrate under the shelf and slope of the beaufort sea. Monterey Bay Aquarium Research Institute (MBARI): Moss Landing, CA.

- Paull, C.K., Dallimore, S.R., Caress, D.W., Gwiazda, R., Melling, H., Riedel, M., Jin, Y.K., Hong, J.K., Kim, Y.G., Graves, D., Sherman, A., Lundsten, E., Anderson, K., Lundsten, L., Villinger, H., Kopf, A., Johnson, S.B., Hughes Clarke, J., Blasco, S., Conway, K., Neelands, P., Thomas, H., Côté, M., 2015. Active mud volcanoes on the continental slope of the Canadian Beaufort Sea. *Geochemistry, Geophys. Geosystems* 16, 3160–3181. <https://doi.org/10.1002/2015GC005928>
- Penton, C.R., Devol, A.H., Tiedje, J.M., 2006. Molecular evidence for the broad distribution of anaerobic ammonium-oxidizing bacteria in freshwater and marine sediments. *Appl. Environ. Microbiol.* 72, 6829–6832. <https://doi.org/10.1128/AEM.01254-06>
- Petro, C., Zäncker, B., Starnawski, P., Jochum, L.M., Ferdelman, T.G., Jørgensen, B.B., Røy, H., Kjeldsen, K.U., Schramm, A., 2019. Marine Deep Biosphere Microbial Communities Assemble in Near-Surface Sediments in Aarhus Bay. *Front. Microbiol.* 10, 758. <https://doi.org/10.3389/fmicb.2019.00758>
- Pickart, R.S., 2004. Shelfbreak circulation in the Alaskan Beaufort Sea: Mean structure and variability. *J. Geophys. Res. C Ocean.* 109, 1–14. <https://doi.org/10.1029/2003JC001912>
- Pjevac, P., Kamyshny, A., Dyksma, S., Mußmann, M., 2014. Microbial consumption of zero-valence sulfur in marine benthic habitats. *Environ. Microbiol.* 16, 3416–3430. <https://doi.org/10.1111/1462-2920.12410>
- Probandt, D., Knittel, K., Tegetmeyer, H.E., Ahmerkamp, S., Holtappels, M., Amann, R., 2017. Permeability shapes bacterial communities in sublittoral surface sediments. *Environ. Microbiol.* 19, 1584–1599. <https://doi.org/10.1111/1462-2920.13676>
- Qin, W., Amin, S.A., Martens-Habbena, W., Walker, C.B., Urakawa, H., Devol, A.H., Ingalls, A.E., Moffett, J.W., Armbrust, E.V., Stahl, D.A., 2014. Marine ammonia-oxidizing archaeal

- isolates display obligate mixotrophy and wide ecotypic variation. *Proc. Natl. Acad. Sci. U. S. A.* 111, 12504–9. <https://doi.org/10.1073/pnas.1324115111>
- Qin, W., Martens-Habbena, W., Kobelt, J.N., Stahl, D.A., 2016. *Candidatus Nitrosopumilales*, in: *Bergey's Manual of Systematics of Archaea and Bacteria*. John Wiley & Sons, Ltd, Chichester, UK, pp. 1–2. <https://doi.org/10.1002/9781118960608.obm00122>
- R Core Team, 2017. R: A language and environment for statistical computing.
- Rachold, V., Eicken, H., Gordeev, V. V, Grigoriev, M.N., Hubberten, H., 2004. The Organic Carbon Cycle in the Arctic Ocean. *Org. Carbon Cycle Arct. Ocean*. <https://doi.org/10.1007/978-3-642-18912-8>
- Rapp, J.Z., Fernández-Méndez, M., Bienhold, C., Boetius, A., 2018. Effects of Ice-Algal Aggregate Export on the Connectivity of Bacterial Communities in the Central Arctic Ocean. *Front. Microbiol.* 9, 1035. <https://doi.org/10.3389/fmicb.2018.01035>
- Ravenschlag, K., Sahm, K., Amann, R., 2001. Quantitative molecular analysis of the microbial community in marine arctic sediments (Svalbard). *Appl. Environ. Microbiol.* 67, 387–395. <https://doi.org/10.1128/AEM.67.1.387-395.2001>
- Renaud, P.E., Wallhead, P., Kotta, J., Włodarska-Kowalczyk, M., Bellerby, R.G.J., Rätsep, M., Slagstad, D., Kukliński, P., 2019. Arctic Sensitivity? Suitable Habitat for Benthic Taxa Is Surprisingly Robust to Climate Change. *Front. Mar. Sci.* 6, 538. <https://doi.org/10.3389/fmars.2019.00538>
- Retelletti Brogi, S., Kim, J.-H., Ryu, J.-S., Jin, Y.K., Lee, Y.K., Hur, J., 2019. Exploring sediment porewater dissolved organic matter (DOM) in a mud volcano: Clues of a thermogenic DOM source from fluorescence spectroscopy. *Mar. Chem.* <https://doi.org/10.1016/J.MARCHEM.2019.03.009>

- Roussel, E.G., Sauvadet, A.-L., Chaduteau, C., Fouquet, Y., Charlou, J.-L., Prieur, D., Cambon Bonavita, M.-A., 2009. Archaeal communities associated with shallow to deep seafloor sediments of the New Caledonia Basin. *Environ. Microbiol.* 11, 2446–2462.
<https://doi.org/10.1111/j.1462-2920.2009.01976.x>
- Ruff, S.E., Biddle, J.F., Teske, A.P., Knittel, K., Boetius, A., Ramette, A., 2015. Global dispersion and local diversification of the methane seep microbiome. *Proc. Natl. Acad. Sci.* 112, 4015–4020. <https://doi.org/10.1073/pnas.1421865112>
- Rysgaard, S., Glud, R.N., Risgaard-Petersen, N., Dalsgaard, T., 2004. Denitrification and anammox activity in Arctic marine sediments. *Limnol. Oceanogr.* 49, 1493–1502.
<https://doi.org/10.4319/lo.2004.49.5.1493>
- Salter, S.J., Cox, M.J., Turek, E.M., Calus, S.T., Cookson, W.O., Moffatt, M.F., Turner, P., Parkhill, J., Loman, N.J., Walker, A.W., 2014. Reagent and laboratory contamination can critically impact sequence-based microbiome analyses. *BMC Biol.* 12, 87.
<https://doi.org/10.1186/s12915-014-0087-z>
- Schloss, P.D., Westcott, S.L., Ryabin, T., Hall, J.R., Hartmann, M., Hollister, E.B., Lesniewski, R. a., Oakley, B.B., Parks, D.H., Robinson, C.J., Sahl, J.W., Stres, B., Thallinger, G.G., Van Horn, D.J., Weber, C.F., 2009. Introducing mothur: Open-source, platform-independent, community-supported software for describing and comparing microbial communities. *Appl. Environ. Microbiol.* 75, 7537–7541. <https://doi.org/10.1128/AEM.01541-09>
- Schreiber, L., Holler, T., Knittel, K., Meyerdierks, A., Amann, R., 2010. Identification of the dominant sulfate-reducing bacterial partner of anaerobic methanotrophs of the ANME-2 clade. *Environ. Microbiol.* 12. <https://doi.org/10.1111/j.1462-2920.2010.02275.x>
- Sheik, C.S., Jain, S., Dick, G.J., 2014. Metabolic flexibility of enigmatic SAR324 revealed

- through metagenomics and metatranscriptomics. *Environ. Microbiol.* 16, 304–317.
<https://doi.org/10.1111/1462-2920.12165>
- Siegert, M., Krüger, M., Teichert, B., Wiedicke, M., Schippers, A., 2011. Anaerobic Oxidation of Methane at a Marine Methane Seep in a Forearc Sediment Basin off Sumatra, Indian Ocean. *Front. Microbiol.* 2. <https://doi.org/10.3389/fmicb.2011.00249>
- Simpson, K.G., Tremblay, J.-É., Gratton, Y., Price, N.M., 2008. An annual study of inorganic and organic nitrogen and phosphorus and silicic acid in the southeastern Beaufort Sea. *J. Geophys. Res.* 113, C07016. <https://doi.org/10.1029/2007JC004462>
- Sinkko, H., Lukkari, K., Sihvonen, L.M., Sivonen, K., Leivuori, M., Rantanen, M., Paulin, L., Lyra, C., 2013. Bacteria Contribute to Sediment Nutrient Release and Reflect Progressed Eutrophication-Driven Hypoxia in an Organic-Rich Continental Sea. *PLoS One* 8, e67061. <https://doi.org/10.1371/journal.pone.0067061>
- Smoot, C.A., Hopcroft, R.R., 2017. Depth-stratified community structure of Beaufort Sea slope zooplankton and its relations to water masses. *J. Plankton Res.* 39, 79–91.
<https://doi.org/10.1093/plankt/fbw087>
- Sørensen, K.B., Teske, A., 2006. Stratified communities of active archaea in deep marine subsurface sediments. *Appl. Environ. Microbiol.* 72, 4596–4603.
<https://doi.org/10.1128/AEM.00562-06>
- Sparrow, K.J., Kessler, J.D., Southon, J.R., Garcia-Tigreros, F., Schreiner, K.M., Ruppel, C.D., Miller, J.B., Lehman, S.J., Xu, X., 2018. Limited contribution of ancient methane to surface waters of the U.S. Beaufort Sea shelf. *Sci. Adv.* 4, eaao4842.
<https://doi.org/10.1126/sciadv.aao4842>
- Stahl, D.A., de la Torre, J.R., 2012. Physiology and diversity of ammonia-oxidizing archaea.

- Annu. Rev. Microbiol. 66, 83–101. <https://doi.org/10.1146/annurev-micro-092611-150128>
- Stokes, C.R., Clark, C.D., Winsborrow, M.C.M., Winsborrow, C.M., 2006. Subglacial bedform evidence for a major palaeo-ice stream and its retreat phases in Amundsen Gulf, Canadian Arctic Archipelago. *J. Quat. Sci.* 21, 399–412. <https://doi.org/10.1002/jqs.991>
- Takeuchi, M., Katayama, T., Yamagishi, T., Hanada, S., Tamaki, H., Kamagata, Y., Oshima, K., Hattori, M., Marumo, K., Nedachi, M., Maeda, H., Suwa, Y., Sakata, S., 2014. *Methyloceanibacter caenitepidi* gen. nov., sp. nov., a facultatively methylotrophic bacterium isolated from marine sediments near a hydrothermal vent. *Int. J. Syst. Evol. Microbiol.* 64, 462–468. <https://doi.org/10.1099/ijss.0.053397-0>
- Tanaka, N., Romanenko, L.A., Ino, T., Frolova, G.M., Mikhailov, V. V., 2011. *Cocleimonas flava* gen. nov., sp. nov., a gammaproteobacterium isolated from sand snail (*Umbonium costatum*). *Int. J. Syst. Evol. Microbiol.* 61, 412–416. <https://doi.org/10.1099/ijss.0.020263-0>
- Teeling, H., Fuchs, B.M., Becher, D., Klockow, C., Gardebrecht, A., Bennis, C.M., Kassabgy, M., Huang, S., Mann, A.J., Waldmann, J., Weber, M., Klindworth, A., Otto, A., Lange, J., Bernhardt, J., Reinsch, C., Hecker, M., Peplies, J., Bockelmann, F.D., Callies, U., Gerdt, G., Wichels, A., Wiltshire, K.H., Glöckner, F.O., Schweder, T., Amann, R., 2012. Substrate-controlled succession of marine bacterioplankton populations induced by a phytoplankton bloom. *Science* 336, 608–11. <https://doi.org/10.1126/science.1218344>
- Teeling, H., Fuchs, B.M., Bennis, C.M., Krüger, K., Chafee, M., Kappelmann, L., Reintjes, G., Waldmann, J., Quast, C., Glöckner, F.O., Lucas, J., Wichels, A., Gerdt, G., Wiltshire, K.H., Amann, R.I., 2016. Recurring patterns in bacterioplankton dynamics during coastal spring algae blooms. *Elife* 5. <https://doi.org/10.7554/eLife.11888>
- Thamdrup, B., Dalsgaard, T., 2002. Production of N₂ through anaerobic ammonium oxidation

- coupled to nitrate reduction in marine sediments. *Appl. Environ. Microbiol.* 68, 1312–1318.
<https://doi.org/10.1128/AEM.68.3.1312-1318.2002>
- Trembath-Reichert, E., Case, D.H., Orphan, V.J., 2016. Characterization of microbial associations with methanotrophic archaea and sulfate-reducing bacteria through statistical comparison of nested Magneto-FISH enrichments. *PeerJ* 2016.
<https://doi.org/10.7717/peerj.1913>
- Treude, T., Krause, S., Maltby, J., Dale, A.W., Coffin, R., Hamdan, L.J., 2014. Sulfate reduction and methane oxidation activity below the sulfate-methane transition zone in Alaskan Beaufort Sea continental margin sediments: Implications for deep sulfur cycling. *Geochim. Cosmochim. Acta* 144, 217–237. <https://doi.org/10.1016/j.gca.2014.08.018>
- Trivedi, C.B., Lau, G.E., Grasby, S.E., Templeton, A.S., Spear, J.R., 2018. Low-Temperature Sulfidic-Ice Microbial Communities, Borup Fiord Pass, Canadian High Arctic. *Front. Microbiol.* 9, 1622. <https://doi.org/10.3389/fmicb.2018.01622>
- Ullman, W.J., Aller, R.C., 1982. *No Title, Limnology and Oceanography*. Wiley-Blackwell.
<https://doi.org/10.4319/lo.1982.27.3.0552>
- Van de Vossenberg, J., Woebken, D., Maalcke, W.J., Wessels, H.J.C.T., Dutilh, B.E., Kartal, B., Janssen-Megens, E.M., Roeselers, G., Yan, J., Speth, D., Gloerich, J., Geerts, W., Van der Biezen, E., Pluk, W., Francoijs, K.J., Russ, L., Lam, P., Malfatti, S.A., Tringe, S.G., Haaijer, S.C.M., Op den Camp, H.J.M., Stunnenberg, H.G., Amann, R., Kuypers, M.M.M., Jetten, M.S.M., 2013. The metagenome of the marine anammox bacterium “*Candidatus Scalindua profunda*” illustrates the versatility of this globally important nitrogen cycle bacterium. *Environ. Microbiol.* 15, 1275–1289. <https://doi.org/10.1111/j.1462-2920.2012.02774.x>

- van der Waals, M.J., Atashgahi, S., da Rocha, U.N., van der Zaan, B.M., Smidt, H., Gerritse, J., 2017. Benzene degradation in a denitrifying biofilm reactor: activity and microbial community composition. *Appl. Microbiol. Biotechnol.* 101, 5175–5188.
<https://doi.org/10.1007/s00253-017-8214-8>
- Vekeman, B., Kerckhof, F.-M.M., Cremers, G., de Vos, P., Vandamme, P., Boon, N., Op den Camp, H.J.M., Heylen, K., 2016a. New Methyloceanibacter diversity from North Sea sediments includes methanotroph containing solely the soluble methane monooxygenase. *Environ. Microbiol.* 18, 4523–4536. <https://doi.org/10.1111/1462-2920.13485>
- Vekeman, B., Speth, D., Wille, J., Cremers, G., De Vos, P., Op den Camp, H.J.M., Heylen, K., 2016b. Genome Characteristics of Two Novel Type I Methanotrophs Enriched from North Sea Sediments Containing Exclusively a Lanthanide-Dependent XoxF5-Type Methanol Dehydrogenase. *Microb. Ecol.* 72, 503–509. <https://doi.org/10.1007/s00248-016-0808-7>
- Vollmers, J., Voget, S., Dietrich, S., Gollnow, K., Smits, M., Meyer, K., Brinkhoff, T., Simon, M., Daniel, R., 2013. Poles Apart: Arctic and Antarctic Octadecabacter strains Share High Genome Plasticity and a New Type of Xanthorhodopsin. *PLoS One* 8, e63422.
<https://doi.org/10.1371/journal.pone.0063422>
- Waidner, L.A., Kirchman, D.L., 2007. Aerobic anoxygenic phototrophic bacteria attached to particles in turbid waters of the Delaware and Chesapeake estuaries. *Appl. Environ. Microbiol.* 73, 3936–3944. <https://doi.org/10.1128/AEM.00592-07>
- Walsh, J.E., Overland, J.E., Groisman, P.Y., Rudolf, B., 2011. Ongoing climate change in the arctic. *Ambio* 40, 6–16. <https://doi.org/10.1007/s13280-011-0211-z>
- Walters, W., Hyde, E.R., Berg-Lyons, D., Ackermann, G., Humphrey, G., Parada, A., Gilbert, J.A., Jansson, J.K., Caporaso, J.G., Fuhrman, J.A., Apprill, A., Knight, R., 2016. Improved

- Bacterial 16S rRNA Gene (V4 and V4-5) and Fungal Internal Transcribed Spacer Marker Gene Primers for Microbial Community Surveys. *mSystems* 1, e00009-15.
<https://doi.org/10.1128/mSystems.00009-15>
- Wang, L., Yu, M., Liu, Y., Liu, Jiwen, Wu, Y., Li, L., Liu, Jihua, Wang, M., Zhang, X.-H., 2018. Comparative analyses of the bacterial community of hydrothermal deposits and seafloor sediments across Okinawa Trough. *J. Mar. Syst.* 180, 162–172.
<https://doi.org/10.1016/j.jmarsys.2016.11.012>
- Wang, Q., Garrity, G.M., Tiedje, J.M., Cole, J.R., 2007. Naive Bayesian Classifier for Rapid Assignment of rRNA Sequences into the New Bacterial Taxonomy. *Appl. Environ. Microbiol.* 73, 5261–5267. <https://doi.org/10.1128/AEM.00062-07>
- Wang, X., Yan, Y., Gao, D., 2018. The threshold of influent ammonium concentration for nitrate over-accumulation in a one-stage deammonification system with granular sludge without aeration. *Sci. Total Environ.* 634, 843–852. <https://doi.org/10.1016/j.scitotenv.2018.04.053>
- Wasmund, K., Mußmann, M., Loy, A., 2017. The life sulfuric: microbial ecology of sulfur cycling in marine sediments. *Environ. Microbiol. Rep.* 9, 323–344.
<https://doi.org/10.1111/1758-2229.12538>
- Weingartner, T., Okkonen, S., Danielson, S., 2005. Circulation and water property variations in the nearshore Alaskan Beaufort Sea. *US Miner. Manag. Serv. Outer Cont. Shelf Study* 2005–028, 1–103.
- Westcott, S.L., Schloss, P.D., 2017. OptiClust, an Improved Method for Assigning Amplicon-Based Sequence Data to Operational Taxonomic Units. *mSphere* 2, e00073-17.
<https://doi.org/10.1128/mSphereDirect.00073-17>
- Williams, T.J., Lefèvre, C.T., Zhao, W., Beveridge, T.J., Bazylinski, D.A., 2012. *Magnetospira*

- thiophila gen. nov., sp. nov., a marine magnetotactic bacterium that represents a novel lineage within the Rhodospirillaceae (Alphaproteobacteria). *Int. J. Syst. Evol. Microbiol.* 62, 2443–2450. <https://doi.org/10.1099/ijms.0.037697-0>
- Winkel, M., Mitzscherling, J., Overduin, P.P., Horn, F., Winterfeld, M., Rijkers, R., Grigoriev, M.N., Knoblauch, C., Mangelsdorf, K., Wagner, D., Liebner, S., 2018. Anaerobic methanotrophic communities thrive in deep submarine permafrost. *Sci. Rep.* 8, 1291. <https://doi.org/10.1038/s41598-018-19505-9>
- Wu, C.H., Sercu, B., van de Werfhorst, L.C., Wong, J., deSantis, T.Z., Brodie, E.L., Hazen, T.C., Holden, P.A., Andersen, G.L., 2010. Characterization of coastal urban watershed bacterial communities leads to alternative community-based indicators. *PLoS One* 5. <https://doi.org/10.1371/journal.pone.0011285>
- Wu, H., Liu, M., Zhang, W., Xiao, T., 2014. Phylogenetic analysis of epibacterial communities on the surfaces of four red macroalgae. *J. Ocean Univ. China* 13, 1025–1032. <https://doi.org/10.1007/s11802-014-2325-y>
- Xia, Y., Wang, Yubo, Wang, Yi, Chin, F.Y.L., Zhang, T., 2016. Cellular adhesiveness and cellulolytic capacity in Anaerolineae revealed by omics-based genome interpretation. *Biotechnol. Biofuels* 9, 111. <https://doi.org/10.1186/s13068-016-0524-z>
- Xing, P., Hahnke, R.L., Unfried, F., Markert, S., Huang, S., Barbeyron, T., Harder, J., Becher, D., Schweder, T., Glöckner, F.O., Amann, R.I., Teeling, H., 2015. Niches of two polysaccharide-degrading Polaribacter isolates from the North Sea during a spring diatom bloom. *ISME J.* 9, 1410–1422. <https://doi.org/10.1038/ismej.2014.225>
- Yamada, T., Sekiguchi, Y., 2018. *Anaerolineaceae*, in: *Bergey's Manual of Systematics of Archaea and Bacteria*. John Wiley & Sons, Ltd, Chichester, UK, pp. 1–5.

<https://doi.org/10.1002/9781118960608.fbm00301>

Yekutieli, D., Benjamini, Y., 2002. The control of the false discovery rate in multiple testing under dependency. *Ann. Stat.* 29, 1165–1188. <https://doi.org/10.1214/aos/1013699998>

Zeng, Y.-X., Yu, Y., Li, H.-R., Luo, W., 2017. Prokaryotic Community Composition in Arctic Kongsfjorden and Sub-Arctic Northern Bering Sea Sediments As Revealed by 454 Pyrosequencing. *Front. Microbiol.* 8, 2498. <https://doi.org/10.3389/fmicb.2017.02498>

Zinger, L., Amaral-Zettler, L.A., Fuhrman, J.A., Horner-Devine, M.C., Huse, S.M., Welch, D.B.M., Martiny, J.B.H., Sogin, M., Boetius, A., Ramette, A., 2011. Global Patterns of Bacterial Beta-Diversity in Seafloor and Seawater Ecosystems. *PLoS One* 6, e24570. <https://doi.org/10.1371/journal.pone.0024570>

Zinke, L.A., Reese, B.K., McManus, J., Wheat, C.G., Orcutt, B.N., Amend, J.P., 2018. Sediment microbial communities influenced by cool hydrothermal fluid migration. *Front. Microbiol.* 9. <https://doi.org/10.3389/fmicb.2018.01249>

2.8 FIGURES

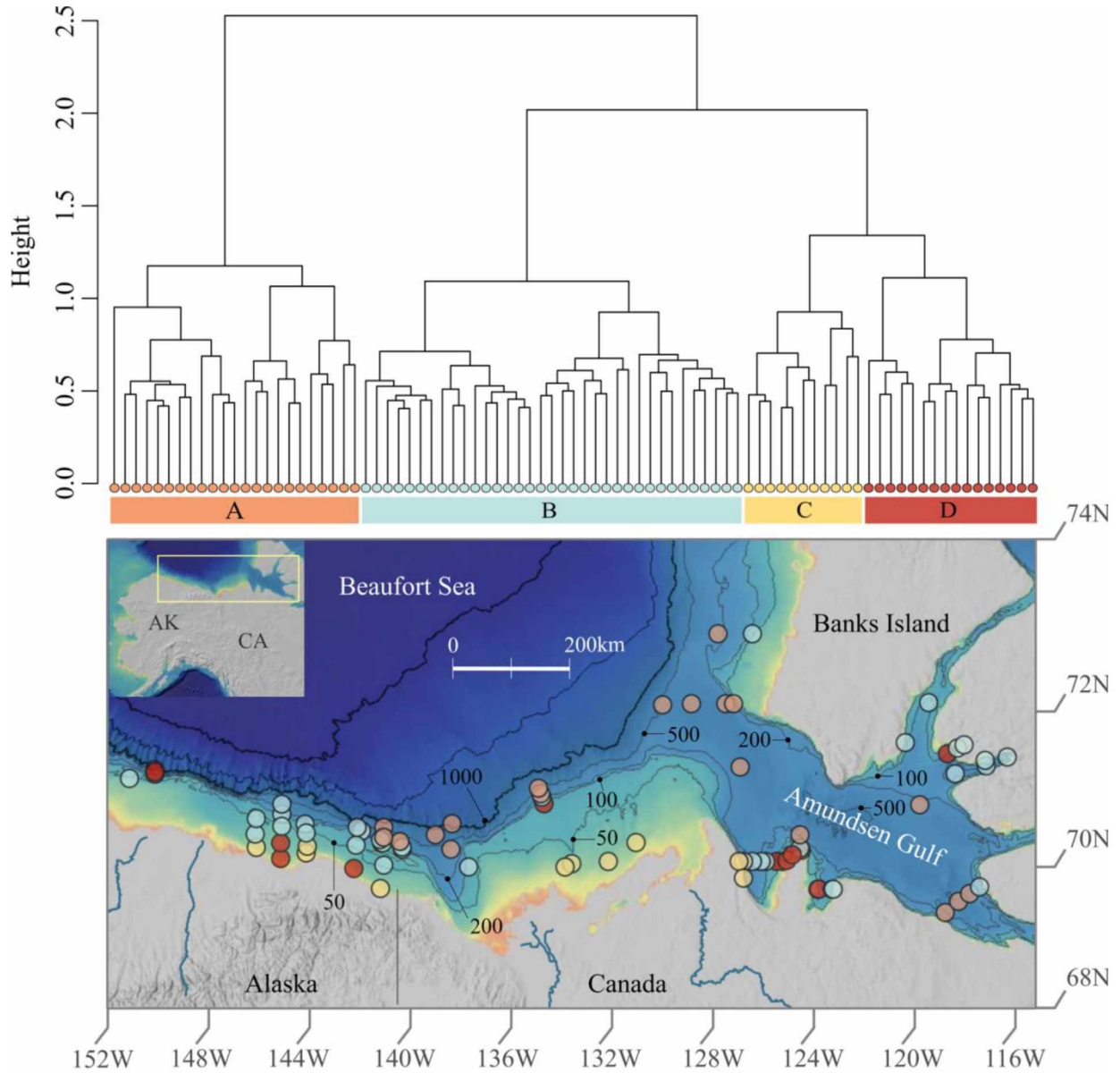


Figure 2.1. Prokaryotic cluster assemblages and spatial distribution in Beaufort Sea sediments. This figure shows the dendrogram of the four assemblages revealed via hierarchical clustering above the study area map which exhibits sample locations colored by assemblage. The map was created using ArcGIS online with the following layers: Northwest Territories, Esri, Garmin, FAO, NOAA, USGS, EPA, NRCan, and Parks Canada.

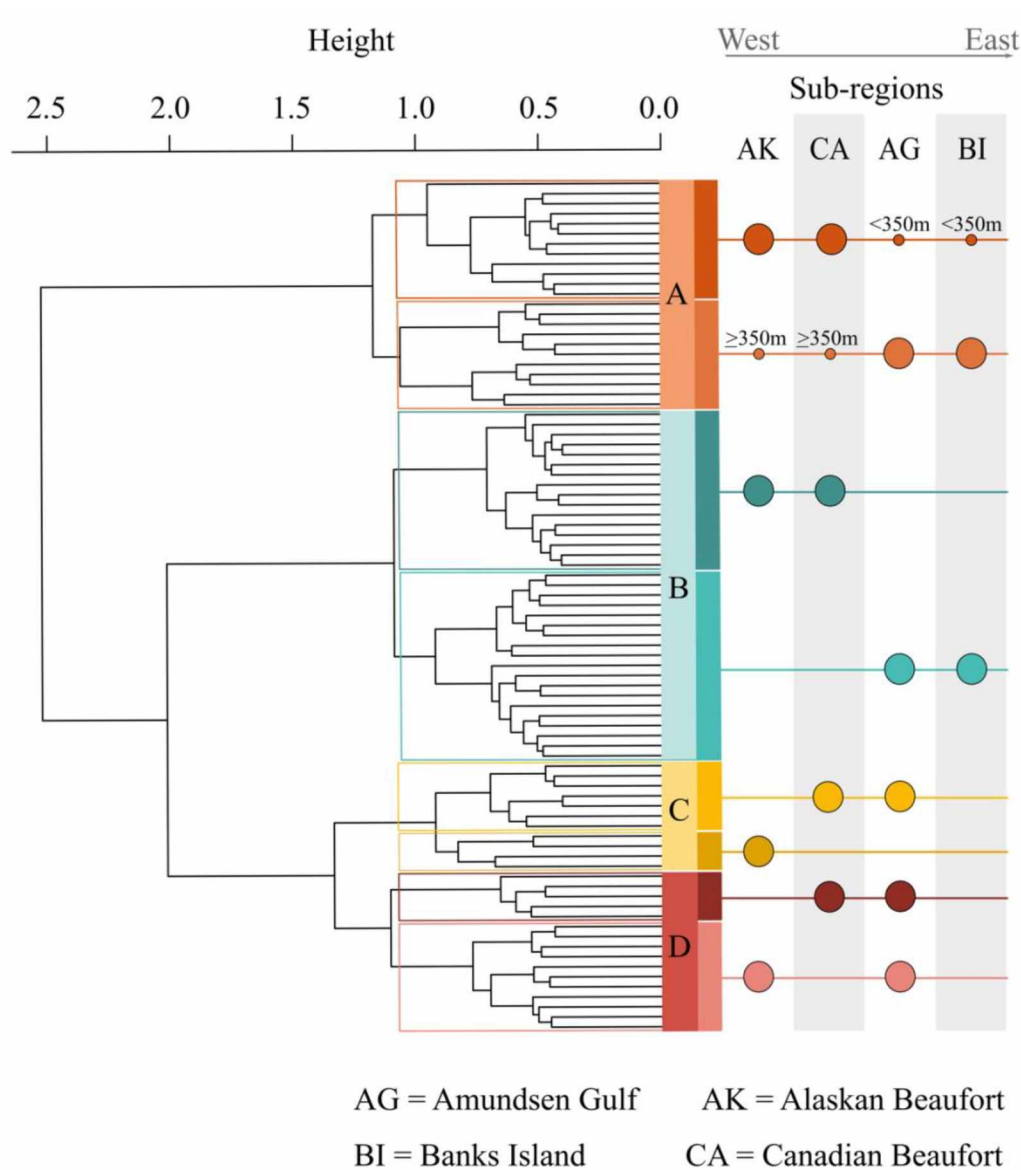


Figure 2.2. Substructure of prokaryotic assemblages. This dendrogram highlights the substructure within each assemblage and the differing east to west gradients reflected by the substructure. Assemblage A was divided by location and depth, with one sub-cluster dominated by Amundsen Gulf (AG) samples combined with broader Beaufort (AKCA) slope samples deeper than 350 m. The other assemblage A sub-cluster was dominated by broader Beaufort slope samples with AG samples shallower than 350 m. Assemblage B divided cleanly between broader Beaufort and Amundsen Gulf samples. Assemblage C divided between the west of the Mackenzie River, AK samples, and east of the Mackenzie River, CA Beaufort and AG samples. Assemblage D divided into combinations of AG samples with either AK or CA samples with no obvious demarcations.

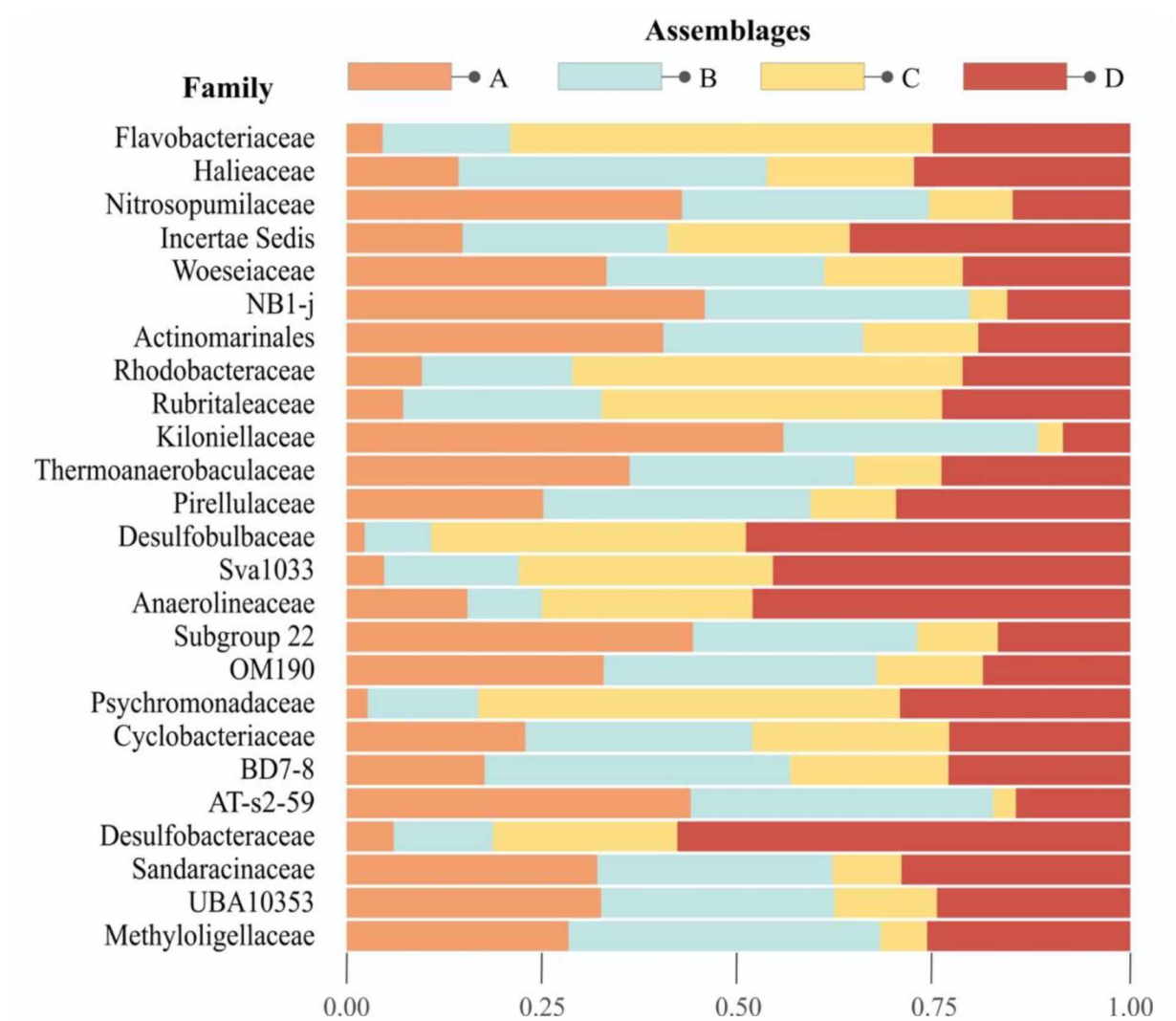
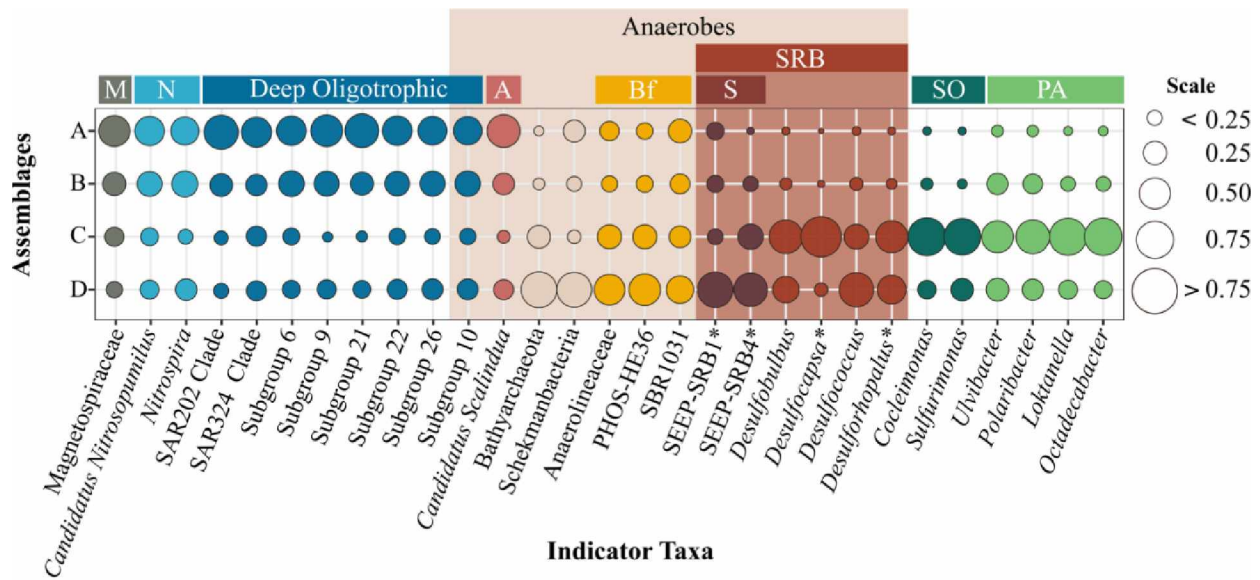


Figure 2.3. Top 25 abundant families in Beaufort Sea surface sediments. The stacked barplot illustrates the proportion of the top 25 families for each assemblage on the left-hand y-axis. The plot is arranged such that the most abundant taxa starts from the top and decreases toward the bottom. Note that Gammaproteobacteria Inc. sed., NB1-j, Actinomarinales, Sva1033, OM190, BD7-8, AT-s2-59, and UBA10353 are not classified to family, but order level.



Abbreviation Key

M = Magnetotactic N = Nitrifiers A = Annamox Bf = Biofilms S = Seeps
 SRB = Sulfate Reducing Bacteria SO = Sulfur Oxizers PA = Phytoplankton Associated

Figure 2.4. Proportion of assemblage-specific indicator taxa across prokaryotic assemblages. Indicator taxa are identified to the lowest taxonomic level possible. The plot is colored by functional groups which provide insight into characteristics associated with specific assemblages. *Indicates those taxa that were not yielded as indicators, but represent OTUs belonging to the same family as unidentified indicator taxa.

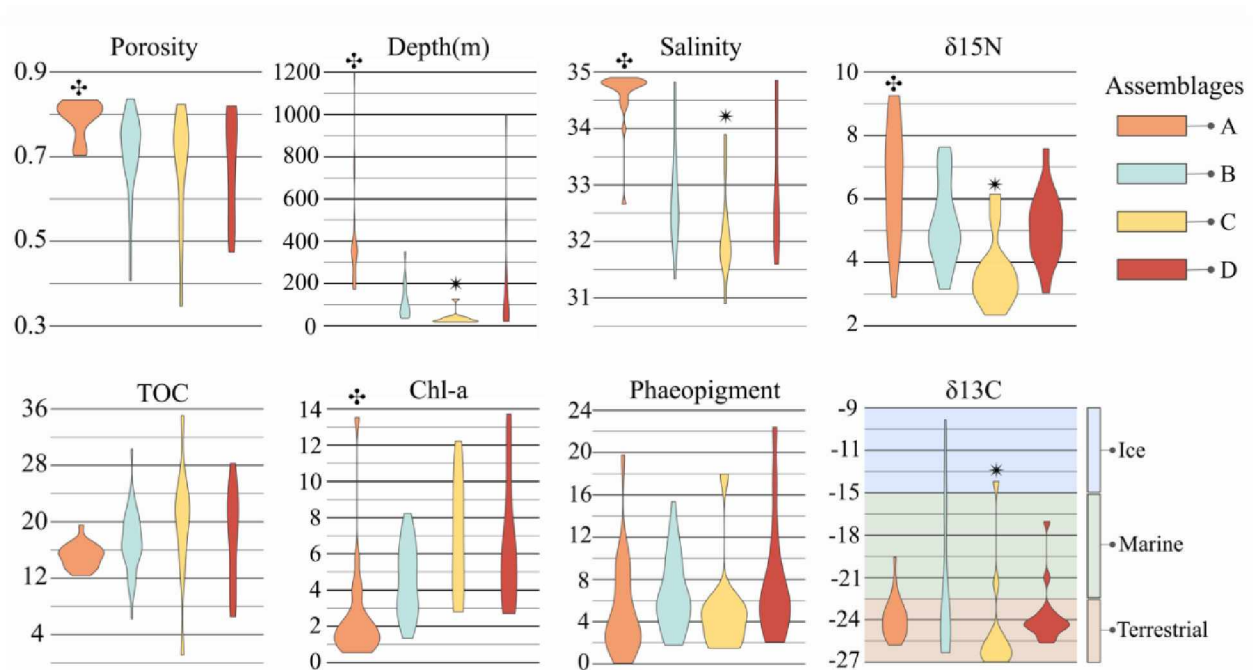


Figure 2.5. Distribution of environmental parameters for each assemblage. Each violin plot shows the distribution, within each assemblage, of the environmental parameters indicated as significant correlates in the ideal model for CAP analysis. Note that salinity is also included in this figure, though it was not run in CAP analysis due to the covariance inflation factor with depth. The symbols † and * indicate significant differences between un-matching symbols with other assemblages. $\delta^{13}\text{C}$ values for ice, marine, and terrestrial OM sources was derived from Dunton et al. (2006).

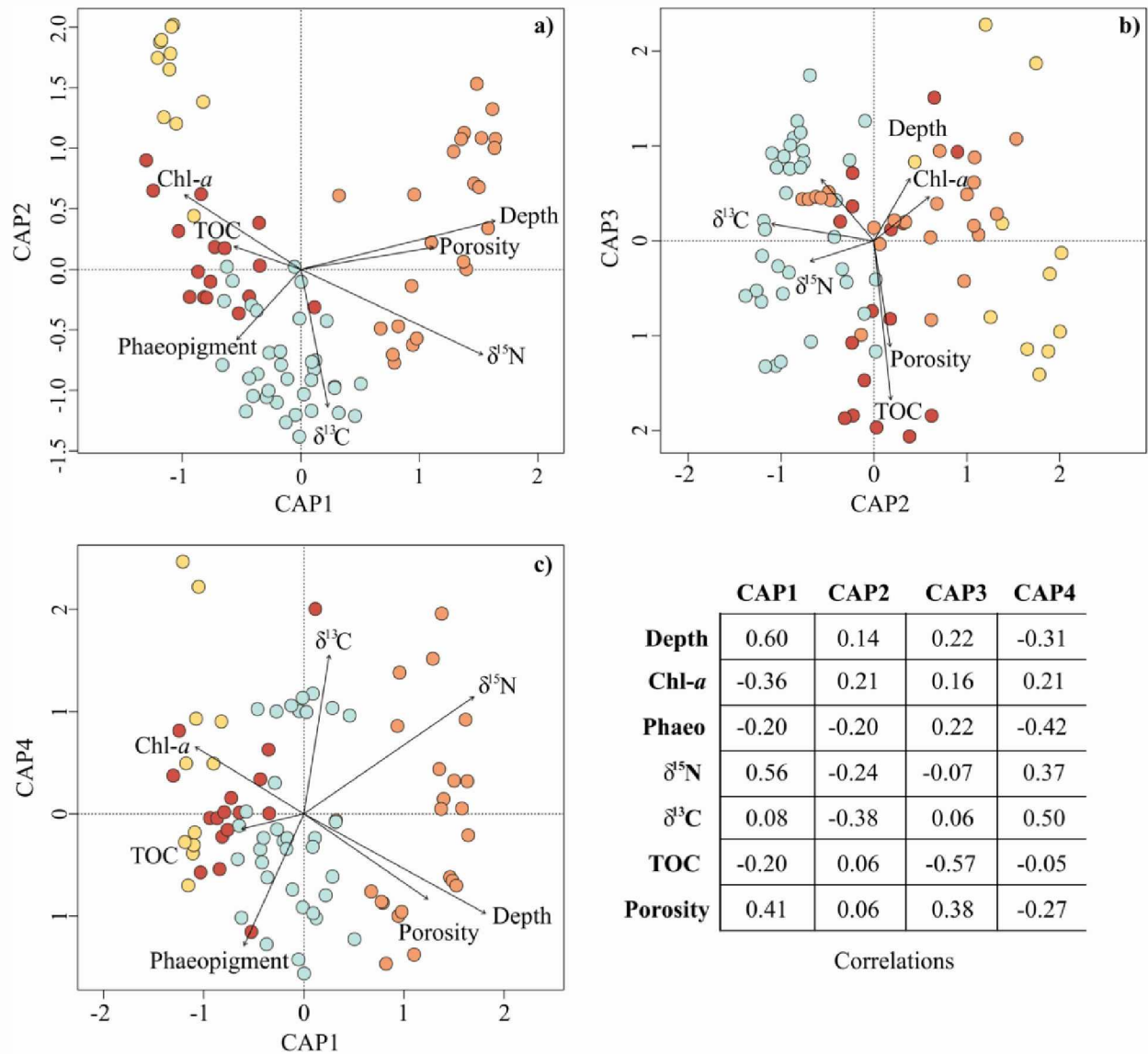


Figure 2.6. Environmental parameters influencing prokaryotic assemblage structure. The ordination plots above depict the results of Constrained Analysis of Principal Coordinates. All included environmental parameters are significant correlates ($P < 0.001$) to the first four CAP axes (A–C) and, in total, explained 18% of the variation in prokaryotic community structure ($R^2 = 0.18$). The corresponding correlations are reported in the table for all axes.

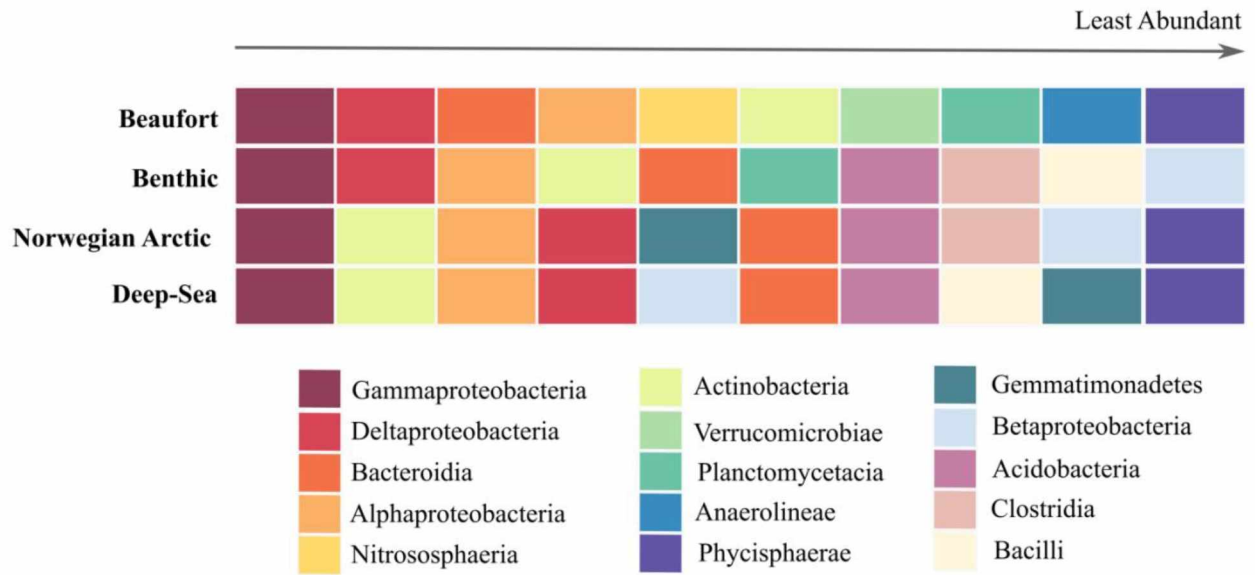
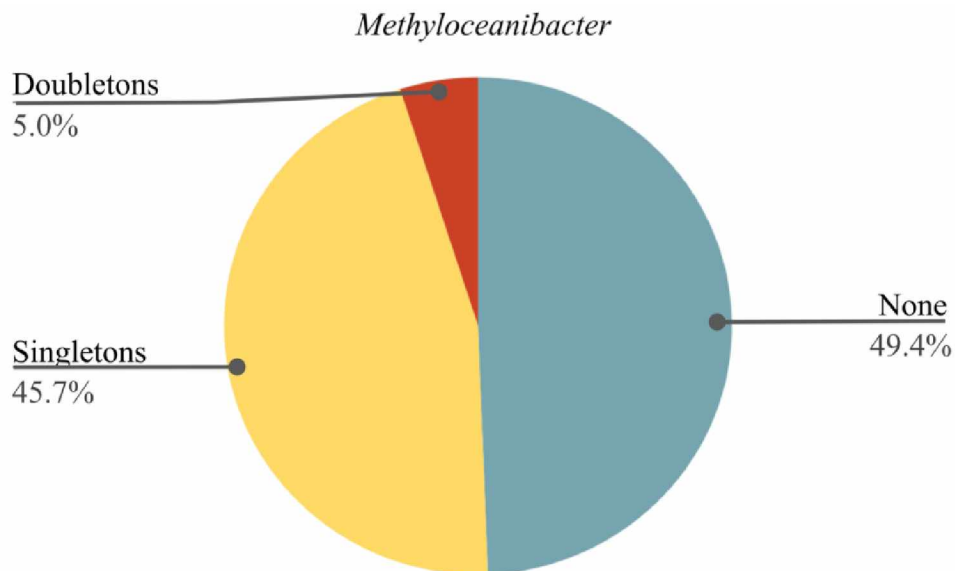
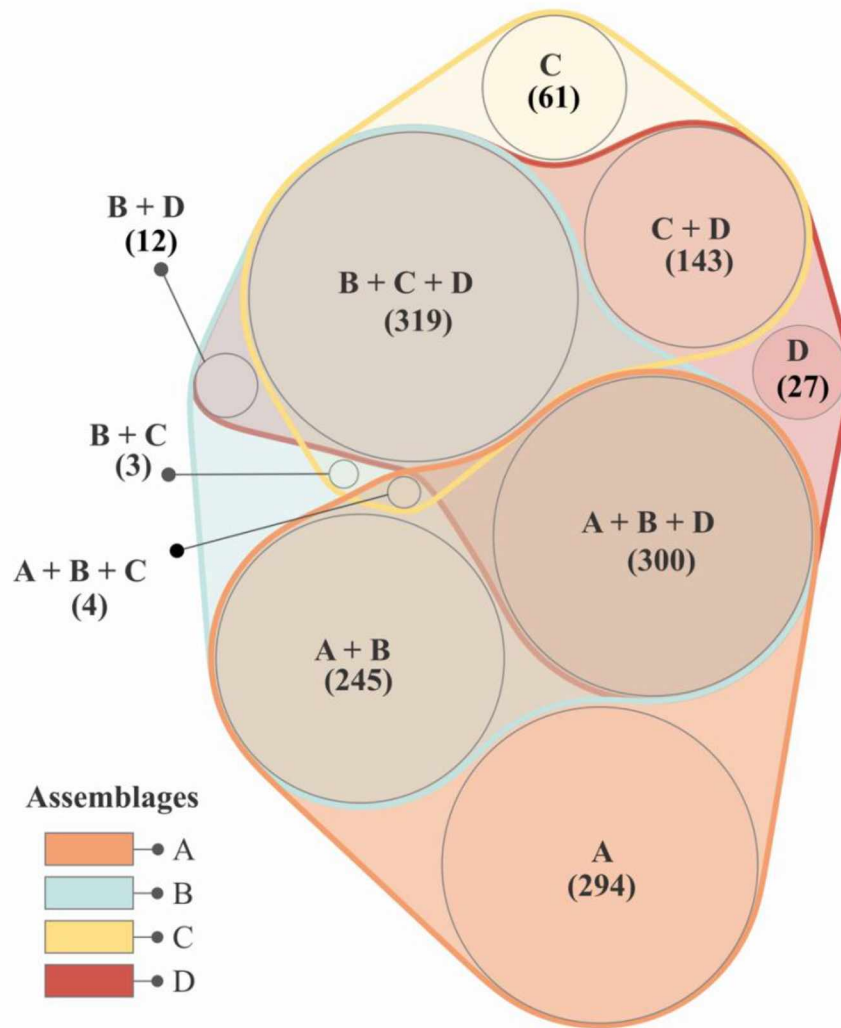


Figure 2.7. Top 10 abundant prokaryotes at class level exhibited in marine sediments. The colored grid above is arranged with surface sediment microbiomes on the y-axis, Beaufort, global benthic, Norwegian Arctic, and deep-sea (Zinger et al., 2011; Bienhold et al., 2016). The x-axis represents the rank from the most abundant taxa on the left to the least abundant taxa on the right exhibited by these microbiomes. The colors represent the class-level taxonomy of these prokaryotes.

2.9 APPENDICES



Appendix 2.1. Distribution of *Methyloceanibacter* at different levels of sequence removal. The pie chart above illustrates an example, using the genus *Methyloceanibacter*, of how relative abundances change with removal of singletons and doubletons compared to no removal (none). The difference in abundance is attributed to the removal of OTUs that would likely not have been removed if clustered at 97% similarity as they belong to the same genus. This is an important consideration when using amplicon sequence variants (ASVs), and software which automatically remove singletons and doubletons such as DADA2.



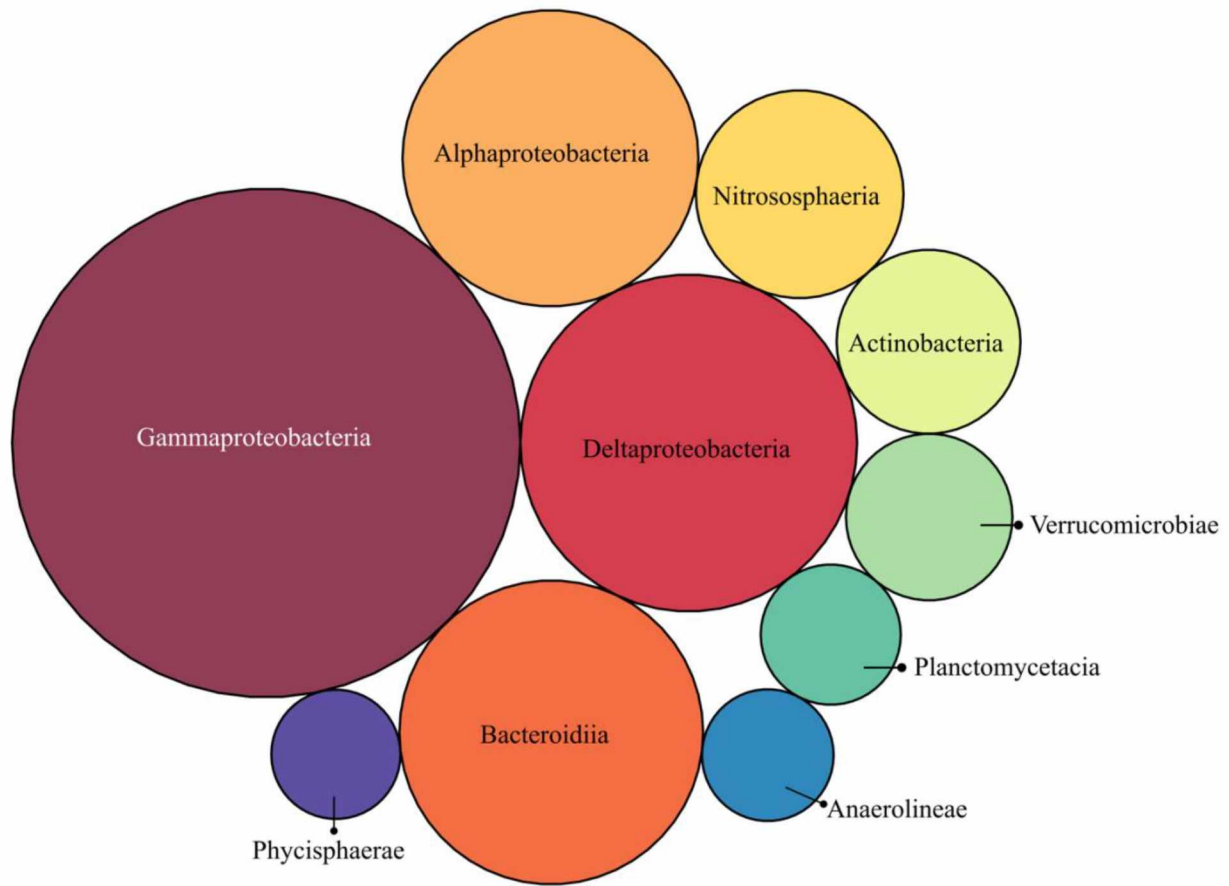
Appendix 2.2. Indicator OTUs for individual and combinations of prokaryotic assemblages. This Venn diagram illustrates the number of indicator OTUs in parentheses identified for individual assemblages and those shared in different combinations of assemblages.

Appendix 2.3. Indicator taxa for each prokaryotic assemblage. Taxa are arranged from most abundant starting at the top to least abundant toward the bottom. Those without a semi-colon indicate OTUs which could not be IDed past the taxonomic level provided.

A	B	C	D
NB1-J	-	Rhodobacteraceae	Anaerolineaceae
Nitrosopumilaceae; <i>Nitrosopumilus</i>	-	Flavobacteriaceae	Desulfobacteraceae
Subgroup 22	-	Flavobacteriaceae; <i>Ulvibacter</i>	4572-13
Nitrosopumilaceae	-	Saprosiraceae	Anaerolineaceae
Thermoanaerobaculaceae; Subgroup 10	-	Alphaproteobacteria	Bacteroidetes BD2-2
Alphaproteobacteria	-	Flavobacteriaceae; <i>Lutibacter</i>	Bathyarchaeota
Gammaproteobacteria Incertae Sedis	-	Flavobacteriaceae; <i>Maribacter</i>	BD2-11 terrestrial group
Kiloniellaceae	-	NS11-12 marine group	Desulfobacteraceae; <i>Desulfococcus</i>
Woeseiaceae ; <i>Woeseia</i>	-	Thiotrichaceae; <i>Cocleimonas</i>	Desulfobulbaceae
Nitrosococcaceae ; <i>AqS1</i>	-	Thiovulaceae; <i>Sulfurimonas</i>	PHOS-HE36
SAR324 clade (Marine group B)	-	Unknown Family; <i>Marinicella</i>	SBR1031
Subgroup 21	-	Actinobacteria	Schekmanbacteria
Latescibacteria	-	Alteromonadaceae	WCHB1-41
Magnetospiraceae	-	Anaerolineaceae	-
Nitrospiraceae ; <i>Nitrospira</i>	-	Burkholderiaceae; <i>Polaromonas</i>	-
OM190	-	Clostridiales	-
PAUC43f marine benthic group	-	Colwelliaceae	-
Subgroup 6	-	Crocinitomicaceae	-
Subgroup 9	-	Desulfobulbaceae	-

A	B	C	D
Bacteriap25	-	Desulfuromonadales	-
Cyclobacteriaceae	-	EPR3968-O8a-Bc78	-
KI89A clade	-	Flavobacteriaceae; <i>Arcticiflavibacter</i>	-
S085	-	Flavobacteriaceae; <i>Gaetbulibacter</i>	-
SAR202	-	Flavobacteriaceae; <i>Maritimimonas</i>	-
BD2-11 terrestrial group	-	Flavobacteriaceae; <i>Muriicola</i>	-
Chloroflexi	-	Methylophilaceae; <i>Methylotenera</i>	-
Phycisphaeraceae; Urania-1B-19 marine sediment group	-	Nitrincolaceae	-
Subgroup 26	-	Nitrosococcaceae; <i>Cm1-21</i>	-
Dadabacteriales	-	Rhodobacteraceae; Roseobacter clade NAC11-7 lineage	-
<i>EPR3968-O8a-Bc78</i>	-	Rubritaleaceae; <i>Persicirhabdus</i>	-
<i>JG30-KF-CM66</i>	-	Sphingomonadaceae	-
Kiloniellaceae	-	Spirochaetaceae	-
MBNT15	-	Spirosomaceae; <i>Taeseokella</i>	-
Pla3 lineage	-	-	-
Planctomycetes	-	-	-
Rhodobacteraceae	-	-	-
Rhodothermaceae	-	-	-
Saprospiraceae	-	-	-
Scalinduaceae; <i>Scalindua</i>	-	-	-
Sneathiellaceae; <i>AT-s3-44</i>	-	-	-
TK17	-	-	-
VadinHA49	-	-	-
67-14	-	-	-
AT-s2-59	-	-	-

A	B	C	D
C86	-	-	-
CCM11a	-	-	-
DEV007	-	-	-
Eel-36e1D6	-	-	-
Flavobacteriaceae	-	-	-
Gemmatimonadaceae	-	-	-
<i>KD4-96</i>	-	-	-
KF-JG30-B3	-	-	-
Kiloniellaceae; <i>Limibacillus</i>	-	-	-
Latescibacteraceae	-	-	-
OM182 clade	-	-	-
P9X2b3D02	-	-	-
Phycisphaeraceae	-	-	-
Rhizobiales Incertae Sedis; <i>Anderseniella</i>	-	-	-
Sandaracinaceae	-	-	-
Solibacteraceae (Subgroup 3)	-	-	-
Subgroup 7	-	-	-
TRA3-20	-	-	-
UBA10353 marine group	-	-	-



Appendix 2.4. Proportion of top 10 most abundant taxa in Beaufort sediments at class level. This bubble plot illustrates the proportion of the 10 most abundant taxa at class level for Beaufort Sea surface sediments.

CHAPTER 3: BENTHIC BACTERIA AND ARCHAEA IN THE NORTH AMERICAN ARCTIC REFLECT FOOD SUPPLY REGIMES AND IMPACTS OF COASTAL AND RIVERINE INPUTS³

3.1 ABSTRACT

Benthic bacteria and archaea can be considered biogeochemical engineers as they play a major role in organic matter (OM) degradation and nutrient cycling. As such, prokaryotic community structure, yielded from 16S rRNA amplicon sequencing, can reflect environmental conditions such as OM composition and quantity, nutrient availability, redox conditions, and natural/anthropogenic contaminants (e.g. petroleum hydrocarbons). To assess prokaryotic community structure, we sequenced marine sediments in the upper 10-cm layer on the northern Bering and southern Chukchi Sea shelves, a high-latitude region undergoing rapid environmental change. We then explored broader spatial patterns in community structure for surface sediments (upper 1cm), incorporating samples from the Northeast Chukchi and Beaufort Seas in relation to environmental variables. Three assemblages were characterized at distinct depth horizons in the upper 10-cm sediment layer from the Northern Bering and Southern Chukchi benthos. One assemblage was exclusively found in sediments at greater than 1 cm sediment depth and contained a relatively higher proportion of anaerobic taxa (e.g. Anaerolineaceae, Desulfobulbaceae, and Desulfosarcinaceae). Overall, community distribution in the upper 10-cm reflected sediment grain size, OM quantity and composition, and possibly the influence of

³ Walker, Alexis M., Mary Beth Leigh, and Sarah L. Mincks. "Benthic bacteria and archaea in the North American Arctic reflect food supply regimes and impacts of coastal and riverine inputs." *Deep Sea Research Part II: Topical Studies in Oceanography* (2022): 105224.

bioturbation. Two assemblages were characterized in surface sediments (upper 1 cm) across the broader Northern Bering and Chukchi Sea study area. A relatively high abundance of anaerobic taxa (e.g. SEEP-SRB4, Subgroup 23, and R76-B128) in one assemblage suggested comparatively suboxic sediments, and the other suggested allochthonous input of phytodetritus based on high abundance of diatom/particle associated microbes (e.g. *Polaribacter*, *Dokdonia*, and *Ulvibacter*), combined with high sediment chl-*a* concentration. This latter assemblage may reflect depositional areas influenced by hydrographic patterns. Prokaryotic community structure across the North American Arctic region highlights regional differences in environmental controls, with food-supply regimes influencing structure on the Bering-Chukchi inflow shelves, in contrast to the Beaufort interior shelves where nearshore heterogeneity (riverine input and terrigenous material) are major drivers of sediment prokaryote communities.

3.2 INTRODUCTION

Benthic prokaryotes, bacteria and archaea, are major mediators of biogeochemical processes at the sediment-water interface and within marine sediments. Unlike their more ephemeral counterparts residing in the water column, sediment prokaryotic communities can reflect both short-term changes in the environment as well as more consistent, long-term environmental features in a given habitat (Fuhrman et al., 2015; Zinger et al., 2011). Although taxonomic identity via 16S rRNA amplicon sequencing is not a reliable predictor of ecological function for most prokaryotes, the presence of certain families or genera can provide some indication of the quantity or quality of available organic matter (OM), trace metals, bioturbation, presence of naturally- or anthropogenically-derived hydrocarbons, and even redox conditions along a sediment depth gradient. (Baltar et al., 2018; Chen et al., 2017; Deng et al., 2020;

Ferguson et al., 2017; Hoffmann et al., 2017; Kostka et al., 2011; Steenbergh et al., 2014).

Despite the vast increase in research coverage of marine prokaryotes over the past few decades, many regions around the globe have yet to be surveyed. In the Northern Bering and Chukchi seas, benthic prokaryotic community structure has been patchily surveyed, with just one study in Northern Bering sediments and a handful of studies in deep-water Chukchi Plateau sediments, leaving the vast majority of the broad, shallow Bering-Chukchi shelf unexplored with respect to bacteria and archaea (Dong et al., 2017, 2015; Park et al., 2014; Zeng et al., 2011).

The Bering-Chukchi shelf is considered a highly productive and ecologically important habitat that supports foraging by an array of organisms including whales, pinnipeds, and sea birds, which in turn support subsistence hunting by indigenous coastal communities (Grebmeier, 2012; Grebmeier et al., 2015, 2006; Grebmeier and Maslowski, 2014). The high productivity of this region is fueled by the northward flow of three major water masses: nutrient-rich Anadyr-influenced water in the west, centrally located summer and winter variants of Bering Sea water, and warmer lower-nutrient Alaska Coastal Water to the east along the Alaskan coast (Gong and Pickart, 2015; Weingartner et al., 2005; Woodgate, 2018).

On productive continental shelves, such as the Northern Bering and Chukchi shelf, redox layering in marine sediments is relatively truncated, as the high OM input fosters shallower suboxic and anoxic conditions where only the upper few millimeters of sediment may be oxygenated (Jørgensen et al., 2005; Orcutt et al., 2011). Redox conditions dictate OM degradation and burial, with accelerated degradation rates in oxic conditions, and higher rates of burial under anoxic conditions (Arndt et al., 2013; Jessen et al., 2017; Zonneveld et al., 2010). Redox reactions and layering are almost completely microbially mediated, and several studies have observed vertical stratification of microbial community structure reflecting different redox

conditions (Durbin and Teske, 2011; Gao et al., 2011; Jorgensen, 2006; Luna et al., 2013; Ravenschlag et al., 2000). In the absence of direct geochemical measurements, benthic prokaryotes may provide a rough sense of redox conditions with sediment depth. Many factors affect how microbes catalyze the reactions that drive redox layering, such as sedimentation rates, bioturbation, sediment type, and bottom/pore-water nutrient concentrations, which can vary widely in time and space (Aller, 1994; Canfield et al., 2005; Edlund et al., 2008; Emerson et al., 2004). As microbial community structure varies across multiple spatiotemporal scales and along biogeochemical gradients, broad baseline surveys of prokaryotic patterns are essential in understanding more localized patterns in a region of interest (Ladau and Elie-Fadrosh, 2019; Shade et al., 2018).

In addition to being a dynamic environment, Arctic shelves are also highly susceptible to climate change effects, which have already manifested in reduced sea-ice extent, species range shifts, and changes in pelagic primary productivity, OM deposition, and hydrography, all of which may have major and varying impacts on macro- to microorganisms (Arrigo and van Dijken, 2015, 2011; Grebmeier, 2012; Moore and Staben, 2015; Nelson et al., 2014). In this ecologically important region that is relatively unstudied with respect to benthic prokaryotes and is experiencing rapid environmental change, we used 16S rRNA amplicon surveys of sediment samples to 1) assess vertical structure of prokaryotic communities in sediments of the Northern (N) Bering and Southeastern (SE) Chukchi Seas, 2) investigate environmental correlates of prokaryotic community structure in surface sediments (0-1 cm) on a broader spatial scale from the N Bering to the Northeast (NE) Chukchi Sea shelf, and 3) provide a contextual baseline for benthic prokaryotes in surface sediments across the North American Arctic from the N Bering to the Eastern (E) Beaufort Sea.

3.3 METHODS

3.3.1 Collection

To assess prokaryotic community structure with sediment depth, samples were collected in June 2018 from eleven stations in the N Bering and SE Chukchi seas as part of the Arctic Shelf Growth, Respiration, and Deposition Rate (ASGARD) field program, a component of the North Pacific Research Board Arctic Integrated Ecosystem Research Program (NPRB IERP; Baker, M.R. et al., 2022; Baker et al., 2020; <https://www.nprb.org/arctic-program/about-the-program>) (Fig. 3.1a). Samples were collected via multi-corer (Ocean Instruments MC-800) with 10-cm diameter tubes. One tube per station was allocated for the assessment of prokaryotic community structure via amplicon sequencing. The top water was siphoned from the surface of the core, which was then sectioned at 1-cm intervals down to 5 cm, then 5-7 cm, and 7-10 cm. Samples were immediately frozen in individual sterile bags at -80°C.

To place the ASGARD study area into broader spatial context, we also analyzed additional samples of surface sediments (upper 1 cm) collected in July 2014 during the annual Canadian Coast Guard Service survey aboard the Sir Wilfred Laurier (SWL) across all five transects of the Distributed Biological Observatory (DBO1-5; Fig. 3.2). Seven of these sample stations directly corresponded to locations sampled in 2018 during ASGARD, allowing for limited comparison of community structure between the two sampling years.

Prokaryotic community structure from the Bering-Chukchi (ASGARD + DBO) was also compared with data from our previous work in the adjacent Beaufort Sea for a broader regional comparison (Walker et al., 2021). Both DBO samples and Beaufort Sea samples were collected in 2014 via 0.1-m² double van Veen grab using a 60-cc, 2.5 cm diameter sterilized syringe and

frozen at -20°C shipboard then stored at -80°C onshore (Grebmeier and Cooper, 2014; Walker et al., 2021). The term North American Arctic will be used in discussions involving all analyses spanning the Bering-Chukchi (ASGARD + DBO) and Beaufort Sea sampling areas.

3.3.2 Environmental Data

Environmental data were provided by each of the respective field programs, with some differences between programs in the suite of variables measured. For ASGARD stations, sediment environmental variables were measured from replicate multi-core deployments at each station, including porosity, grain size, total organic carbon and total nitrogen (TOC, TN mg/g), stable isotope signature ($\delta^{15}\text{N}$, $\delta^{13}\text{C}$), and phytopigment concentration (Chl-*a* and phaeopigment $\mu\text{g/g}$) (Table S1). Porosity calculations and detailed methods for analysis of phytopigment concentration are described elsewhere (Walker et al., 2021, Charrier et al., submitted). TOC, TN, and stable isotope analysis were conducted at the Alaska Stable Isotope Facility at the University of Alaska Water and Environmental Research Center. Sediments were rinsed in 1N HCl to remove carbonates prior to analysis. Elemental and stable isotope analyses were conducted via continuous-flow isotope ratio mass spectrometry using a Thermo Scientific Flash 2000 elemental analyzer and Thermo Scientific Conflo IV interfaced with a Thermo Scientific DeltaV Plus Mass Spectrometer. Stable isotope ratios were reported in δ notation as parts per thousand (‰) deviation from the international standard Vienna Pee Dee Belemnite (VPDB; carbon). Typically, instrument precision is <0.2 ‰.

A single multi-core tube was allocated for grain-size analysis at each ASGARD station. After removing top water, the upper 5 cm of the core was subsampled using a 60-cc syringe with the end cut off. In the onshore lab, the samples were wet- and dry-sieved after homogenization

in 20 mL of 2 g L⁻¹ sodium hexametaphosphate and 30 mL of reverse osmosis (RO) water per 30-40 g of sediment. For wet sieving we used stainless steel 2-mm and 63- μ m sieves; sediment remaining on each sieve was collected into a separate container and dried at 90°C until a constant mass was reached. Dried sediment from the 63- μ m sieve was further sieved through brass stacked sieves (mesh sizes 18, 35, 60, 120, and 230) on a shaker for 10 min. After sediment from each sieve was weighed, the silty-clay fraction was rehydrated with RO water and 30% hydrogen peroxide was added until bubbling ceased in order to remove organic material. The silt-clay fraction was incubated on a block heater (70°C) for 60 minutes to decompose hydrogen peroxide, and then dried at 90°C until constant mass was reached. Mean phi was calculated using the Grain Size Distribution and Statistics (GRADISTAT v.8.0) package (Blott, 2010; Blott and Pye, 2006). Only the parameters mean phi and % silt-clay were used in environmental data analysis.

Bottom-water temperature and salinity data were collected during the ASGARD field program using R/V Sikuliaq's Sea-Bird 9/11 CTD system. Data processing methods are briefly described in Charrier et al. (submitted). Bottom seawater characteristics were also measured via water collected from Niskin bottles during CTD deployments. Samples for nutrients were collected from the deepest sampled depths (~ 5 m above seafloor), filtered through 0.45- μ m cellulose acetate filters, and frozen for later analysis at NOAA's Pacific Marine Environmental Laboratory. Nutrients (nitrate [NO₃⁻], nitrite [NO₂⁻], phosphate [PO₄³⁻], ammonium [NH₄⁺], and silicic acid [H₄SiO₄]) were measured following protocols described in Becker et al. (2020) and utilizing the ortho-phthaldialdehyde (OPA) method for analysis of ammonium. It is important to note that ammonium analysis in frozen samples is less accurate than those carried out onboard. To assess community structure correlations with possible denitrification, we calculated the ratio of ammonium + nitrate + nitrite to phosphate (DIN:P) for each sample.

Environmental data for the DBO sites sampled aboard the SWL are publicly available, and in this study we included bottom water salinity, temperature, and bottom-water nutrient concentrations (mmol/m³; nitrite and nitrate, silicic acid, phosphate, and ammonium), and sediment chl-*a* (mg/m²), TOC (%), TN (%), C:N and grain size (phi 1-4, >5) (Table S2). Details of sample collection and processing for 2014 DBO environmental data are provided elsewhere (Cooper et al., 2014; Grebmeier and Cooper, 2014).

3.3.3 *16S rRNA Amplicon Sequencing*

Genomic DNA was extracted from freeze-dried sediment samples using the Qiagen PowerSoil kit. Sample gDNA and a mock community DNA standard (Zymobiotics) were then run in parallel from gene amplification through library preparation. Revised forward (515FB) and reverse primers (806RB) from the Earth Microbiome Project (EMP) were used to amplify the V4 region following the EMP one-step PCR amplification protocol of the 16S rRNA gene, and library preparation was conducted using iTru adapters (Apprill et al., 2015; Caporaso et al., 2012, 2011; Parada et al., 2016; Walters et al., 2016). Samples were sequenced on an Illumina MiSeq at the UAF Institute of Arctic Biology Genomics Core Laboratory.

Sequenced samples were de-multiplexed using the Mr. Demuxy package (Cock et al., 2009). Demultiplexed sequences were run with mothur v1.43.0 on a high performance-computing cluster through UAF Research Computing Systems using a modified MiSeq standard operating procedure (Schloss et al., 2009). The sequencing error rate was calculated using the mock community samples which were subsequently removed prior to clustering. OTUs were clustered at 100% similarity using the OptiClust option in mothur, taxonomy was assigned to

OTUs using the SILVA 138 mothur formatted reference database with a bootstrap cutoff of 100% (Edgar, 2018; Glöckner et al., 2017; Wang et al., 2007; Westcott and Schloss, 2017).

Three OTU tables were created using this method so that we could subsample to a higher number of sequence reads with the ASGARD samples and assess surface sediment samples among all the Bering-Chukchi shelf sites (ASGARD + DBO) prior to clustering OTUs with our published dataset from the Beaufort Sea. Therefore, an OTU table was created with each of the following: ASGARD samples only, all Bering-Chukchi surface-sediment samples (ASGARD + DBO), and all North American Arctic surface (0-1 cm) sediment samples (ASGARD + DBO + Beaufort Sea). The samples in the resulting OTU tables were normalized to 29,000, 16,000 and 16,000 sequences respectively and converted to relative abundances. The OTU table with ASGARD samples was used to investigate how N. Bering and SE Chukchi benthic prokaryotic community structure varied with sediment depth, whereas the other two OTU tables were used to evaluate regional-scale spatial patterns in surface sediments (0 – 1 cm) across the Bering-Chukchi-Beaufort study area.

3.3.4 Data Analysis

Statistical analyses and figure generation were all conducted using R (R Core Team, 2017). To assess the vertical (with depth in sediments) and horizontal spatial variation in prokaryotic community structure in Chukchi sediments as well as compare community structure between Chukchi and Beaufort sediments, we used hierarchical clustering analysis with the ward.D2 method using the vegan package (Murtagh and Legendre, 2014; Oksanen et al., 2007). The validity of the clusters, within-cluster dispersion, and significance differences in composition between clusters were investigated via a silhouette test, dispersion test (betadisper),

and PERMANOVA (adonis) respectively (Oksanen et al., 2017). To investigate how taxonomic composition differed with sediment depth, we looked at individual vertical profiles of relative abundance for each of the top-100-most-abundant family-level taxa that exhibited clear changes with sediment depth. Indicator taxa analysis was performed using the *indicspecies* package to identify OTUs that distinguished clusters within Northern Bering and Southern Chukchi Sea sediments and in surface sediments across the broader Bering-Chukchi (De Cáceres et al., 2010; De Cáceres and Legendre, 2009). The *multipatt* function was used to identify taxa specific to a single cluster, or indicative of combinations of clusters, with a significance of ≤ 0.001 and a strength of ≥ 0.850 (i.e., $\geq 85\%$ probability of occurrence within a given cluster or combination of clusters; Cáceres and Legendre, 2009). In order to assess how environmental parameters influenced community structure with depth in sediments, we qualitatively compared vertical assemblage patterns (Groups 1-4) and vertical environmental profiles using data from Table S1. To identify significant environmental correlates of prokaryotic community structure on a broader spatial scale with Bering-Chukchi Sea samples we used Canonical Analysis of Principle coordinates (CAP) with a Bray-Curtis distance matrix using the *capscale* function in the R package *vegan*. The best model for CAP was identified based on variance inflation factors for each environmental parameter and a forward and backward stepwise model selection via permutation tests on adjusted R^2 and p -values using the *ordistep* function. The significance of the correlations identified by CAP was investigated in R using PERMANOVA (*adonis* function), and correlation strengths were calculated using the *cor* function (Oksanen et al., 2017). CAP was conducted using only surface sediments (0-1cm) from ASGARD and DBO sites combined, and a subset of environmental variables that were consistently sampled in both field programs (Table S3.2).

3.4 RESULTS

3.4.1 Vertical Distribution of Prokaryotic Communities Within Sediments (N Bering, SE Chukchi)

When vertical prokaryotic community structure was assessed within the ASGARD study area, three clusters, i.e. assemblages, were identified (Figs 3.1b, S3.1, and S3.2). Two assemblages, A and B, were restricted to the upper 5-cm layers, and one (assemblage C) exclusively occurred in subsurface sediments (below 1 cm). These assemblages occurred at different sediment depths among stations, but stations could be grouped based on similar distribution of taxa with depth (Fig. 3.1b). At the coastal stations in the Southeast Chukchi Sea (Group 1; CL3, CL1, DBO3.3, IL4), surface assemblage B occupied the upper 1 cm, with assemblage C found in 1-5-cm layers. Farther offshore at stations DBO 3.6 and DBO 3.8 (Group 2), surface sediments were occupied by a different assemblage (A), which was also distributed more deeply into sediments (0–7 cm). At two offshore stations farther south (group 3; CNL3 and CNL5), assemblage B occupied the entire 0-5-cm layer sampled. At stations south of the Bering Strait (Group 4; DBO 2.2, DBO 2.4, and CBE3), only surface assemblages A and B were observed, with assemblage A occupying all sampled depths with the exception of DBO2.4 where assemblage B was found in the upper 1-cm layer. These station groupings were used to further investigate the distribution of specific taxa with depth in sediments.

Ten of the 100 most abundant families across sediment horizons showed clear qualitative variations in relative abundance with sediment depth, based on qualitative assessment of relative-abundance plots for each taxon (not shown). Stations with similar vertical distribution of assemblages A, B and C also exhibited similar taxonomic changes with depth (Fig. 3.4).

Overall, the families Chitinovibrionaceae, Flavobacteriaceae, Nitrosopumilaceae, and Psychromonadaceae decreased in relative abundance with sediment depth, while Anaerolineaceae, Desulfobulbaceae, and Desulfosarcinaceae increased with sediment depth (Fig. 3). These trends are most apparent for station Groups 1 and 2, where the magnitude of change in relative abundance with sediment depth was greater than for Groups 3 and 4. The following families were most abundant within certain station groups: Anaerolineaceae (Group 1), Thiotrichaceae (Groups 2 and 3), Chitinovibrionaceae and Psychromonadaceae (Group 3), Nitrosopumilaceae and Pirellulaceae (Group 4).

Three environmental variables exhibited significant correlations ($P < 0.001$) with community structure when plotted with the four station profile groups: porosity ($R^2 = 0.59$), TOC ($R^2 = 0.55$), and TN ($R^2 = 0.45$). Overall, porosity, TOC, and TN values were higher for Groups 1 and 2, and lower for Groups 3 and 4 (Fig. 3.4).

3.4.2 Spatial Distribution of Sediment Prokaryotic Communities on a Broader Spatial Scale

When surface sediments (0-1cm) from the ASGARD study area and DBO transects were examined separately via hierarchical clustering, only the two surface assemblages, A and B, were observed (Fig. 3.2). Of the seven stations that were sampled in both 2014 and 2018, only one (DBO2.2) differed in assemblage designation between years. When surface sediments of all samples from the Bering-Chukchi were combined and analyzed via hierarchical clustering, all ASGARD samples were designated as assemblage B (Fig. S3.3). We compared the most abundant 25 families between assemblages A and B, and found that Desulfobulbaceae, Sva1033, Desulfocapsaceae, Desulfosarcinaceae Kiritimatiellaceae, Thermoanaerobaculaceae, BD2-2, and Anaerolineaceae were more abundant in assemblage A, whereas Rubritaleaceae,

Psychromonadaceae, Pirellulaceae, Rhodobacteraceae, and Colwelliaceae were more abundant in assemblage B (Fig. S3.4).

Major differences between assemblage A and B were less apparent at the family level, and were further explored at the genus level by comparing relative abundance of the most abundant taxa and indicator taxa analysis (Fig. 5). The most abundant genera in assemblage A were *SEEP-SRB4*, Subgroup 23, *R76-B128*, *MSBL3*, *Actibacter*, and *Maritimimonas*. The most abundant genera in assemblage B were *Dokdonia*, *Colwellia*, *Persicirhabdus*, *Formosa*, *Portibacter*, *Roseibacillus*, *Roseobacter clade NAC11-7*, *Rubritalea*, *Sulfitobacter*, *Ulvibacter*, *Yoonia-Loktanella*, *Polaribacter*, *Rubripirellula*, *Blastopirellula*, *Bythiopirellula*, *Rhodopirellula*, *Geopsychrobacter*, and *Oleiphilus*. Indicator taxa for assemblage A were *R76-B128*, *MSBL3*, and *Blastopirellula*, *Dokdonia*, *Rubritalea*, *Geopsychrobacter*, and *Oleiphilus* for assemblage B. Iron reducing (*Geopsychrobacter*) and oil-degrading (*Oleiphilus*) taxa were markedly more abundant in stations CL3, CL1, DBO3.3 and IL4, offshore of Pt. Hope Alaska (Fig. 3.6).

CAP performed on all Bering-Chukchi surface sediment samples indicated that temperature, salinity, Chl-*a*, NH₄⁺, PO₄³⁻, DIN:P, H₄SiO₄, and silt-clay were significant correlates across four CAP axes and accounted for 20% of the variance in community structure ($R^2 = 0.37$, adj. $R^2 = 0.20$, $P < 0.001$). Differences between assemblage A and B were most apparent along the CAP1 axis such that assemblage A stations were generally correlated with high % silt-clay sediments, in cooler bottom water, and higher nutrient concentrations (NH₄⁺, PO₄³⁻, and H₄SiO₄), whereas assemblage B sediments were sandier and characterized by a higher concentration of fresh phytodetritus (Chl-*a*) and warmer bottom waters (Fig. 3.7a).

Variation within assemblage A was most apparent on the CAP2 and CAP4 axes, with separation between DBO1 (St Lawrence Island), DBO3 (SE Chukchi Sea biomass hot spot), and DBO4 (NE Chukchi Sea) stations (Fig. 3.7a, b). The distribution of assemblage A stations along the CAP4 axis indicated that DBO3 sediments had lower Chl-*a* and higher bottom-water DIN:P, whereas the two DBO1 stations nearest to St. Lawrence Island were highly correlated with Chl-*a* and moderately correlated with NH₄⁺ concentration and lower DIN:P in bottom waters. Along the CAP2 axis, stations designated as assemblage A in the DBO4 area were highly correlated with elevated bottom water H₄SiO₄. DBO3 stations had higher bottom-water salinity and NH₄⁺ with siltier sediments, and DBO1 stations were distributed more closely along the midpoint of the axes suggesting overlapping characteristics.

Variation within assemblage B was exhibited along the CAP 3 and CAP4 axes (Fig. 3.7a, b). Along the CAP4 axis, ASGARD nearshore samples and those just north of the Bering Strait were in sediments with high Chl-*a* concentration and low DIN:P in bottom waters, whereas DBO2 (N Bering) and DBO3 stations were in high DIN:P bottom waters with low sediment Chl-*a*. ASGARD and DBO3 samples from further offshore (e.g. DBO3.6, 3.8) were spread along the CAP4 axes, suggesting that these stations are located within an environmental gradient. Along the CAP3 axis, DBO2 and ASGARD stations were in more saline and higher-nutrient waters overlying siltier sediments, compared to nearshore DBO3 stations.

3.4.3 Chukchi vs. Beaufort Sediments

Three major homogeneously dispersed clusters, or prokaryotic assemblages, were identified in surface sediments when additional samples were incorporated from the Beaufort Sea, including a Chukchi-Bering assemblage and two Beaufort Sea assemblages: nearshore and offshore Beaufort (Fig. 3.8). Substructure within these three assemblages suggested the Bering-

Chukchi included a similar community at DBO1 and DBO4, and another community DBO5, DBO3, and DBO2, with ASGARD samples clustering among the nearest DBO stations nearest to them. One station in DBO4 and another station in DBO5 did not fit this pattern and were designated under the opposite assemblage. The Beaufort Sea offshore samples encompassed distinct assemblages east and west of the Mackenzie River.

3.5 DISCUSSION

Three prokaryotic assemblages were detected in the upper 10 cm of northern Bering and southern Chukchi sediments; two assemblages (A and B) that were exhibited in surface sediments down to 7 cm, and one exclusively subsurface (below 1cm) assemblage (C). A qualitative assessment of vertical profiles for sediment variables did not clearly identify specific sediment characteristics associated with the three prokaryotic assemblages, but rather indicated assemblage Groups with similar vertical structure in the prokaryotic community (Figs. 3.1b, 3.3). Stations characterized by Groups 1 and 2 were found in silty sediments with high porosity and high OM content, including higher nitrogen, and were the only stations to exhibit subsurface assemblage C. Groups 3 and 4 were found in sandier sediments with lower OM and nitrogen content and exhibited either assemblage A or B throughout.

Assemblages A and B were also found in surface sediments (0-1 cm) throughout the broader Bering-Chukchi study area (ASGARD + DBO sites). Although these field programs occurred four years apart, the same assemblages were found at the seven stations sampled in both years, indicating that prokaryotic community structure on this spatial scale is likely a consistent feature of these surface sediments (Fig. 3.2). The strongest, significant correlations with environmental parameters indicated that assemblage A was characterized by silty sediments in

cooler bottom water with higher nutrient concentrations (NH_4^+ , PO_4^{3-} , and H_4SiO_4), whereas assemblage B was associated with warmer bottom waters and sandier sediments with higher Chl-*a* content, indicating fresh phytodetritus deposition (Fig. 3.7a). In the following sections, we dive deeper into taxonomic composition in relation to significant environmental correlates for prokaryote communities with sediment depth and within Bering-Chukchi surface sediments, and provide a broader context for distribution of benthic microbes in surface sediments across the North American Arctic.

3.5.1 Vertical Distribution of Prokaryotic Communities Within Sediments (N Bering, SE Chukchi)

Vertical structure of prokaryotic communities in the ASGARD study area (Fig. 3.1a) reflects OM loading, sediment grain size, and potentially the composition of OM as well as effects of bioturbation on sediment properties. Sites with higher OM content (Groups 1 and 2) exhibited a marked shift from aerobic to anaerobic taxa with sediment depth. Subsurface assemblage C occurred only in these siltier OM-rich sediments and was dominated by strict anaerobes, including OTUs from the bacterial families Anaerolineaceae, often associated with heavy OM loading, and the sulfate reducers Desulfobulbaceae and Desulfosarcinaceae (Kuever, 2014; Sinkko et al., 2013; Wang et al., 2017; Watanabe et al., 2021). The genus *Electrothrix*, a member of the Desulfobulbaceae family, was relatively more abundant at stations where surface assemblage A was predominant (Groups 2 and 4). *Electrothrix* spp. are known as cable bacteria, which form a cable-like chain between deeper sulfidic sediments and surficial oxic sediments, performing electrogenic sulfur oxidation in the former and oxygen reduction in the latter (Burdorf et al., 2017; Nielsen et al., 2010; Pfeffer et al., 2012). The metabolism of *Electrothrix* contributes to the formation of three distinct redox zones within the sediment: oxic, suboxic, and

sulfidic/anoxic (Burdorf et al., 2017; Nielsen et al., 2010). The abundance of *Electrothrix* thus suggests that assemblage A reflects relatively suboxic conditions supporting sulfur oxidation, which extend from the surface to >5 cm depth, as opposed to an abrupt and shallow oxic/ anoxic boundary at 1cm (Group 1 sites) or a deeper oxic zone down to 5 cm (Group 3; Fig. 3.1b).

Sandy sediments with low OM and nitrogen content (station Groups 3 and 4) exhibited very little change in the relative abundance of taxa along the sediment depth profile and hosted just one assemblage throughout. Though low-OM sandy sediments generally exhibit more relaxed redox layering, the relatively uniform taxonomic profiles exhibited at these sites, as well as in siltier high-OM stations in Group 2, suggest bioturbation may also be homogenizing conditions across the upper layers of sediment (Kristensen, 2000). Bioturbation (i.e. advective mixing of sediments via movement of metazoan infauna) includes multiple activities such as burrowing, deposit-feeding, and excretion that can alter sediment biogeochemistry and thus redox layering (Aller, 1994, 1982; Kristensen et al., 2012). Based on macrofaunal sampling conducted in parallel during the ASGARD field program (Charrier et al., submitted), stations in Groups 2 and 3 were dominated by larger-bodied burrowing infauna such as bivalves. Bivalve biomass was highest at station CNL3 (Group 3), just north of Bering Strait and at Group 2 stations (DBO 3.6 and DBO 3.8; Charrier et al., submitted). Similarly, the homogeneous distribution of microbial taxa throughout the upper 5 cm of sediment was also observed at station DBO 2.2 (Group 4), where ampeliscid amphipods dominate the macrofaunal biomass (Charrier et al., submitted). The dense networks of burrows created by these amphipods have a significant impact on oxygen and nutrient fluxes (Grebmeier and McRoy, 1989), which surely influence distribution of microbes at this sandy site. In contrast, biomass of small polychaetes was high at the nearshore Group 1 stations, where a shallow transition to the subsurface prokaryote

assemblage (C) was observed; these smaller-bodied burrowers may also play an important role in bioturbation at these coastal sites, albeit over a more limited depth range in siltier, high-OM sediments.

In addition to homogenizing and oxygenating sediments through bioturbation, the high biomass of bivalves in the deeper ~5 – 7-cm sediment layers may enhance OM concentration at depth through subduction of detritus and/or deposition of waste products. At station CNL3 (Group 3) in particular, we found the highest relative abundance of OTUs belonging to the bacterial family Chitinivibrionaceae, typified by *Chitinivibrio*. This genus is composed of anaerobic bacteria which use chitin as their sole substrate, and have thus far been sequenced from livestock gut rumen and anoxic soda lake sediments (Henderson et al., 2019; Sorokin et al., 2020, 2014). High abundances of chitin degrading microbes of the order Chitinophagales, as well as members of the orders Rhodobacterales and Thiotrichales, have been found in clam biodeposits (e.g. feces, pseudofeces; (Murphy et al., 2019). Though the family Chitinivibrionaceae is not within the order Chitinophagales, members of both groups anaerobically degrade chitin. Furthermore, CNL stations also exhibited the highest abundances of OTUs within the Rhodobacteraceae family (order Rhodobacterales) and the second highest abundances of OTUs within the sulfur-oxidizing Thiotrichaceae family (order Thiotrichales), which supports the presence of clam biodeposits (Murphy et al., 2019). Chitinivibrionaceae may also signal allochthonous chitin detritus such as zooplankton carapaces. Experimental evidence shows that addition of chitinous detritus to Arctic sediments leads to increased abundance of chitin-degrading bacteria and members of the Psychromonadaceae and Colwelliaceae families (Hoffmann et al., 2017), which were also comparatively more abundant in CNL stations (Group 3).

The effects of bioturbation on surrounding sediment microbes may vary among different types of burrowing infaunal organisms. In contrast to the activities of bivalves, many infaunal polychaetes construct burrows, which increases the sediment surface area available for aerobic nitrification and can thus increase microbial nitrification rates and the abundance of nitrifying bacteria and ammonia oxidizing archaea (Aller, 1988; Dale et al., 2019; Gilbertson et al., 2012). Polychaetes also produce mucus which can stimulate ammonium production and have a species-specific effect on nitrification (Gilbertson et al., 2012). Relatively small, motile burrowing polychaetes were concentrated in the surface layers at stations in Groups 1 and 4 (Charrier et al., submitted), coincident with the highest relative abundances of the nitrifying archaea, *Candidatus Nitrosopumilus*. In addition, nitrifying bacteria in the genus *Nitrospira* were twice as abundant at Group 4 stations (Daims, 2014; Daims et al., 2015). Microbes in the *Candidatus Nitrosopumilus* and *Nitrospira* genera can perform complete nitrification, oxidizing ammonia to nitrate (Daims et al., 2015; Stahl and de la Torre, 2012). This pattern is consistent with results of sediment-core incubation experiments conducted during ASGARD, which measured the highest efflux of nitrate (7x the mean concentration across all stations) at DBO 2.4 (Group 4; Mincks et al. unpublished data), where high biomass of motile burrowing polychaetes was also detected in the surface layer.

Overall, sediment characteristics and interactions with the macrofaunal community seem to explain turnover in microbial taxonomic composition with sediment depth and the occurrence of the subsurface assemblage (C). However, these factors do not clearly explain the distribution of the two surface assemblages A and B within the ASGARD study area. We incorporated samples from a broader area to further investigate regional distribution of these surface assemblages.

3.5.2 Spatial Patterns in Bering-Chukchi Surface Sediments

Spatially overlapping samples from two different years suggests that prokaryotic assemblage patterns, remain broadly consistent through time at a given site. Moreover, incorporation of the additional DBO samples with the ASGARD dataset yielded the same assemblages A and B in surface sediments over the broader study area that included sites farther south in the Bering Sea (DBO 1) and into the Northeast Chukchi (DBO4 and 5). Distribution of these two assemblages was best described by sediment grain size, fresh phytodetritus (Chl-*a*), and bottom water characteristics (temperature, NH_4^+ , PO_4^{3-} , and H_4SiO_4). The majority of assemblage A stations were located beneath nutrient-rich Anadyr-influenced waters, and assemblage B stations were commonly located in nearshore areas more likely influenced by less saline, low-nutrient Alaska Coastal Water (Danielson et al., 2017). However, variation in community structure among assemblage B sites reflects differentiation between Alaska Coastal Water (ACW) and an Anadyr-influenced mixed water mass known as Bering-Chukchi Summer Water (BCSW), which is intermediate with respect to salinity and temperature and higher in nutrients than the ACW (Danielson et al., 2017). Similarly, variation among assemblage A sites indicated some differences between DBO4 stations in the NE Chukchi, which had lower salinity and higher H_4SiO_4 concentration suggesting influence of sea-ice melt and Chukchi Shelf Winter Water (high- H_4SiO_4 bottom water), compared to offshore DBO3 stations with Anadyr-influenced bottom water (Danielson et al., 2017).

Analysis of environmental correlates also suggests that microbial community structure may reflect denitrification in sediments at certain stations. Bottom water with low DIN:P ratios may indicate active denitrification in underlying sediments, as nitrate and nitrite concentrations are drawn down (reduced) while phosphate concentrations remain relatively stable (Codispoti et

al., 1991; Cooper et al., 1999; Souza et al., 2014). Low DIN:P ratios were moderately correlated to nearshore DBO3 stations (DBO 3.1-3.6), CL1, CNL3, IL4, CL3, DBO2.4, and DBO1 stations nearest to St. Lawrence Island (DBO1.6 and 1.8) (Fig. 3.7). When we investigated indicator taxa from these specific sites, 11 taxa were yielded, however they could not be classified past family-level and therefore we could not reliably attribute denitrification as a potential function of these microbes. Additional investigation into these taxa, via meta- or transcriptomic work could shed light on whether denitrification could be or is occurring. Thus far, studies investigating denitrification have largely focused on the NE Chukchi and broader Bering shelves, so it is difficult to draw direct comparisons with our findings (Chang and Devol, 2009; Devol et al., 1997; McTigue et al., 2016; Mills et al., 2015). However, bottom-water DIN:P ratios at our stations near St. Lawrence Island and Barrow Canyon area are consistent with reports of relatively high nitrogen deficits and denitrification rates in these areas (Codispoti et al., 1991; Cooper et al., 1999; Horak et al., 2013; Mordy et al., 2021; Souza et al., 2014). While stations in Barrow Canyon were not included in our CAP analysis due to missing Chl-*a* values, the two nearshore DBO5 sites (Barrow Canyon area) did exhibit the lowest DIN:P ratios of any sites sampled here. Low DIN:P ratios may result from processes other than denitrification, including bottom water residence time (Mordy et al., 2021) or the abiotic desorption of PO₄ from particles results in high bottom water PO₄ concentration and thus lower DIN:P ratios (Defforey and Paytan, 2018). Bottom water and sediment phosphate (dissolved and particulate) values tend to be high in the North American Arctic, but the DIN:P ratios overall are still typically within range of the Redfield ratio (Cooper et al., 1999; Goñi et al., 2019; Piper et al., 2016),

Genus-level taxonomic composition of prokaryotes in surficial sediments from across the broader Bering-Chukchi study area provides further evidence that assemblage A reflects low-

oxygen sediments relative to assemblage B locations. Anaerobic taxa such as SEEP-SRB4, Subgroup 23, R76-B128, MSBL3 and uncultured genera of the families Anaerolineaceae and Desulfobulbaceae were more frequently found at sites designated as assemblage A, and in higher relative abundance (Fig. 5; Dedysh and Yilmaz, 2018; Kuever, 2014; Schreiber et al., 2010; Sinkko et al., 2013; Van Vliet et al., 2019). Uncultured Desulfobulbaceae and the SEEP-SRB4 clade are sulfate-reducing bacteria, with the latter group most commonly sequenced from cold seeps where they may couple sulfate reduction to the anaerobic oxidation of non-methane and methane hydrocarbons (Kleindienst et al., 2012; Petro et al., 2019; Ruff et al., 2015; Schreiber et al., 2010). R76-B128, MSBL3, and uncultured Anaerolineaceae bacteria have largely been studied in the context of sludge digesters, but have been sequenced in marine sediments where they are thought to indicate heavy OM loading (Giongo et al., 2020; McIlroy et al., 2017; van Vliet et al., 2019a; Vetterli et al., 2015; Zinke et al., 2018). Though OM loading was not a significant correlate of prokaryotic community structure, sediment TOC concentrations were significantly higher at assemblage A stations, suggesting that these stations did experience heavier OM loading.

In contrast, assemblage B exhibited comparatively high abundances of diatom-associated aerobic bacteria such as *Polaribacter*, *Persicirhabdus*, *Formosa*, *Dokdonia*, *Loktanella*, *Portibacter*, *Ulvibacter*, *Roseobacillus*, and *Rubripirella* (Figure 5) (Alejandre-Colomo et al., 2020; Cheng et al., 2021; Crenn et al., 2018; Purohit et al., 2020; Tanaka et al., 2014; Unfried et al., 2018), which is consistent with the strong, positive correlation between assemblage B stations and sediment Chl-*a*. Several of these taxa have also been linked to marine microplastics (Mu et al., 2019). In Northern Bering and Chukchi Sea sediments, the most abundant microplastics were found offshore of Point Hope (near our stations CL1 and nearshore DBO3)

and the Diomedes Islands north of Bering Strait (CNL3, CNL5, DBO2), which were characterized by assemblage B including higher diversity and abundance of aerobic microplastic-associated taxa such as *Dokdonia*, *Portibacter*, *Colwellia*, *Persicirhabdus*, *Rubripirellula*, and *Roseobacter* (Basili et al., 2020; Cheng et al., 2021; Harrison et al., 2014; Kallscheuer et al., 2020; Oberbeckmann et al., 2016; Purohit et al., 2020).

Indicator taxa from both assemblages included microbes reported to have similar functional potential, with more taxa being associated with anaerobic metabolism in assemblage A and aerobic metabolism in assemblage B. For instance, in assemblage B, organisms such as *Bacteroidetes* spp. (*Polaribacter*) and *Planctomycetes* spp. (*Rhodo-* and *Blastopirellula*) are known to aerobically breakdown sulfated polysaccharides, whereas indicator taxa associated with assemblage A, both the R76-B128 and MSBL3 clades, anaerobically break down sulfated polysaccharides (Jeske et al., 2013; van Vliet et al., 2020, 2019a; Wegner et al., 2013; Xing et al., 2015). Sulfated polysaccharides are exuded by micro- and macroalgae and bacteria, comprising a large proportion of marine snow, and are important in the global carbohydrate cycle. It is useful to know which organisms are capable of degrading them in both oxic and anoxic conditions, as these sulfate groups typically act as a barrier to organic matter breakdown by other microbes (Arnosti et al., 2020; van Vliet et al., 2019a). Therefore, these taxa characteristic of both assemblages A and B suggest that both communities are involved in the breakdown of sulfated polysaccharides but are likely performing this role under different redox conditions given the predominance of anaerobic taxa (assemblage A) over aerobic taxa (assemblage B).

Indicator taxa analyses conducted separately for ASGARD and DBO samples also revealed higher relative abundances of obligate oil-degrading bacterial taxa (*Oleiphilus* and

Oleispira) at stations near Pt. Hope (DBO3.3, CL3, IL4) compared to all other stations (Fig. 3.6), although much lower than abundances exhibited following acute oil exposure (Golyshin et al., 2002; Walker in prep). *Oleispira* was only found at trace abundances throughout the region. It is a relatively ubiquitous oil degrader commonly found in cold and polar habitats, and aerobically degrades branched and straight alkanes (Guibert et al., 2012; Ribicic et al., 2018; Yakimov et al., 2007, 2003). *Oleiphilus* has been found in uncontaminated sediments underlying oligotrophic waters, and aerobically degrades both linear or branched aliphatic hydrocarbons (alkanes, alkenes, and alkynes) (Golyshin et al., 2002; Gutierrez, 2019; Head et al., 2006; Toshchakov et al., 2017; Yakimov et al., 2007). Elevated abundance of *Oleiphilus* relative to *Oleispira* suggests higher concentrations of certain hydrocarbon compounds at these stations. Given the interest in petroleum resource extraction in this region, we considered the possibility of natural seeps or oil contamination via exploratory drilling as potential sources of petroleum exposure for these sediment communities (Goldsmith et al., 2009). However, oil degraders were most abundant in surface sediments (0-1 cm), and are not likely responding to a deeper hydrocarbon source. Alternatively, obligate oil degraders may be responding to phytoplankton-derived alkanes and alkenes (Rontani et al., 2014, 2018; Volkman et al., 1994), which have been detected in this area as high concentrations of highly branched isoprenoids (HBI), specifically HBI III which is a C_{25:3} alkane typically utilized as a biomarker for pelagic phytoplankton (Koch et al., 2020; Meskhidze et al., 2015; Rontani et al., 2018). Consistently high deposition of phytodetritus and associated HBI III in this area may result from slow currents and subsequent settling of phytodetritus (Koch et al., 2020); slow currents (< 0.05 cm s⁻¹) are reported around Pt. Hope (Charrier et al., submitted). Thus far, *Oleiphilus* has not been shown to degrade HBI, but does have genes which are upregulated during isoprenoid degradation in other taxa well known to degrade HBI (Alvarez

et al., 2009; Toshchakov et al., 2018; Yakimov et al., 2007). The reportedly high concentrations of HBI III and Chl-*a* combined with the elevated abundances of *Oleiphilus* in this area suggests it is capable of degrading phyto-derived alkanes and alkenes.

Indicator taxa may also reflect other environmental characteristics that are influencing prokaryotic communities that were not measured here. For example, elevated abundance of *Geopsychrobacter* was observed in specific locations (Fig. 3.6d). This genus is comprised of cold-tolerant anaerobic bacteria which can produce electrode-harvestable electrons, reduce iron and manganese, and form magnetite when reducing crystalline Fe (III) (Greene, 2014; Holmes et al., 2004). High abundances of these bacteria were observed near Pt. Hope (DBO3, CL1) and Pt. Barrow, which overlap with areas that have exhibited some of the highest surface sediment iron concentrations in the region (Fig. 3.6d,e) (Astakhov et al., 2013). In addition, the Chukchi Sea shelf is relatively replete with iron-rich diagenetic and hydrothermal ferromanganese nodules (Cui et al., 2020; Kolesnik and Kolesnik, 2015). Diagenetic processes favoring the precipitation of metals via sediment redox reactions are largely catalyzed by microbes (Burdige, 1993; Hein et al., 1997; Lyu et al., 2021); therefore, manganese and iron reduction by microbes may catalyze the formation of ferromanganese nodules (Burdige, 1993; Molari et al., 2020; Templeton et al., 2005). Several studies report specific microbes associated with metalliferous nodules, including *Geopsychrobacter* which was associated with ferromanganese nodules on the Arctic shelf in the Kara Sea (Shulga et al., 2021; Templeton et al., 2005; Tully and Heidelberg, 2013). Iron reduction can also lead to an efflux of iron-bound phosphate from sediment pore waters, which could be contributing to the low DIN:P ratios observed at nearshore DBO3 and CL1 stations, further highlighting the complex role benthic microbes play in marine biogeochemical cycling (Jensen et al., 1995; Rozan et al., 2002).

3.5.3 Prokaryotic Community Structure in North American Arctic Sediments

The distribution of prokaryotic assemblages across the broader North American Arctic region provides further insights into the factors influencing community structure on different shelf systems. Beaufort and Bering-Chukchi sediments represent two different shelf systems: narrow interior shelf and shallow inflow shelf systems, respectively (Carmack and Wassmann, 2006). The northward advection of nutrient-rich waters supports high primary productivity and a robust benthic faunal population on the Bering-Chukchi Shelf, whereas turbidity, terrigenous material, depth variation, and longer sea-ice cover promote a latitudinally and longitudinally heterogeneous Beaufort Shelf environment which is comparatively lower in primary productivity and benthic biomass (Carmack and Wassmann, 2006; Goñi et al., 2013). The different prokaryotic community structures observed underscored the heterogeneity of the Beaufort Shelf, with sediments exhibiting distinct nearshore and offshore shelf assemblages, whereas Bering-Chukchi sediments exhibited just one assemblage throughout (Figure 3.8; Walker et al., 2021). The nearshore Beaufort Sea is influenced by sea ice, coastal erosion, and several rivers including the Mackenzie River (4th largest in the Arctic), so this distinction between prokaryotic communities is not surprising (Dunton et al., 2006; Macdonald and Thomas, 1991; McClelland et al., 2014). Substructure within the offshore Beaufort shelf assemblage indicates a division between communities that occurred either west or east of the Mackenzie River, further highlighting the major impact of this river even in offshore shelf sediments near the slope (Walker et al., 2021)

Two sub-groups within the Bering-Chukchi assemblage almost exactly corresponded to two predominant food-supply regimes recently described by Feng et al. (2021), where long-term (decades) patterns of high biomass and abundance of benthic macrofauna have been observed;

from north to south are the Barrow Canyon (BC), Northeastern Chukchi Sea (NECS), Southern Chukchi Sea (SECS), Chirikov Basin (Chirikov), and St. Lawrence Island Polyna (SLIP) hotspots (Feng et al., 2021; Grebmeier, 2012; Grebmeier et al., 2015, 2006). The local production of particulate food characterizes the NECS (DBO4) and SLIP (DBO1) hotspots, while the advective-supply regime encompasses the BC (DBO5), SECS (DBO3), and Chirikov (DBO2) hotspots (Feng et al., 2021). We saw this same pattern reflected in prokaryotes, with the exception of one nearshore station in the NECS (DBO4) hotspot that clustered with those in the advective-supply regime and one offshore station in the BC (DBO5) hotspot that clustered with the local-supply regime (Fig. 3.8). The local-supply regime is characterized by comparatively weaker currents, greater influence of sea-ice algae, and greater reliance on locally produced organic carbon, whereas the advective regime is largely reliant on horizontal transport of organic carbon produced “upstream” in the Northern Bering Sea and deposited “downstream” (NE Chukchi), with benthic consumption exceeding local primary production (Feng et al., 2021). Prokaryote community structure at the anomalous DBO4 station may reflect an advective-supply regime due to its proximity to the Alaska Coastal Current, similar to DBO5 stations nearer to shore in the BC hotspot which are also within the advective-supply food regime. Conversely the offshore station in the BC hotspot may reflect a local-supply food regime in waters closest to Barrow Canyon which are less likely affected by the faster moving currents along the coast (Edlund et al., 2008; Emerson et al., 2004). It is likely that the suboxic assemblage (A) and the diatom/particle-associated assemblage (B) are reflective of the local-supply and advective-supply food regimes respectively. On a smaller spatial scale within the Bering-Chukchi shelf, microbial assemblages are likely reflecting the complex flow through the Bering Strait which results in a

combination of local and advective food sources, particularly with respect to the DBO3 stations in the SECS hotspot.

3.6 CONCLUSIONS

The vertical distribution of microbial communities within the upper 10 cm in Bering-Chukchi sediments reflects OM and nitrogen loading, sediment type, and OM type (fresh phytodetritus or chitinous detritus/biodeposits) and provides a rough indication of redox conditions; sediment conditions are also likely influenced by bioturbation. Combined, these insights can be used to predict areas in the sediment where high carbon burial or mineralization is more likely to occur. For instance, nearshore stations with silty clay, high OM and TN, and bioturbation via polychaetes (Group 1) would likely exhibit higher OM burial rates, and slower OM degradation rates below the 1-cm sediment layer due to the prevalence of anaerobic microbes. Conversely, sandy sediments with lower OM and TN with a high biomass of bivalves, found at offshore stations north of the Bering Strait, would likely exhibit less burial and faster rates of OM degradation throughout the 5-cm sediment horizon.

Broader spatial coverage of Bering-Chukchi surface sediments from two different years suggests that there is a long-term/consistent two-assembly prokaryotic community structure, one which is representative of comparatively suboxic sediments (A) and one which is characterized by allochthonous input as evidenced by the abundance of diatom/particle-associated microbes (B). Although hydrography over the Bering-Chukchi shelf is complex and exhibits both intra- and interannual variation, the overall distribution of prokaryotic assemblages reflected the consistent feature of cooler nutrient rich Anadyr-influenced water offshore, low-nutrient warmer water nearshore, and the associated depositional conditions. Zooming in to a

smaller scale, looking at variation within each assemblage suggests that prokaryotic community structure may also reflect finer scale hydrography and deposition, and points to locations where microbial communities may influence bottom water nutrient profiles.

The presence of specific taxa in surface sediments may indicate elevated levels of hydrocarbons and/or iron reduction particularly at stations surrounding Pt. Hope. Combined with the shallow turnover to relatively abundant anaerobic sulfate-reducing taxa, this pattern points to declining habitat quality in this area (Group 1 stations). In 2004, researchers found sulfidic dead zones in sediments near Pt. Hope where sediments were black, smelled of sulfide, and were littered with decaying epifauna (Feder et al., 2004). With potentially increasing primary production and subsequent deposition, we may be seeing more sulfidic dead zones in years to come. These data highlight the need for more regular and long-term sampling and characterization of benthic microbes in this region. Just two surveys of microbial community structure conducted here support findings from long-term macro-benthic studies on the Bering-Chukchi shelf and reveal biogeochemical information that tend to be overlooked with respect to typical long-term environmental sampling designs. However, these surveys were conducted four years apart and lack the resolution needed to place benthic microbes into the spatiotemporal context required for monitoring of ecosystem health and function (Buttigieg et al., 2018).

As a whole, microbial community structure in the North American Arctic highlights the differences between the Bering-Chukchi inflow and Beaufort interior shelves. The cumulative environmental characteristics and associated food-supply regimes influence sediments and produce heterogeneous conditions (e.g., via riverine input of terrigenous material) in nearshore Beaufort sediments. Changes in OM and riverine input, coastal erosion, and sea-ice extent are expected to continue under climate change, and surveys of microorganisms would be valuable to

infer any changes in burial vs. degradation of OM. We recommend incorporating benthic microbial community structure surveys into any long-term monitoring programs in this rapidly changing Arctic marine ecosystem. For monitoring purposes, it would be beneficial to capture broad spatial coverage as a priority and collect vertical profiles where possible, being strategic about sampling cores in areas where there are marked differences in TOC, sediment type, and bioturbation.

3.7 ACKNOWLEDGEMENTS

The authors thank Brittany Charrier for all of her hard work on the proposal for this project, generating environmental data, and providing insight into corresponding macrofaunal community patterns. We thank the crew of the R/V Sikuliaq, and the many ASGARD scientists who collected samples for this project (Andrew Thurber, Sarah Seabrook, Jessica Pretty, Opik Ahkinga, Sylvana Gonzales) and who shared supporting environmental data. Jackie Grebmeier was instrumental in collecting surface sediment samples for microbial community analysis across the broader Bering-Chukchi. This manuscript is a product of the North Pacific Research Board Arctic Integrated Ecosystem Research Program (<https://www.nprb.org/arctic-program>); NPRB publication number ArcticIERP-27.

3.8 REFERENCES

- Alejandre-Colomo, C., Harder, J., Fuchs, B.M., Rosselló-Móra, R., Amann, R., 2020. High-throughput cultivation of heterotrophic bacteria during a spring phytoplankton bloom in the North Sea. *Syst. Appl. Microbiol.* 43, 126066. <https://doi.org/10.1016/j.syapm.2020.126066>
- Aller, R.C., 1994. Bioturbation and remineralization of sedimentary organic matter: effects of redox oscillation. *Chem. Geol.* 114, 331–345. [https://doi.org/10.1016/0009-2541\(94\)90062-0](https://doi.org/10.1016/0009-2541(94)90062-0)
- Aller, R.C., 1988. Benthic fauna and biogeochemical processes in marine sediments: the role of burrow structures., in: *Nitrogen Cycling in Coastal Marine Environments. Nitrogen cycling in coastal marine environments.*, pp. 301–338.
- Aller, R.C., 1982. The effects of macrobenthos on chemical properties of marine sediments and overlying waters. *Anim. Relations Biog. Alter. Sediments* 53–102.
https://doi.org/10.1007/978-1-4757-1317-6_2
- Alvarez, L.A., Exton, D.A., Timmis, K.N., Suggett, D.J., McGenity, T.J., 2009. Characterization of marine isoprene-degrading communities. *Environ. Microbiol.* 11, 3280–3291.
<https://doi.org/10.1111/j.1462-2920.2009.02069.x>
- Apprill, A., McNally, S., Parsons, R., Weber, L., 2015. Minor revision to V4 region SSU rRNA 806R gene primer greatly increases detection of SAR11 bacterioplankton. *Aquat. Microb. Ecol.* 75, 129–137. <https://doi.org/10.3354/ame01753>
- Arndt, S., Jørgensen, B.B., Larowe, D.E., Middelburg, J.J., Pancost, R.D., Regnier, P., 2013.

Earth-Science Reviews Quantifying the degradation of organic matter in marine sediments :
A review and synthesis. *Earth Sci. Rev.* 123, 53–86.

<https://doi.org/10.1016/j.earscirev.2013.02.008>

Arnosti, C., Wietz, M., Brinkhoff, T., Hehemann, J.-H., Probandt, D., Zeugner, L., Amann, R.,
2020. The Biogeochemistry of Marine Polysaccharides: Sources, Inventories, and Bacterial
Drivers of the Carbohydrate Cycle. <https://doi.org/10.1146/annurev-marine-032020>

Arrigo, K.R., van Dijken, G.L., 2015. Continued increases in Arctic Ocean primary production.
Prog. Oceanogr. 136, 60–70. <https://doi.org/10.1016/j.pocean.2015.05.002>

Arrigo, K.R., van Dijken, G.L., 2011. Secular trends in Arctic Ocean net primary production. *J.*
Geophys. Res. 116, C09011. <https://doi.org/10.1029/2011JC007151>

Astakhov, A.S., Gusev, E.A., Kolesnik, A.N., Shakirov, R.B., 2013. Conditions of the
accumulation of organic matter and metals in the bottom sediments of the Chukchi Sea.
Russ. Geol. Geophys. 54, 1056–1070. <https://doi.org/10.1016/j.rgg.2013.07.019>

Baker, M.R., Farley, E. V., Danielson, S.L., Mordy, C., Stafford, K.M., Dickson, D.M.S., 2022.
Integrated Research in the Arctic – ecosystem linkages and shifts in the northern Bering Sea
and eastern and western Chukchi Sea. *Deep. Res. II.*

Baker, M.R., Farley, E. V., Ladd, C., Danielson, S.L., Stafford, K.M., Huntington, H.P.,
Dickson, D.M.S., 2020. Integrated ecosystem research in the Pacific Arctic – understanding
ecosystem processes, timing and change. *Deep Sea Res. Part II Top. Stud. Oceanogr.* 177,
104850. <https://doi.org/10.1016/J.DSR2.2020.104850>

- Baltar, F., Gutiérrez-Rodríguez, A., Meyer, M., Skudelny, I., Sander, S., Thomson, B., Nodder, S., Middag, R., Morales, S.E., 2018. Specific Effect of Trace Metals on Marine Heterotrophic Microbial Activity and Diversity: Key Role of Iron and Zinc and Hydrocarbon-Degrading Bacteria. *Front. Microbiol.* 9, 3190.
<https://doi.org/10.3389/fmicb.2018.03190>
- Basili, M., Quero, G.M., Giovannelli, D., Manini, E., Vignaroli, C., Avio, C.G., De Marco, R., Luna, G.M., 2020. Major Role of Surrounding Environment in Shaping Biofilm Community Composition on Marine Plastic Debris. *Front. Mar. Sci.* 7, 262.
<https://doi.org/10.3389/fmars.2020.00262>
- Becker, S., Aoyama, M., Woodward, E.M.S., Bakker, K., Coverly, S., Mahaffey, C., Tanhua, T., 2020. GO-SHIP Repeat Hydrography Nutrient Manual: The Precise and Accurate Determination of Dissolved Inorganic Nutrients in Seawater, Using Continuous Flow Analysis Methods. *Front. Mar. Sci.* 7, 908.
<https://doi.org/10.3389/FMARS.2020.581790/BIBTEX>
- Blott, S.J., 2010. GRADISTAT Version 8.0: A grain size distribution and statistics package for the analysis of unconsolidated sediments by sieving or laser granulometer.
- Blott, S.J., Pye, K., 2006. Particle size distribution analysis of sand-sized particles by laser diffraction: An experimental investigation of instrument sensitivity and the effects of particle shape. *Sedimentology* 53, 671–685. <https://doi.org/10.1111/J.1365-3091.2006.00786.X>
- Burdige, D.J., 1993. The biogeochemistry of manganese and iron reduction in marine sediments.

Earth-Science Rev. 35, 249–284. [https://doi.org/10.1016/0012-8252\(93\)90040-E](https://doi.org/10.1016/0012-8252(93)90040-E)

Burdorf, L.D.W., Tramper, A., Seitaj, D., Meire, L., Hidalgo-Martinez, S., Zetsche, E.-M., Boschker, H.T.S., Meysman, F.J.R., 2017. Long-distance electron transport occurs globally in marine sediments. *Biogeosciences* 14, 683–701. <https://doi.org/10.5194/bg-14-683-2017>

Buttigieg, P.L., Fadeev, E., Bienhold, C., Hehemann, L., Offre, P., Boetius, A., 2018. Marine microbes in 4D — using time series observation to assess the dynamics of the ocean microbiome and its links to ocean health. *Curr. Opin. Microbiol.* 43, 169–185. <https://doi.org/10.1016/j.mib.2018.01.015>

Canfield, D.E., Bo Thamdrup, Erik Kristensen, 2005. Heterotrophic Carbon Metabolism. *Adv. Mar. Biol.* 48, 129–166. [https://doi.org/10.1016/S0065-2881\(05\)48005-0](https://doi.org/10.1016/S0065-2881(05)48005-0)

Caporaso, J.G., Lauber, C.L., Walters, W. a, Berg-Lyons, D., Huntley, J., Fierer, N., Owens, S.M., Betley, J., Fraser, L., Bauer, M., Gormley, N., Gilbert, J. a, Smith, G., Knight, R., 2012. Ultra-high-throughput microbial community analysis on the Illumina HiSeq and MiSeq platforms. *ISME J.* 6, 1621–1624. <https://doi.org/10.1038/ismej.2012.8>

Caporaso, J.G., Lauber, C.L., Walters, W.A., Berg-Lyons, D., Lozupone, C.A., Turnbaugh, P.J., Fierer, N., Knight, R., 2011. Global patterns of 16S rRNA diversity at a depth of millions of sequences per sample. *Proc. Natl. Acad. Sci.* 108, 4516–4522. <https://doi.org/10.1073/pnas.1000080107>

Carmack, E., Wassmann, P., 2006. Food webs and physical–biological coupling on pan-Arctic shelves: Unifying concepts and comprehensive perspectives. *Prog. Oceanogr.* 71, 446–477. <https://doi.org/10.1016/j.pocean.2006.10.004>

- Chang, B.X., Devol, A.H., 2009. Seasonal and spatial patterns of sedimentary denitrification rates in the Chukchi sea. *Deep Sea Res. Part II Top. Stud. Oceanogr.* 56, 1339–1350.
<https://doi.org/10.1016/j.dsr2.2008.10.024>
- Chen, X., Andersen, T.J., Morono, Y., Inagaki, F., Jørgensen, B.B., Lever, M.A., 2017. Bioturbation as a key driver behind the dominance of Bacteria over Archaea in near-surface sediment. *Sci. Rep.* 7, 2400. <https://doi.org/10.1038/s41598-017-02295-x>
- Cheng, J., Jacquin, J., Conan, P., Pujo-Pay, M., Barbe, V., George, M., Fabre, P., Bruzaud, S., Ter Halle, A., Meistertzheim, A.L., Ghiglione, J.F., 2021. Relative Influence of Plastic Debris Size and Shape, Chemical Composition and Phytoplankton-Bacteria Interactions in Driving Seawater Plasticsphere Abundance, Diversity and Activity. *Front. Microbiol.* 11.
<https://doi.org/10.3389/fmicb.2020.610231>
- Cock, P.J.A., Antao, T., Chang, J.T., Chapman, B.A., Cox, C.J., Dalke, A., Friedberg, I., Hamelryck, T., Kauff, F., Wilczynski, B., de Hoon, M.J.L., 2009. Biopython: freely available Python tools for computational molecular biology and bioinformatics. *Bioinformatics* 25, 1422–1423. <https://doi.org/10.1093/bioinformatics/btp163>
- Codispoti, L.A., Friederich, G.E., Sakamoto, C.M., Gordon, L.I., 1991. Nutrient cycling and primary production in the marine systems of the Arctic and Antarctic, *Journal of Marine Systems*.
- Cooper, L.W., Cota, G.F., Pomeroy, L.R., Grebmeier, J.M., Whitley, T.E., 1999. Modification of NO, PO, and NO/PO during flow across the Bering and Chukchi shelves: Implications for use as Arctic water mass tracers. *J. Geophys. Res. Ocean.* 104, 7827–7836.

<https://doi.org/10.1029/1999JC900010>

- Cooper, L.W., Grebmeier, J.M., Frey, K.E., Vagle, S., 2014. SWL14 Bottle Data [WWW Document]. Arct. Data Cent. URL <https://arcticdata.io/catalog/view/urn:uuid:26786355-86f3-4554-8e68-a5b668fd2698> (accessed 7.8.21).
- Crenn, K., Duffieux, D., Jeanthon, C., 2018. Bacterial Epibiotic Communities of Ubiquitous and Abundant Marine Diatoms Are Distinct in Short- and Long-Term Associations. *Front. Microbiol.* 0, 2879. <https://doi.org/10.3389/FMICB.2018.02879>
- Cui, Y., Liu, X., Liu, C., Gao, J., Fang, X., Liu, Y., Wang, W., Li, Y., 2020. Mineralogy and geochemistry of ferromanganese oxide deposits from the Chukchi Sea in the Arctic Ocean. *Arctic, Antarct. Alp. Res.* 52, 120–129. <https://doi.org/10.1080/15230430.2020.1738824>
- Daims, H., 2014. The Family Nitrospiraceae, in: *The Prokaryotes*. Springer Berlin Heidelberg, Berlin, Heidelberg, pp. 733–749. https://doi.org/10.1007/978-3-642-38954-2_126
- Daims, H., Lebedeva, E. V., Pjevac, P., Han, P., Herbold, C., Albertsen, M., Jehmlich, N., Palatinszky, M., Vierheilig, J., Bulaev, A., Kirkegaard, R.H., von Bergen, M., Rattei, T., Bendinger, B., Nielsen, P.H., Wagner, M., 2015. Complete nitrification by *Nitrospira* bacteria. *Nature* 528, 504–509. <https://doi.org/10.1038/nature16461>
- Dale, H., Taylor, J.D., Solan, M., Lam, P., Cunliffe, M., 2019. Polychaete mucopolysaccharide alters sediment microbial diversity and stimulates ammonia-oxidising functional groups. *FEMS Microbiol. Ecol.* 95. <https://doi.org/10.1093/femsec/fiy234>
- Danielson, S.L., Eisner, L., Ladd, C., Mordy, C., Sousa, L., Weingartner, T.J., 2017. A

- comparison between late summer 2012 and 2013 water masses, macronutrients, and phytoplankton standing crops in the northern Bering and Chukchi Seas. *Deep. Res. Part II Top. Stud. Oceanogr.* 135, 7–26. <https://doi.org/10.1016/j.dsr2.2016.05.024>
- De Cáceres, M., Legendre, P., 2009. Associations between species and groups of sites: indices and statistical inference. *Ecology* 90, 3566–3574. <https://doi.org/10.1890/08-1823.1>
- De Cáceres, M., Legendre, P., Moretti, M., 2010. Improving indicator species analysis by combining groups of sites. *Oikos* 119, 1674–1684. <https://doi.org/10.1111/j.1600-0706.2010.18334.x>
- Dedysh, S.N., Yilmaz, P., 2018. Refining the taxonomic structure of the phylum Acidobacteria. *Int. J. Syst. Evol. Microbiol.* 68, 3796–3806. <https://doi.org/10.1099/ijsem.0.003062>
- Defforey, D., Paytan, A., 2018. Phosphorus cycling in marine sediments: Advances and challenges. *Chem. Geol.* 477, 1–11. <https://doi.org/10.1016/J.CHEMGEO.2017.12.002>
- Deng, L., Bölsterli, D., Kristensen, E., Meile, C., Su, C.-C., Bernasconi, S.M., Seidenkrantz, M.-S., Glombitza, C., Lagostina, L., Han, X., Jørgensen, B.B., Røy, H., Lever, M.A., 2020. Macrofaunal control of microbial community structure in continental margin sediments. *Proc. Natl. Acad. Sci. U. S. A.* 117, 15911–15922. <https://doi.org/10.1073/pnas.1917494117>
- Devol, A.H., Codispoti, L.A., Christensen, J.P., 1997. Summer and winter denitrification rates in western Arctic shelf sediments. *Cont. Shelf Res.* 17, 1029–1050. [https://doi.org/10.1016/S0278-4343\(97\)00003-4](https://doi.org/10.1016/S0278-4343(97)00003-4)
- Dong, C., Bai, X., Sheng, H., Jiao, L., Zhou, H., Shao, Z., 2015. Distribution of PAHs and the

- PAH-degrading bacteria in the deep-sea sediments of the high-latitude Arctic Ocean. *Biogeosciences* 12, 2163–2177. <https://doi.org/10.5194/bg-12-2163-2015>
- Dong, C., Sheng, H., Wang, W., Zhou, H., Shao, Z., 2017. Bacterial distribution pattern in the surface sediments distinctive among shelf, slope and basin across the western Arctic Ocean. *Polar Biol.* 40, 423–436. <https://doi.org/10.1007/s00300-016-1970-6>
- Dunton, K.H., Weingartner, T., Carmack, E.C., 2006. The nearshore western Beaufort Sea ecosystem: Circulation and importance of terrestrial carbon in arctic coastal food webs. *Prog. Oceanogr.* 71, 362–378. <https://doi.org/10.1016/j.pocean.2006.09.011>
- Durbin, A.M., Teske, A., 2011. Microbial diversity and stratification of South Pacific abyssal marine sediments. *Environ. Microbiol.* 13, 3219–3234. <https://doi.org/10.1111/j.1462-2920.2011.02544.x>
- Edgar, R.C., 2018. Updating the 97% identity threshold for 16S ribosomal RNA OTUs. *Bioinformatics* 34, 2371–2375. <https://doi.org/10.1093/bioinformatics/bty113>
- Edlund, A., Hårdeman, F., Jansson, J.K., Sjöling, S., 2008. Active bacterial community structure along vertical redox gradients in Baltic Sea sediment. *Environ. Microbiol.* 10, 2051–2063. <https://doi.org/10.1111/j.1462-2920.2008.01624.x>
- Emerson, S., Hedges, J., Holland, H.D., Turekian, K.K., 2004. Sediment diagenesis and benthic flux. *Ocean. Mar. Geochemistry* 6, 293–319.
- Feder, H.M., Jewett, S.C., Blanchard, A., 2004. Southeastern Chukchi Sea (Alaska) epibenthos. *Polar Biol.* 28, 402–421. <https://doi.org/10.1007/S00300-004-0683-4>

- Feng, Z., Ji, R., Ashjian, C., Zhang, J., Campbell, R., Grebmeier, J.M., 2021. Benthic hotspots on the northern Bering and Chukchi continental shelf: Spatial variability in production regimes and environmental drivers. *Prog. Oceanogr.* 191, 102497. <https://doi.org/10.1016/j.pocean.2020.102497>
- Ferguson, R.M.W., Gontikaki, E., Anderson, J.A., Witte, U., 2017. The variable influence of dispersant on degradation of oil hydrocarbons in subarctic deep-sea sediments at low temperatures (0-5 °C). *Sci. Rep.* 7, 1–13. <https://doi.org/10.1038/s41598-017-02475-9>
- Fuhrman, J.A., Cram, J.A., Needham, D.M., 2015. Marine microbial community dynamics and their ecological interpretation. *Nat. Rev. Microbiol.* 13, 133–146. <https://doi.org/10.1038/nrmicro3417>
- Gao, Z., Wang, X., Hannides, A.K., Sansone, F.J., Wang, G., 2011. Impact of redox-stratification on the diversity and distribution of bacterial communities in sandy reef sediments in a microcosm. *Chinese J. Oceanol. Limnol.* 29, 1209–1223. <https://doi.org/10.1007/s00343-011-0316-z>
- Gilbertson, W.W., Solan, M., Prosser, J.I., 2012. Differential effects of microorganism-invertebrate interactions on benthic nitrogen cycling. *FEMS Microbiol. Ecol.* 82, 11–22. <https://doi.org/10.1111/j.1574-6941.2012.01400.x>
- Giongo, A., Granada, C.E., Borges, L.G.A., Pereira, L.M., Trindade, F.J., Mattiello, S.P., Oliveira, R.R., Shubeita, F.M., Lovato, A., Marcon, C., Medina-Silva, R., 2020. Microbial communities in anaerobic digesters change over time and sampling depth. *Brazilian J.*

Microbiol. 51, 1177–1190. <https://doi.org/10.1007/s42770-020-00272-7>

Glöckner, F.O., Yilmaz, P., Quast, C., Gerken, J., Beccati, A., Ciuprina, A., Bruns, G., Yarza, P., Peplies, J., Westram, R., Ludwig, W., 2017. 25 years of serving the community with ribosomal RNA gene reference databases and tools. *J. Biotechnol.* 261, 169–176. <https://doi.org/10.1016/j.jbiotec.2017.06.1198>

Goldsmith, S. S., Cuyno, L., Kovacs, K., Mundy, N., Bungler, A., Mccoy, T., 2009. Economic Analysis of Future Offshore Oil & Gas Development: Beaufort Sea, Chukchi Sea, and North Aleutian Basin.

Golyshin, P.N., Chernikova, T.N., Abraham, W.-R., Lünsdorf, H., Timmis, K.N., Yakimov, M.M., 2002. *Oleiphilaceae* fam. nov., to include *Oleiphilus messinensis* gen. nov., sp. nov., a novel marine bacterium that obligately utilizes hydrocarbons. *Int. J. Syst. Evol. Microbiol.* 52, 901–911. <https://doi.org/10.1099/00207713-52-3-901>

Gong, D., Pickart, R.S., 2015. Summertime circulation in the eastern Chukchi Sea. *Deep Sea Res. Part II Top. Stud. Oceanogr.* 118, 18–31. <https://doi.org/10.1016/J.DSR2.2015.02.006>

Goñi, M. a., O'Connor, A.E., Kuzyk, Z.Z., Yunker, M.B., Gobeil, C., Macdonald, R.W., 2013. Distribution and sources of organic matter in surface marine sediments across the North American Arctic margin. *J. Geophys. Res. Ocean.* 118, 4017–4035. <https://doi.org/10.1002/jgrc.20286>

Goñi, M.A., Corvi, E.R., Welch, K.A., Buktenica, M., Lebon, K., Alleau, Y., Juranek, L.W., 2019. Particulate organic matter distributions in surface waters of the Pacific Arctic shelf during the late summer and fall season. *Mar. Chem.* 211, 75–93.

<https://doi.org/10.1016/J.MARCHEM.2019.03.010>

Grebmeier, J., McRoy, C., 1989. Pelagic-benthic coupling on the shelf of the northern Bering and Chukchi Seas. III Benthic food supply and carbon cycling. *Mar. Ecol. Prog. Ser.* 53, 79–91. <https://doi.org/10.3354/meps053079>

Grebmeier, J.M., 2012. Shifting Patterns of Life in the Pacific Arctic and Sub-Arctic Seas. *Ann. Rev. Mar. Sci.* 4, 63–78. <https://doi.org/10.1146/annurev-marine-120710-100926>

Grebmeier, J.M. and, Maslowski, W., 2014. *The Pacific Arctic Region*. Springer Netherlands, Dordrecht. <https://doi.org/10.1007/978-94-017-8863-2>

Grebmeier, J.M., Bluhm, B.A., Cooper, L.W., Danielson, S.L., Arrigo, K.R., Blanchard, A.L., Clarke, J.T., Day, R.H., Frey, K.E., Gradinger, R.R., Kędra, M., Konar, B., Kuletz, K.J., Lee, S.H., Lovvorn, J.R., Norcross, B.L., Okkonen, S.R., 2015. Ecosystem characteristics and processes facilitating persistent macrobenthic biomass hotspots and associated benthivory in the Pacific Arctic. *Prog. Oceanogr.* 136, 92–114. <https://doi.org/10.1016/j.pocean.2015.05.006>

Grebmeier, J.M., Cooper, L.W., 2014. SWL14 Sediment Parameters [WWW Document]. *Arct. Data Cent.* URL <https://arcticdata.io/catalog/view/doi:10.5065/D6M043GJ> (accessed 7.8.21).

Grebmeier, J.M., Cooper, L.W., Feder, H.M., Sirenko, B.I., 2006. Ecosystem dynamics of the Pacific-influenced Northern Bering and Chukchi Seas in the Amerasian Arctic. *Prog. Oceanogr.* 71, 331–361. <https://doi.org/10.1016/j.pocean.2006.10.001>

- Greene, A.C., 2014. The Family Desulfuromonadaceae, in: *The Prokaryotes*. Springer Berlin Heidelberg, Berlin, Heidelberg, pp. 143–155. https://doi.org/10.1007/978-3-642-39044-9_380
- Guibert, L.M., Loviso, C.L., Marcos, M.S., Commendatore, M.G., Dionisi, H.M., Lozada, M., 2012. Alkane Biodegradation Genes from Chronically Polluted Subantarctic Coastal Sediments and Their Shifts in Response to Oil Exposure. *Microb. Ecol.* 64, 605–616. <https://doi.org/10.1007/s00248-012-0051-9>
- Gutierrez, T., 2019. Occurrence and Roles of the Obligate Hydrocarbonoclastic Bacteria in the Ocean When There Is No Obvious Hydrocarbon Contamination, in: *Taxonomy, Genomics and Ecophysiology of Hydrocarbon-Degrading Microbes*. Springer International Publishing, Cham, pp. 337–352. https://doi.org/10.1007/978-3-030-14796-9_14
- Harrison, J.P., Schratzberger, M., Sapp, M., Osborn, A.M., 2014. Rapid bacterial colonization of low-density polyethylene microplastics in coastal sediment microcosms. *BMC Microbiol.* 14, 232. <https://doi.org/10.1186/s12866-014-0232-4>
- Head, I.M., Jones, D.M., Röling, W.F.M., 2006. Marine microorganisms make a meal of oil. *Nat. Rev. Microbiol.* 4, 173–182. <https://doi.org/10.1038/nrmicro1348>
- Hein, J.R., Koschinsky, A., Halbach, P., Manheim, F.T., Bau, M., Kang, J.K., Lubick, N., 1997. Iron and manganese oxide mineralization in the Pacific. *Geol. Soc. Spec. Publ.* 119, 123–138. <https://doi.org/10.1144/GSL.SP.1997.119.01.09>
- Henderson, G., Yilmaz, P., Kumar, S., Forster, R.J., Kelly, W.J., Leahy, S.C., Guan, L.L., Janssen, P.H., 2019. Improved taxonomic assignment of rumen bacterial 16S rRNA

sequences using a revised SILVA taxonomic framework. PeerJ 2019, e6496.

<https://doi.org/10.7717/peerj.6496>

Hoffmann, K., Hassenrück, C., Salman-Carvalho, V., Holtappels, M., Bienhold, C., 2017.

Response of Bacterial Communities to Different Detritus Compositions in Arctic Deep-Sea Sediments. *Front. Microbiol.* 8, 1–18. <https://doi.org/10.3389/fmicb.2017.00266>

Holmes, D.E., Nicoll, J.S., Bond, D.R., Lovley, D.R., 2004. Potential role of a novel

psychrotolerant member of the family Geobacteraceae, *Geopsychrobacter electrodiphilus* gen. nov., sp. nov., in electricity production by a marine sediment fuel cell. *Appl. Environ. Microbiol.* 70, 6023–6030. <https://doi.org/10.1128/AEM.70.10.6023-6030.2004>

Horak, R.E.A., Whitney, H., Shull, D.H., Mordy, C.W., Devol, A.H., 2013. The role of

sediments on the Bering Sea shelf N cycle: Insights from measurements of benthic denitrification and benthic DIN fluxes. *Deep Sea Res. Part II Top. Stud. Oceanogr.* 94, 95–105. <https://doi.org/10.1016/J.DSR2.2013.03.014>

Jensen, H.S., Mortensen, P.B., Andersen, F. O., Rasmussen, E., Jensen, A., 1995. Phosphorus

cycling in a coastal marine sediment, Aarhus Bay, Denmark. *Limnol. Oceanogr.* 40, 908–917. <https://doi.org/10.4319/LO.1995.40.5.0908>

Jeske, O., Jogler, M., Petersen, J., Sikorski, J., Jogler, C., 2013. From genome mining to

phenotypic microarrays: Planctomycetes as source for novel bioactive molecules. *Antonie van Leeuwenhoek* 2013 1044 104, 551–567. <https://doi.org/10.1007/S10482-013-0007-1>

Jessen, G.L., Lichtschlag, A., Ramette, A., Pantoja, S., Rossel, P.E., Schubert, C.J., Struck, U.,

Boetius, A., 2017. Hypoxia causes preservation of labile organic matter and changes

seafloor microbial community composition (Black Sea). *Sci. Adv.* 3, e1601897.

<https://doi.org/10.1126/sciadv.1601897>

Jørgensen, B., Glud, R., Holby, O., 2005. Oxygen distribution and bioirrigation in Arctic fjord sediments (Svalbard, Barents Sea). *Mar. Ecol. Prog. Ser.* 292, 85–95.

<https://doi.org/10.3354/meps292085>

Jorgensen, B.B., 2006. Bacteria and marine biogeochemistry. *Mar. Geochemistry* 169–206.

https://doi.org/10.1007/3-540-32144-6_5

Kallscheuer, N., Jogler, M., Wiegand, S., Peeters, S.H., Heuer, A., Boedeker, C., Jetten, M.S.M.M., Rohde, M., Jogler, C., 2020. Three novel *Rubripirellula* species isolated from plastic particles submerged in the Baltic Sea and the estuary of the river Warnow in northern Germany. *Antonie Van Leeuwenhoek* 113, 1767–1778.

<https://doi.org/10.1007/s10482-019-01368-3>

Kleindienst, S., Ramette, A., Amann, R., Knittel, K., 2012. Distribution and in situ abundance of sulfate-reducing bacteria in diverse marine hydrocarbon seep sediments. *Environ. Microbiol.* 14, 2689–2710. <https://doi.org/10.1111/j.1462-2920.2012.02832.x>

<https://doi.org/10.1111/j.1462-2920.2012.02832.x>

Koch, C.W., Cooper, L.W., Lalande, C., Brown, T.A., Frey, K.E., Grebmeier, J.M., 2020.

Seasonal and latitudinal variations in sea ice algae deposition in the Northern Bering and Chukchi seas determined by algal biomarkers. *PLoS One* 15, e0231178.

<https://doi.org/10.1371/journal.pone.0231178>

Kolesnik, O.N., Kolesnik, A.N., 2015. Rare earth elements in ferromanganese nodules of the Chukchi Sea. *Lithol. Miner. Resour.* 50, 181–191.

<https://doi.org/10.1134/S0024490215030050>

Kostka, J.E., Prakash, O., Overholt, W.A., Green, S.J., Freyer, G., Canion, A., Delgado, J., Norton, N., Hazen, T.C., Huettel, M., 2011. Hydrocarbon-degrading bacteria and the bacterial community response in Gulf of Mexico beach sands impacted by the deepwater horizon oil spill. *Appl. Environ. Microbiol.* 77, 7962–7974.

<https://doi.org/10.1128/AEM.05402-11>

Kristensen, E., 2000. Organic matter diagenesis at the oxic/anoxic interface in coastal marine sediments, with emphasis on the role of burrowing animals. *Hydrobiologia* 426, 1–24.

<https://doi.org/10.1023/A:1003980226194>

Kristensen, E., Penha-Lopes, G., Delefosse, M., Valdemarsen, T., Quintana, C.O., Banta, G.T., 2012. What is bioturbation? the need for a precise definition for fauna in aquatic sciences. *Mar. Ecol. Prog. Ser.* 446, 285–302. <https://doi.org/10.3354/meps09506>

Kuever, J., 2014. The Family Desulfobulbaceae, in: *The Prokaryotes*. Springer Berlin Heidelberg, Berlin, Heidelberg, pp. 75–86. https://doi.org/10.1007/978-3-642-39044-9_267

Ladau, J., Eloë-Fadrosh, E.A., 2019. Spatial, Temporal, and Phylogenetic Scales of Microbial Ecology. *Trends Microbiol.* 27, 662–669. <https://doi.org/10.1016/J.TIM.2019.03.003>

Luna, G.M., Corinaldesi, C., Rastelli, E., Danovaro, R., 2013. Patterns and drivers of bacterial α - and β -diversity across vertical profiles from surface to subsurface sediments. *Environ. Microbiol. Rep.* 5, 731–739. <https://doi.org/10.1111/1758-2229.12075>

Lyu, J., Yu, X., Jiang, M., Cao, W., Saren, G., Chang, F., 2021. The Mechanism of Microbial-

Ferromanganese Nodule Interaction and the Contribution of Biomineralization to the Formation of Oceanic Ferromanganese Nodules. *Microorganisms* 9, 1247.

<https://doi.org/10.3390/microorganisms9061247>

Macdonald, R.W., Thomas, D.J., 1991. Chemical interactions and sediments of the western Canadian arctic shelf. *Cont. Shelf Res.* 11, 843–863. [https://doi.org/10.1016/0278-4343\(91\)90082-H](https://doi.org/10.1016/0278-4343(91)90082-H)

McClelland, J.W., Townsend-Small, A., Holmes, R.M., Pan, F., Stieglitz, M., Khosh, M., Peterson, B.J., 2014. River export of nutrients and organic matter from the North Slope of Alaska to the Beaufort Sea. *Water Resour. Res.* 50, 1823–1839. <https://doi.org/10.1002/2013WR014722>

McIlroy, S.J., Kirkegaard, R.H., Dueholm, M.S., Fernando, E., Karst, S.M., Albertsen, M., Nielsen, P.H., 2017. Culture-Independent Analyses Reveal Novel Anaerolineaceae as Abundant Primary Fermenters in Anaerobic Digesters Treating Waste Activated Sludge. *Front. Microbiol.* 8, 1134. <https://doi.org/10.3389/fmicb.2017.01134>

McTigue, N.D., Gardner, W.S., Dunton, K.H., Hardison, A.K., 2016. Biotic and abiotic controls on co-occurring nitrogen cycling processes in shallow Arctic shelf sediments. *Nat. Commun.* 7, 13145. <https://doi.org/10.1038/ncomms13145>

Meskhidze, N., Sabolis, A., Reed, R., Kamykowski, D., 2015. Quantifying environmental stress-induced emissions of algal isoprene and monoterpenes using laboratory measurements. *Biogeosciences* 12, 637–651. <https://doi.org/10.5194/bg-12-637-2015>

Mills, M.M., Brown, Z.W., Lowry, K.E., van Dijken, G.L., Becker, S., Pal, S., Benitez-Nelson,

- C.R., Downer, M.M., Strong, A.L., Swift, J.H., Pickart, R.S., Arrigo, K.R., 2015. Impacts of low phytoplankton $\text{NO}_3^-:\text{PO}_4^{3-}$ utilization ratios over the Chukchi Shelf, Arctic Ocean. *Deep Sea Res. Part II Top. Stud. Oceanogr.* 118, 105–121.
<https://doi.org/10.1016/J.DSR2.2015.02.007>
- Molari, M., Janssen, F., Vonnahme, T.R., Wenzhöfer, F., Boetius, A., 2020. The contribution of microbial communities in polymetallic nodules to the diversity of the deep-sea microbiome of the Peru Basin (4130-4198 m depth). *Biogeosciences* 17, 3203–3222.
<https://doi.org/10.5194/bg-17-3203-2020>
- Moore, S.E., Stabeno, P.J., 2015. Synthesis of Arctic Research (SOAR) in marine ecosystems of the Pacific Arctic. *Prog. Oceanogr.* 136, 1–11. <https://doi.org/10.1016/j.pocean.2015.05.017>
- Mordy, C.W., Eisner, L., Kearney, K., Kimmel, D., Lomas, M.W., Mier, K., Proctor, P., Ressler, P.H., Stabeno, P., Wisegarver, E., 2021. Spatiotemporal variability of the nitrogen deficit in bottom waters on the eastern Bering Sea shelf. *Cont. Shelf Res.* 224, 104423.
<https://doi.org/10.1016/j.csr.2021.104423>
- Mu, J., Qu, L., Jin, F., Zhang, S., Fang, C., Ma, X., Zhang, W., Huo, C., Cong, Y., Wang, J., 2019. Abundance and distribution of microplastics in the surface sediments from the northern Bering and Chukchi Seas. *Environ. Pollut.* 245, 122–130.
<https://doi.org/10.1016/j.envpol.2018.10.097>
- Murphy, A.E., Kolkmeier, R., Song, B., Anderson, I.C., Bowen, J., 2019. Bioreactivity and Microbiome of Biodeposits from Filter-Feeding Bivalves. *Microb. Ecol.* 77, 343–357.
<https://doi.org/10.1007/s00248-018-01312-4>

Murtagh, F., Legendre, P., 2014. Ward's Hierarchical Agglomerative Clustering Method: Which Algorithms Implement Ward's Criterion? *J. Classif.* 31, 274–295.

<https://doi.org/10.1007/s00357-014-9161-z>

Nelson, R.J., Ashjian, C.J., Bluhm, B.A., Conlan, K.E., Gradinger, R.R., Grebmeier, J.M., Hill, V.J., Hopcroft, R.R., Hunt, B.P.V., Joo, H.M., Kirchman, D.L., Kosobokova, K.N., Lee, S.H., Li, W.K.W., Lovejoy, C., Poulin, M., Sherr, E., Young, K. V., 2014. Biodiversity and biogeography of the lower trophic taxa of the pacific arctic region: Sensitivities to climate change, in: *The Pacific Arctic Region: Ecosystem Status and Trends in a Rapidly Changing Environment*. Springer Netherlands, pp. 269–336. https://doi.org/10.1007/978-94-017-8863-2_10

Nielsen, L.P., Risgaard-Petersen, N., Fossing, H., Christensen, P.B., Sayama, M., 2010. Electric currents couple spatially separated biogeochemical processes in marine sediment. *Nature* 463, 1071–1074. <https://doi.org/10.1038/nature08790>

Oberbeckmann, S., Osborn, A.M., Duhaime, M.B., 2016. Microbes on a bottle: Substrate, season and geography influence community composition of microbes colonizing marine plastic debris. *PLoS One* 11, e0159289. <https://doi.org/10.1371/journal.pone.0159289>

Oksanen, J., Blanchet, F.G., Friendly, M., Kindt, R., Legendre, P., Mcglinn, D., Minchin, P.R., O'hara, R.B., Simpson, G.L., Solymos, P., Henry, M., Stevens, H., Szoecs, E., Wagner, H., Oksanen, M.J., 2017. *Community Ecology Package*.

Oksanen, J., Kindt, R., Legendre, P., O'hara, B., Henry, M., Maintainer, H.S., 2007. *Vegan: Community Ecology Package*.

- Orcutt, B.N., Sylvan, J.B., Knab, N.J., Edwards, K.J., 2011. Microbial Ecology of the Dark Ocean above, at, and below the Seafloor. *Microbiol. Mol. Biol. Rev.* 75, 361–422.
<https://doi.org/10.1128/MMBR.00039-10>
- Parada, A.E., Needham, D.M., Fuhrman, J.A., 2016. Every base matters: assessing small subunit rRNA primers for marine microbiomes with mock communities, time series and global field samples. *Environ. Microbiol.* 18, 1403–1414. <https://doi.org/10.1111/1462-2920.13023>
- Park, H.J., Lee, Y.M., Kim, S., Wi, A.R., Han, S.J., Kim, H.-W., Kim, I.-C., Yim, J.H., Kim, D., 2014. Identification of proteolytic bacteria from the Arctic Chukchi Sea expedition cruise and characterization of cold-active proteases. *J. Microbiol.* 52, 825–833.
<https://doi.org/10.1007/s12275-014-4226-6>
- Petro, C., Zäncker, B., Starnawski, P., Jochum, L.M., Ferdelman, T.G., Jørgensen, B.B., Røy, H., Kjeldsen, K.U., Schramm, A., 2019. Marine Deep Biosphere Microbial Communities Assemble in Near-Surface Sediments in Aarhus Bay. *Front. Microbiol.* 10, 758.
<https://doi.org/10.3389/fmicb.2019.00758>
- Pfeffer, C., Larsen, S., Song, J., Dong, M., Besenbacher, F., Meyer, R.L., Kjeldsen, K.U., Schreiber, L., Gorby, Y.A., El-Naggar, M.Y., Leung, K.M., Schramm, A., Risgaard-Petersen, N., Nielsen, L.P., 2012. Filamentous bacteria transport electrons over centimetre distances. *Nature* 491, 218–221. <https://doi.org/10.1038/nature11586>
- Piper, M.M., Benitez-Nelson, C.R., Frey, K.E., Mills, M.M., Pal, S., 2016. Dissolved and particulate phosphorus distributions and elemental stoichiometry throughout the Chukchi Sea. *Deep Sea Res. Part II Top. Stud. Oceanogr.* 130, 76–87.

<https://doi.org/10.1016/j.dsr2.2016.05.009>

Purohit, J., Chattopadhyay, A., Teli, B., 2020. Metagenomic Exploration of Plastic Degrading Microbes for Biotechnological Application. *Curr. Genomics* 21, 253–270.

<https://doi.org/10.2174/1389202921999200525155711>

R Core Team, 2017. R: A language and environment for statistical computing.

Ravenschlag, K., Sahm, K., Knoblauch, C., Jørgensen, B.B., Amann, R., 2000. Community Structure, Cellular rRNA Content, and Activity of Sulfate-Reducing Bacteria in Marine Arctic Sediments. *Appl. Environ. Microbiol.* 66, 3592–3602.

<https://doi.org/10.1128/AEM.66.8.3592-3602.2000>

Ribicic, D., Netzer, R., Hazen, T.C., Techtmann, S.M., Drabløs, F., Brakstad, O.G., 2018. Microbial community and metagenome dynamics during biodegradation of dispersed oil reveals potential key-players in cold Norwegian seawater. *Mar. Pollut. Bull.* 129, 370–378.

<https://doi.org/10.1016/j.marpolbul.2018.02.034>

Rontani, J.-F., Belt, S.T., Vaultier, F., Brown, T.A., Massé, G., 2014. Autoxidative and Photooxidative Reactivity of Highly Branched Isoprenoid (HBI) Alkenes. *Lipids* 49, 481–494. <https://doi.org/10.1007/s11745-014-3891-x>

Rontani, J.F., Belt, S.T., Amiraux, R., 2018. Biotic and abiotic degradation of the sea ice diatom biomarker IP25 and selected algal sterols in near-surface Arctic sediments. *Org. Geochem.* 118, 73–88. <https://doi.org/10.1016/j.orggeochem.2018.01.003>

Rozan, T.F., Taillefert, M., Trouwborst, R.E., Glazer, B.T., Ma, S., Herszage, J., Valdes, L.M.,

- Price, K.S., III, G.W.L., 2002. Iron-sulfur-phosphorus cycling in the sediments of a shallow coastal bay: Implications for sediment nutrient release and benthic macroalgal blooms. *Limnol. Oceanogr.* 47, 1346–1354. <https://doi.org/10.4319/LO.2002.47.5.1346>
- Ruff, S.E., Biddle, J.F., Teske, A.P., Knittel, K., Boetius, A., Ramette, A., 2015. Global dispersion and local diversification of the methane seep microbiome. *Proc. Natl. Acad. Sci.* 112, 4015–4020. <https://doi.org/10.1073/pnas.1421865112>
- Schloss, P.D., Westcott, S.L., Ryabin, T., Hall, J.R., Hartmann, M., Hollister, E.B., Lesniewski, R. a., Oakley, B.B., Parks, D.H., Robinson, C.J., Sahl, J.W., Stres, B., Thallinger, G.G., Van Horn, D.J., Weber, C.F., 2009. Introducing mothur: Open-source, platform-independent, community-supported software for describing and comparing microbial communities. *Appl. Environ. Microbiol.* 75, 7537–7541. <https://doi.org/10.1128/AEM.01541-09>
- Schreiber, L., Holler, T., Knittel, K., Meyerdierks, A., Amann, R., 2010. Identification of the dominant sulfate-reducing bacterial partner of anaerobic methanotrophs of the ANME-2 clade. *Environ. Microbiol.* 12. <https://doi.org/10.1111/j.1462-2920.2010.02275.x>
- Shade, A., Dunn, R.R., Blowes, S.A., Keil, P., Bohannan, B.J.M., Herrmann, M., Küsel, K., Lennon, J.T., Sanders, N.J., Storch, D., Chase, J., 2018. Macroecology to Unite All Life, Large and Small. *Trends Ecol. Evol.* 33, 731–744. <https://doi.org/10.1016/J.TREE.2018.08.005>
- Shulga, N., Abramov, S., Gavrilov, S., Ryazantsev, K., 2021. Arctic Fe-Mn deposits from the Kara Sea: fastgrowing refuges for cosmopolitan marine microorganisms under sharp changes of redox conditions. *EGU Gen. Assem. Conf. Abstr.* EGU21-15925.

<https://doi.org/https://doi.org/10.21203/rs.3.rs-1816563/v1>

Sinkko, H., Lukkari, K., Sihvonen, L.M., Sivonen, K., Leivuori, M., Rantanen, M., Paulin, L., Lyra, C., 2013. Bacteria Contribute to Sediment Nutrient Release and Reflect Progressed Eutrophication-Driven Hypoxia in an Organic-Rich Continental Sea. *PLoS One* 8, e67061. <https://doi.org/10.1371/journal.pone.0067061>

Sorokin, D.Y., Gumerov, V.M., Rakitin, A.L., Beletsky, A. V., Damsté, J.S.S., Muyzer, G., Mardanov, A. V., Ravin, N. V., 2014. Genome analysis of *Chitinivibrio alkaliphilus* gen. nov., sp. nov., a novel extremely haloalkaliphilic anaerobic chitinolytic bacterium from the candidate phylum Termite Group 3. *Environ. Microbiol.* 16, 1549–1565. <https://doi.org/10.1111/1462-2920.12284>

Sorokin, D.Y., Mardanov, A. V., Ravin, N. V., 2020. *Chitinivibrio*, in: Oren, A. (Ed.), *Bergey's Manual of Systematics of Archaea and Bacteria*. Wiley, pp. 1–5. <https://doi.org/10.1002/9781118960608.gbm01979>

Souza, A.C., Kim, I.N., Gardner, W.S., Dunton, K.H., 2014. Dinitrogen, oxygen, and nutrient fluxes at the sediment–water interface and bottom water physical mixing on the eastern Chukchi Sea shelf. *Deep Sea Res. Part II Top. Stud. Oceanogr.* 102, 77–83. <https://doi.org/10.1016/J.DSR2.2014.01.002>

Stahl, D.A., de la Torre, J.R., 2012. Physiology and diversity of ammonia-oxidizing archaea. *Annu. Rev. Microbiol.* 66, 83–101. <https://doi.org/10.1146/annurev-micro-092611-150128>

Steenbergh, A.K., Bodelier, P.L.E., Slomp, C.P., Laanbroek, H.J., 2014. Effect of Redox Conditions on Bacterial Community Structure in Baltic Sea Sediments with Contrasting

Phosphorus Fluxes. PLoS One 9, e92401. <https://doi.org/10.1371/journal.pone.0092401>

Tanaka, N., Romanenko, L.A., Kurilenko, V. V, Svetashev, V.I., Kalinovskaya, N.I., Mikhailov, V. V, 2014. *Loktanella maritima* sp. nov. isolated from shallow marine sediments. *Int. J. Syst. Evol. Microbiol.* 64, 2370–2375. <https://doi.org/10.1099/ijs.0.061747-0>

Templeton, A.S., Staudigel, H., Tebo, B.M., Bailey, B., Johnson, H., Sheehan, C., Rogers, D., 2005. Diverse Mn(II)-Oxidizing Bacteria Isolated from Submarine Basalts at Loihi Seamount. *Geomicrobiol. J.* 22, 127–139. <https://doi.org/10.1080/01490450590945951>

Toshchakov, S. V., Korzhenkov, A.A., Chernikova, T.N., Ferrer, M., Golyshina, O. V., Yakimov, M.M., Golyshin, P.N., 2017. The genome analysis of *Oleiphilus messinensis* ME102 (DSM 13489T) reveals backgrounds of its obligate alkane-devouring marine lifestyle. *Mar. Genomics* 36, 41–47. <https://doi.org/10.1016/j.margen.2017.07.005>

Toshchakov, S. V, Korzhenkov, A.A., Chernikova, T.N., Ferrer, M., Golyshina, O. V, Yakimov, M.M., Golyshin, P.N., 2018. The genome analysis of *Oleiphilus messinensis* ME102 (DSM 13489 T) reveals backgrounds of its obligate alkane-devouring marine lifestyle. <https://doi.org/10.1016/j.margen.2017.07.005>

Tully, B.J., Heidelberg, J.F., 2013. Microbial communities associated with ferromanganese nodules and the surrounding sediments. *Front. Microbiol.* 4, 161. <https://doi.org/10.3389/fmicb.2013.00161>

Unfried, F., Becker, S., Robb, C.S., Hehemann, J.-H., Markert, S., Heiden, S.E., Hinzke, T., Becher, D., Reintjes, G., Krüger, K., Avci, B., Kappelmann, L., Hahnke, R.L., Fischer, T., Harder, J., Teeling, H., Fuchs, B., Barbeyron, T., Amann, R.I., Schweder, T., 2018.

- Adaptive mechanisms that provide competitive advantages to marine bacteroidetes during microalgal blooms. *ISME J.* 12, 2894–2906. <https://doi.org/10.1038/s41396-018-0243-5>
- van Vliet, D.M., Lin, Y., Bale, N.J., Koenen, M., Villanueva, L., Stams, A.J.M., Sánchez-Andrea, I., 2020. *Pontiella desulfatans* gen. Nov., sp. nov., and *pontiella sulfatireligans* sp. nov., two marine anaerobes of the pontiellaceae fam. nov. producing sulfated glycosaminoglycan-like exopolymers. *Microorganisms* 8, 1–22. <https://doi.org/10.3390/microorganisms8060920>
- van Vliet, D.M., Palakawong Na Ayudthaya, S., Diop, S., Villanueva, L., Stams, A.J.M., Sánchez-Andrea, I., 2019a. Anaerobic Degradation of Sulfated Polysaccharides by Two Novel Kiritimatiellales Strains Isolated From Black Sea Sediment. *Front. Microbiol.* 10, 253. <https://doi.org/10.3389/fmicb.2019.00253>
- van Vliet, D.M., Palakawong Na Ayudthaya, S., Diop, S., Villanueva, L., Stams, A.J.M.M., Sánchez-Andrea, I., 2019b. Anaerobic Degradation of Sulfated Polysaccharides by Two Novel Kiritimatiellales Strains Isolated From Black Sea Sediment. *Front. Microbiol.* 10, 253. <https://doi.org/10.3389/fmicb.2019.00253>
- Vetterli, A., Hyytiäinen, K., Ahjos, M., Auvinen, P., Paulin, L., Hietanen, S., Leskinen, E., 2015. Seasonal patterns of bacterial communities in the coastal brackish sediments of the Gulf of Finland, Baltic Sea. *Estuar. Coast. Shelf Sci.* 165, 86–96. <https://doi.org/10.1016/j.ecss.2015.07.049>
- Volkman, J.K., Barrett, S.M., Dunstan, G.A., 1994. C25 and C30 highly branched isoprenoid alkenes in laboratory cultures of two marine diatoms. *Org. Geochem.* 21, 407–414.

[https://doi.org/10.1016/0146-6380\(94\)90202-X](https://doi.org/10.1016/0146-6380(94)90202-X)

- Walker, A.M., Leigh, M.B., Mincks, S.L., 2021. Patterns in Benthic Microbial Community Structure Across Environmental Gradients in the Beaufort Sea Shelf and Slope. *Front. Microbiol.* 12, 37. <https://doi.org/10.3389/fmicb.2021.581124>
- Walters, W., Hyde, E.R., Berg-Lyons, D., Ackermann, G., Humphrey, G., Parada, A., Gilbert, J.A., Jansson, J.K., Caporaso, J.G., Fuhrman, J.A., Apprill, A., Knight, R., 2016. Improved Bacterial 16S rRNA Gene (V4 and V4-5) and Fungal Internal Transcribed Spacer Marker Gene Primers for Microbial Community Surveys. *mSystems* 1, e00009-15. <https://doi.org/10.1128/mSystems.00009-15>
- Wang, L., Liu, X., Yu, S., Shi, X., Wang, X., Zhang, X.-H., 2017. Bacterial community structure in intertidal sediments of Fildes Peninsula, maritime Antarctica. *Polar Biol.* 40, 339–349. <https://doi.org/10.1007/s00300-016-1958-2>
- Wang, Q., Garrity, G.M., Tiedje, J.M., Cole, J.R., 2007. Naive Bayesian Classifier for Rapid Assignment of rRNA Sequences into the New Bacterial Taxonomy. *Appl. Environ. Microbiol.* 73, 5261–5267. <https://doi.org/10.1128/AEM.00062-07>
- Watanabe, M., Galushko, A., Fukui, M., Kuever, J., 2021. Desulfosarcinaceae, in: Whitman, W.B. (Ed.), *Bergey's Manual of Systematics of Archaea and Bacteria*. Wiley, pp. 1–4. <https://doi.org/10.1002/9781118960608.fbm00329>
- Wegner, C.E., Richter-Heitmann, T., Klindworth, A., Klockow, C., Richter, M., Achstetter, T., Glöckner, F.O., Harder, J., 2013. Expression of sulfatases in *Rhodopirellula baltica* and the diversity of sulfatases in the genus *Rhodopirellula*. *Mar. Genomics* 9, 51–61.

- Weingartner, T., Aagaard, K., Woodgate, R., Danielson, S., Sasaki, Y., Cavalieri, D., 2005. Circulation on the north central Chukchi Sea shelf. *Deep Sea Res. Part II Top. Stud. Oceanogr.* 52, 3150–3174. <https://doi.org/10.1016/J.DSR2.2005.10.015>
- Westcott, S.L., Schloss, P.D., 2017. OptiClust, an Improved Method for Assigning Amplicon-Based Sequence Data to Operational Taxonomic Units. *mSphere* 2, e00073-17. <https://doi.org/10.1128/mSphereDirect.00073-17>
- Woodgate, R.A., 2018. Increases in the Pacific inflow to the Arctic from 1990 to 2015, and insights into seasonal trends and driving mechanisms from year-round Bering Strait mooring data. *Prog. Oceanogr.* 160, 124–154. <https://doi.org/10.1016/J.POCEAN.2017.12.007>
- Xing, P., Hahnke, R.L., Unfried, F., Markert, S., Huang, S., Barbeyron, T., Harder, J., Becher, D., Schweder, T., Glöckner, F.O., Amann, R.I., Teeling, H., 2015. Niches of two polysaccharide-degrading *Polaribacter* isolates from the North Sea during a spring diatom bloom. *ISME J.* 9, 1410–1422. <https://doi.org/10.1038/ismej.2014.225>
- Yakimov, M.M., Giuliano, L., Gentile, G., Crisafi, E., Chernikova, T.N., Abraham, W.-R., Lünsdorf, H., Timmis, K.N., Golyshin, P.N., 2003. *Oleispira antarctica* gen. nov., sp. nov., a novel hydrocarbonoclastic marine bacterium isolated from Antarctic coastal sea water. *Int. J. Syst. Evol. Microbiol.* 53, 779–785. <https://doi.org/10.1099/ijs.0.02366-0>
- Yakimov, M.M., Timmis, K.N., Golyshin, P.N., 2007. Obligate oil-degrading marine bacteria. *Curr. Opin. Biotechnol.* 18, 257–266. <https://doi.org/10.1016/j.copbio.2007.04.006>
- Zeng, Y., Zou, Y., Chen, B., Grebmeier, J.M., Li, H., Yu, Y., Zheng, T., 2011. Phylogenetic

diversity of sediment bacteria in the northern Bering Sea. *Polar Biol.* 34, 907–919.

<https://doi.org/10.1007/s00300-010-0947-0>

Zinger, L., Amaral-Zettler, L.A., Fuhrman, J.A., Horner-Devine, M.C., Huse, S.M., Welch, D.B.M., Martiny, J.B.H., Sogin, M., Boetius, A., Ramette, A., 2011. Global Patterns of Bacterial Beta-Diversity in Seafloor and Seawater Ecosystems. *PLoS One* 6, e24570.

<https://doi.org/10.1371/journal.pone.0024570>

Zinke, L.A., Reese, B.K., McManus, J., Wheat, C.G., Orcutt, B.N., Amend, J.P., 2018. Sediment microbial communities influenced by cool hydrothermal fluid migration. *Front. Microbiol.*

9. <https://doi.org/10.3389/fmicb.2018.01249>

Zonneveld, K.A.F., Versteegh, G.J.M., Kasten, S., Eglinton, T.I., Emeis, K.-C., Huguët, C., Koch, B.P., De Lange, G.J., De Leeuw, J.W., Middelburg, J.J., Mollenhauer, G., Prahl, F.G., Rethemeyer, J., Wakeham, S.G., 2010. Selective preservation of organic matter in marine environments; processes and impact on the sedimentary record. *Biogeosciences* 7, 483–511.

3.9 FIGURES

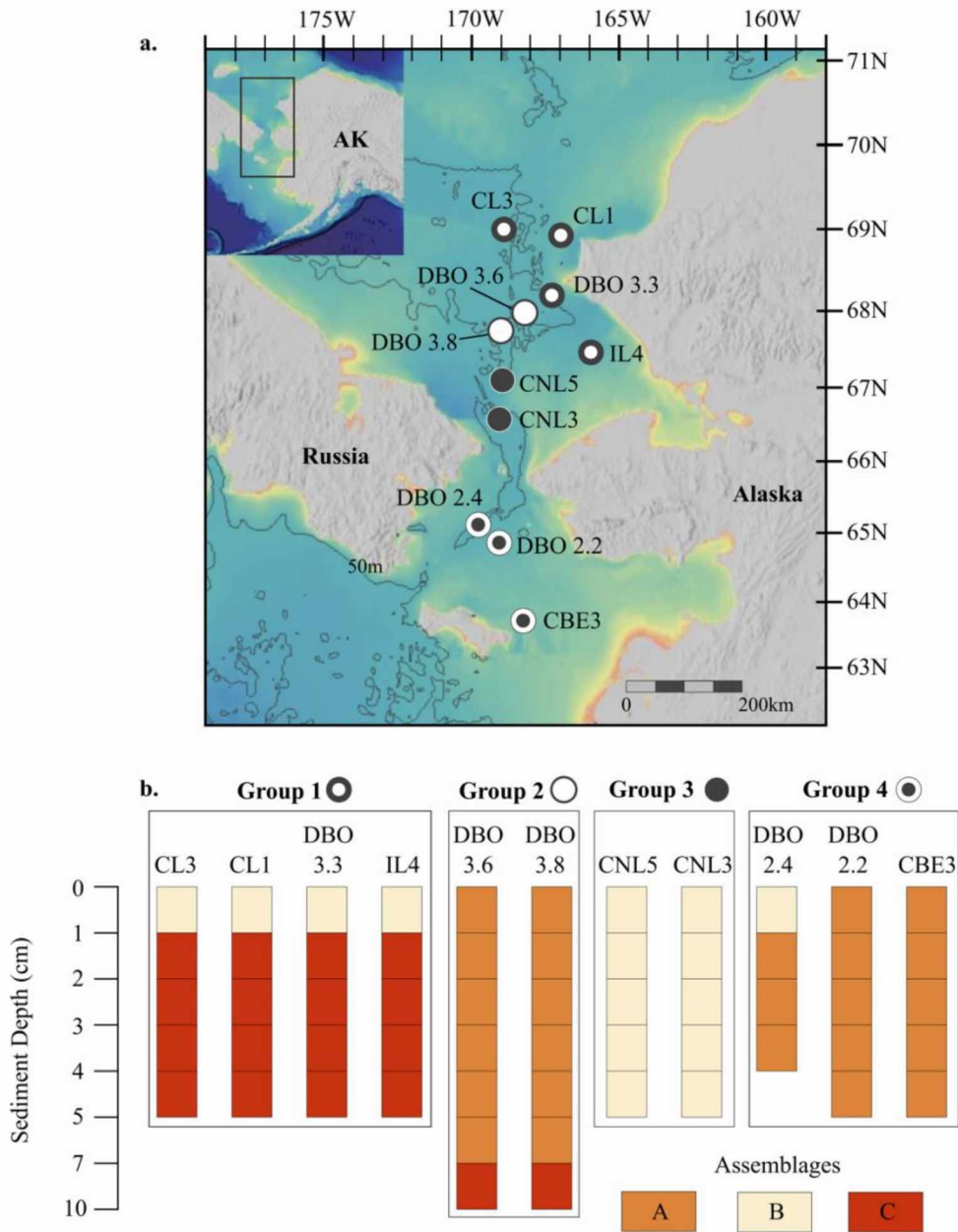


Figure 3.1. Map of ASgard sample stations and associated vertical sediment depth distributions of prokaryotic assemblages. Map (a). The stations on this map show where sediment cores were collected for prokaryotic community and environmental parameter analyses in 2018 as a part of the ASgard program. The different symbols marking each station indicate the assemblage profile group across different sediment depth horizons (b). A depiction of the assemblage profile groups (Group 1, Group 2, Group 3, Group 4), which exhibited similar assemblage patterns with sediment depth.

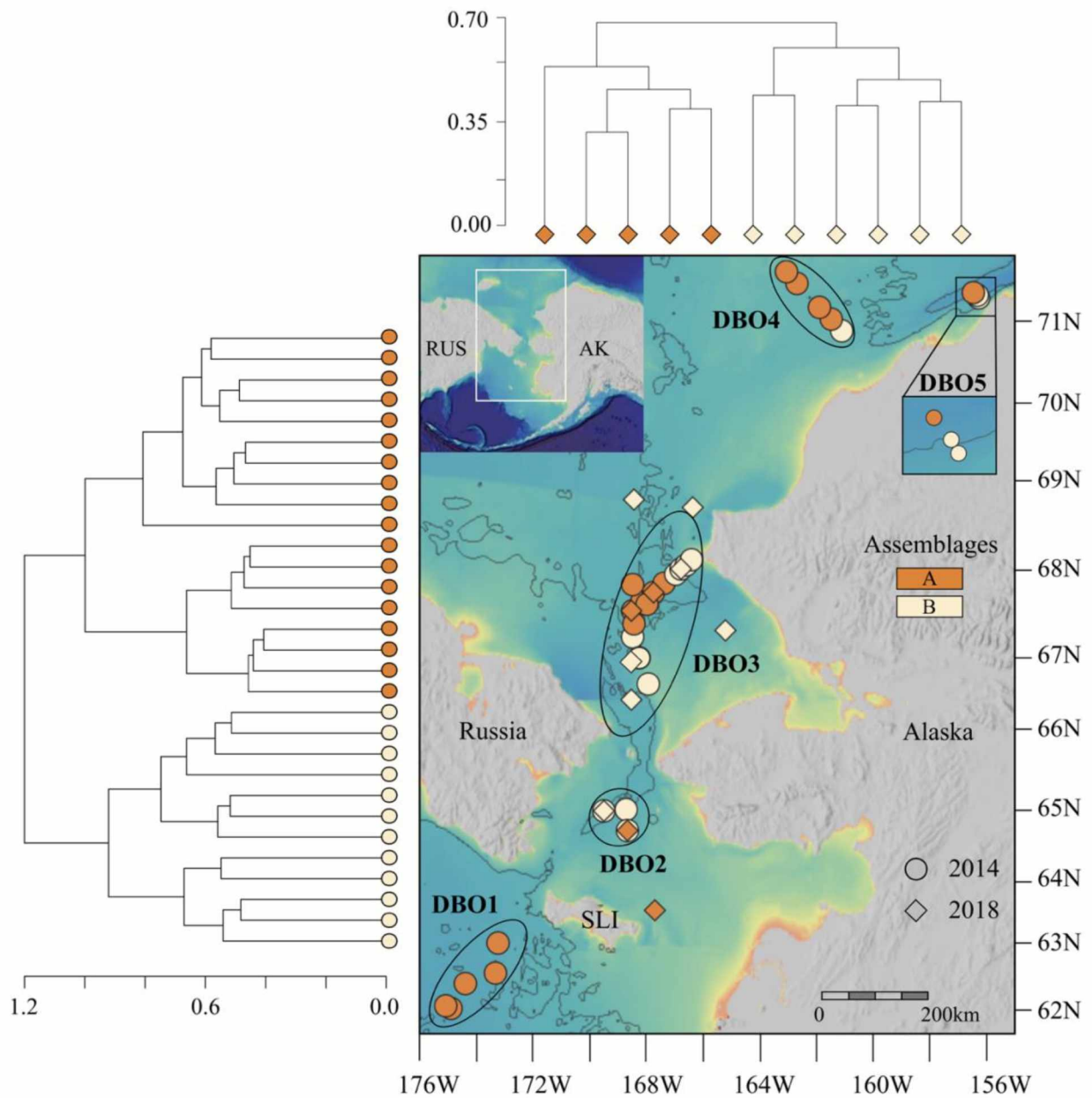


Figure 3.2. Map and dendrograms of prokaryotic community structure exhibited in Bering-Chukchi surface sediments from ASGARD and DBO samples. The dendrogram above the map shows the assemblages for ASGARD surface sediments and the dendrogram to the left shows the assemblages exhibited in DBO surface sediments. The stations on the map are colored by assemblage and shaped based on year. The stations on the map are also put into context with respect to the DBO 1-5 transects located on the Bering-Chukchi Shelf. St. Lawrence Island is denoted by the abbreviation SLI.

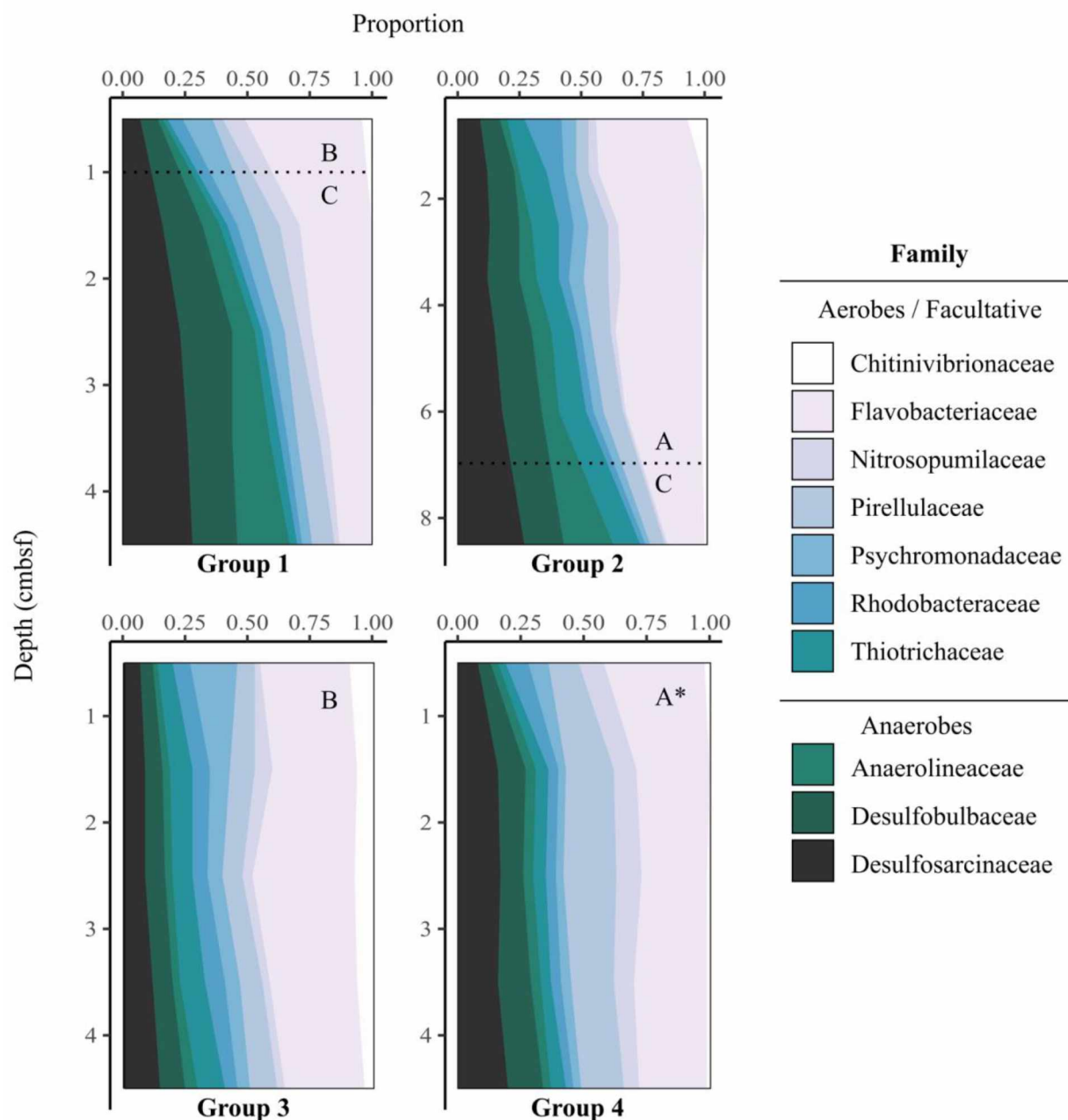


Figure 3.3. Depth trends in relative abundance of 10 dominant taxa (family-level) for groups sharing the same downcore microbial assemblage patterns. Overlaid on each plot are letters denoting the assemblage exhibited by each group and dotted lines where a transition between assemblages occurred. The figure legend is organized such that the aerobic and/or facultative taxa are depicted in lighter colors and anaerobic taxa are depicted in darker colors. Depth is measure as cm below seafloor (cmbsf).

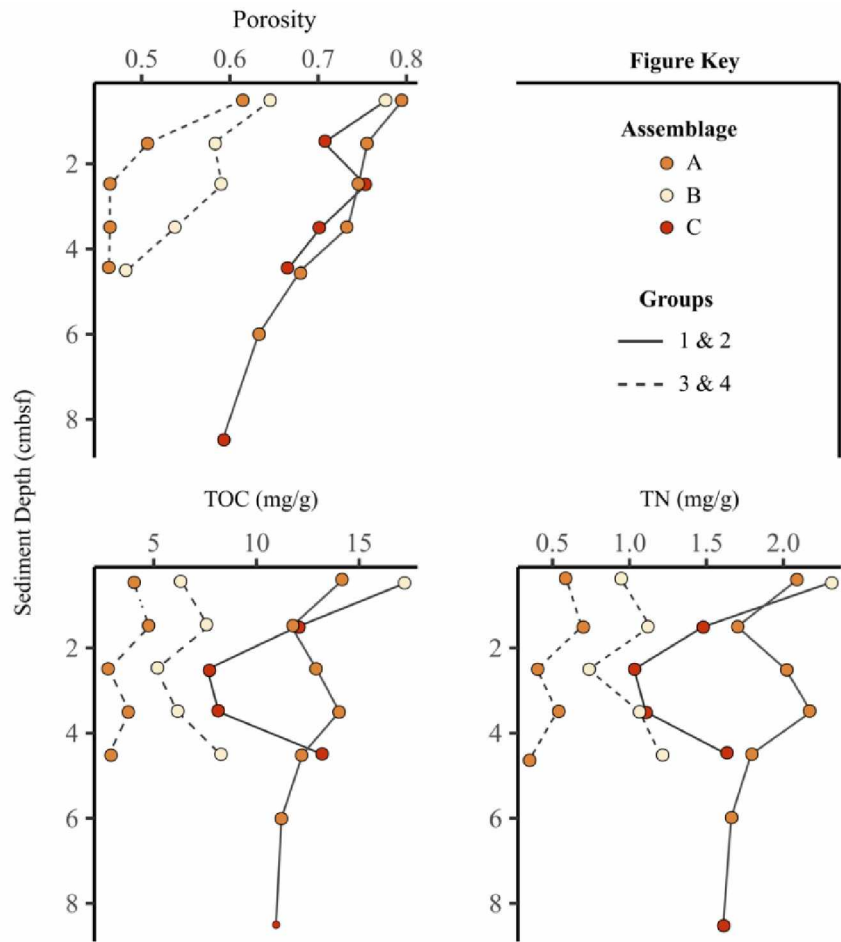


Figure 3.4. Sediment characteristics profiles for prokaryotic assemblage structure with sediment depth. Depth profiles of environmental parameters (porosity, TOC, and TN) that were significantly correlated with microbial community structure for each group. Groups are denoted by different line patterns, and colors of the points reflect the assemblage that was exhibited at the corresponding sediment depth on the y-axis. Sediment depth is measure as cm below seafloor (cmbsf).

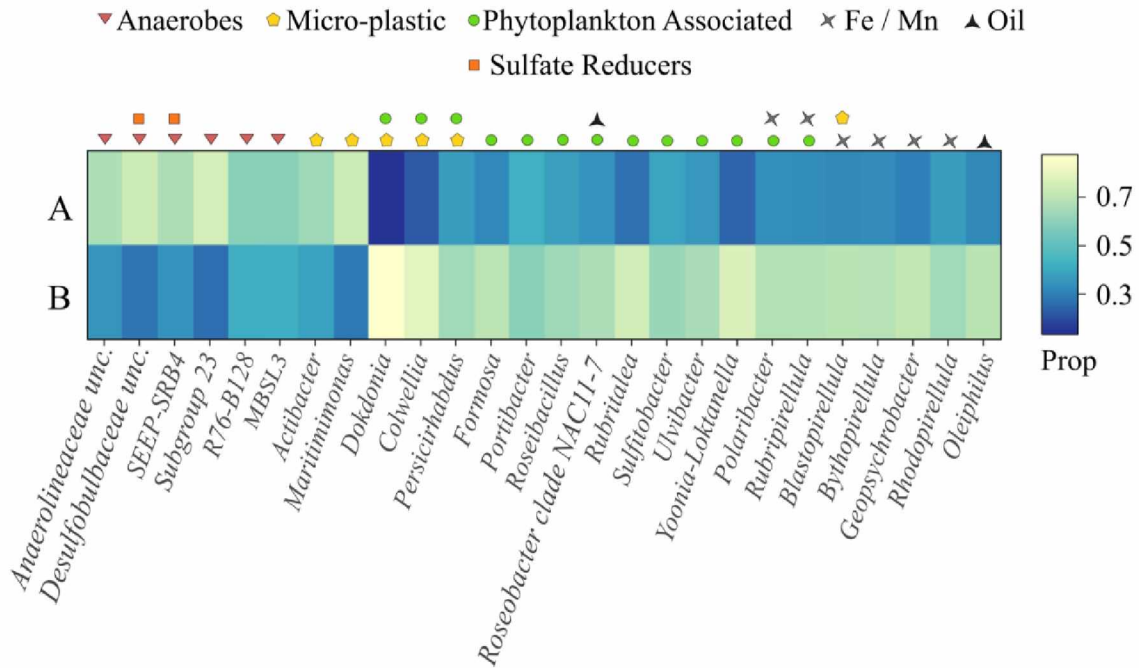


Figure 3.5. Heatmap of indicator taxa and most abundant genus-level taxa for assemblages A and B across Bering-Chukchi sediments. Indicator taxa included in the heatmap are *R76-B128*, *MSBL3*, *Blastopirellula*, *Dokdonia*, *Rubritalea*, *Geopsychrobacter*, and *Oleiphilus*. The symbols above the heatmap represent functional groups reported in the literature for each taxon.

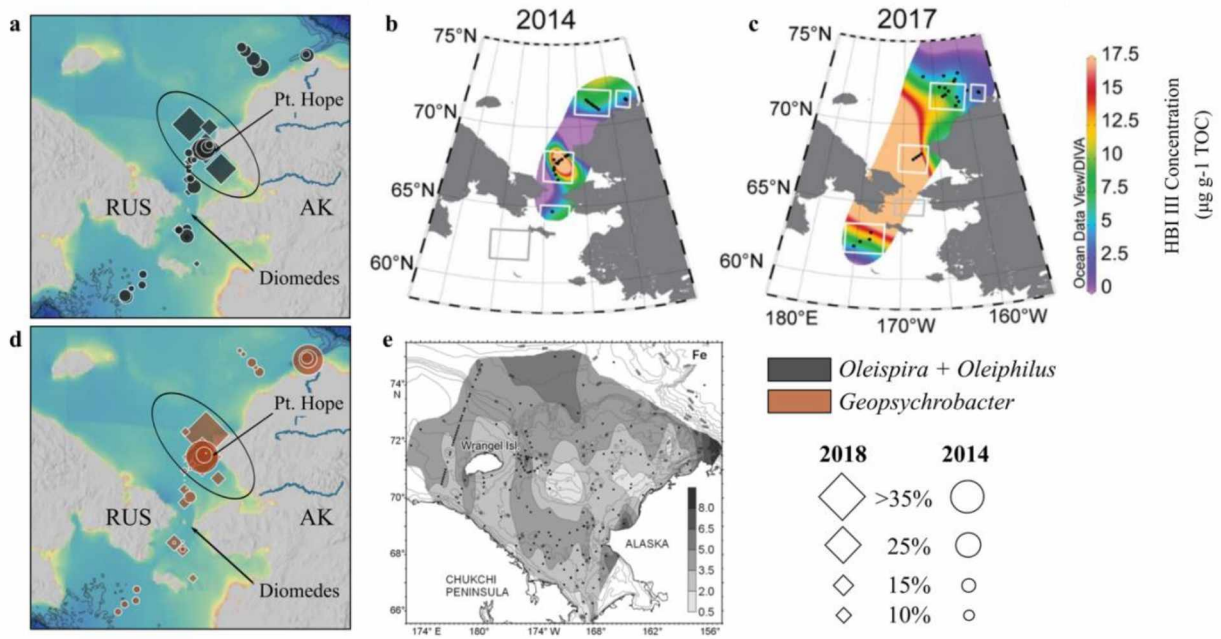


Figure 3.6. Distribution of oil degraders and iron reducers in relation to isoprenoid III and Fe concentrations in Northern Bering and Chukchi sediments on the Bering Chukchi Shelf. Maps of the distribution and relative abundance (%) of oil degraders (*Oleispira* and *Oleiphilus*) and iron reducers (*Geopsychrobacter*) in sediments collected from a) ASGARD (2018) and d) DBO (2014). Concentrations of highly branched isoprenoid III in b) 2014 and c) 2017 (Koch et al., 2020). Iron (Fe) content (%) measured in Chukchi sediments in 2012 (e) (Astakhov et al., 2013).

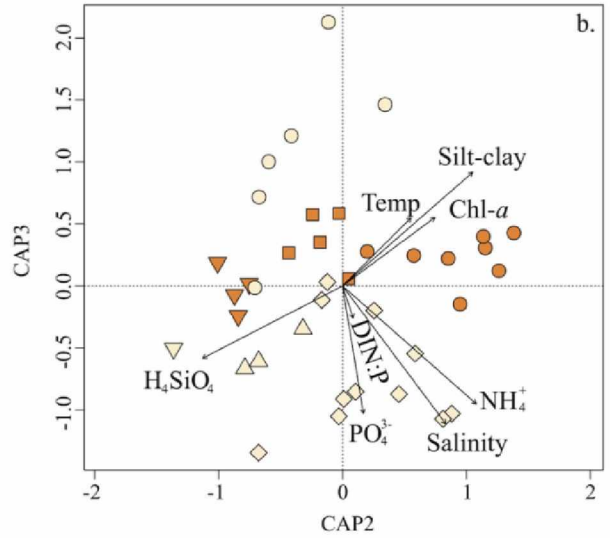
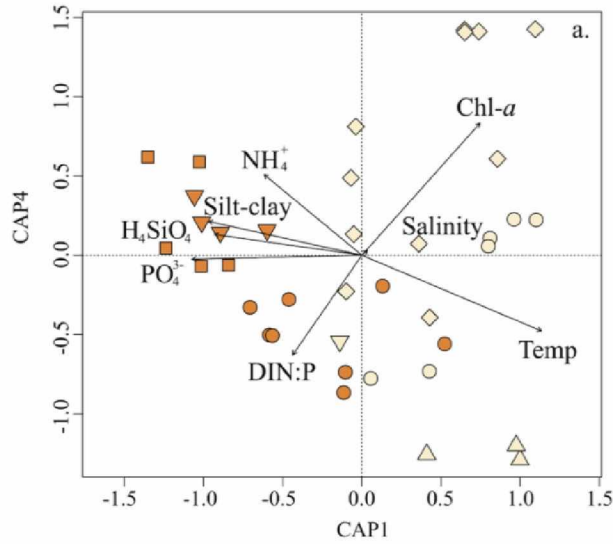


Figure Key

Assemblages	A	B
Samples	◇ ASGARD	□ DBO1
	△ DBO2	○ DBO3
		▽ DBO4

	CAP1	CAP2	CAP3	CAP4
Temp	0.66	-0.24	0.23	-0.29
Salinity	0.02	0.36	-0.47	0.02
Chl- <i>a</i>	0.43	0.32	0.23	0.50
NH ₄ ⁺	-0.36	0.47	-0.40	0.31
PO ₄ ³⁻	-0.62	0.07	-0.43	-0.01
DIN:P	-0.25	0.04	-0.11	-0.38
H ₄ SiO ₄	-0.54	-0.49	-0.24	0.08
% Silt-Clay	-0.56	0.46	0.38	0.13

Figure 3.7. Environmental parameters correlating with prokaryotic assemblage structure in Bering-Chukchi surface sediments. Ordination plots exhibiting the significant environmental correlates with the community structure of Bering-Chukchi sediment prokaryotes and are depicted in 2 different axes combinations: a) CAP1 and CAP4 axes and b) CAP2 and CAP3 axes. The table provides the correlation strength (R^2) between the statistically significant ($P < 0.001$) environmental variables and associated axes. Note that DBO5 was not included as all three samples were lacking Chl-*a* measurements.

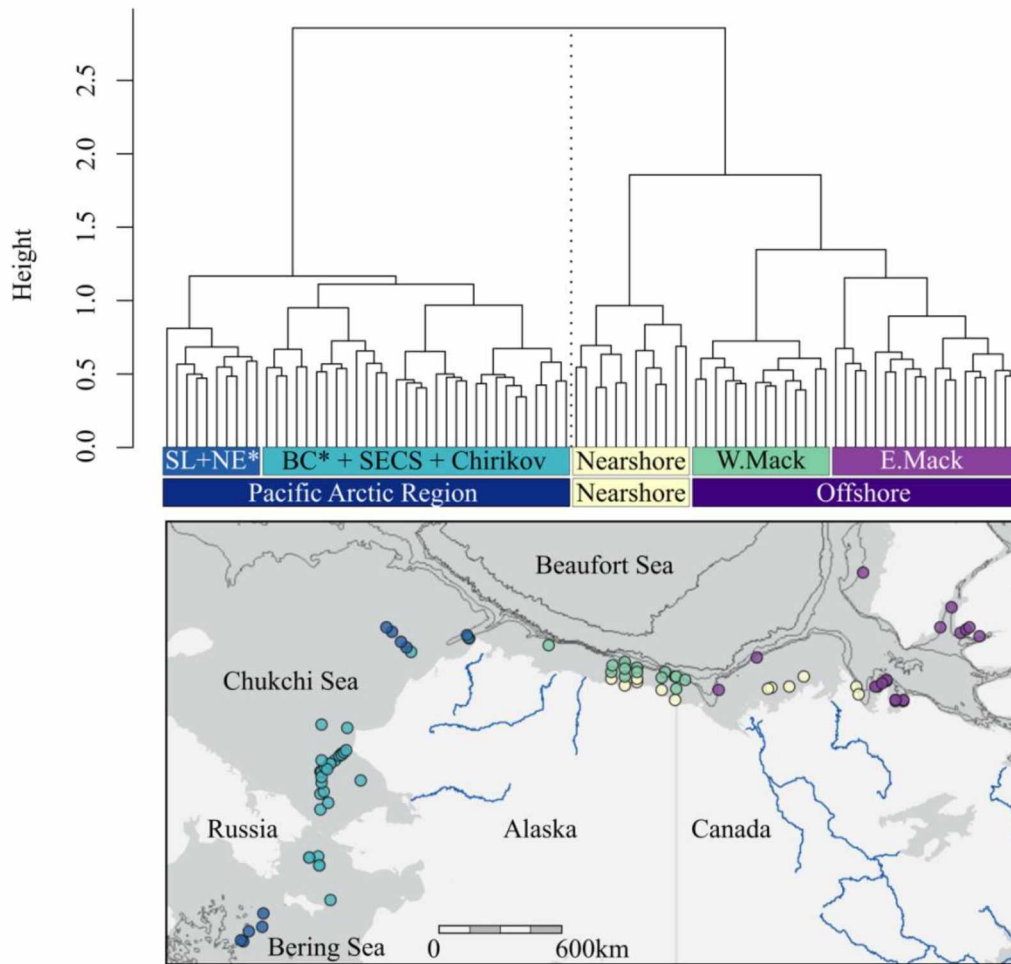


Figure 3.8. Dendrogram and map of prokaryotic community structure in surface sediments of the North American Arctic. The dotted line in the dendrogram denotes the division between the Bering-Chukchi and Beaufort seas and depicts the differences between the 3 major assemblages in the North American Arctic: The Bering-Chukchi assemblage and the nearshore and offshore assemblages within the Beaufort Sea. The substructure within the Bering-Chukchi assemblage was such that the transects overlaying corresponding benthic hotspots DBO1 (SLIP) and DBO4 (NECS) hotspots were clustered together (SL+NE*), and the DBO5 (BC), DBO3 (SECS), and DBO2 (Chirikov) hotspots were clustered together (BC* +SECS + Chirikov). The asterisks denote that there is one station within the NECS (DBO4) transect which clusters with the BC +SECS + Chirikov (DBO5+DBO3+DBO2) samples, and one station in the BC (DBO5) transect that were clustered with the SLIP+NECS (DBO1 + DBO4) samples. In the Beaufort Sea, substructure within the offshore shelf assemblage was such that there were offshore sub-assemblages west and east of the Mackenzie River. The stations on the map are colored by substructure.

APPENDICES

Appendix Table 3.1. Sediment characteristic data for ASGARD samples.

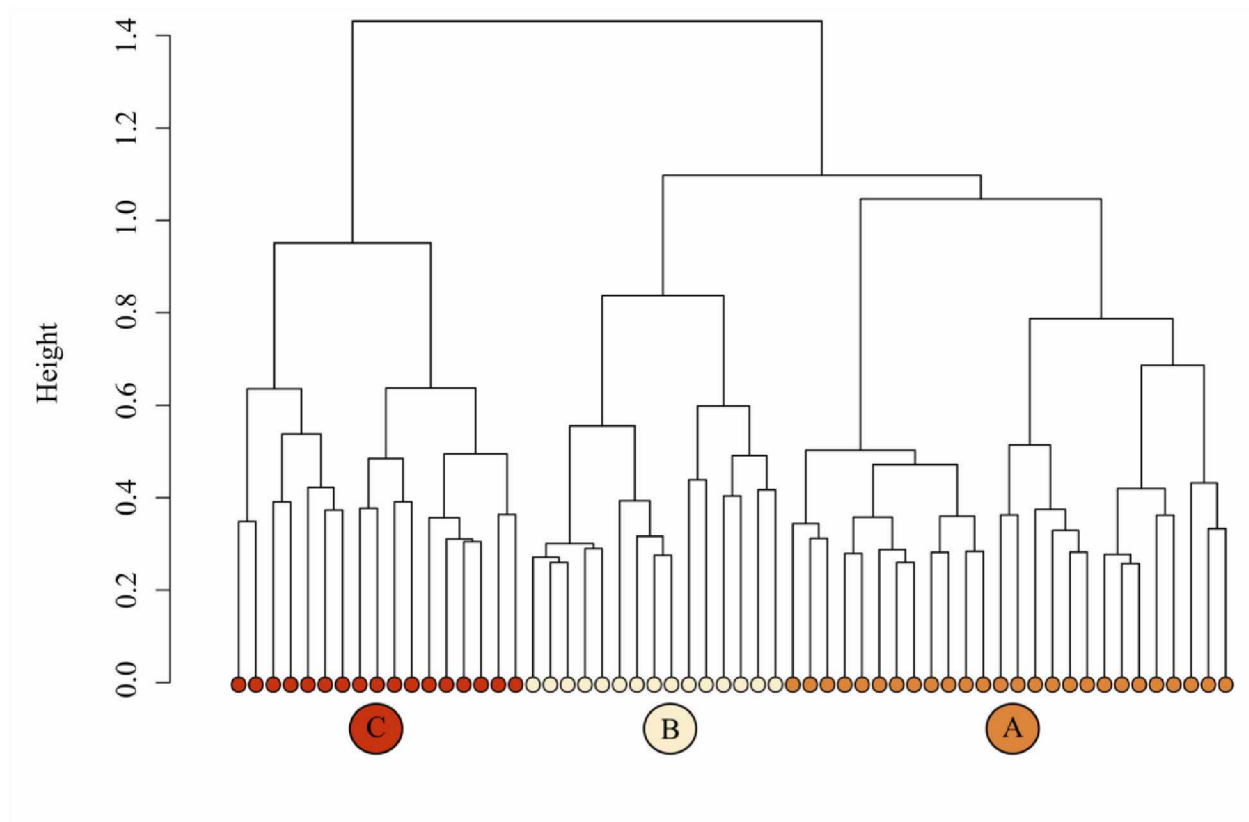
Sample_ID	Porosity	Mean Phi	Sorting	Kurtosis	SiltyClay (phi>5)	Chl- <i>a</i> (µg/g)	Phaeo (µg/g)	d ¹⁵ N (o/oo)	d ¹³ C (o/oo)	TOC (mg/g)	TN (mg/g)	CN
CBE3_0_1cm	0.816	4.514	1.887	1.554	29.7	1.22	4.10	7.51	-22.45	4.06	0.60	6.80
CBE3_1_2cm	0.527	4.514	1.887	1.554	29.7	0.89	4.14	8.16	-22.50	4.78	0.69	6.95
CBE3_2_3cm	0.464	4.514	1.887	1.554	29.7	0.87	3.66	8.18	-22.47	8.18	1.19	6.87
CBE3_3_4cm	0.531	4.514	1.887	1.554	29.7	0.70	2.64	7.92	-22.92	4.53	0.59	7.74
CBE3_4_5cm	0.463	4.514	1.887	1.554	29.7	0.61	2.83	7.71	-22.70	4.04	0.58	7.00
CL1_0_1cm	0.754	6.161	2.240	0.681	76.2	10.12	7.95	8.61	-22.96	16.39	2.20	7.44
CL1_1_2cm	0.649	6.161	2.240	0.681	76.2	2.02	4.25	5.36	-23.57	8.06	0.83	9.75
CL1_3_4cm	0.661	6.161	2.240	0.681	76.2	0.89	3.18	8.87	-23.81	7.67	0.84	9.15
CL1_4_5cm	0.609	6.161	2.240	0.681	76.2	0.85	3.03	6.18	-23.70	12.59	1.45	8.70
CL3_0_1cm	0.802	6.669	2.093	0.797	89.7	6.85	12.02	7.74	-21.84	19.46	3.07	6.35
CL3_1_2cm	0.764	6.669	2.093	0.797	89.7	2.80	8.74	8.75	-22.15	17.58	2.53	6.95
CL3_2_3cm	0.754	6.669	2.093	0.797	89.7	1.90	7.60	7.27	-22.49	14.62	1.97	7.43
CL3_3_4cm	0.767	6.669	2.093	0.797	89.7	1.89	7.92	8.83	-22.48	15.27	2.03	7.50
CL3_4_5cm	0.749	6.669	2.093	0.797	89.7	1.43	6.73	9.04	-22.57	16.00	2.11	7.57
CNL3_0_1cm	0.628	2.337	1.731	2.189	14.4	5.92	5.65	6.90	-21.55	5.59	0.94	5.96
CNL3_1_2cm	0.527	2.337	1.731	2.189	14.4	1.66	3.67	8.16	-21.73	4.58	0.75	6.07
CNL3_2_3cm	0.517	2.337	1.731	2.189	14.4	1.21	3.41	8.27	-22.63	2.24	0.34	6.52
CNL3_3_4cm	0.443	2.337	1.731	2.189	14.4	1.09	3.17	7.95	-20.85	7.10	1.26	5.65
CNL3_4_5cm	0.373	2.337	1.731	2.189	14.4	0.85	2.92	8.30	-22.01	10.31	1.54	6.68
CNL5_0_1cm	0.667	4.995	2.302	0.802	47.9	2.39	7.93	7.01	-22.55	7.28	0.99	7.36
CNL5_1_2cm	0.637	4.995	2.302	0.802	47.9	2.34	7.10	7.79	-22.34	10.75	1.52	7.09
CNL5_2_3cm	0.665	4.995	2.302	0.802	47.9	2.31	5.51	6.91	-22.30	8.00	1.13	7.11
CNL5_3_4cm	0.633	4.995	2.302	0.802	47.9	2.41	3.52	3.43	-22.52	5.23	0.87	6.04
CNL5_4_5cm	0.594	4.995	2.302	0.802	47.9	3.12	4.42	6.68	-22.48	6.19	0.86	7.19

DBO2.2_0_1cm	0.526	2.915	1.197	1.946	10.7	3.82	6.50	8.78	-21.81	6.83	1.00	6.80
DBO2.2_1_2cm	0.508	2.915	1.197	1.946	10.7	1.28	4.38	7.77	-22.24	3.19	0.45	7.00
DBO2.2_2_3cm	0.472	2.915	1.197	1.946	10.7	1.18	2.94	10.07	-22.07	2.70	0.40	6.75
DBO2.2_3_4cm	0.464	2.915	1.197	1.946	10.7	0.89	3.21	7.70	-21.68	2.32	0.37	6.29
DBO2.2_4_5cm	0.484	2.915	1.197	1.946	10.7	0.55	2.76	6.67	-22.02	2.07	0.31	6.60
DBO2.4_0_1cm	0.615	3.062	1.164	1.821	10.7	2.30	3.67	6.38	-21.37	3.65	0.54	6.76
DBO2.4_1_2cm	0.442	3.062	1.164	1.821	10.7	0.60	2.67	6.68	-21.66	4.89	0.72	6.82
DBO2.4_2_3cm	0.464	3.062	1.164	1.821	10.7	0.55	2.62	6.89	-21.87	2.82	0.39	7.20
DBO2.4_3_4cm	0.447	3.062	1.164	1.821	10.7	0.67	2.42	6.74	-21.89	3.81	0.53	7.20
DBO2.4_4_5cm	0.417	3.062	1.164	1.821	10.7	0.57	2.34	6.71	-22.14	2.82	0.37	7.57
DBO3.3_0_1cm	0.439	3.052	3.800	0.612	37.7	5.65	4.41	8.00	-21.96	3.77	0.61	6.19

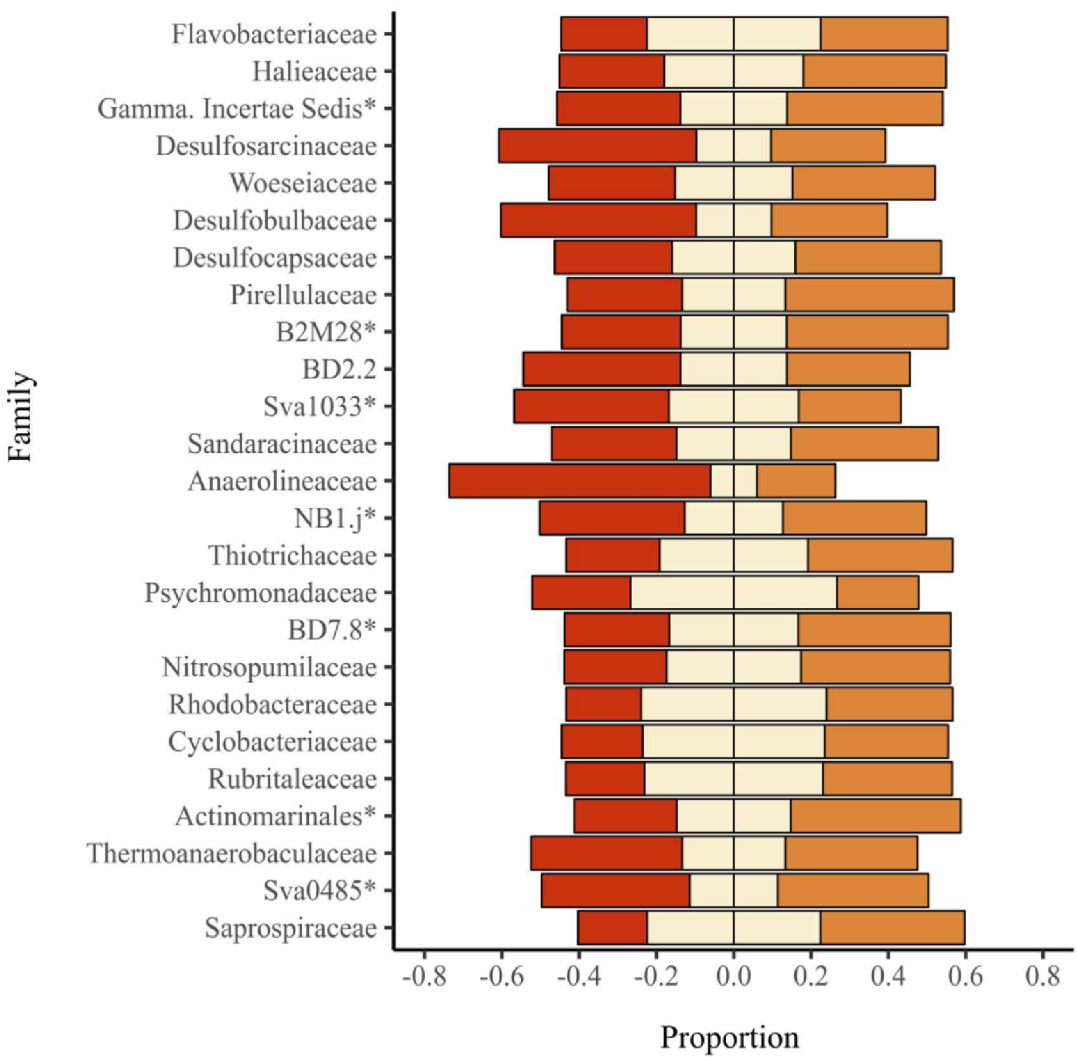
Appendix Table 3.2. Environmental data for ASGARD and DBO surface samples (0-1cm).

Station	Cruise	Year	Latitude	Longitude	Depth (m)	Temp (C)	Salinity	NH4 (mmol/m3)	NO2+NO3 (mmol/m3)	PO4 (mmol/m3)	H ₄ SiO ₄ (mmol/m3)	SiltyClay (phi _≥ 5)	TOC (mg/g)	TN (mg/g)	CN	Chla (mg/m2)	DIN:P
CBE3	ASGARD	2018	63.514	-168.179	32	1.82	31.76	1.79	5.49	1.393	22.8	29.7	4.06	0.60	6.80	11.95	3.94
CL1	ASGARD	2018	68.948	-166.910	46	0.02	31.92	2.42	9.01	1.517	18.6	76.2	16.39	2.20	7.44	49.21	5.94
CL3	ASGARD	2018	69.034	-168.890	53	-0.62	32.39	1.97	16.54	2.021	37.1	89.7	19.46	3.07	6.35	26.48	8.18
CNL3	ASGARD	2018	66.501	-168.956	56	1.74	32.76	2.5	7.96	1.227	12.7	14.4	5.59	0.94	5.96	58.5	6.49
CNL5	ASGARD	2018	67.000	-168.960	48	1.48	32.97	3.71	8.96	1.532	19.8	47.9	7.28	0.99	7.36	14.06	5.85
DBO2.2	ASGARD	2018	64.680	-169.101	46	2.31	32.36	0.83	7.33	1.254	10.4	10.7	6.83	1.00	6.80	28.96	5.85
DBO2.4	ASGARD	2018	64.960	-169.890	48	0.90	32.94	1.41	12.06	1.505	16.1	10.7	3.65	0.54	6.76	23.91	8.01
DBO3.3	ASGARD	2018	68.186	-167.310	48	0.48	32.67	3.43	4.22	1.215	8.2	37.7	3.77	0.61	6.19	38.99	3.47
DBO3.6	ASGARD	2018	67.898	-168.244	58	0.56	32.70	5.51	2.94	1.437	11.6	45.3	11.34	1.66	6.85	19.52	2.05
DBO3.8	ASGARD	2018	67.671	-168.959	51	1.74	32.86	5.8	4.85	1.543	12.9	61.7	15.43	2.32	6.63	8.02	3.14
IL4	ASGARD	2018	67.406	-165.824	39	2.07	32.46	1.36	0.94	0.76	1.1	93.3	17.88	2.36	7.59	36.6	1.24
DBO5.3	DBO	2014	71.331	-157.317	91	0.45	31.67	0.80	1.49	0.80	11.74	12	4.4	0.5	8.13	NA	1.86
DBO5.4	DBO	2014	71.358	-157.358	108	-0.93	31.98	1.30	3.15	0.90	18.15	9.68	3.4	0.3	12.84	NA	3.50
DBO5.5	DBO	2014	71.399	-157.465	126	-1.60	32.40	2.00	9.81	1.58	34.16	NA	5	0.5	9.2	NA	6.21
DBO4.1	DBO	2014	70.973	-161.901	45	-1.24	32.13	1.86	5.42	1.25	20.28	28.77	3.9	0.5	8.57	7.15	4.34
DBO4.2	DBO	2014	71.104	-162.264	47	-1.52	32.33	1.92	9.01	1.42	28.11	50.23	8.1	0.9	8.82	10.97	6.35
DBO4.3	DBO	2014	71.233	-162.635	46	-1.67	32.54	2.48	11.47	1.72	37.37	87.15	11.3	1.6	7.04	14.68	6.67
DBO4.5	DBO	2014	71.490	-163.388	43	-1.72	32.66	1.85	14.72	1.95	50.53	57.54	9.6	1.4	6.74	9.94	7.55
DBO4.6	DBO	2014	71.618	-163.771	42	-1.68	32.57	2.43	13.88	1.88	43.77	67.47	9.2	1.3	6.95	6.86	7.38
DBO3.1	DBO	2014	67.671	-168.909	50	2.24	32.68	2.43	7.79	1.37	4.63	92.64	12.5	2	6.22	20.1	5.69
DBO3.2	DBO	2014	67.783	-168.601	50	2.08	32.56	2.91	10.43	1.66	6.41	97.08	12.2	1.9	6.41	29.22	6.28
DBO3.3	DBO	2014	67.898	-168.235	59	2.14	32.45	2.64	10.07	1.27	3.56	62.63	11.3	1.8	6.4	37.69	7.93
DBO3.4	DBO	2014	68.012	-167.869	53	2.00	32.11	1.98	0.9	0.82	5.34	33.08	6.5	1	6.44	23.57	1.10
DBO3.5	DBO	2014	68.128	-167.496	50	3.28	31.64	0.64	0.27	0.52	3.56	28.91	6.4	0.9	7.33	23.99	0.52
DBO3.6	DBO	2014	68.185	-167.307	48	4.69	31.51	0.42	0.66	0.40	4.63	18.55	6.4	1	6.69	20.39	1.65
DBO3.7	DBO	2014	68.242	-167.122	43	5.71	31.22	0.38	0.29	0.49	6.41	33.96	6.8	0.9	7.54	35.49	0.59

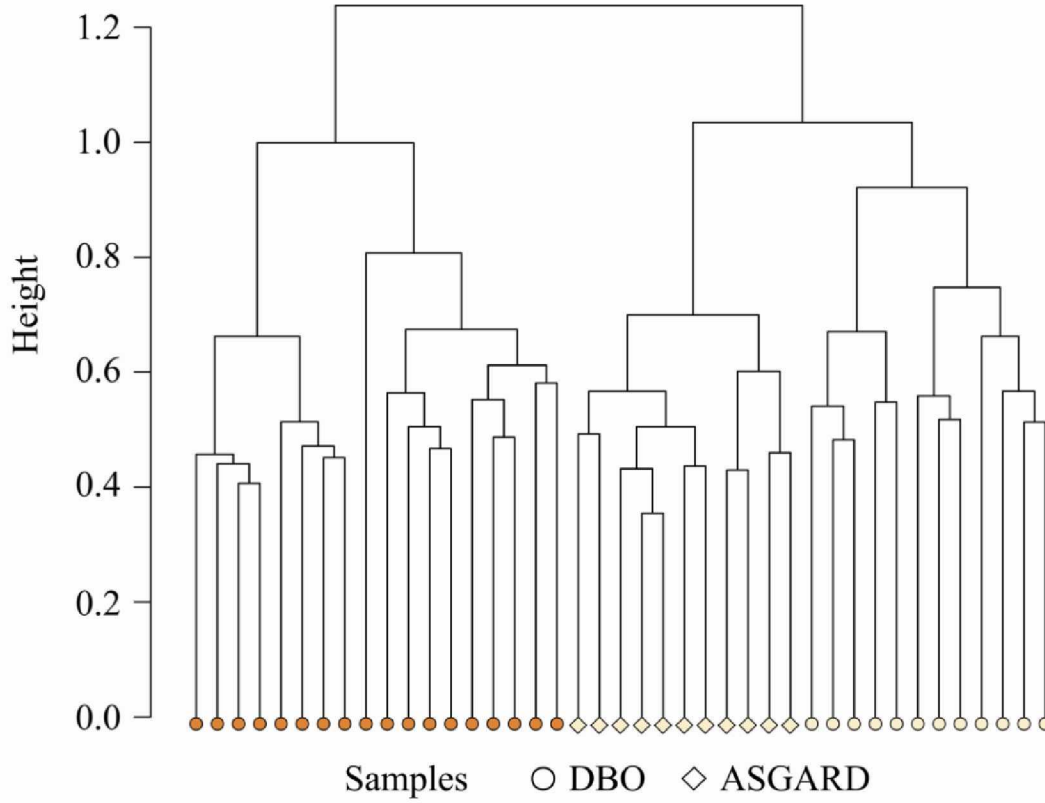
DBO3.8	DBO	2014	68.300	-166.936	35	5.49	30.94	0.92	0.44	0.59	8.90	26.3	6.2	0.8	8.2	11.75	0.75
DBO1.1	DBO	2014	62.011	-175.059	81	-1.55	31.74	0.85	16.36	1.77	27.76	73.59	11.2	1.8	6.32	27.18	9.24
DBO1.2	DBO	2014	62.050	-175.209	84	-1.54	31.75	0.63	15.79	1.77	26.33	87.09	15.1	2.5	6.15	23.67	8.92
DBO1.4	DBO	2014	62.390	-174.570	71	-1.33	31.86	2.39	15.86	1.90	46.26	84.97	11	1.7	6.52	17.5	8.35
DBO1.8	DBO	2014	63.030	-173.460	71	-1.56	32.45	4.07	15.21	2.04	40.93	91.44	15.5	2.7	5.8	17.63	7.46
DBO1.6	DBO	2014	62.560	-173.549	65	-1.47	32.11	3.75	12.93	1.71	44.13	74.75	10.7	1.7	6.18	19.29	7.56
DBO2.5	DBO	2014	64.991	-169.141	48	1.67	32.72	1.15	17.64	1.71	29.89	23.48	4.7	0.7	6.47	16.88	10.32
DBO2.2	DBO	2014	64.682	-169.100	45	1.48	32.69	1.09	17.21	1.49	26.69	6.08	1.8	0.3	6.8	14.45	11.55
DBO2.4	DBO	2014	64.960	-169.891	49	2.21	32.66	1.30	23.29	1.63	33.81	21.52	3.3	0.5	6.86	19.19	14.29
UTN1	DBO	2014	66.712	-168.399	35	3.15	32.01	0.54	3.01	0.63	1.78	83.69	10.9	1.5	7.25	32.63	4.78
UTN3	DBO	2014	67.330	-168.909	50	2.27	32.53	1.38	7.57	1.26	3.20	70.75	8.5	1.2	6.82	22.5	6.01
UTN4	DBO	2014	67.501	-168.904	50	1.82	32.45	2.04	13.86	1.67	7.12	86.05	10.3	1.7	6.11	18.34	8.30
UTN6	DBO	2014	67.741	-168.440	50	2.10	32.39	2.20	11.07	1.43	2.85	97.98	11.8	1.9	6.07	29.22	7.74
UTN7	DBO	2014	68.000	-168.931	57	2.02	32.60	3.08	12.71	1.46	3.91	94.14	13.7	2.2	6.1	20.29	8.71
UTN2	DBO	2014	67.050	-168.729	47	2.44	32.54	0.54	10.07	1.05	4.98	81.37	7.4	1.1	6.85	28.6	9.59



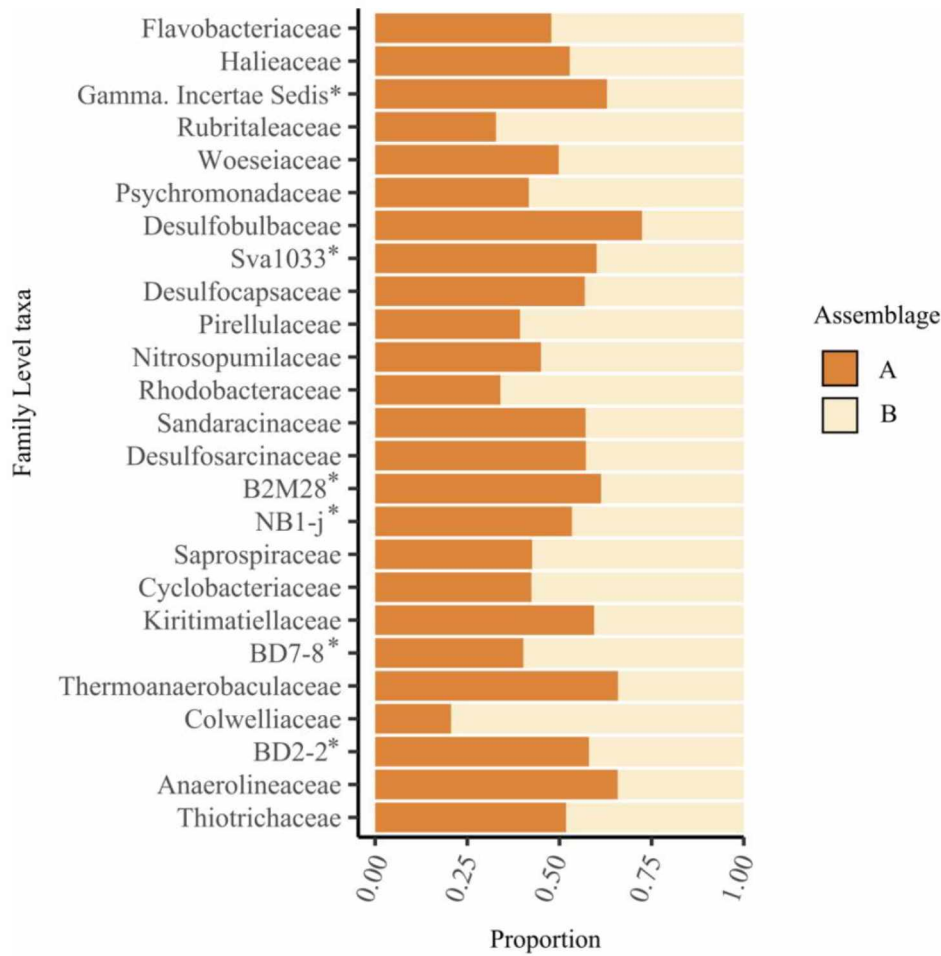
Appendix 3.3. Dendrogram depicting the three prokaryotic assemblage clusters resulting from hierarchical clustering analysis.



Appendix 3.4. Most abundant prokaryotic families across 3 assemblages exhibited in Chukchi sediments in 2018. The stacked barplot illustrates the relative abundance of the top 25 families for each cluster found in the upper 5-10cm in Chukchi Sea sediments collected in 2018. The plot is arranged such that the most abundant taxa starts from the top and decreases towards the bottom. Note that Gammaproteobacteria (Gamma.) Incertae Sedis, B2M28, Sva1033, NB1-j, Actinomarinales, and Sva0485 are not classified to family, but order level.



Appendix 3.5. Dendrogram from hierarchical clustering analysis with combined OTU table for ASGARD and DBO sediment samples.



Appendix 3.6. Top-25 most abundant prokaryotic families across 2 assemblages exhibited in Chukchi sediments in 2014 and 2018. The stacked barplot illustrates the relative abundance of the top 25 families for each assemblage found in the upper 1 cm layer in Northern Bering and Chukchi sediments collected in 2014 and 2018. The plot is arranged such that the most abundant taxa start from the top and decreases towards the bottom. Note that Gammaproteobacteria (Gamma.) Incertae Sedis, Sva1033, B2M28, NB1-j, and BD2-2 are not classified to family, but to order level.

CHAPTER 4: MICROBIAL COMMUNITY RESPONSE TO CRUDE OIL EXPOSURE IN ARCTIC MARINE SEDIMENTS

4.1 ABSTRACT

As sea-ice cover declines, the risk of marine oil spills in the Arctic has grown due to increased ship traffic and offshore oil and gas exploration. With the increasing likelihood of an oil exposure event, it is important to understand the fate and effects of crude oil in the Arctic marine system. This study investigated the benthic microbial response to crude oil in Arctic marine sediments to better understand the effect of spilled oil on benthic habitat. Sediments amended with fresh and weathered crude oil were incubated at *in-situ* bottom water temperature under anoxic and oxic conditions to identify microbial community shifts and putative oil-degrading microbes in the benthos. Molecular analyses via 16S rRNA amplicon surveys of the sediment microbial community response to oil revealed that significant community shifts occurred in the oiled treatments, with distinct microbial communities emerging following exposure to fresh versus weathered oil under both oxic and anoxic conditions. The relative abundance of several taxa increased in response to oil exposure, including *Oleispira*, *Neptuniibacter*, *Cycloclasticus*, *Zhongshania*, *Roseobacter NAC117*, *Aquibacter*, *Lutibacter*, *Lutimonas*, *Persicirhabdus*, and *Sva1033*, implicating these taxa in oil biodegradation. This study underscores both the diversity and ubiquity of hydrocarbon-degrading microbes and the strong influence of environmental parameters (i.e. oxygen, habitat, and oil type) on post-spill microbial community succession.

4.2 INTRODUCTION

Rapid change is occurring in the Arctic marine environment due to climbing atmospheric temperatures, and current projections include ice-free summers in the Beaufort (4 months) and Chukchi (5 months) seas by 2040 (Årthun et al., 2021; Wang and Overland, 2015). Thus, previously ice-covered waters will become more accessible to human activities, increasing the likelihood of anthropogenic disturbance and contaminant exposure through oil and gas development and increased marine traffic. Oil in the benthos can adversely impact the health of the marine ecosystems, including benthic and pelagic food webs, immediately following an oil spill and for decades into the future (Peterson et al., 2003; Shigenaka, 2014). Oil can be toxic or fatal to a multitude of demersal fishes and invertebrates and is persistent in the environment and the tissues of exposed organisms years after a spill event (Jewett et al., 2002; Short et al., 2003; Sun et al., 2018). Ten years following the Exxon-Valdez oil spill (EVOS), oil compounds persisted in marine sediments and at toxic levels within the tissues of organisms such as Pacific halibut (*Hippoglossus stenolepis*), mussels, and clams (Jewett et al., 2002). In Arctic ecosystems, benthic fishes and invertebrates compose all or some of the diets of marine birds and mammals including walruses (*Odobenus rosmarus divergens*), seals, and whales, which are also important for subsistence hunting by Indigenous communities (Huntington et al., 2021). Thus, understanding the fate of oil in Arctic marine sediments is important to assessing the potential environmental and human health impacts of an oil spill in this ecosystem.

Following an oil spill, the cleanup effort generally focuses on treating visible oil slicks on the sea surface or shorelines, while less attention is afforded to offshore subtidal sediments, even with conservative estimates that 20-30% of total oil from a spill event settles to the seafloor

(Ghaly and Dave, 2011; Muschenheim and Lee, 2002; Wang et al., 2020). Despite the positive buoyancy of oil in seawater, deposition to sediments can occur naturally through aggregation with suspended particles and weathering of oil (Gregson et al., 2021; Gustitus and Clement, 2017). Aggregates form through adhesion of oil droplets to suspended particulate material with higher density, such as sediment grains, phytoplankton, and other detritus at the sea surface or in the water column, increasing the likelihood of sedimentation (Daly et al., 2016; Gregson et al., 2021; Quigg et al., 2020). Following a spill, the chemical composition and physical characteristics of oil change over time through a variety of processes collectively termed “weathering”, including photo-oxidation, evaporation, biodegradation, dissolution, and emulsification (Tarr et al., 2016; Ward and Overton, 2020). Typically, the lighter and more volatile oil compounds are lost first during weathering, leaving the heavier and more metabolically recalcitrant petroleum products, which tend to sink out to the benthos (Wang et al., 2020). Weathered oil components are the most persistent in marine environments and include many of the polycyclic aromatic hydrocarbons (PAHs) (Sekar and Dichristina, 2017; Sieradzki et al., 2021). Oil-spill response methods can also contribute to oil sedimentation. Dispersants, which are widely used to separate oil slicks into smaller droplets following a spill, have been reported to accelerate oil transport to the benthos, as it promotes oil-particle aggregation (Cai et al., 2016; Daly et al., 2016; Gong et al., 2014; Passow et al., 2017; Quigg et al., 2020).

Because microbial biodegradation is the primary means through which oil is removed from the marine environment following a spill, understanding oil biodegradation potential is important to accurately predicting the fate and effects of oil exposure (Braddock et al., 1995; Hazen et al., 2015; McFarlin et al., 2014; Prince et al., 2013, 2002). This information is also

valuable to developing appropriate spill response strategies, including those that rely on biodegradation. Oxygen exposure and degree of weathering both influence oil biodegradation in marine sediments, which exhibit oxic and anoxic pockets even in the surface layer and a transition to anoxic conditions typically within the upper few cm in most muddy nearshore environments (Glud et al., 1998; Rysgaard et al., 1994). Anoxic conditions can significantly slow oil biodegradation and/or provide the necessary conditions for anaerobic biodegradation of more recalcitrant, weathered oil compounds (Hazen et al., 2015). Fresh oil is generally broken down through microbial processing much more quickly than weathered oil due to the presence of more labile components (Head et al., 2006). Once the oil has been heavily weathered and the recalcitrant chemical compounds remain, oil biodegradation is very limited. However, some anaerobic microbes, which require suboxic or anoxic environments, are capable of breaking down some of these recalcitrant compounds (Braddock et al., 1995; Rysgaard et al., 2004).

In this study we used incubation experiments containing Arctic marine sediments and sea water from the Chukchi Sea (Pacific Arctic) to assess the benthic microbial response to fresh and weathered oil exposure. Using high-throughput DNA sequencing techniques, we tracked microbial community shifts in response to oil exposure under oxic and anoxic conditions, and identified key taxonomic groups that increased in relative abundance during fresh and weathered oil biodegradation, identifying them as putative oil degraders that could be used to survey for biodegradation potential throughout the region.

4.3 METHODS

4.3.1 Experimental Design

Community composition shifts were observed during oxic seawater-sediment-oil incubations at 6 time points, at 12-day intervals over the course of 60 days via destructive harvesting of samples. Anoxic incubations were only analyzed at 790 days. The treatments, i.e., unoiled, fresh oil, and weathered oil samples, were used to assess community composition shifts with type of oil and without oil under oxic and anoxic conditions. For each treatment there were 3 replicates. Community shifts observed in the incubation experiment were also compared to the community from sediments frozen immediately upon collection, referred to in this study as *in-situ* samples, to track bottle effects and community drift in relation to oil exposure.

Marine sediment and seawater samples for the incubation experiment were collected on the Chukchi Sea shelf (69.91°N, 166.05°W) during the AMBON cruise in August 2017 at 45 m water depth (<https://ambon-us.org/field-work/2017-cruise/>). Surface sediments were collected via van Veen grab, and seawater was collected from the seawater intake hose on board the ship. Sediments and seawater were stored in sterile, acid-washed containers and kept at the *in-situ* temperature of 5 °C until shipped on ice to the University of Alaska Fairbanks (UAF), where they were kept in a cold room set at 5°C. A subset of these sediments (*in-situ* samples) was frozen immediately after collection to characterize the *in-situ* community. Seawater was vacuum filtered through 0.2-um filters and autoclaved to remove pelagic microbes. Seawater was cooled to 5°C prior to experimental setup and spiked with 1% Sigma-Aldrich resazurin solution with a final concentration of 0.002% so that oxygenation states (oxic, suboxic, anoxic) could be determined for individual samples.

Serum bottles used for incubations were washed with lab-grade detergent, acid-washed in a 10% HCl solution, and autoclaved. Each 100-mL bottle was filled with 40 mL of sterile seawater and 8 mL of sediment. To expedite bottle preparation while remaining relatively precise, we used the mass of 8 mL of sediment to assure each bottle had comparable sediment volumes. To determine the mass of sediment in the 8-ml aliquots added to each serum bottle, 10 different 8-mL sediment samples were weighed revealing an average mass of 12.2 g sediment per 8 ml. Each serum bottle was then prepared using a sterile stainless-steel funnel to transfer the 12.2 g (SD = 0.02 g) of marine sediment to serum bottles. Residual sediment was then rinsed from the funnel into the serum bottle with 40 mL of 1% resazurin-spiked seawater.

A total of 334 100- mL glass serum bottles were prepared for incubation experiments to accommodate 3 replicates of each treatment: unoiled, fresh-oil, and weathered-oil under oxic, anoxic, abiotic and biotic conditions (Figure 4.1). To quantify abiotic oil degradation half (167) of the sediment/seawater prepared bottles were autoclaved, re-oxygenated, and cooled down to 5°C (*in situ* bottom water temp.) prior to oil addition. Alaska North-Slope (ANS) crude oil was obtained from Polar Tankers Inc., in Valdez, Alaska, on July 12, 2017. Half of the crude oil was sealed and stored in an amber glass bottle in a dark area of the cold room at 5°C for use as fresh oil treatment. The other half was used to create the “weathered” oil by transferring to a 500-mL graduated cylinder loosely capped with sterile foil, and slowly agitating on a shaker table until 20% of its mass had been lost to volatilization (Prince et al., 2013). For oiled treatments, 1 mL of either fresh or weathered oil was added to each bottle via positive displacement pipette and homogenized, for a total oil concentration of 2% (Braddock et al., 2004; Ferguson et al., 2017).

All serum bottles were encased in a custom-made foam-lined holder on a shaker table. A subset of oxic incubation bottles, 3 replicates of unoiled, fresh oil, and weathered oil, were

destructively harvested on the first day of oil addition (day 0) and every 12 days until the end of the experiment at 60 days. When bottles were harvested, samples destined for DNA extraction were transferred to DNA/RNAase-free 50-mL Falcon tubes and immediately frozen at -80°C until extraction.

4.3.2 Sequencing, Bioinformatics, and Data Analysis

To assess the diversity, structure, and composition of prokaryotes in the Beaufort Sea benthos, 16S ribosomal RNA (rRNA) amplicon sequencing was conducted on lyophilized sediments. To prepare samples for sequencing, total genomic DNA was extracted from sediment samples using the Qiagen PowerSoil kit. Revised forward (515FB) and reverse primers (806RB) from the Earth Microbiome Project (EMP) were used to amplify the V4 region of the 16S rRNA gene. Library preparation was completed with iTru adapters for sequencing following the one-step PCR protocol with indexed primers (Apprill et al., 2015; Caporaso et al., 2012; Parada et al., 2016; Walters et al., 2016). Samples were sequenced on an Illumina MiSeq at the UAF Institute of Arctic Biology Genomics Core Lab.

The 16S rRNA amplicon sequences were de-multiplexed using the Mr. Demuxy package (Cock et al., 2009) and analyzed with mothur v1.43.0 on a high performance-computing cluster through UAF Research Computing Systems using a modified MiSeq standard operating procedure (Schloss et al., 2009). Operational taxonomic units (OTUs) were clustered at 100% similarity using OptiClust option in mothur; taxonomy was assigned to OTUs using the SILVA 138.1 mothur formatted reference database with a bootstrap cutoff of 100%, and the samples in the resulting OTU table were converted to relative abundances (Edgar, 2018; Glöckner et al.,

2017; Wang et al., 2007; Westcott and Schloss, 2017). The resulting OTU table was used to identify prokaryotes likely involved in the biodegradation of oil in Arctic marine sediments.

We examined treatment effects on prokaryotic diversity by calculating the inverse Simpson index ($1/\lambda$) for each sample, which takes into account both evenness and richness, including the *in situ* community (Morris et al., 2014). To assess prokaryotic community structure across all treatments, we used hierarchical clustering analysis with Bray-Curtis dissimilarities using the ward.D2 method in the vegan package in R (R Core Team, 2017). To test the validity, homogeneity, and significance of resulting clusters we used a silhouette test, a dispersion test (betadisper function), and a PERMANOVA via the adonis function respectively (Clarke et al., 2016; Oksanen, 2015; R Core Team, 2017; Rousseeuw, 1987). Area plots were used to visualize the change in the most abundant taxa from *in situ* samples (10 days prior to start of experiment) to the end of oxic experiments (60 days after start of experiment) and finally at the conclusion of the anoxic incubation (790 days after start of experiment). Indicator taxa analysis using the multipatt function in vegan was used to understand how rare taxa changed with time and differed among treatments.

4.4 RESULTS

4.4.1 Community Structure

Hierarchical clustering indicated that the sediment microbial communities grouped into 3 clusters. The sample set was homogeneously dispersed among clusters, and the community structures of samples in each cluster were significantly different from that of other clusters ($P < 0.001$, Figure 4.2). The first cluster consisted of all unoiled samples, both oxic and anoxic, across

all time points. This cluster, which we will refer to as the unoiled assemblage also included all oxic oiled samples from day 0 of the experiment (i.e., harvested immediately following oil addition). The second cluster, the oiled oxic assemblage, contained all fresh and weathered oil samples from day 12 to day 60, and the third cluster, the anoxic oiled assemblage, encompassed all the anoxic oiled samples at day 790.

After 12 days, the community structure of the unoiled oxic samples were more similar to those from the time of field collection, whereas day-0 samples from the incubation (both oiled and unoiled) were more similar to all oxic unoiled samples between day 24 and day 60 and anoxic unoiled samples at day 790 (Figure 4.2). Under oxic conditions, microbial communities were similar in the fresh and weathered oil treatments on days 12 and 24, and then began to diverge such that weathered-oil-treated communities were distinct from fresh oiled communities from day 36 to day 60. Under anoxic conditions, clear differences in community structure were again detected between fresh and weathered-oil treatments. Oxic and anoxic samples were thus pooled within each oil treatment for subsequent analyses and visualizations of diversity and taxonomic composition (Figure 4.3, 4.4, 4.5).

4.4.2 Core Community

To investigate changes in community structure over time in response to oil addition, we first identified the most abundant taxa from *in situ* and unoiled samples to serve as the baseline or dominant “core community”. The most abundant genera in the core community were:

Aquibacter, *B2M28 genus*, *BD7-8 genus*, *Candidatus Nitrosopumilus*, *Halioglobus*, *Lutibacter*, *Lutimonas*, *Persicirhabdus*, *Psychromonas*, *Sva0081 genus*, *Sva1033 genus*, and *Woeseia* (Figure 4.3). Note that unknown genera *B2M28 genus*, *BD7-8 genus*, *Sva0081 genus*, and

Sva1033 genus were clustered at genus level and identified to order. The relative abundance of several core taxa increased in unoiled samples over time including *B2M28*, *BD7-8*, *Halioglobus*, *Nitrosopumilis*, *Psychromonas*, *Sva0081*, and *Woeseia*. *Sva0081* and *Woeseia* remained relatively stable over time in the oxic samples but increased in abundance in anoxic samples at day 790, along with emergence of *Arcobacter* which was only present in high abundances in anoxic samples (Figure 4.3, 4.4). *Persicirhabdus*, and *Sva1033* remained relatively stable throughout the experiment, whereas, *Aquibacter*, *Lutibacter*, and *Lutimonas* decreased in relative abundance in unoiled samples. Generally, taxa that increased in relative abundance in unoiled samples became less abundant in oiled samples, and vice versa (Figure 4.3).

4.4.3 Putative Oil Degraders

The core community taxa that were comparatively enriched in oiled samples were *Aquibacter*, *Lutibacter*, *Lutimonas*, *Persicirhabdus*, and *Sva1033*. Several taxa that were not dominant in the core community substantially increased in relative abundance by day 12 in response to oil addition, differing in relative abundance between fresh and weathered oil (Figure 4.4). Some of these taxa became more dominant than certain core taxa (Figure 4.4). Those that were relatively abundant in both fresh and weathered-oil samples (oxic and anoxic) included *Cycloclasticus*, *Neptuniibacter*, *Oleispira*, *Zhongshania* and *Marinifilum*. *Fusibacter*, *Pseudomonas*, and *Shewanella* were only abundant in fresh-oiled samples, whereas *Roseobacter* clade *NAC117* was only abundant in weathered-oil samples.

The genus *Oleispira* appeared to respond most quickly to oil addition under oxic conditions, increasing in relative abundance after 12 days in both the fresh- and weathered-oil samples. The initial spike in *Oleispira* relative abundance was followed by an increase of both

Neptuniibacter and *Cycloclasticus* at 24 days in both fresh- and weathered-oil samples. The increase in *Neptuniibacter* was more pronounced in the fresh oil samples while the increase in *Cycloclasticus* was more pronounced in weathered-oil samples, particularly over time. Following the peak in *Neptuniibacter* abundance, *Oleispira* exhibited a second peak of higher abundances at day 48 in fresh-oil samples. *Cycloclasticus* exhibited the most substantial increase between days 12 and 36 in the fresh-oil samples and remained relatively stable through the end of the experiment. However, in weathered-oil samples, *Cycloclasticus* continued to increase in abundance substantially from day 12 to day 60 and showed no sign of plateauing. *Oleispira* increased at day 12 and steadily decreased from day 30 to day 60. *Zhongshania* exhibited a slight increase at day 36, but was overall less abundant in the weathered-oil samples than in the fresh-oil samples. *Roseobacter clade NAC117*, which was only in higher abundances in the weathered oil samples, did not start to increase in relative abundance until day 24 and increased slightly, though steadily, until day 60.

4.4.4 Diversity

In the oiled treatments, diversity (Inverse Simpson index) initially increased relative to *in situ* samples, but began to significantly ($P < 0.001$) decrease at day 24 in fresh-oil samples and at day 12 in weathered-oil samples (Figure 4.5). All anoxic samples, including unoiled, were less diverse than *in situ* sediments.

4.5 DISCUSSION

Over the course of incubation experiment we observed a significant decrease in microbial diversity in oiled samples, a trend also reported by others in marine habitats following oil exposure (Acosta-González et al., 2015; Acosta-González and Marqués, 2016; King et al., 2015; Rodriguez-R et al., 2015). Diversity was drastically lower in anoxic oiled samples at day 790 than both *in situ* and anoxic unoiled sample diversity. Research on the effects of the Deep Water Horizon (DWH) spill reported that microbial taxonomic diversity markedly decreased in oxic sediments and did not return to previous levels until 1 year following the exposure event (Kostka et al., 2011; Rodriguez-R et al., 2015). Here we did not measure the diversity of oxic samples beyond two months of incubation, however, diversity was significantly lower in anoxic oiled samples compared to unoiled samples after 2.5 years (Figure 4.5).

Our incubation experiment revealed that oxygen availability as well as the presence and condition of oil, fresh versus weathered, were major factors influencing microbial community structure. The *in situ* and unoiled assemblages were similar to each other, and representative of communities previously recorded in Chukchi Sea sediments (Walker et al., in review; Figure 4.2). Generally, core community taxa that increased in relative abundance in unoiled samples over time, decreased in oiled samples (Figure 4.3). We also observed core community taxa that were enriched upon oil exposure and taxa that emerged with high relative abundances only upon oil exposure. Core community taxa that exhibited increased relative abundances in oiled samples relative to unoiled samples were *Aquibacter*, *Lutibacter*, *Lutimonas*, *Persicirhabdus*, and *Sva1033* (Figure 4.3). In oxic samples, these taxa were generally enriched in both fresh and weathered oil samples, however peak abundances varied over time based on oil treatment. For

instance, at days 24 and 60, *Persicirhabdus* exhibited peaks in relative abundance in fresh oiled samples, in contrast to weathered oil samples where peaks were observed on days 12 and 48. Additionally, in anoxic samples, *Persicirhabdus* exhibited much higher relative abundances in fresh oil treatments, while *Aquibacter*, *Lutibacter*, and *Sva1033* were more enriched in weathered oil samples and *Lutimonas* in both fresh and weathered oil samples. This suggests that these core community taxa may be capable of oil degradation, and respond differently to oil type under oxic and anoxic conditions.

Many of these putative oil-degrading core community taxa are not commonly researched within the scope of oil degradation. *Persicirhabdus* is sparsely mentioned in the literature, however it has been sequenced in seawater treated with fresh naphthenic oil and gut microbiota of sole exposed to light crude oil (Brakstad et al., 2018; Cerqueda-García et al., 2020). *Aquibacter* is also not well researched, though a few studies have observed this genus in plastic and oil-polluted sediments (Hamdan et al., 2019; Krause et al., 2020; Wang et al., 2021; Zoppini et al., 2020). *Lutibacter* has been predominately observed under oxic conditions, and most described species of this genus are aerobic or facultative anaerobes, which is interesting given its peak relative abundance here was observed in anoxic weathered-oil samples (Choi and Cho, 2006; Nedashkovskaya et al., 2015). In oxic conditions *Lutibacter* has been indirectly linked with PAH degradation and in anoxic conditions it has been enriched in nitrate-reducing conditions with naphthenic acids (Clothier and Gieg, 2016; Gao et al., 2018; Isaac et al., 2013; Marietou et al., 2018; Milton et al., 2015). Naphthenic acids, which can be enriched during the weathering process, preferentially bind to sediments, rather than being released into the water column (Rogers et al., 2002; Yang et al., 2019). Therefore, *Lutibacter* may play some role in anaerobic naphthenic acid degradation in weathered oil samples here. *Lutibacter* may also be

degrading extracellular DNA and cell debris, as these bacteria have been shown to do in anoxic sediments (Wasmund et al., 2021). Given the length of incubation time with respect to anoxic samples coupled with the weathered oil exposure there is likely an abundance of extracellular DNA and cell debris from the lysis and death of other sediment microbes.

Research linking *Sva1033* to petroleum biodegradation is also sparse, however it has been strongly correlated with PAHs in polluted lagoon sediments (Zoppini et al., 2020). Though members of *Sva1033* are not yet cultured, multiple studies in polar marine sediments suggest that they are capable of dissimilatory iron and sulfate reduction (Aromokeye et al., 2021; Buongiorno et al., 2019; Wunder et al., 2021). *Lutimonas* has exhibited declines in abundance upon oil exposure and PAHs, but enrichment in those same studies with respect to polychlorinated biphenyls (Koo et al., 2015; Quero et al., 2015; Zanaroli et al., 2012)

Taxa that were in trace abundances in unoiled samples and emerged as the most abundant in the oxic fresh and weathered-oil samples were *Oleispira*, *Neptuniibacter*, *Cycloclasticus*, and *Zhongshania*. *Oleispira* spp. are among the most well-known marine oil-degrading microbes and have been implicated in aerobic oil biodegradation, primarily of branched and straight-chain alkanes, in both seawater and marine sediments (Guibert et al., 2016, 2012; Netzer et al., 2018; Yakimov et al., 2003). The substantial increase of *Oleispira* in the early stages of the experiment in both fresh and weathered samples is congruent with the typical succession of chemical compounds in oil, as branched and straight-chain alkanes, otherwise known as saturated hydrocarbons, are generally the first compounds to be biodegraded (Head et al., 2006).

Neptuniibacter has been implicated in hydrocarbon degradation via genomic analyses which have indicated that specific strains can degrade the PAHs carbazole and phenanthrene (Achberger et al., 2021; Ahmad et al., 2015; Dombrowski et al., 2016; Maeda et al., 2010;

Nagashima et al., 2010). In the fresh-oil samples, *Neptuniibacter* reached its peak abundance roughly halfway through the experiment, which is also when a trough in *Oleispira* was observed. Following the peak in *Neptuniibacter* abundance, *Oleispira* exhibited a second abundance peak indicating that *Neptuniibacter* may produce labile degradation products favorable to *Oleispira*. This trend was not observed in the weathered-oil samples where *Neptuniibacter* was at relatively stable, lower abundances throughout the remainder of the experiment.

Bacteria belonging to the *Cycloclasticus* genus have been implicated physiologically and experimentally in the aerobic degradation of a multitude of PAHs (Dyksterhouse et al., 1995; Kasai et al., 2003). Members of *Cycloclasticus* are considered the dominant aerobic PAH-degraders in marine sediments, and were one of the most abundant taxa in PAH-enriched Arctic marine sediments where they utilized naphthalene and phenanthrene as sole carbon sources (Dong et al., 2015). *Cycloclasticus spp.* specialize in more recalcitrant crude-oil components that tend to persist at later stages in the oil degradation process (Ribicic et al., 2018; Yakimov et al., 2007, 2003).

OTUs affiliated with *Zhongshania* matched at 100% identity in the BLAST database to *Zhongshania aliphaticivorans* and uncultured clones. *Zhongshania aliphaticivorans* isolated from oil-contaminated marine sediments has been implicated in aliphatic hydrocarbon degradation based on the presence of several alkane degradation genes, including alkane 1-monooxygenase and haloalkane dehalogenase (Jia et al., 2016; Naysim et al., 2014). *Zhongshania* also played a major role in initial alkane degradation of chemically dispersed oil in Norwegian seawater (Ribicic et al., 2018). Metagenome analysis suggests that *Zhongshania* may be capable of degrading aromatics such as biphenyl, benzoate, catechol, and cyclopentanol (Jia et al., 2016). To our knowledge, bacteria belonging to the genus *Zhongshania* have not yet been

identified or isolated from Arctic marine sediments. *Zhongshania*, more abundant in the fresh-oil samples, gradually increased from day 12 to day 36 and spiked at day 48, co-incident with the second peak in *Oleispira* abundance (Figure 4.4). Degradation products generated by *Cycloclasticus*, *Neptuniibacter*, or both, were likely also favorable to *Zhongshania*.

The *Roseobacter* NAC11-7 lineage, which was predominant in the weathered-oil samples, increased in abundance from day 12 to day 48, after which it gradually declined until day 60 (Figure 3.4). This lineage is commonly associated with phytoplankton blooms and has mostly been identified and described from seawater, though it was recently found in high abundances in Arctic marine sediments of the Beaufort Sea (Hahnke et al., 2013; Luo and Moran, 2014; Teeling et al., 2016; Walker et al., 2021). Brakstad et al. (2004) reported that *Roseobacter* NAC11-7 was abundant during oil biodegradation in low-temperature (5.9-7.4°C) seawater. Additionally, Netzer et al. (2018) found that bacteria in the *Roseobacter* NAC11-7 lineage were prevalent only in oiled seawater (versus unoiled), with slightly higher abundances associated with oiled diatom aggregates. Genomic studies have investigated the metabolic capabilities of 24 representatives of the *Roseobacter* lineage and found different pathways pertaining to the aerobic degradation of aromatic compounds (Buchan et al., 2019, 2000; Giebel et al., 2016).

Several putative anaerobic oil degraders ranked within the most abundant taxa in anoxic oiled samples and were reflective of oil type. Only *Marinifilum* was enriched in both fresh and weathered oil, whereas *Pseudomonas*, *Shewanella* and *Fusibacter* were enriched only in fresh oil samples, and *Roseobacter* NAC11-7 and *Oleispira* in weathered oil samples. *Marinifilum* spp. have exhibited enrichment in oil-impacted marine environments, however their role in oil biodegradation is currently unknown (Marietou et al., 2018; Scoma et al., 2018; Yang et al., 2016). Multiple *Marinifilum* species contain reductive dehalogenases in their genomes, which

could be utilized in the transformation of halogenated hydrocarbons into more biodegradable and less toxic compounds (Atashgahi, 2019; Oyewusi et al., 2020; Zanaroli et al., 2015). Though halogenated hydrocarbons are not components of crude oil, conditions may be met in the marine environment for the formation of these compounds such as methyl chloride (CH₃CL) (Atashgahi et al., 2018; Ballschmiter, 2003; Field, 2016; Khan et al., 2008; Ruecker et al., 2014). In the Arctic and elsewhere, several studies have observed marine microbes capable of reductive dehalogenation present in high abundances following oil exposure (Manzetti, 2014; Oyewusi et al., 2020; Yu et al., 2018). Here we propose two hypotheses for this: 1) metabolic versatility of anaerobic microbes, and 2) possible formation of halogenated hydrocarbons via biodegradation products and/or naturally occurring organohalides.

Pseudomonas, *Shewanella*, and *Fusibacter*, taxa that were substantially enriched in anoxic fresh-oil samples, have been linked to anaerobic degradation of petroleum compounds, largely PAHs. *Pseudomonas* is one of the most diverse bacterial genera, encompassing hundreds of species that vary widely in their metabolic potential and ecology and are difficult to identify based solely on the 16S rRNA gene (Gomila et al., 2015; Hesse et al., 2018; Peix et al., 2009). Our most abundant OTU (OTU3) showed a 100% identity match to just one taxon, *Pseudomonas sabulinigri*. *P. sabulinigri* has been shown to be psychrotolerant and to degrade PAHs, specifically naphthalene, in cold marine sediments (Isaac et al., 2013; Sánchez et al., 2014). *Fusibacter* has often been observed co-occurring with *Pseudomonas* in anoxic conditions associated with oil-producing wells and petroleum contaminated marine sediments (Deng et al., 2022; Mu et al., 2021; Santos et al., 2020; Xue et al., 2015). *Fusibacter* can anaerobically convert PAHs such as 2-methylnaphthalene, aromatics, and alkanes to volatile fatty acids via fermentation (Folwell et al., 2016; Hasegawa et al., 2014; Mu et al., 2021). *Shewanella* has been

linked to oil biodegradation under aerobic and anaerobic conditions in the marine environment, as well as heavy metal degradation and reductive dehalogenation specifically in anoxic conditions (Atashgahi, 2019; Deppe et al., 2005; Ferguson et al., 2017; Gerdes et al., 2005; Lohner and Spormann, 2013; Martín-Gil et al., 2004; Toes et al., 2008; Yin et al., 2022). In addition to degrading PAHs such as phenanthrene, *Shewanella* species, due to their ability to use a vast number of diverse electron acceptors, are likely able to degrade anthracene and pyrene, highly recalcitrant petroleum compounds, *in situ* (Edlund and Jansson, 2008; Hau and Gralnick, 2007; Sekar and Dichristina, 2017).

There were two taxa that markedly increased in anoxic weathered-oil samples, *Roseobacter NAC11-7* and *Oleispira* that, to our knowledge, have not previously been shown to anaerobically degrade petroleum hydrocarbons. As previously mentioned, the *Roseobacter NAC11-7* lineage has largely been associated with oil degradation in seawater, i.e., in oxic conditions, however we observed a marked increase in abundance of these bacteria in anoxic oiled samples at day 790. Essentially nothing is known about the role of this group with respect to anaerobic degradation, although genomic evidence suggests some *Roseobacter* clades may thrive in anoxic environments (Feng et al., 2021; Pohlner et al., 2019). Ample evidence supports the role of *Oleispira* spp. in aerobic biodegradation of petroleum hydrocarbons, but this function has not been documented under anoxic conditions. Lab cultures and genomic data indicate *Oleispira lenta* and *O. antarctica*, the two most abundant species found here, are facultative anaerobes capable of surviving in anoxic conditions (Kube et al., 2013; Wang et al., 2012; Yakimov et al., 2003).

4.5.1 Conclusions

This study revealed putative oil degraders that are common players in oil degradation as well as lesser-known taxa whose roles remain elusive with respect to biodegradation in oxic and anoxic marine sediments. The genera putatively implicated here as major contributors to oil degradation in sediments are largely different from those reported from Chukchi seawater, with the exception of two taxa *Roseobacter* NAC117 and *Oleispira* (Gofstein et al., 2019). Although not surprising, as sediment and seawater microbial communities are typically significantly different, this may have implications related to differences in degradation potential in sediments vs. seawater (Zinger et al., 2011). The shifts in microbial community structure during oil incubations likely reflected the succession of hydrocarbon compounds present in fresh and weathered oil over time, a trend also reported in Arctic seawater (Gofstein et al., 2019; McFarlin et al., 2018). Though this type of succession has been well-documented in the marine environment, the combination of abundant putative oil degraders exhibited here are relatively novel in comparison to the majority of studies published on marine sediments (Dong et al., 2015; Ferguson et al., 2017; Rodriguez-R et al., 2015; Yang et al., 2016). Taxa, such as *Zhongshania*, *Neptuniibacter*, and *Roseobacter* NAC117 not commonly associated with oil degradation were prominent in this study, whereas bacteria reported to degrade oil such as *Alcanivorax* and *Marinobacter* were less abundant in our incubation experiment (Acosta-González and Marqués, 2016; Dong et al., 2015; Ferguson et al., 2017; Rodriguez-R et al., 2015; Yang et al., 2016). Future analyses of petroleum hydrocarbon concentrations and composition may shed more light on the taxa that degrade different fractions under oxic and anoxic conditions, as well as how degradation rates in the Arctic benthos compare to pelagic habitats and to other geographic regions.

4.6 REFERENCES

- Achberger, A.M., Doyle, S.M., Mills, M.I., Holmes, C.P., Quigg, A., Sylvan, J.B., 2021. Bacteria-Oil Microaggregates Are an Important Mechanism for Hydrocarbon Degradation in the Marine Water Column. *mSystems* 6. <https://doi.org/10.1128/mSystems.01105-21>
- Acosta-González, A., Marqués, S., 2016. Bacterial diversity in oil-polluted marine coastal sediments. *Curr. Opin. Biotechnol.* 38, 24–32. <https://doi.org/10.1016/j.copbio.2015.12.010>
- Acosta-González, A., Martirani-von Abercron, S.M., Rosselló-Móra, R., Wittich, R.M., Marqués, S., 2015. The effect of oil spills on the bacterial diversity and catabolic function in coastal sediments: a case study on the Prestige oil spill. *Environ. Sci. Pollut. Res.* 22, 15200–15214. <https://doi.org/10.1007/s11356-015-4458-y>
- Ahmad, A.B., Zulkharnain, A.B., Husaini, A.A.S.B.A., 2015. Substrate specificity of angular dioxygenase from carbazole-degrading bacterium *Neptuniibacter* sp. Strain CAR-SF. *J. Chem. Pharm. Sci.* 8, 382–388.
- Apprill, A., McNally, S., Parsons, R., Weber, L., 2015. Minor revision to V4 region SSU rRNA 806R gene primer greatly increases detection of SAR11 bacterioplankton. *Aquat. Microb. Ecol.* 75, 129–137. <https://doi.org/10.3354/ame01753>
- Aromokeye, D.A., Willis-Poratti, G., Wunder, L.C., Yin, X., Wendt, J., Richter-Heitmann, T., Henkel, S., Vázquez, S., Elvert, M., Mac Cormack, W., Friedrich, M.W., 2021. Macroalgae degradation promotes microbial iron reduction via electron shuttling in coastal Antarctic sediments. *Environ. Int.* 156, 106602. <https://doi.org/10.1016/j.envint.2021.106602>
- Årthun, M., Onarheim, I.H., Dörr, J., Eldevik, T., 2021. The Seasonal and Regional Transition to

an Ice-Free Arctic. *Geophys. Res. Lett.* 48, e2020GL090825.

<https://doi.org/10.1029/2020GL090825>

Atashgahi, S., 2019. Discovered by genomics: putative reductive dehalogenases with N-terminus transmembrane helices. *FEMS Microbiol. Ecol.* 95, 48.

<https://doi.org/10.1093/femsec/fiz048>

Atashgahi, S., Häggblom, M.M., Smidt, H., 2018. Organohalide respiration in pristine environments: implications for the natural halogen cycle. *Environ. Microbiol.* 20, 934–948.

<https://doi.org/10.1111/1462-2920.14016>

Ballschmiter, K., 2003. Pattern and sources of naturally produced organohalogens in the marine environment: biogenic formation of organohalogens. *Chemosphere* 52, 313–324.

[https://doi.org/10.1016/S0045-6535\(03\)00211-X](https://doi.org/10.1016/S0045-6535(03)00211-X)

Braddock, J.F., Gannon, K. a, Rasley, B.T., 2004. OCS Study MMS 2004-061 Petroleum Hydrocarbon – Degrading Microbial Communities in Beaufort – Chukchi Sea Sediments by Project Organization. Univ. Alaska Fairbanks 38.

Braddock, J.F., Lindstrom, J.E., Brown, E.J., 1995. Distribution of hydrocarbon-degrading microorganisms in sediments from Prince William Sound, Alaska, following the Exxon Valdez oil spill. *Mar. Pollut. Bull.* 30, 125–132. [https://doi.org/10.1016/0025-326X\(94\)00110-U](https://doi.org/10.1016/0025-326X(94)00110-U)

Brakstad, O.G., Davies, E.J., Ribicic, D., Winkler, A., Brønner, U., Netzer, R., 2018. Biodegradation of dispersed oil in natural seawaters from Western Greenland and a Norwegian fjord. *Polar Biol.* 41, 2435–2450. <https://doi.org/10.1007/s00300-018-2380-8>

- Buchan, A., Collier, L.S., Neidle, E.L., Moran, M.A., 2000. Key aromatic-ring-cleaving enzyme, protocatechuate 3,4-dioxygenase, in the ecologically important marine *Roseobacter* lineage. *Appl. Environ. Microbiol.* 66, 4662–4672. <https://doi.org/10.1128/AEM.66.11.4662-4672.2000>
- Buchan, A., González, J.M., Chua, M.J., 2019. Aerobic Hydrocarbon-Degrading Alphaproteobacteria: Rhodobacteraceae (*Roseobacter*), in: *Taxonomy, Genomics and Ecophysiology of Hydrocarbon-Degrading Microbes*. Springer International Publishing, Cham, pp. 93–104. https://doi.org/10.1007/978-3-030-14796-9_8
- Buongiorno, J., Herbert, L.C., Wehrmann, L.M., Michaud, A.B., Laufer, K., Røy, H., Jørgensen, B.B., Szykiewicz, A., Faiia, A., Yeager, K.M., Schindler, K., Lloyd, K.G., 2019. Complex Microbial Communities Drive Iron and Sulfur Cycling in Arctic Fjord Sediments. *Appl. Environ. Microbiol.* 85, 1–16. https://doi.org/10.1128/AEM.00949-19/SUPPL_FILE/AEM.00949-19-S0001.PDF
- Cai, Z., Fu, J., Liu, W., Fu, K., O'reilly, S.E., Zhao, D., 2016. Effects of oil dispersants on settling of marine sediment particles and particle-facilitated distribution and transport of oil components. <https://doi.org/10.1016/j.marpolbul.2016.09.057>
- Caporaso, J.G., Lauber, C.L., Walters, W. a, Berg-Lyons, D., Huntley, J., Fierer, N., Owens, S.M., Betley, J., Fraser, L., Bauer, M., Gormley, N., Gilbert, J. a, Smith, G., Knight, R., 2012. Ultra-high-throughput microbial community analysis on the Illumina HiSeq and MiSeq platforms. *ISME J.* 6, 1621–1624. <https://doi.org/10.1038/ismej.2012.8>
- Cerqueda-García, D., Améndola-Pimenta, M., Zamora-Briseño, J.A., González-Penagos, C.E.,

- Árcega-Cabrera, F., Ceja-Moreno, V., Rodríguez-Canul, R., 2020. Effects of chronic exposure to water accommodated fraction (WAF) of light crude oil on gut microbiota composition of the lined sole (*Achirus lineatus*). *Mar. Environ. Res.* 161, 105116. <https://doi.org/10.1016/J.MARENRES.2020.105116>
- Choi, D.H., Cho, B.C., 2006. *Lutibacter litoralis* gen. nov., sp. nov., a marine bacterium of the family Flavobacteriaceae isolated from tidal flat sediment. *Int. J. Syst. Evol. Microbiol.* 56, 771–776. <https://doi.org/10.1099/IJS.0.64146-0>
- Clarke, K.R., Somerfield, P.J., Gorley, R.N., 2016. Clustering in non-parametric multivariate analyses. *J. Exp. Mar. Bio. Ecol.* 483, 147–155. <https://doi.org/10.1016/J.JEMBE.2016.07.010>
- Clothier, L.N., Gieg, L.M., 2016. Anaerobic biodegradation of surrogate naphthenic acids. *Water Res.* 90, 156–166. <https://doi.org/10.1016/J.WATRES.2015.12.019>
- Daly, K.L., Passow, U., Chanton, J., Hollander, D., 2016. Assessing the impacts of oil-associated marine snow formation and sedimentation during and after the Deepwater Horizon oil spill. *Anthropocene* 13, 18–33. <https://doi.org/10.1016/j.ancene.2016.01.006>
- Deng, S., Wang, B., Su, S., Zeng, H., Chen, R., Ma, H., Hu, Y., Zheng, A., Shu, C., Zou, J., Li, Y., Zhu, H., Sun, S., She, Y., Zhang, F., 2022. Microbial community diversity and potential bioremediation of drill cuttings in two oil reservoirs. *Pet. Sci. Technol.* 40, 1462–1478. <https://doi.org/10.1080/10916466.2021.2024228>
- Deppe, U., Richnow, H.-H., Michaelis, W., Antranikian, G., 2005. Degradation of crude oil by an arctic microbial consortium. *Extremophiles* 9, 461–70. <https://doi.org/10.1007/s00792->

- Dombrowski, N., Donaho, J.A., Gutierrez, T., Seitz, K.W., Teske, A.P., Baker, B.J., 2016. Reconstructing metabolic pathways of hydrocarbon-degrading bacteria from the Deepwater Horizon oil spill. *Nat. Microbiol.* 1, 16057. <https://doi.org/10.1038/nmicrobiol.2016.57>
- Dong, C., Bai, X., Sheng, H., Jiao, L., Zhou, H., Shao, Z., 2015. Distribution of PAHs and the PAH-degrading bacteria in the deep-sea sediments of the high-latitude Arctic Ocean. *Biogeosciences* 12, 2163–2177. <https://doi.org/10.5194/bg-12-2163-2015>
- Dyksterhouse, S.E., Gray, J.P., Herwig, R.P., Lara, J.C., Staley, J.T., 1995. *Cycloclasticus pugetii* gen. nov., sp. nov., an aromatic hydrocarbon-degrading bacterium from marine sediments. *Int. J. Syst. Bacteriol.* 45, 116–123. <https://doi.org/10.1099/00207713-45-1-116>
- Edgar, R.C., 2018. Updating the 97% identity threshold for 16S ribosomal RNA OTUs. *Bioinformatics* 34, 2371–2375. <https://doi.org/10.1093/bioinformatics/bty113>
- Edlund, A., Jansson, J.K., 2008. Use of bromodeoxyuridine immunocapture to identify psychrotolerant phenanthrene-degrading bacteria in phenanthrene-enriched polluted Baltic Sea sediments. <https://doi.org/10.1111/j.1574-6941.2008.00513.x>
- Feng, X., Chu, X., Qian, Y., Henson, M.W., Lanclos, V.C., Qin, F., Barnes, S., Zhao, Y., Thrash, J.C., Luo, H., 2021. Mechanisms driving genome reduction of a novel *Roseobacter* lineage. *ISME J.* 2021 1512 15, 3576–3586. <https://doi.org/10.1038/s41396-021-01036-3>
- Ferguson, R.M.W., Gontikaki, E., Anderson, J.A., Witte, U., 2017. The variable influence of dispersant on degradation of oil hydrocarbons in subarctic deep-sea sediments at low

- temperatures (0-5 °C). *Sci. Rep.* 7, 1–13. <https://doi.org/10.1038/s41598-017-02475-9>
- Field, J.A., 2016. Natural production of organohalide compounds in the environment. *Organohalide-Respiring Bact.* 7–29. https://doi.org/10.1007/978-3-662-49875-0_2/COVER
- Folwell, B.D., McGenity, T.J., Price, A., Johnson, R.J., Whitby, C., 2016. Exploring the capacity for anaerobic biodegradation of polycyclic aromatic hydrocarbons and naphthenic acids by microbes from oil-sands-process-affected waters. *Int. Biodeterior. Biodegradation* 108, 214–221. <https://doi.org/10.1016/j.ibiod.2014.12.016>
- Gao, W., Yin, X., Mi, T., Zhang, Y., Lin, F., Han, B., Zhao, X., Luan, X., Cui, Z., Zheng, L., 2018. Microbial diversity and ecotoxicity of sediments 3 years after the Jiaozhou Bay oil spill. *AMB Express* 8, 1–10. <https://doi.org/10.1186/S13568-018-0603-6/FIGURES/7>
- Gerdes, B., Brinkmeyer, R., Dieckmann, G., Helmke, E., 2005. Influence of crude oil on changes of bacterial communities in Arctic sea-ice. *FEMS Microbiol. Ecol.* 53, 129–139.
- Ghaly, A.E., Dave, D., 2011. Remediation Technologies for Marine Oil Spills: A Critical Review and Comparative Analysis. *Am. J. Environ. Sci.* 7, 423–440.
- Giebel, H.A., Klotz, F., Voget, S., Poehlein, A., Grosser, K., Teske, A., Brinkhoff, T., 2016. Draft genome sequence of the marine Rhodobacteraceae strain O3.65, cultivated from oil-polluted seawater of the Deepwater Horizon oil spill. *Stand. Genomic Sci.* 11. <https://doi.org/10.1186/s40793-016-0201-7>
- Glöckner, F.O., Yilmaz, P., Quast, C., Gerken, J., Beccati, A., Ciuprina, A., Bruns, G., Yarza, P., Peplies, J., Westram, R., Ludwig, W., 2017. 25 years of serving the community with

- ribosomal RNA gene reference databases and tools. *J. Biotechnol.* 261, 169–176.
<https://doi.org/10.1016/j.jbiotec.2017.06.1198>
- Glud, R.N., Holby, O., Hoffmann, F., Canfield, D.E., 1998. Benthic mineralization and exchange in Arctic sediments (Svalbard, Norway). *Mar. Ecol. Prog. Ser.* 173, 237–251.
<https://doi.org/10.3354/meps173237>
- Gofstein, T.R., Perkins, M., Field, J., Leigh, M.B., 2019. Sequential co-degradation of crude oil and Corexit 9500. *Environ. Sci. Technol.*
- Gomila, M., Peña, A., Mulet, M., Lalucat, J., García-Valdés, E., 2015. Phylogenomics and systematics in *Pseudomonas*. *Front. Microbiol.* 0, 214.
<https://doi.org/10.3389/FMICB.2015.00214>
- Gong, Y., Zhao, X., Cai, Z., O'Reilly, S.E., Hao, X., Zhao, D., 2014. A review of oil, dispersed oil and sediment interactions in the aquatic environment: Influence on the fate, transport and remediation of oil spills. *Mar. Pollut. Bull.* 79, 16–33.
<https://doi.org/10.1016/j.marpolbul.2013.12.024>
- Gregson, B.H., McKew, B.A., Holland, R.D., Nedwed, T.J., Prince, R.C., McGenity, T.J., 2021. Marine Oil Snow, a Microbial Perspective. *Front. Mar. Sci.* 8, 619484.
<https://doi.org/10.3389/fmars.2021.619484>
- Guibert, L.M., Loviso, C.L., Borglin, S., Jansson, J.K., Dionisi, H.M., Lozada, M., 2016. Diverse Bacterial Groups Contribute to the Alkane Degradation Potential of Chronically Polluted Subantarctic Coastal Sediments. *Microb. Ecol.* 71, 100–112.
<https://doi.org/10.1007/s00248-015-0698-0>

- Guibert, L.M., Loviso, C.L., Marcos, M.S., Commendatore, M.G., Dionisi, H.M., Lozada, M., 2012. Alkane Biodegradation Genes from Chronically Polluted Subantarctic Coastal Sediments and Their Shifts in Response to Oil Exposure. *Microb. Ecol.* 64, 605–616. <https://doi.org/10.1007/s00248-012-0051-9>
- Gustitus, S.A., Clement, T.P., 2017. Formation, Fate, and Impacts of Microscopic and Macroscopic Oil-Sediment Residues in Nearshore Marine Environments: A Critical Review. *Rev. Geophys.* 55, 1130–1157. <https://doi.org/10.1002/2017RG000572>
- Hahnke, S., Brock, N.L., Zell, C., Simon, M., Dickschat, J.S., Brinkhoff, T., 2013. Physiological diversity of Roseobacter clade bacteria co-occurring during a phytoplankton bloom in the North Sea. *Syst. Appl. Microbiol.* 36, 39–48. <https://doi.org/10.1016/j.syapm.2012.09.004>
- Hamdan, H.Z., Salam, D.A., Saikaly, P.E., 2019. Characterization of the microbial community diversity and composition of the coast of Lebanon: Potential for petroleum oil biodegradation. *Mar. Pollut. Bull.* 149, 110508. <https://doi.org/10.1016/J.MARPOLBUL.2019.110508>
- Hasegawa, R., Toyama, K., Miyanaga, K., Tanji, Y., 2014. Identification of crude-oil components and microorganisms that cause souring under anaerobic conditions. *Appl. Microbiol. Biotechnol.* 98, 1853–1861. <https://doi.org/10.1007/s00253-013-5107-3>
- Hau, H.H., Gralnick, J.A., 2007. Ecology and Biotechnology of the Genus *Shewanella*. <https://doi.org/10.1146/annurev.micro.61.080706.093257>
- Hazen, T.C., Prince, R.C., Mahmoudi, N., 2015. Marine Oil Biodegradation. *Environ. Sci. Technol.* 50, 2121–2129. <https://doi.org/10.1021/acs.est.5b03333>

- Head, I.M., Jones, D.M., Röling, W.F.M., 2006. Marine microorganisms make a meal of oil. *Nat. Rev. Microbiol.* 4, 173–182. <https://doi.org/10.1038/nrmicro1348>
- Hesse, C., Schulz, F., Bull, C.T., Shaffer, B.T., Yan, Q., Shapiro, N., Hassan, K.A., Varghese, N., Elbourne, L.D.H., Paulsen, I.T., Kyrpides, N., Woyke, T., Loper, J.E., 2018. Genome-based evolutionary history of *Pseudomonas* spp. *Environ. Microbiol.* 20, 2142–2159. <https://doi.org/10.1111/1462-2920.14130>
- Huntington, H.P., Raymond-Yakoubian, J., Noongwook, G., Naylor, N., Harris, C., Harcharek, Q., Adams, B., 2021. “We Never Get Stuck.” A Collaborative Analysis of Change and Coastal Community Subsistence Practices in the Northern Bering and Chukchi Seas, Alaska. *ARCTIC* 74, 113–126. <https://doi.org/10.14430/ARCTIC72446>
- Isaac, P., Sánchez, L.A., Bourguignon, N., Cabral, M.E., Ferrero, M.A., 2013. Indigenous PAH-degrading bacteria from oil-polluted sediments in Caleta Cordova, Patagonia Argentina. *Int. Biodeterior. Biodegradation* 82, 207–214. <https://doi.org/10.1016/J.IBIOD.2013.03.009>
- Jewett, S.C., Dean, T.A., Woodin, B.R., Hoberg, M.K., Stegeman, J.J., 2002. Exposure to hydrocarbons 10 years after the Exxon Valdez oil spill: Evidence from cytochrome P4501A expression and biliary FACs in nearshore demersal fishes. *Mar. Environ. Res.* 54, 21–48. [https://doi.org/10.1016/S0141-1136\(02\)00093-4](https://doi.org/10.1016/S0141-1136(02)00093-4)
- Jia, B., Jeong, H.I., Kim, K.H., Jeon, C.O., 2016. Complete genome of *Zhongshania* aliphaticivorans SM-2T, an aliphatic hydrocarbon-degrading bacterium isolated from tidal flat sediment. *J. Biotechnol.* 226, 22–23. <https://doi.org/10.1016/j.jbiotec.2016.03.039>
- Kasai, Y., Shindo, K., Harayama, S., Misawa, N., 2003. Molecular Characterization and

Substrate Preference of a Polycyclic Aromatic Hydrocarbon Dioxygenase from
Cycloclasticus sp. Strain A5. *Appl. Environ. Microbiol.* 69, 6688–6697.

<https://doi.org/10.1128/AEM.69.11.6688-6697.2003>

Khan, M.A.Q., Khan, S.F., Shattari, F., 2008. Halogenated Hydrocarbons. *Encycl. Ecol. Five-
Volume Set 1831–1843*. <https://doi.org/10.1016/B978-008045405-4.00399-2>

King, G.M., Kostka, J.E., Hazen, T.C., Sobczyk, P.A., 2015. Microbial Responses to the
Deepwater Horizon Oil Spill: From Coastal Wetlands to the Deep Sea. *Annu. Rev. Mar.
Sci.* Vol 7 7, 377–401. <https://doi.org/10.1146/annurev-marine-010814-015543>

Koo, H., Mojib, N., Huang, J.P., Donahoe, R.J., Bej, A.K., 2015. Bacterial community shift in
the coastal Gulf of Mexico salt-marsh sediment microcosm in vitro following exposure to
the Mississippi Canyon Block 252 oil (MC252). *3 Biotech* 5, 379–392.

<https://doi.org/10.1007/S13205-014-0233-X/TABLES/3>

Kostka, J.E., Prakash, O., Overholt, W.A., Green, S.J., Freyer, G., Canion, A., Delgado, J.,
Norton, N., Hazen, T.C., Huettel, M., 2011. Hydrocarbon-degrading bacteria and the
bacterial community response in Gulf of Mexico beach sands impacted by the deepwater
horizon oil spill. *Appl. Environ. Microbiol.* 77, 7962–7974.

<https://doi.org/10.1128/AEM.05402-11>

Krause, S., Molari, M., Gorb, E. V., Gorb, S.N., Kossel, E., Haeckel, M., 2020. Persistence of
plastic debris and its colonization by bacterial communities after two decades on the abyssal
seafloor. *Sci. Reports* 2020 101 10, 1–15. <https://doi.org/10.1038/s41598-020-66361-7>

Kube, M., Chernikova, T.N., Al-Ramahi, Y., Beloqui, A., Lopez-Cortez, N., Guazzaroni, M.E.,

- Heipieper, H.J., Klages, S., Kotsyurbenko, O.R., Langer, I., Nechitaylo, T.Y., Lünsdorf, H., Fernández, M., Juárez, S., Ciordia, S., Singer, A., Kagan, O., Egorova, O., Alain Petit, P., Stogios, P., Kim, Y., Tchigvintsev, A., Flick, R., Denaro, R., Genovese, M., Albar, J.P., Reva, O.N., Martínez-Gomariz, M., Tran, H., Ferrer, M., Savchenko, A., Yakunin, A.F., Yakimov, M.M., Golyshina, O. V., Reinhardt, R., Golyshin, P.N., 2013. Genome sequence and functional genomic analysis of the oil-degrading bacterium *Oleispira antarctica*. *Nat. Commun.* 2013 41 4, 1–11. <https://doi.org/10.1038/ncomms3156>
- Lohner, S.T., Spormann, A.M., 2013. Identification of a reductive tetrachloroethene dehalogenase in *Shewanella sediminis*. *Philos. Trans. R. Soc. B Biol. Sci.* 368, 20120326. <https://doi.org/10.1098/rstb.2012.0326>
- Luo, H., Moran, M.A., 2014. Evolutionary Ecology of the Marine Roseobacter Clade. *Microbiol. Mol. Biol. Rev.* 78, 573–587. <https://doi.org/10.1128/membr.00020-14>
- Maeda, R., Ito, Y., Iwata, K., Omori, T., 2010. Comparison of marine and terrestrial carbazole-degrading bacteria. *Appl. Microbiol.* 1311–1321.
- Manzetti, S., 2014. Remediation technologies for oil-drilling activities in the Arctic: oil-spill containment and remediation in open water. *Environ. Technol. Rev.* 3, 49–60. <https://doi.org/10.1080/21622515.2014.966156>
- Marietou, A., Chastain, R., Beulig, F., Scoma, A., Hazen, T.C., Bartlett, D.H., 2018. The Effect of Hydrostatic Pressure on Enrichments of Hydrocarbon Degrading Microbes From the Gulf of Mexico Following the Deepwater Horizon Oil Spill. *Front. Microbiol.* 9, 808. <https://doi.org/10.3389/fmicb.2018.00808>

- Martín-Gil, J., Ramos-Sánchez, M.C., Martín-Gil, F.J., 2004. *Shewanella putrefaciens* in a fuel-in-water emulsion from the Prestige oil spill. *Antonie Van Leeuwenhoek* 86, 283–285. <https://doi.org/10.1023/B:ANTO.0000047939.49597.eb>
- McFarlin, K.M., Perkins, M.J., Field, J.A., Leigh, M.B., 2018. Biodegradation of Crude Oil and Corexit 9500 in Arctic Seawater. *Front. Microbiol.* 9. <https://doi.org/10.3389/fmicb.2018.01788>
- McFarlin, K.M., Prince, R.C., Perkins, R., Leigh, M.B., 2014. Biodegradation of dispersed oil in Arctic seawater at -1°C. *PLoS One* 9, 1–8. <https://doi.org/10.1371/journal.pone.0084297>
- Militon, C., Jézéquel, R., Gilbert, F., Corsellis, Y., Sylvi, L., Cravo-Laureau, C., Duran, R., Cuny, P., 2015. Dynamics of bacterial assemblages and removal of polycyclic aromatic hydrocarbons in oil-contaminated coastal marine sediments subjected to contrasted oxygen regimes. *Environ. Sci. Pollut. Res.* 22, 15260–15272. <https://doi.org/10.1007/s11356-015-4510-y>
- Morris, E.K., Caruso, T., Buscot, F., Fischer, M., Hancock, C., Maier, T.S., Meiners, T., Müller, C., Obermaier, E., Prati, D., Socher, S.A., Sonnemann, I., Wäschke, N., Wubet, T., Wurst, S., Rillig, M.C., 2014. Choosing and using diversity indices: insights for ecological applications from the German Biodiversity Exploratories. *Ecol. Evol.* 4, 3514–24. <https://doi.org/10.1002/ece3.1155>
- Mu, J., Leng, Q., Yang, G., Zhu, B., 2021. Anaerobic degradation of high-concentration polycyclic aromatic hydrocarbons (PAHs) in seawater sediments. *Mar. Pollut. Bull.* 167, 112294. <https://doi.org/10.1016/J.MARPOLBUL.2021.112294>

- Muschenheim, D.K., Lee, K., 2002. Removal of oil from the sea surface through particulate interactions: Review and prospectus. *Spill Sci. Technol. Bull.* 8, 9–18.
[https://doi.org/10.1016/S1353-2561\(02\)00129-9](https://doi.org/10.1016/S1353-2561(02)00129-9)
- Nagashima, H., Zulkharnain, A. Bin, Maeda, R., Fuse, H., Iwata, K., Omori, T., 2010. Cloning and Nucleotide Sequences of Carbazole Degradation Genes from Marine Bacterium *Neptuniibacter* sp. Strain CAR-SF. *Curr. Microbiol.* 61, 50–56.
<https://doi.org/10.1007/s00284-009-9575-8>
- Naysim, L.O., Kang, H.J., Jeon, C.O., 2014. *Zhongshania aliphaticivorans* sp. nov., an aliphatic hydrocarbon-degrading bacterium isolated from marine sediment, And transfer of *Spongiibacter borealis* Jang et al. 2011 to the genus *Zhongshania* as *Zhongshania borealis* comb. nov. *Int. J. Syst. Evol. Microbiol.* 64, 3768–3774.
- Nedashkovskaya, O.I., Van Trappen, S., Zhukova, N. V., de Vos, P., 2015. *Lutibacter holmesii* sp. Nov., A marine bacterium of the family Flavobacteriaceae isolated from the sea urchin *Strongylocentrotus intermedius*, and emended description of the genus *Lutibacter*. *Int. J. Syst. Evol. Microbiol.* 65, 3991–3996.
<https://doi.org/10.1099/IJSEM.0.000525/CITE/REFWORKS>
- Netzer, R., Henry, I.A., Ribicic, D., Wibberg, D., Brönner, U., Brakstad, O.G., 2018. Petroleum hydrocarbon and microbial community structure successions in marine oil-related aggregates associated with diatoms relevant for Arctic conditions. *Mar. Pollut. Bull.* 135, 759–768. <https://doi.org/10.1016/j.marpolbul.2018.07.074>
- Oksanen, J., 2015. *Multivariate Analysis of Ecological Communities in R: vegan tutorial.*

- Oyewusi, H.A., Wahab, R.A., Huyop, F., 2020. Dehalogenase-producing halophiles and their potential role in bioremediation. *Mar. Pollut. Bull.* 160, 111603.
<https://doi.org/10.1016/J.MARPOLBUL.2020.111603>
- Parada, A.E., Needham, D.M., Fuhrman, J.A., 2016. Every base matters: assessing small subunit rRNA primers for marine microbiomes with mock communities, time series and global field samples. *Environ. Microbiol.* 18, 1403–1414. <https://doi.org/10.1111/1462-2920.13023>
- Passow, U., Sweet, J., Quigg, A., 2017. How the dispersant Corexit impacts the formation of sinking marine oil snow. *Mar. Pollut. Bull.* 125, 139–145.
<https://doi.org/10.1016/j.marpolbul.2017.08.015>
- Peix, A., Ramírez-Bahena, M.H., Velázquez, E., 2009. Historical evolution and current status of the taxonomy of genus *Pseudomonas*. *Infect. Genet. Evol.* 9, 1132–1147.
<https://doi.org/10.1016/J.MEEGID.2009.08.001>
- Peterson, C.H., Rice, S.D., Short, J.W., Esler, D., Bodkin, J.L., Ballachey, B.E., Irons, D.B., 2003. Long-Term Ecosystem Response to the Exxon Valdez Oil Spill. *Science* (80-.). 302, 2082–2086.
https://doi.org/10.1126/SCIENCE.1084282/SUPPL_FILE/PETERSON.SOM.PDF
- Pohlner, M., Dlugosch, L., Wemheuer, B., Mills, H., Engelen, B., Reese, B.K., 2019. The Majority of Active Rhodobacteraceae in Marine Sediments Belong to Uncultured Genera: A Molecular Approach to Link Their Distribution to Environmental Conditions. *Front. Microbiol.* 10, 659. <https://doi.org/10.3389/fmicb.2019.00659>
- Prince, R.C., McFarlin, K.M., Butler, J.D., Febbo, E.J., Wang, F.C.Y., Nedwed, T.J., 2013. The

primary biodegradation of dispersed crude oil in the sea. *Chemosphere* 90, 521–526.

<https://doi.org/10.1016/j.chemosphere.2012.08.020>

Prince, R.C., Owens, E.H., Sergy, G.A., 2002. Weathering of an Arctic oil spill over 20 years: the BIOS experiment revisited. *Mar Pollut Bull* 44, 1236–1242.

[https://doi.org/10.1016/s0025-326x\(02\)00214-x](https://doi.org/10.1016/s0025-326x(02)00214-x)

Quero, G.M., Cassin, D., Botter, M., Perini, L., Luna, G.M., 2015. Patterns of benthic bacterial diversity in coastal areas contaminated by heavy metals, polycyclic aromatic hydrocarbons (PAHs) and polychlorinated biphenyls (PCBs). *Front. Microbiol.* 6, 1053.

<https://doi.org/10.3389/FMICB.2015.01053/BIBTEX>

Quigg, Antonietta, Passow, Uta, Daly, Kendra L, Burd, Adrian, Hollander, D.J., Schwing, P.T., Lee, Kenneth, Quigg, A, Passow, U, Daly, K L, Hollander, · D J, Schwing, · P T, Burd, A, Lee, K, 2020. Marine Oil Snow Sedimentation and Flocculent Accumulation (MOSSFA) Events: Learning from the Past to Predict the Future. *Deep Oil Spills* 196–220.

https://doi.org/10.1007/978-3-030-11605-7_12

R Core Team, 2017. R: A language and environment for statistical computing.

Ribicic, D., Netzer, R., Hazen, T.C., Techtmann, S.M., Drabløs, F., Brakstad, O.G., 2018.

Microbial community and metagenome dynamics during biodegradation of dispersed oil reveals potential key-players in cold Norwegian seawater. *Mar. Pollut. Bull.* 129, 370–378.

<https://doi.org/10.1016/j.marpolbul.2018.02.034>

Rodriguez-R, L.M., Overholt, W.A., Hagan, C., Huettel, M., Kostka, J.E., Konstantinidis, K.T., 2015. Microbial community successional patterns in beach sands impacted by the

- Deepwater Horizon oil spill. *ISME J.* 9, 1928–1940. <https://doi.org/10.1038/ismej.2015.5>
- Rogers, V. V., Liber, K., MacKinnon, M.D., 2002. Isolation and characterization of naphthenic acids from Athabasca oil sands tailings pond water. *Chemosphere* 48, 519–527. [https://doi.org/10.1016/S0045-6535\(02\)00133-9](https://doi.org/10.1016/S0045-6535(02)00133-9)
- Rousseeuw, P.J., 1987. Silhouettes: A graphical aid to the interpretation and validation of cluster analysis. *J. Comput. Appl. Math.* 20, 53–65. [https://doi.org/10.1016/0377-0427\(87\)90125-7](https://doi.org/10.1016/0377-0427(87)90125-7)
- Ruecker, A., Weigold, P., Behrens, S., Jochmann, M., Laaks, J., Kappler, A., 2014. Predominance of biotic over abiotic formation of halogenated hydrocarbons in hypersaline sediments in Western Australia. *Environ. Sci. Technol.* 48, 9170–9178. https://doi.org/10.1021/ES501810G/SUPPL_FILE/ES501810G_SI_001.PDF
- Rysgaard, S., Glud, R.N., Risgaard-Petersen, N., Dalsgaard, T., 2004. Denitrification and anammox activity in Arctic marine sediments. *Limnol. Oceanogr.* 49, 1493–1502. <https://doi.org/10.4319/lo.2004.49.5.1493>
- Rysgaard, S., Risgaard-Petersen, N., Sloth, N.P., Jensen, K., Nielsen, L.P., Nielsen, P., 1994. Oxygen Regulation of Nitrification and Denitrification in Sediments. *Source Limnol. Oceanogr. Limnol. Ocean.* 39, 1643–1652. <https://doi.org/10.4319/lo.1994.39.7.1643>
- Sánchez, D., Mulet, M., Rodríguez, A.C., David, Z., Lalucat, J., García-Valdés, E., 2014. *Pseudomonas aestusnigri* sp. nov., isolated from crude oil-contaminated intertidal sand samples after the Prestige oil spill. *Syst. Appl. Microbiol.* 37, 89–94.
- Santos, J.C. dos, Lopes, D.R.G., Da Silva, J.D., De Oliveira, M.D., Dias, R.S., Lima, H.S., De

- Sousa, M.P., De Paula, S.O., Silva, C.C. da, 2020. Diversity of sulfate-reducing prokaryotes in petroleum production water and oil samples. *Int. Biodeterior. Biodegrad.* 151. <https://doi.org/10.1016/J.IBIOD.2020.104966>
- Scoma, A., Heyer, R., Rifai, R., Dandyk, C., Marshall, I., Kerckhof, F.M., Marietou, A., Boshker, H.T.S., Meysman, F.J.R., Malmos, K.G., Vosegaard, T., Vermeir, P., Banat, I.M., Benndorf, D., Boon, N., 2018. Reduced TCA cycle rates at high hydrostatic pressure hinder hydrocarbon degradation and obligate oil degraders in natural, deep-sea microbial communities. *ISME J.* 2018 134 13, 1004–1018. <https://doi.org/10.1038/s41396-018-0324-5>
- Sekar, R., Dichristina, T.J., 2017. Degradation of the recalcitrant oil spill components anthracene and pyrene by a microbially driven Fenton reaction. *FEMS Microbiol. Lett.* 364, 203. <https://doi.org/10.1093/FEMSLE/FNX203>
- Shigenaka, G., 2014. Twenty-Five Years After the Exxon Valdez Oil Spill ; National Oceanic and Atmospheric Administration Scientific Support, Monitoring and Research.
- Short, J.W., Rice, S.D., Heintz, R.A., Carls, M.G., Moles, A., 2003. Long-term effects of crude oil on developing fish: Lessons from the Exxon Valdez oil spill. *Energy Sources* 25, 509–517. <https://doi.org/10.1080/00908310390195589>
- Sieradzki, E.T., Morando, M., Fuhrman, J.A., 2021. Metagenomics and Quantitative Stable Isotope Probing Offer Insights into Metabolism of Polycyclic Aromatic Hydrocarbon Degraders in Chronically Polluted Seawater. *mSystems* 6.
- Sun, R., Sun, Y., Li, Q.X., Zheng, X., Luo, X., Mai, B., 2018. Polycyclic aromatic hydrocarbons

in sediments and marine organisms: Implications of anthropogenic effects on the coastal environment. *Sci. Total Environ.* 640–641, 264–272.

<https://doi.org/10.1016/J.SCITOTENV.2018.05.320>

Tarr, M.A., Zito, P., Overton, E.B., Olson, G.M., Adhikari, P.L., Reddy, C.M., 2016. Weathering of oil spilled in the marine environment. *Oceanography* 29, 126–135.

<https://doi.org/10.5670/oceanog.2016.77>

Teeling, H., Fuchs, B.M., Bennke, C.M., Krüger, K., Chafee, M., Kappelmann, L., Reintjes, G., Waldmann, J., Quast, C., Glöckner, F.O., Lucas, J., Wichels, A., Gerdt, G., Wiltshire, K.H., Amann, R.L., 2016. Recurring patterns in bacterioplankton dynamics during coastal spring algae blooms. *Elife* 5. <https://doi.org/10.7554/eLife.11888>

Toes, A.C.M., Geelhoed, J.S., Kuenen, J.G., Muyzer, G., 2008. Characterization of Heavy Metal Resistance of Metal-Reducing *Shewanella* Isolates From Marine Sediments. <https://doi.org/10.1080/01490450802258329> 25, 304–314.

<https://doi.org/10.1080/01490450802258329>

Walker, A.M., Leigh, M.B., Mincks, S.L., 2021. Patterns in Benthic Microbial Community Structure Across Environmental Gradients in the Beaufort Sea Shelf and Slope. *Front. Microbiol.* 12, 37. <https://doi.org/10.3389/fmicb.2021.581124>

Walters, W., Hyde, E.R., Berg-Lyons, D., Ackermann, G., Humphrey, G., Parada, A., Gilbert, J.A., Jansson, J.K., Caporaso, J.G., Fuhrman, J.A., Apprill, A., Knight, R., 2016. Improved Bacterial 16S rRNA Gene (V4 and V4-5) and Fungal Internal Transcribed Spacer Marker Gene Primers for Microbial Community Surveys. *mSystems* 1, e00009-15.

<https://doi.org/10.1128/mSystems.00009-15>

Wang, J., Lu, J., Zhang, Y., Wu, J., Luo, Y., 2021. Unique Bacterial Community of the Biofilm on Microplastics in Coastal Water. *Bull. Environ. Contam. Toxicol.* 107, 597–601.

<https://doi.org/10.1007/s00128-020-02875-0>

Wang, M., Overland, J.E., 2015. Projected future duration of the sea-ice-free season in the Alaskan Arctic. (J.E. Overland). *Prog. Oceanogr.* 136, 50–59.

<https://doi.org/10.1016/j.pocean.2015.01.001>

Wang, Q., Garrity, G.M., Tiedje, J.M., Cole, J.R., 2007. Naive Bayesian Classifier for Rapid Assignment of rRNA Sequences into the New Bacterial Taxonomy. *Appl. Environ. Microbiol.* 73, 5261–5267. <https://doi.org/10.1128/AEM.00062-07>

Wang, Y., Yu, M., Austin, B., Zhang, X.-H.H., 2012. *Oleispira lenta* sp. nov., a novel marine bacterium isolated from Yellow sea coastal seawater in Qingdao, China. *Antonie Van Leeuwenhoek* 101, 787–794. <https://doi.org/10.1007/s10482-011-9693-8>

Wang, Z., An, C., Lee, K., Owens, E., Chen, Z., Boufadel, M., Taylor, E., Feng, Q., 2020.

Factors influencing the fate of oil spilled on shorelines: a review. *Environ. Chem. Lett.* 2020

192 19, 1611–1628. <https://doi.org/10.1007/S10311-020-01097-4>

Ward, C.P., Overton, E.B., 2020. How the 2010 Deepwater Horizon spill reshaped our

understanding of crude oil photochemical weathering at sea: a past, present, and future perspective. *Environ. Sci. Process. Impacts* 22, 1125–1138.

<https://doi.org/10.1039/D0EM00027B>

- Wasmund, K., Pelikan, C., Schintlmeister, A., Wagner, M., Watzka, M., Richter, A., Bhatnagar, S., Noel, A., Hubert, C.R.J.J., Rattei, T., Hofmann, T., Hausmann, B., Herbold, C.W., Loy, A., 2021. Genomic insights into diverse bacterial taxa that degrade extracellular DNA in marine sediments. *Nat. Microbiol.* 2021 67 6, 885–898. <https://doi.org/10.1038/s41564-021-00917-9>
- Westcott, S.L., Schloss, P.D., 2017. OptiClust, an Improved Method for Assigning Amplicon-Based Sequence Data to Operational Taxonomic Units. *mSphere* 2, e00073-17. <https://doi.org/10.1128/mSphereDirect.00073-17>
- Wunder, L.C., Aromokeye, D.A., Yin, X., Richter-Heitmann, T., Willis-Poratti, G., Schnakenberg, A., Otersen, C., Dohrmann, I., Römer, M., Bohrmann, G., Kasten, S., Friedrich, M.W., 2021. Iron and sulfate reduction structure microbial communities in (sub-)Antarctic sediments. *ISME J.* 2021 1512 15, 3587–3604. <https://doi.org/10.1038/s41396-021-01014-9>
- Xue, J., Yu, Y., Bai, Y., Wang, L., Wu, Y., 2015. Marine Oil-Degrading Microorganisms and Biodegradation Process of Petroleum Hydrocarbon in Marine Environments: A Review. *Curr. Microbiol.* 71, 220–228. <https://doi.org/10.1007/s00284-015-0825-7>
- Yakimov, M.M., Giuliano, L., Gentile, G., Crisafi, E., Chernikova, T.N., Abraham, W.-R., Lünsdorf, H., Timmis, K.N., Golyshin, P.N., 2003. *Oleispira antarctica* gen. nov., sp. nov., a novel hydrocarbonoclastic marine bacterium isolated from Antarctic coastal sea water. *Int. J. Syst. Evol. Microbiol.* 53, 779–785. <https://doi.org/10.1099/ijs.0.02366-0>
- Yakimov, M.M., Timmis, K.N., Golyshin, P.N., 2007. Obligate oil-degrading marine bacteria.

- Curr. Opin. Biotechnol. 18, 257–266. <https://doi.org/10.1016/j.copbio.2007.04.006>
- Yang, C., Zhang, G., Serhan, M., Koivu, G., Yang, Z., Hollebhone, B., Lambert, P., Brown, C.E., 2019. Characterization of naphthenic acids in crude oils and refined petroleum products. Fuel 255. <https://doi.org/10.1016/J.FUEL.2019.115849>
- Yang, T., Speare, K., McKay, L., MacGregor, B.J., Joye, S.B., Teske, A., 2016. Distinct bacterial communities in surficial seafloor sediments following the 2010 deepwater horizon blowout. Front. Microbiol. 7, 1384. <https://doi.org/10.3389/FMICB.2016.01384/BIBTEX>
- Yin, Y., Liu, C., Zhao, G., Chen, Y., 2022. Versatile mechanisms and enhanced strategies of pollutants removal mediated by *Shewanella oneidensis*: A review. J. Hazard. Mater. 129703. <https://doi.org/10.1016/J.JHAZMAT.2022.129703>
- Yu, J., Chen, C., Liu, C., Yu, D., Chen, S., Yuan, F., Fu, Y., Liu, Q., 2018. Insight into relationship between micro-consortia, nitrogen source and petroleum degradation at low temperature anaerobic condition. bioRxiv. <https://doi.org/10.1101/358838>
- Zanaroli, G., Negroni, A., Häggblom, M.M., Fava, F., 2015. Microbial dehalogenation of organohalides in marine and estuarine environments. Curr. Opin. Biotechnol. 33, 287–295. <https://doi.org/10.1016/J.COPBIO.2015.03.013>
- Zanaroli, G., Negroni, A., Vignola, M., Nuzzo, A., Shu, H.Y., Fava, F., 2012. Enhancement of microbial reductive dechlorination of polychlorinated biphenyls (PCBs) in a marine sediment by nanoscale zerovalent iron (NZVI) particles. J. Chem. Technol. Biotechnol. 87, 1246–1253. <https://doi.org/10.1002/jctb.3835>

Zinger, L., Amaral-Zettler, L.A., Fuhrman, J.A., Horner-Devine, M.C., Huse, S.M., Welch, D.B.M., Martiny, J.B.H., Sogin, M., Boetius, A., Ramette, A., 2011. Global Patterns of Bacterial Beta-Diversity in Seafloor and Seawater Ecosystems. *PLoS One* 6, e24570. <https://doi.org/10.1371/journal.pone.0024570>

Zoppini, A., Bongiorni, L., Ademollo, N., Patrolecco, L., Cibic, T., Franzo, A., Melita, M., Bazzaro, M., Amalfitano, S., 2020. Bacterial diversity and microbial functional responses to organic matter composition and persistent organic pollutants in deltaic lagoon sediments. *Estuar. Coast. Shelf Sci.* 233, 106508. <https://doi.org/10.1016/J.ECSS.2019.106508>

4.7 FIGURES

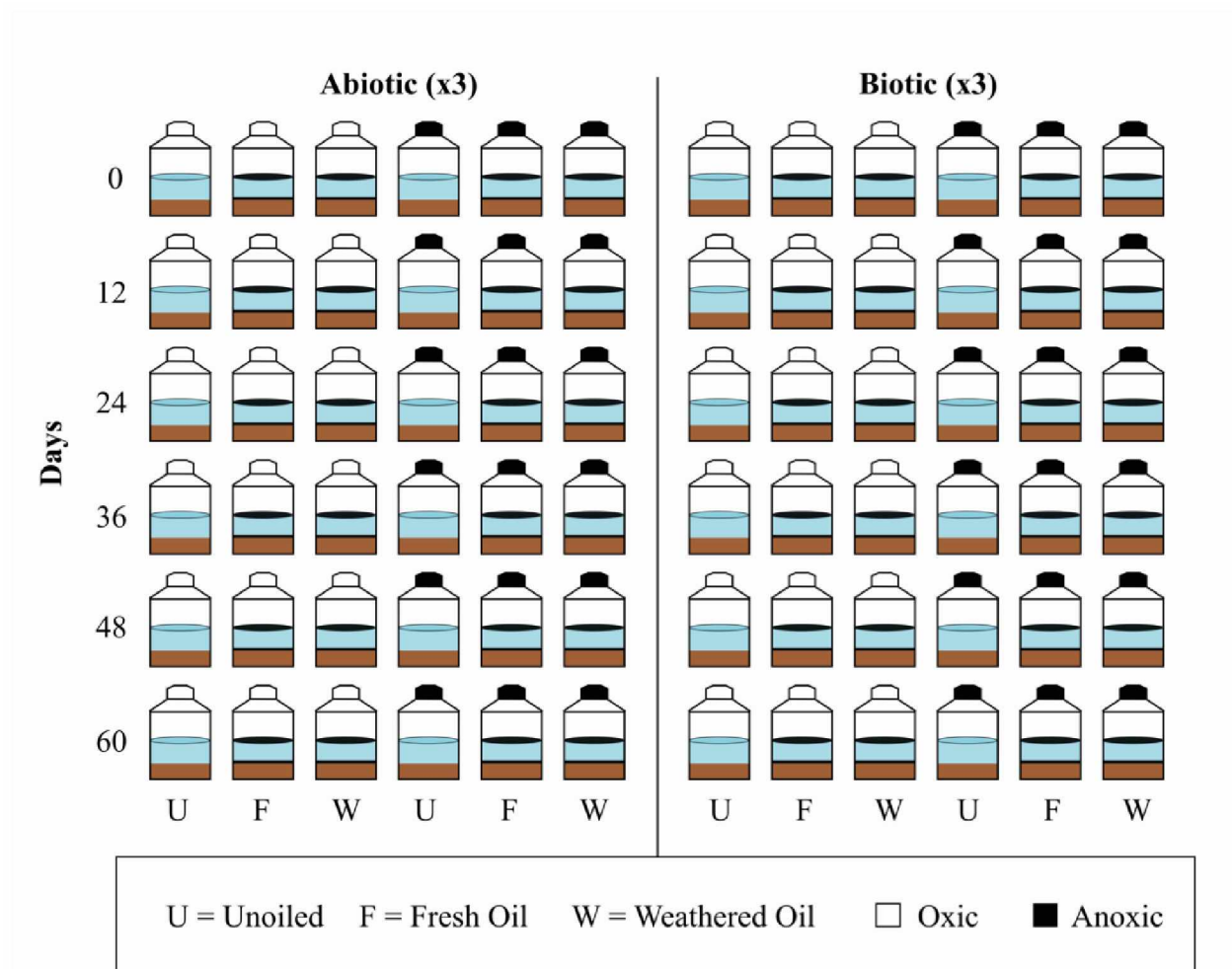


Figure 4.1. Experimental design for sediment oil biodegradation incubation tests. Oil degradation rates and community composition shifts were observed at 6 time points at 12-day intervals over the course of 60 days. For all incubation treatments, i.e., unoiled, fresh oil, weathered oil, oxic, and anoxic, there were 3 replicates. Oxic treatments were analyzed at time 0, 12, 24, 36, 48 and 60 days. Anoxic incubations were only analyzed at 790 days.

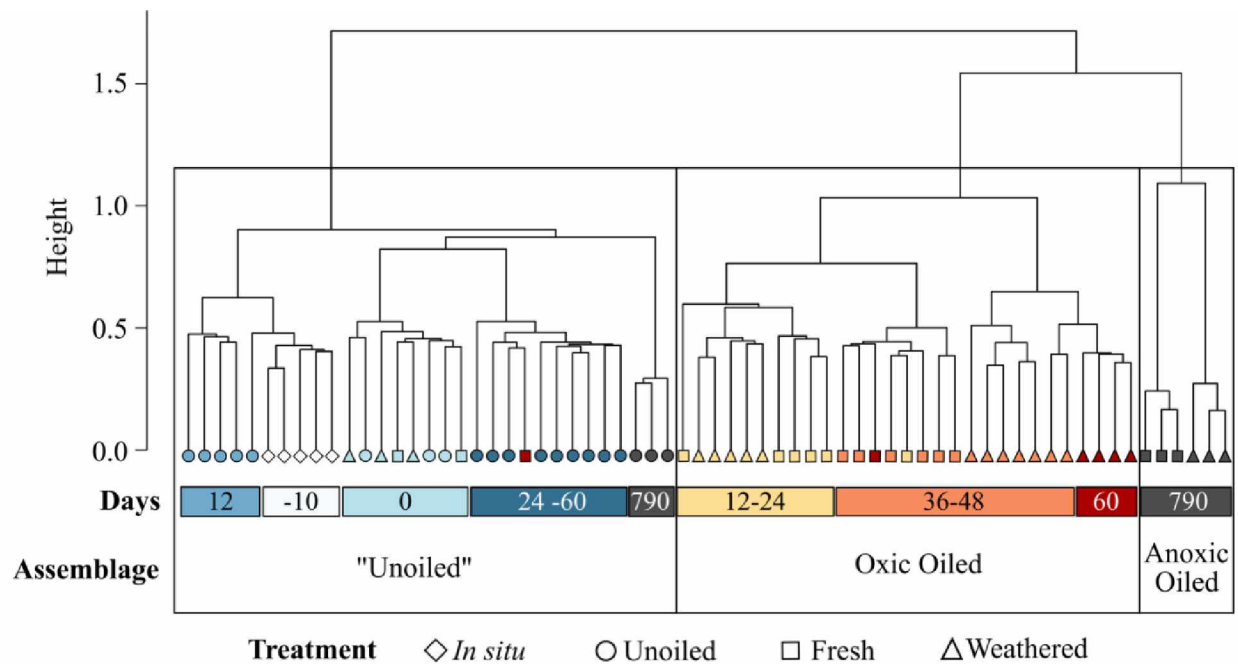


Figure 4.2. Cluster dendrogram of oxic and anoxic sediment samples. In this dendrogram, unooled, oxic oiled, and Anoxic oiled assemblages are enclosed in boxes, and the substructure and time points in days are highlighted in color. The unooled assemblage is in quotations as it does include samples with oil in them from day 0 of the experiment. Shapes are used to denote the treatment for each node on the dendrogram where “*in situ*” represents samples upon collection from the Chukchi Sea benthos, which were collected 10 days prior to the start of the experiment (-10).

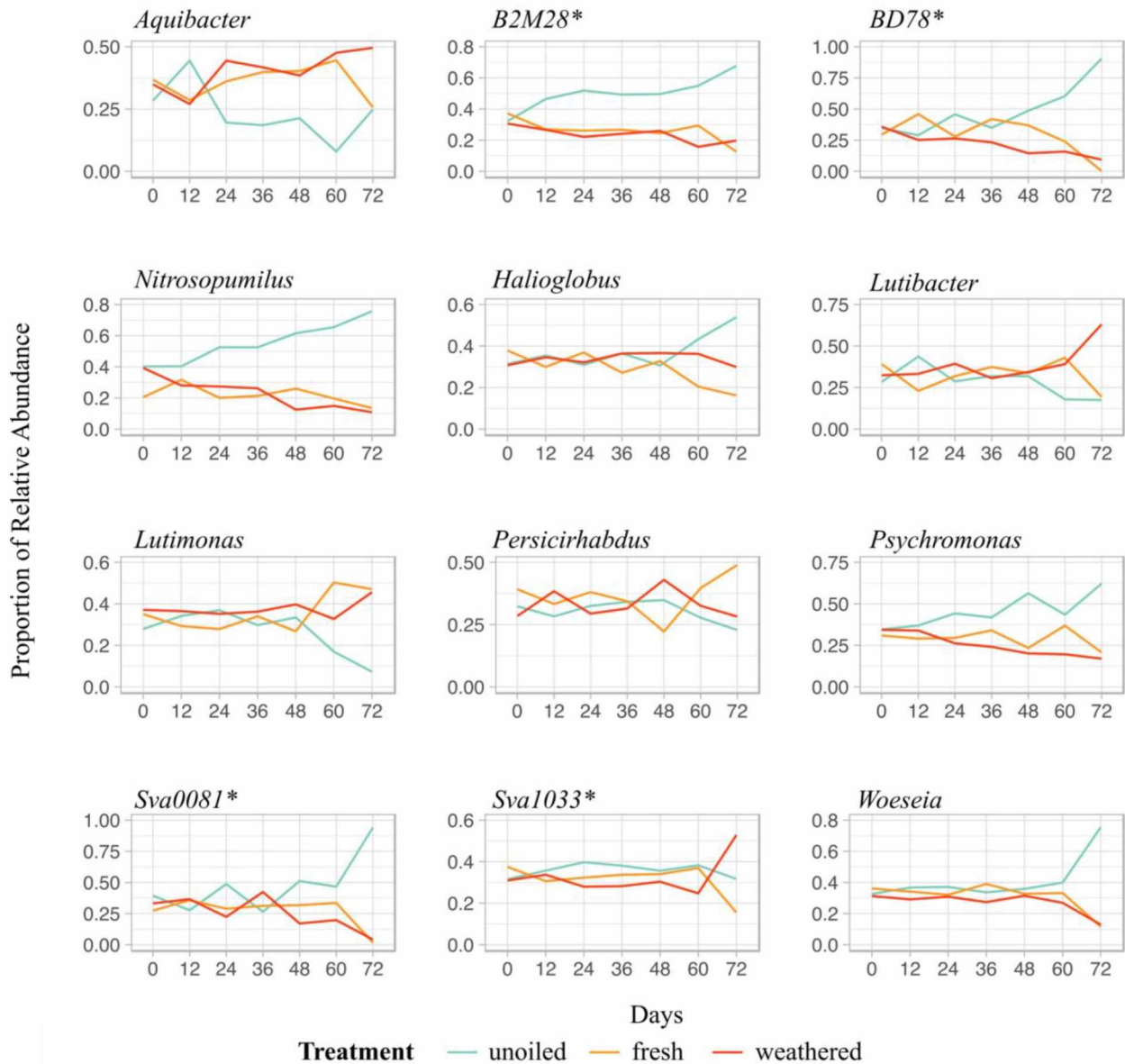


Figure 4.3. Change in core community genera with respect to oil treatment over time. The line plots above depict the proportion (y-axis), which are differing in scale for each taxon, of a given genus within unoiled, fresh oil, and weathered oil samples. The x-axis is such that 0 days is the start of experiment for anoxic and oxic samples, 60 days marks the end of the oxic experiment, and 72 days marks day 790, which is when the anoxic samples were harvested. Taxa with an * are clustered at genus level but could only be classified to order level.

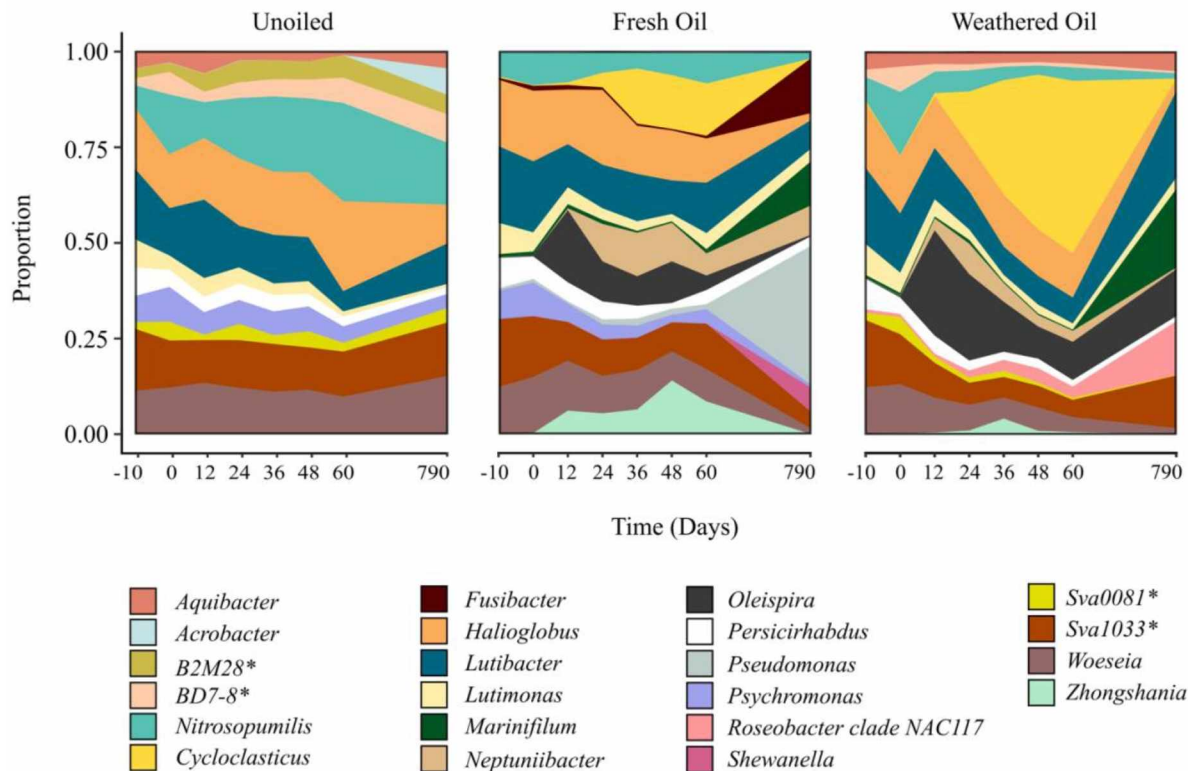


Figure 4.4. Change in most abundant taxa over time across treatments (unoiled fresh oil, and weathered oil under oxic and anoxic conditions) in Chukchi Sea sediments. The area plots above depict the proportional change in core community overtime with select top 50 genera of unoiled, fresh oil, and weathered oil treatments. The x-axis is such that -10 days is the time of sample collection (10 days before experiment start), then day 0 (start of experiment for anoxic and oxic samples), then 12-day intervals when oxic samples were harvested, and finally one anoxic time point at day 790. Asterisks denote taxa which were clustered at genus-level but identified only down to order-level.

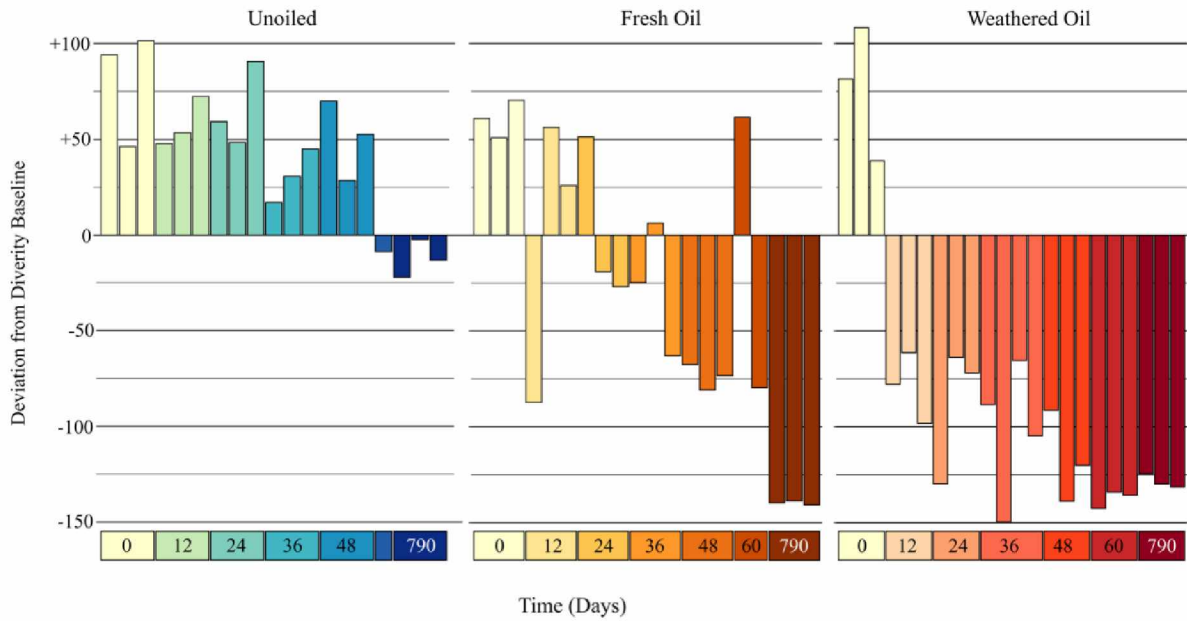


Figure 4.5. Change in prokaryotic diversity overtime across treatments as barplots of unoiled, fresh oil, and weathered oil replicate samples under oxic and anoxic conditions from day 0 to 790 (x-axis) are shown above. The y-axis is the change in inverse Simpson indices from the mean diversity found *in situ* (samples upon collection). All samples from 0-60 days are oxic, and all samples at day 790 are anoxic.

CHAPTER 5: GENERAL CONCLUSION

These data constitute the most comprehensive assessment of sediment microbial communities anywhere in the Arctic, with 126 sampling sites ranging from longitudes -176°W to -116°W, latitudes of 62°N to 73°N, and depths from 17-1,200 m across the Northern Bering, Chukchi, seas, and Alaskan and Canadian regions of the Beaufort Sea shelf and slope. These results expand coverage of microbial communities from the Northern Bering Sea to the Beaufort Sea, where only a handful (N=8) of surface sediment microbial communities have been previously characterized (Hamdan et al., 2013; Wang et al., 2018; Zeng et al., 2011).

On a broad spatial scale spanning two Arctic marginal seas, this analysis of the distribution of prokaryotic assemblages in surface sediments (upper 1 cm) across the Northern Bering-Chukchi-Beaufort seas region provides new insights into the factors influencing microbial community structure on different shelf systems. The Beaufort and Bering-Chukchi seas represent two different high-latitude environments: a narrow interior shelf and a shallow inflow shelf system respectively (Carmack and Wassmann, 2006). The northward advection of nutrient-rich waters supports high primary productivity and a robust benthic faunal population on the Bering-Chukchi Sea shelf, whereas turbidity, terrigenous material, depth variation, and longer sea-ice cover promote a latitudinally and longitudinally heterogeneous Beaufort Sea shelf environment which is comparatively lower in primary productivity and benthic biomass (Carmack and Wassmann, 2006; Goñi et al., 2013). Regional scale prokaryotic community structure underscored the comparative heterogeneity of the Beaufort Sea shelf, with sediments exhibiting distinct nearshore and offshore shelf assemblages, whereas Bering-Chukchi seas sediments exhibited just one assemblage throughout (Figure 2.8; Walker et al., 2021).

Community substructure on this regional spatial scale indicated that within the offshore Beaufort Sea shelf assemblage, there was a division among communities that occurred either west or east of the Mackenzie River, further highlighting the major impact of this river even in offshore shelf sediments near the slope (Walker et al., 2021). Two sub-groups within the Bering-Chukchi seas assemblage (Figure 2.8) corresponded to two predominant food-supply regimes, advective-supply and local-supply (cf., Feng et al., 2021), where long-term (decades) patterns of high biomass and abundance of benthic macrofauna have been observed. The local-supply regime is characterized by comparatively weaker currents, greater influence of sea-ice algae, and greater reliance on locally produced organic carbon, whereas the advective regime is largely reliant on horizontal transport of organic carbon produced “upstream” in the northern Bering Sea and deposited “downstream” (NE Chukchi Sea), with benthic consumption exceeding local primary production.

When we observed prokaryotic community structure on a smaller spatial scale, i.e., Chukchi and Beaufort seas separately, we found that they grouped into two and four assemblages respectively. The four assemblages characterizing Beaufort Sea shelf surface sediments were composed of taxa that, when taken together with environmental correlates, represented shallow-shelf, generalist, upper slope, and anoxic assemblages. A larger proportion of anaerobic taxa occurred in shallow shelf and anoxic assemblages, indicating that, in general, oxygen depletion in nearshore sediments is comparatively more widespread than offshore, particularly in areas where organic matter loading and Chl-*a* were higher and porosity lower. Shallow shelf taxa reflected characteristics of their habitat such as fresh phytodetritus, riverine input, light availability, and sea ice, and were strongly correlated with elevated Chl-*a* and significantly lower values of $\delta^{13}\text{C}$ (terrestrial signal) and salinity. Anoxic assemblage taxa suggested anoxic

conditions even within the upper 1-cm sediment layer, which are likely attributable to patchily distributed pockets of anoxia, such as high organic matter (OM) deposition, benthic seeps, and microbial mats. The upper Beaufort Sea slope assemblage reflected the deeper sampling depths typified by reduced inputs of more degraded OM and pointed to specific areas where nitrification may be a predominant biogeochemical process, as well as local distribution of mud volcanoes and magnetic sediments (Bluhm et al., 2020; Gamboa et al., 2017). The generalist assemblage was largely composed of taxa shared between the shelf and upper-slope assemblages, though the presence of methylotrophs in this assemblage indicates widespread potential for methane degradation across the outer shelf.

On the Bering-Chukchi seas shelf, the two surface sediment assemblages I observed consisted of a diatom/particle-associated assemblage and a comparatively suboxic assemblage, which reflect the aforementioned local and advective food-supply regimes, respectively. A subset of 10-cm deep samples from the Chukchi Sea were used to assess vertical microbial community structure and revealed a subsurface assemblage (1-10 cm) characterized by a comparatively larger proportion of anaerobic taxa than in surface sediment communities. Additionally, downcore microbial community structure in the Bering-Chukchi seas shelf reflected OM and nitrogen loading, sediment type, and OM type (fresh phytodetritus or chitinous detritus/biodeposits) and provided a rough indication of redox conditions and bioturbation influence. Samples collected at the same location in two different years (2014 and 2018) suggests that these two assemblages are consistent over time where they occur. Although hydrography over the Bering-Chukchi shelf is complex and exhibits both intra- and interannual variation, the overall distribution of prokaryotic assemblages reflected the consistent feature of cooler nutrient-rich Anadyr-influenced water offshore, low-nutrient warmer water nearshore, and

the associated depositional conditions. Zooming in to an even smaller scale, and examining the variation within each assemblage, prokaryotic community structure may also reflect finer scale hydrography and deposition, and points to locations where microbial communities may influence bottom water nutrient profiles or reflect environmental conditions unmeasured here. For instance, the presence of certain taxa in surface sediments may indicate elevated levels of hydrocarbons and iron particularly at stations surrounding Pt. Hope, AK. I posited in Chapter 2 that the elevated levels of hydrocarbons, inferred from the high relative abundances of the obligate oil degrader *Oleiphilus*, are likely phytoplankton-derived alkanes and alkenes (Rontani et al., 2014, 2018; Volkman et al., 1994). Due to high deposition rates, phytoplankton-derived alkanes and alkenes have been detected in this area as high concentrations of highly branched isoprenoids (HBI), specifically HBI III which is a C_{25:3} alkane typically utilized as a biomarker for pelagic phytoplankton (Koch et al., 2020; Meskhidze et al., 2015; Rontani et al., 2018). Results from my oil-incubation experiment support this hypothesis as *Oleiphilus* was not among the predominant putative oil degraders in oiled sediments collected near Pt. Hope, suggesting that *Oleiphilus* may be degrading different hydrocarbon compounds *in situ*.

Though *Oleiphilus* did not appear to respond strongly in the oil-incubation experiment, my findings indicated that oil-degradation potential is present in Chukchi sediments as other putative oil degraders were enriched in response to oil exposure. Additionally, I found that oxygen availability as well as the presence and condition of oil, fresh versus weathered, were major factors influencing microbial community structure. Succession of different putative oil degraders over time likely reflected the sequence of hydrocarbon compounds degraded in fresh or weathered oil. This type of succession has been well-documented in the marine environment, however the specific putative oil-degrading consortium exhibited here was relatively novel in

comparison to the majority of studies on marine sediments (Dong et al., 2015; Ferguson et al., 2017; Rodriguez-R et al., 2015; Yang et al., 2016).

5.1.1 Context in a changing Arctic

The Arctic marine ecosystem is undergoing pronounced changes due to climbing atmospheric temperatures, occurring two to three times faster than the global average (Cohen et al., 2014; Previdi et al., 2021). Resulting shifts in sea-ice cover, primary production, and riverine input will likely affect the quality and quantity of OM deposited to the seafloor and the tight pelagic-benthic coupling characteristic of Arctic ecosystems may emphasize the effects of these changes (Grebmeier, 2012; Kortsch et al., 2015, 2012). Previously ice-covered waters will also become more accessible to human activities, increasing the likelihood of anthropogenic disturbance and contaminant exposure through oil and gas development and increased marine traffic. So, what implications do the predicted climate trends have for benthic microbial communities in the Bering-Chukchi and Beaufort seas, and how can microbial community surveys be used to detect change?

In the Beaufort Sea, a larger proportion of anaerobic taxa nearshore occurred on the shallow shelf indicating that, in general, oxygen depletion in nearshore sediments is comparatively more widespread than offshore, particularly in areas where organic matter loading and Chl-*a* are higher and porosity lower. Although this is a common trend when comparing shelf to slope sediments, it may be of particular importance in the Beaufort Sea when viewed through the lens of climate change (Orcutt et al., 2011). An overall net increase of river runoff and terrestrial OM has already been established for the Mackenzie River, and is predicted to continue

over the coming years (Doxaran et al., 2015; Holmes et al., 2012). Thus, we might expect an increase in abundance of anaerobic taxa in the shallow shelf assemblage, with potentially more stations resembling or overlapping with the anoxic assemblage. There may also be increased taxonomic overlap between microbial communities associated with the Mackenzie River outflow and the shallow shelf assemblage. In addition to riverine input, shifts in primary production and sea-ice extent will likely be most apparent in the shallow-shelf sediments, as the majority of indicator taxa identified have been strongly correlated to both phytoplankton blooms and sea-ice microbial communities.

An increase in OM input, whether terrestrial- or marine-derived, will likely translate to an increase in OM burial and subsequent methanogenesis in the already methane-permeated Beaufort Sea sediments (Coffin et al., 2013). Characterizing the microbes involved in both methane production/degradation and associated processes in these sediments is thus of particular interest to investigations of potential greenhouse gas fluxes. The high relative abundance of potential methanotrophs identified in this study could, in addition to highlighting the presence of methane, indicate an important constraint on methane efflux that requires further investigation.

Combined, insights provided by broad-scale surface sediments and downcore sediments analyzed in the Bering-Chukchi seas can be used to predict areas where high carbon burial or mineralization is more likely to occur. For instance, I found that nearshore stations with silty clay, high OM and total organic nitrogen (TN), and bioturbation via polychaetes are likely to exhibit higher OM burial rates, and slower OM degradation rates below the 1-cm sediment layer due to the prevalence of certain anaerobic microbes. In 1987 researchers found sulfidic dead zones in these types of sediments near Pt. Hope where sediments were black, smelled of sulfide, and were littered with decaying epifauna (Feder et al., 2004). With potentially increasing primary

production and subsequent deposition, we may be seeing more sulfidic dead zones in years to come, with microbial community structure shifting to a higher proportion of specific sulfate-reducing taxa. These shifts in deposition and sediment oxygenation also have major implications on microbial community structure changes with respect to a potential oil exposure event. During my incubation experiments I observed substantial changes in relative abundance in the core community, putative oil-degraders, and decreased diversity in anoxic oiled samples. Thus anoxic oiled sediment *in situ* would have a very different community structure than oxic sediments. With additional testing, my experiment also indicates that we may be able to use certain putative oil-degrading taxa and relative proportions of these taxa *in situ* to track the processing of a spill in the benthos.

5.1.2 Future work

These data highlight the need for more regular and long-term sampling and characterization of benthic microbes in this region. The two surveys of microbial community structure conducted here reveal biogeochemical information that tends to be overlooked in typical environmental sampling designs. I recommend incorporating benthic microbial community structure surveys into any long-term monitoring programs in this rapidly changing Arctic marine ecosystem. For monitoring purposes, it would be beneficial to capture broad spatial coverage as a priority and collect vertical profiles where possible, being strategic about sampling in areas where there are marked differences in total organic carbon (TOC), sediment type, and bioturbation.

This study also highlights the vast array of uncultured and unclassified microbes in Arctic marine sediments, and the need for more experimental and culture-based studies to elucidate

their role in biogeochemical processes, with implications for benthic ecosystem function.

Although taxonomic classification does not directly equate to function, this dissertation highlights how taxonomic composition may provide a framework for future studies. For instance, research investigating the role of nitrification and anammox in the Beaufort Sea would be most beneficial in slope sediments where microbes involved in aerobic/anaerobic ammonia oxidation and nitrite oxidation were abundant, and could reveal useful information about regional nitrogen cycling and upwelling dynamics.

Lastly, forthcoming chemical analyses of petroleum hydrocarbon composition and concentration over the course of my oil incubation experiment will aid in inferring which taxa degrade which hydrocarbon classes, provide insight into the putative oil-degrading consortia observed here, and yield quantitative results which will allow us to determine the concentration and degradation rates of petroleum hydrocarbons in North American Arctic sediments.

5.2 REFERENCES

- Bluhm, B.A., Janout, M.A., Danielson, S.L., Ellingsen, I., Gavriilo, M., Grebmeier, J.M., Hopcroft, R.R., Iken, K.B., Ingvaldsen, R.B., Jørgensen, L.L., Kosobokova, K.N., Kwok, R., Polyakov, I. V., Renaud, P.E., Carmack, E.C., 2020. The Pan-Arctic Continental Slope: Sharp Gradients of Physical Processes Affect Pelagic and Benthic Ecosystems. *Front. Mar. Sci.* 7, 1–25. <https://doi.org/10.3389/fmars.2020.544386>
- Carmack, E., Wassmann, P., 2006. Food webs and physical–biological coupling on pan-Arctic shelves: Unifying concepts and comprehensive perspectives. *Prog. Oceanogr.* 71, 446–477. <https://doi.org/10.1016/j.pocean.2006.10.004>
- Coffin, R.B., Smith, J.P., Plummer, R.E., Yoza, B., Larsen, R.K., Millholland, L.C., Montgomery, M.T., 2013. Spatial variation in shallow sediment methane sources and cycling on the Alaskan Beaufort Sea Shelf/Slope. *Mar. Pet. Geol.* 45, 186–197. <https://doi.org/10.1016/J.MARPETGEO.2013.05.002>
- Cohen, J., Screen, J.A., Furtado, J.C., Barlow, M., Whittleston, D., Coumou, D., Francis, J., Dethloff, K., Entekhabi, D., Overland, J., Jones, J., 2014. Recent Arctic amplification and extreme mid-latitude weather. *Nat. Geosci.* 2014 7, 627–637. <https://doi.org/10.1038/ngeo2234>
- Dong, C., Bai, X., Sheng, H., Jiao, L., Zhou, H., Shao, Z., 2015. Distribution of PAHs and the PAH-degrading bacteria in the deep-sea sediments of the high-latitude Arctic Ocean. *Biogeosciences* 12, 2163–2177. <https://doi.org/10.5194/bg-12-2163-2015>
- Doxaran, D., Devred, E., Babin, M., 2015. A 50% increase in the amount of terrestrial particles

delivered by the Mackenzie River into the Beaufort Sea (Canadian Arctic Ocean) over the last 10 years. *Biogeosciences Discuss.* 12, 305–344. <https://doi.org/10.5194/bgd-12-305-2015>

Feder, H.M., Jewett, S.C., Blanchard, A., 2004. Southeastern Chukchi Sea (Alaska) epibenthos. *Polar Biol.* 2004 285 28, 402–421. <https://doi.org/10.1007/S00300-004-0683-4>

Feng, Z., Ji, R., Ashjian, C., Zhang, J., Campbell, R., Grebmeier, J.M., 2021. Benthic hotspots on the northern Bering and Chukchi continental shelf: Spatial variability in production regimes and environmental drivers Keywords: Polar marine ecosystem Benthic biological hotspots Pelagic-benthic coupling Ice-ocean-biogeochemical model. *Prog. Oceanogr.* 191, 102497. <https://doi.org/10.1016/j.pocean.2020.102497>

Ferguson, R.M.W., Gontikaki, E., Anderson, J.A., Witte, U., 2017. The variable influence of dispersant on degradation of oil hydrocarbons in subarctic deep-sea sediments at low temperatures (0-5 °C). *Sci. Rep.* 7, 1–13. <https://doi.org/10.1038/s41598-017-02475-9>

Gamboa, A., Montero-Serrano, J.-C., St-Onge, G., Rochon, A., Desiagne, P.-A., 2017. Mineralogical, geochemical, and magnetic signatures of surface sediments from the Canadian Beaufort Shelf and Amundsen Gulf (Canadian Arctic). *Geochemistry, Geophys. Geosystems* 18, 488–512. <https://doi.org/10.1002/2016GC006477>

Goñi, M. a., O'Connor, A.E., Kuzyk, Z.Z., Yunker, M.B., Gobeil, C., Macdonald, R.W., 2013. Distribution and sources of organic matter in surface marine sediments across the North American Arctic margin. *J. Geophys. Res. Ocean.* 118, 4017–4035. <https://doi.org/10.1002/jgrc.20286>

- Grebmeier, J.M., 2012. Shifting Patterns of Life in the Pacific Arctic and Sub-Arctic Seas. *Ann. Rev. Mar. Sci.* 4, 63–78. <https://doi.org/10.1146/annurev-marine-120710-100926>
- Hamdan, L.J., Coffin, R.B., Sikaroodi, M., Greinert, J., Treude, T., Gillevet, P.M., 2013. Ocean currents shape the microbiome of Arctic marine sediments. *ISME J.* 7, 685–96. <https://doi.org/10.1038/ismej.2012.143>
- Holmes, R.M., Coe, M.T., Fiske, G.J., Gurtovaya, T., McClelland, J.W., Shiklomanov, A.I., Spencer, R.G.M., Tank, S.E., Zhulidov, A. V., 2012. Climate Change Impacts on the Hydrology and Biogeochemistry of Arctic Rivers, in: *Climatic Change and Global Warming of Inland Waters*. John Wiley & Sons, Ltd, Chichester, UK, pp. 1–26. <https://doi.org/10.1002/9781118470596.ch1>
- Koch, C.W., Cooper, L.W., Lalande, C., Brown, T.A., Frey, K.E., Grebmeier, J.M., 2020. Seasonal and latitudinal variations in sea ice algae deposition in the Northern Bering and Chukchi seas determined by algal biomarkers. *PLoS One* 15, e0231178. <https://doi.org/10.1371/journal.pone.0231178>
- Kortsch, S., Primicerio, R., Beuchel, F., Renaud, P.E., Rodrigues, J., Lønne, O.J., Gulliksen, B., 2012. Climate-driven regime shifts in Arctic marine benthos. *Proc. Natl. Acad. Sci. U. S. A.* 109, 14052–14057. <https://doi.org/10.1073/pnas.1207509109>
- Kortsch, S., Primicerio, R., Fossheim, M., Dolgov, A. V., Aschan, M., 2015. Climate change alters the structure of arctic marine food webs due to poleward shifts of boreal generalists. *Proc. R. Soc. B Biol. Sci.* 282. <https://doi.org/10.1098/rspb.2015.1546>
- Meskhidze, N., Sabolis, A., Reed, R., Kamykowski, D., 2015. Quantifying environmental stress-

- induced emissions of algal isoprene and monoterpenes using laboratory measurements. *Biogeosciences* 12, 637–651. <https://doi.org/10.5194/bg-12-637-2015>
- Orcutt, B.N., Sylvan, J.B., Knab, N.J., Edwards, K.J., 2011. Microbial Ecology of the Dark Ocean above, at, and below the Seafloor. *Microbiol. Mol. Biol. Rev.* 75, 361–422. <https://doi.org/10.1128/MMBR.00039-10>
- Previdi, M., Smith, K.L., Polvani, L.M., 2021. Arctic amplification of climate change: a review of underlying mechanisms. *Environ. Res. Lett.* 16, 093003. <https://doi.org/10.1088/1748-9326/AC1C29>
- Rodriguez-R, L.M., Overholt, W.A., Hagan, C., Huettel, M., Kostka, J.E., Konstantinidis, K.T., 2015. Microbial community successional patterns in beach sands impacted by the Deepwater Horizon oil spill. *ISME J.* 9, 1928–1940. <https://doi.org/10.1038/ismej.2015.5>
- Rontani, J.-F., Belt, S.T., Vaultier, F., Brown, T.A., Massé, G., 2014. Autoxidative and Photooxidative Reactivity of Highly Branched Isoprenoid (HBI) Alkenes. *Lipids* 49, 481–494. <https://doi.org/10.1007/s11745-014-3891-x>
- Rontani, J.F., Belt, S.T., Amiraux, R., 2018. Biotic and abiotic degradation of the sea ice diatom biomarker IP25 and selected algal sterols in near-surface Arctic sediments. *Org. Geochem.* 118, 73–88. <https://doi.org/10.1016/j.orggeochem.2018.01.003>
- Volkman, J.K., Barrett, S.M., Dunstan, G.A., 1994. C25 and C30 highly branched isoprenoid alkenes in laboratory cultures of two marine diatoms. *Org. Geochem.* 21, 407–414. [https://doi.org/10.1016/0146-6380\(94\)90202-X](https://doi.org/10.1016/0146-6380(94)90202-X)

- Walker, A.M., Leigh, M.B., Mincks, S.L., 2021. Patterns in Benthic Microbial Community Structure Across Environmental Gradients in the Beaufort Sea Shelf and Slope. *Front. Microbiol.* 12, 37. <https://doi.org/10.3389/fmicb.2021.581124>
- Wang, Y., Chen, X., Guo, W., Zhou, H., 2018. Distinct bacterial and archaeal diversities and spatial distributions in surface sediments of the Arctic Ocean. *FEMS Microbiol. Lett.* 365, 273. <https://doi.org/10.1093/femsle/fny273>
- Yang, T., Speare, K., McKay, L., MacGregor, B.J., Joye, S.B., Teske, A., 2016. Distinct bacterial communities in surficial seafloor sediments following the 2010 deepwater horizon blowout. *Front. Microbiol.* 7, 1384. <https://doi.org/10.3389/FMICB.2016.01384/BIBTEX>
- Zeng, Y., Zou, Y., Chen, B., Grebmeier, J.M., Li, H., Yu, Y., Zheng, T., 2011. Phylogenetic diversity of sediment bacteria in the northern Bering Sea. *Polar Biol.* 34, 907–919. <https://doi.org/10.1007/s00300-010-0947-0>